

Observational Analysis of Tropical Cyclone Formation

by

John L. McBride

P.I. William M. Gray

Department of Atmospheric Science
Colorado State University
Fort Collins, Colorado

NOAA(NHEML)NA-79-RAD-00002
NSF-ATM 78-18962
NEPRF N00228-76-C-2129

Colorado
State
University

Department of
Atmospheric Science

Paper No. 308

OBSERVATIONAL ANALYSIS OF TROPICAL CYCLONE FORMATION

By

John L. McBride

Preparation of this report

has been financially supported by

the National Science Foundation Grant No. ATM 78-18962

and the National Oceanic and Atmospheric Administration,

National Hurricane Experimental Meteorology Laboratory

Grant No. NA 79 RAD 00002 and supplementary support from

the Navy Environmental Prediction Research Facility Grant

No. N00228-76-C-2129

Department of Atmospheric Science

Colorado State University

Fort Collins, Colorado

April, 1979

ABSTRACT

This study investigates the genesis of tropical cyclones through a combination of the compositing approach and the case study approach. Twelve composite data sets are analyzed from the tropical Northwest Pacific and tropical Northwest Atlantic Oceans. Each data set is a composite average of approximately 80 individual disturbances. Four different types of non-developing oceanic tropical disturbances are composited. They are compared with pre-hurricane and pre-typhoon disturbances in each ocean composited at four different stages of intensification. In total 912 different tropical weather systems go into the composites and approximately 40,000 rawinsonde observations are used.

The main findings from the analysis of the composite fields are: (i) pre-typhoon and pre-hurricane systems are located in large areas of high values of low level relative vorticity. The low level vorticity in the vicinity of a developing cloud cluster is approximately twice as large as that observed with non-developing cloud clusters. (ii) Mean divergence and vertical motion for the typical Western Atlantic weather system are well below the magnitudes found in pre-tropical storm systems. (iii) Once a system has sufficient divergence to maintain 100 mb or more per day upward vertical motion over a 4° radius area, there appears to be little relationship between the amount of upward vertical velocity and the potential of the system for development. (iv) Cyclone genesis takes place under conditions of zero vertical wind shear near the system center. (v) There is a requirement for large positive zonal shear to the north and negative zonal shear close to the south of a developing system. There is also a requirement for southerly shear to the west and northerly shear to the east. The scale of this shear pattern is over a 10° latitude radius circle with maximum amplitude at approximately 6° radius. (vi) The large scale flow, therefore, rather than the properties of the system itself, appears to be the main differentiating factor for cyclone genesis.

These six findings can be synthesized into one parameter for the potential of a system for development into a hurricane or typhoon: Genesis Potential (GP) = $\zeta_{900\text{mb}} - \zeta_{200\text{mb}}$, when applied over $0-6^{\circ}$ radius. GP is three times greater for developing tropical weather systems than for non-developing systems.

130 individual weather systems in the Pacific and Atlantic are examined and it is shown that the composite characteristics are always present in the individual situations. In the Atlantic, with the data presently available, it is found that the use of the shear or vorticity criterion would correctly predict the development of 13 out of 16 tropical cyclones. It provides correct predictions for 61 out of 63 non-developing tropical weather systems.

Vertically integrated budgets of heat, momentum and kinetic energy are performed on the composite data sets and physical hypotheses are made on the mechanisms of tropical cyclone genesis and development.

A theory of tropical cyclone genesis is proposed such that the required tropospheric warming is a result of an adjustment of the pre-storm disturbance's mass field to the wind field. The cloud influence on cyclone genesis is not in proportion to the condensation energy released by the system but rather to the ability of the clouds to generate supergradient winds at lower and upper levels. A discussion of the likely physical processes involved with tropical cyclone genesis is presented.

TABLE OF CONTENTS

	Page
1. INTRODUCTION	1
1.1 The compositing philosophy	1
1.2 Compositing technique	3
1.3 Data sets	7
1.4 Discussion.	12
2. BASIC DESCRIPTION OF DATA SETS	17
2.1 Large scale characteristics	17
2.2 The structure of cloud clusters and tropical storms .	20
2.3 Diurnal variation	28
2.4 Dynamic character of the weather systems	31
2.5 Gray's climatological parameter	36
2.6 Contribution from surface evaporation	42
3. COMPARISON: NON-DEVELOPING VS. DEVELOPING SYSTEMS	45
3.1 Pacific cluster: N1 vs. D1, D2	45
3.2 Atlantic cloud clusters: N1, N2 vs. D1	57
3.3 Atlantic depressions: N3 vs. D2	62
3.4 Discussion	70
4. VERTICAL WIND SHEAR	74
5. SUMMARY OF THE DIFFERENCES BETWEEN DEVELOPING AND NON-DEVELOPING TROPICAL DISTURBANCES	88
6. INDIVIDUAL DAY CYCLONE GENESIS	91
6.1 Atlantic tropical storms	91
6.2 Atlantic depressions	102
6.3 Atlantic non-developing systems	104
6.4 Pacific typhoon versus non-developing cloud clusters	110
7. LARGE SCALE FLOW SURROUNDING THE PRE-STORM SYSTEM	114
7.1 The influence of external systems	114
7.2 Vorticity versus divergence	123
7.3 Discussion	131
8. VERTICALLY INTEGRATED BUDGET ANALYSIS	133
8.1 The observed intensification from cloud cluster to typhoon/hurricane	133
8.2 Heat budget	137
8.3 Kinetic energy budget	148
8.4 Angular momentum budget	157
8.5 Summary	171

TABLE OF CONTENTS (cont'd)

	Page
9. THE PHYSICAL PROCESSES OF TROPICAL CYCLONE GENESIS	172
10. CONCLUDING REMARKS	184
BIBLIOGRAPHY	191
APPENDIX: LISTING OF INDIVIDUAL CASE VERTICAL SHEAR DATA	198
A.1 Atlantic tropical storms	198
A.2 Atlantic depressions	205
A.3 Atlantic non-developing systems	207
A.4 Pacific pretyphoon versus non-developing clusters . .	215
A.5 Listing of positions of individual systems	217

1. INTRODUCTION

This study investigates the development of tropical storms. The approach is observational. Two tropical regions, the Northwest Pacific and the Northwest Atlantic Oceans, have been selected for study. Composite data sets have been made up in each region representing weather systems which later intensify into tropical storms, weather systems which do not intensify and tropical cyclones at various different stages of development. The dynamic and physical fields around each of these data sets are analyzed so that the features important for storm development can be distinguished.

An extensive analysis is then performed on 130 separate tropical weather systems to show that these distinguishing features are present in the individual situations. Budget analyses are carried out on the composite data sets and some physical hypotheses are made on the mechanisms of tropical cyclone genesis and intensity change.

1.1 The compositing philosophy

The climatological requirements for the presence of tropical cyclones have been well documented by Gray (1968, 1975, 1979). Charney and Eliassen (1964) and Ooyama (1964) formulated the CISK theory which many claim explains the growth of a tropical storm once the initial deep tropospheric vortex development has occurred.

At present, however, there exists no theory at all for how the initial development of a tropical cyclone from its precursor cloud cluster takes place. The starting point before such a theory can be formulated is a description of the phenomenon to be explained. Some initial steps in this direction have been taken by Riehl (1948), Fett

(1968), Lopez (1968) and Yanai (1961, 1968). These studies were all case studies of individual instances of cyclone formation. They have provided much useful information on the structure of the incipient disturbance and on the changes that take place as cyclone development begins. There are two factors, however, which severely limit the usefulness of the case study approach as an observational basis for the formation of a theory for tropical cyclone genesis.

Firstly, tropical cyclones always form over the warm tropical oceans where traditional data sources are sparse. It is simply not possible to obtain enough rawinsonde data or surface observations around any individual storm or cloud cluster at one time period to permit quantitative analyses of structure, dynamics or energetics.

Secondly, there is a diversity of tropical disturbances. Tropical storms form under various atmospheric conditions; for example, from ITCZ disturbances, from cloud clusters in the deep trade winds, from easterly waves or from the cloudiness associated with a stagnant mid-latitude cold front. Using the case study approach, this variability makes it difficult to distinguish which features are the important ones that lead to storm development.

The current study uses the complementary approach of compositing data. Large amounts of rawinsonde data at many different time periods around many weather systems are averaged together to yield a 'composite' weather system.

All systems which later develop into tropical cyclones are averaged to yield a composite 'pre-typhoon disturbance'. This system is compared with the average of all the systems which do not develop, i.e. with the composite 'non-developing disturbance'.

The first difficulty mentioned above is overcome by the use of many years of data for many different storms, so that the data density becomes great around the composite system. The second difficulty also is overcome as the averaging process smears out the diversity between different systems and enhances the features in common. In the case of cloud clusters which later develop into typhoons or hurricanes, the isolation of these common features is the key to the understanding of how and why tropical storms develop.

Investigations on the applicability of the compositing approach to the study of tropical cyclone genesis have been performed by Gray (1968), Zehr (1976) and S. Erickson (1977). These studies laid most of the framework for the current study and are the source of development for many of the ideas presented later.

1.2 Compositing technique

This study uses ten years (1961-1970) of Northwest Pacific rawinsonde data from the stations shown in Fig. 1. Fourteen years (1961-1974) of Northwest Atlantic rawinsonde data are used from the stations shown in Fig. 2. Twice daily observations (00 and 12 GMT) are utilized.

Compositing is performed on a 15° latitude radius cylindrical grid with 19 vertical levels extending from sea level to 50 mb. The grid is positioned with the disturbance at grid center of the lowest level. Whenever available rawinsonde soundings fall on the grid at a given time period for a given disturbance, each sounding is located relative to the storm center in cylindrical coordinates using plane geometry. Corrections in the relative positions of the balloon and storm center are made for each sounding at each level based on observed winds and

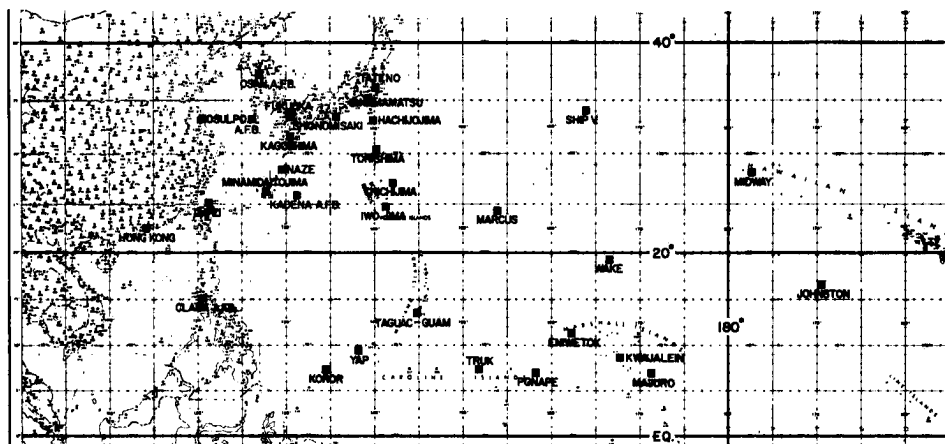


Fig. 1. Northwest Pacific rawinsonde data network.

motions and an assumed balloon ascent rate. It is also assumed that all balloons were released 30 minutes before the nominated observation time.

The cylindrical grid consists of eight octants of 45° azimuthal extent and eleven overlapping radial bands extending from $0-1^{\circ}$, $1-2^{\circ}$, $1-3^{\circ}$, $2-4^{\circ}$, $3-5^{\circ}$, $4-6^{\circ}$, $5-7^{\circ}$, $7-9^{\circ}$, $9-11^{\circ}$, $11-13^{\circ}$ and $13-15^{\circ}$. The grid is aligned geographically. After all parameters have been either measured or computed for each sounding, the value of each parameter is assigned to a point at the center of the grid box in which the sounding falls. All soundings falling in that grid space for the particular type of disturbance being analyzed are composited. An example of the distribution of rawinsonde observations is shown in Fig. 3. The figure shows the number of soundings in each grid box for the eight non-overlapping radial bands: $0-1^{\circ}$, $1-3^{\circ}$, $3-5^{\circ}$, $5-7^{\circ}$, $7-9^{\circ}$, $9-11^{\circ}$, $11-13^{\circ}$ and $13-15^{\circ}$.

Within each direction or octant, a parameter value described as being at 2° radius is actually the composite average of all soundings

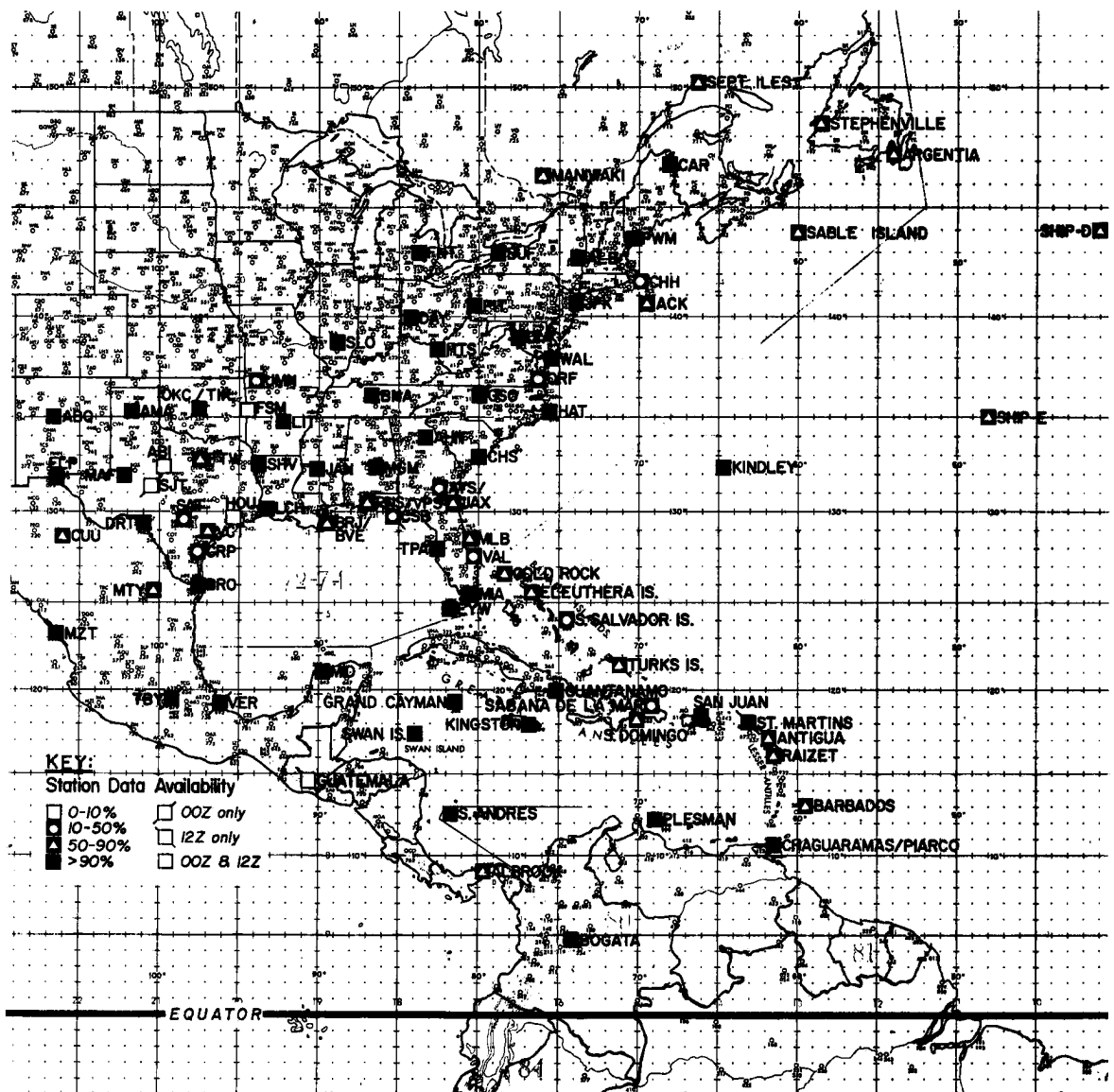


Fig. 2. Northwest Atlantic rawinsonde data network. Only island and coastal stations were used in this study.

falling between 1° latitude distance and 3° latitude distance from the system center. Similarly, the average between 2° and 4° is described as being at 3° , and so on.

In many of the analyses that follow mean values of parameters at a given radius are given. For example, \bar{T} at 3° is the average of the eight octant composites of temperature between 2° and 4° . Vorticity

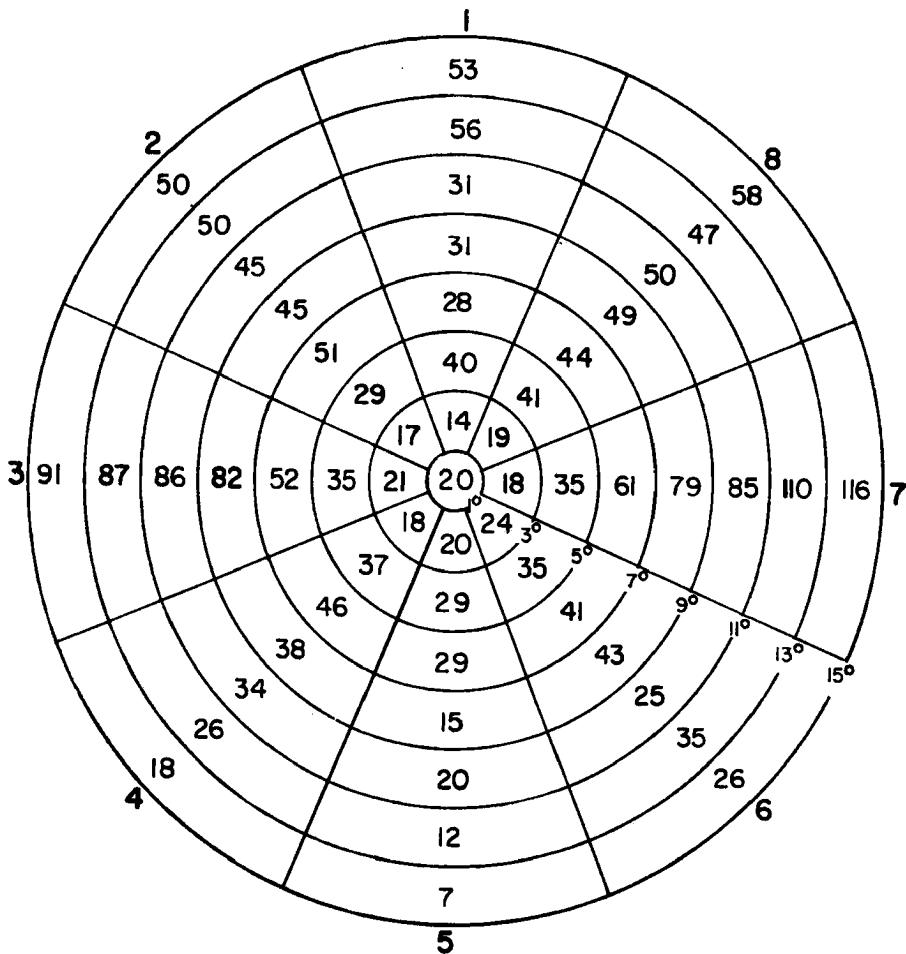


Fig. 3. Cylindrical grid used to composite data and the number of rawinsonde observations included in the grid areas for a particular data set. (This example is for the Pacific D2 pretyphoon cloud cluster.) The grid was centered on the disturbance. Octant 1 was oriented to the north.

and divergence are calculated by line integral methods. Relative vorticity averaged over the $0-4^{\circ}$ radius circle is given by:

$$\begin{aligned}
 \overline{\text{VORT}}^{0-4^{\circ}} &= \frac{1}{\text{AREA}} \oint \mathbf{v}_T \cdot d\ell \\
 &= \frac{1}{\pi R^2} \sum_{i=1}^8 v_{T_i} \frac{2\pi R}{8} \\
 &= \frac{2\bar{v}_T}{R}
 \end{aligned} \tag{1}$$

$$= \frac{2\bar{V}_T \text{ at } 4^\circ \text{ radius}}{4^\circ \text{ latitude}} ,$$

where \bar{V}_T is the tangential component of the wind in cylindrical coordinates. Similarly, divergence is given by $2\bar{V}_R/R$ where \bar{V}_R is the radial component of the wind.

All of the rawinsonde data used in the study are taken from daily Northern Hemisphere Data Tabulation (NHDT) tapes from the Asheville records center and the National Center for Atmospheric Research (NCAR) and from Japanese and East Asian upper air soundings. The latter soundings were card punched by the U.S. Navy Environmental Prediction Research Facility, Monterey, CA for the Colorado State University tropical cyclone research project of W. M. Gray, of which the author is a member.

1.3 Data sets

The typical tropical oceanic weather system is the cloud cluster. This is a westward travelling weather system consisting of a loosely organized collection of deep convective clouds and covered in the upper levels by a thick cirrus shield. The horizontal scale of the cloud cluster is approximately 500-800 km; and it has a lifetime on the order of 1 to 3 days. The structure and mean properties of cloud clusters have been documented by Williams and Gray (1973), Ruprecht and Gray (1976a, 1976b), Martin and Suomi (1972) and S. Erickson (1977).

Many thousand cloud clusters exist over the tropical oceans every year. Of these a very small percentage intensify and become tropical storms. The different stages of development typically follow one another as cloud cluster to tropical depression to tropical storm to typhoon/hurricane. Table 1 defines these classes.

TABLE 1

Definitions of classes of tropical oceanic weather systems.

<u>Class</u>	<u>Definition</u>
<u>Cloud cluster</u>	This is the typical tropical oceanic weather system. It consists of a loosely organized collection of deep convective clouds covered in the upper levels by a thick cirrus shield. The horizontal scale of the cloud cluster is approximately 500-800 km; and it has a lifetime on the order of 1 to 3 days.
<u>The tropical depression</u>	This is defined as a weak tropical cyclone with a definite closed surface circulation, one or more closed surface isobars, and highest sustained wind speeds (average over one minute or longer period) of less than 34 knots (17.5 m/s).
<u>A tropical storm</u>	This is a tropical cyclone with closed isobars and highest sustained wind speeds of 34 to 63 knots inclusive.
<u>The typhoon/hurricane</u>	This is a tropical cyclone with highest sustained winds 64 knots or more. The United States Meteorological Service calls cyclones of this intensity typhoons when they are west of 180° longitude and hurricanes east of 180° longitude.

In this study cyclone genesis is investigated using data from the Northwest Pacific Ocean and from the Northwest Atlantic Ocean as shown in Figs. 1 and 2. Various composite data sets have been made up in each ocean. Prominent tropical cloud clusters or depressions which later develop into hurricanes or typhoons are labelled D. Systems which do not develop are labelled N. In each ocean the developing systems have been placed in a hierarchy of stages of intensification D1 to D4, D1 being the weakest system and D4 the fully developed hurricane or typhoon.

The names of all composite systems analyzed in this study are as follows:

PACIFIC DATA SETSNon-developing

N1 Cloud cluster

Developing

D1 Early pretyphoon cloud cluster
 D2 Pretyphoon cloud cluster
 D3 Intensifying cyclone
 D4 Typhoon

ATLANTIC DATA SETSNon-developing

N1 Cloud cluster
 N2 Wave trough cluster
 N3 Non-developing depression

Developing

D1 Prehurricane cloud cluster
 D2 Prehurricane depression
 D3 Intensifying cyclone
 D4 Hurricane

Following is a more detailed description of each data set.

PACIFIC DATA SETS

N1 - Pacific cloud cluster: summertime Western Pacific cloud clusters. Positions were obtained from ESSA satellite pictures. This data set was composited by Zehr (1976) and is 'Stage 00' of his study. The estimated maximum sustained wind (V_{max}) for these systems is 10 m/s or less. The mean latitude of the system is 11°N ; longitude is 149°E .

D1 - Early pretyphoon cloud cluster: cloud clusters which later develop into typhoons. Positions were obtained from DMSP satellite pictures by S. Erickson (1977). Positions for each system go back as far as detectable by satellite tracing of the system's cloud patterns. This is a small data sample compared to every other composite. It was included in the study because of the very accurate positioning of the clusters, and because it represents the very earliest stage of the storm's existence, 2 to 3 days prior to the beginning of the Joint Typhoon Warning Center (JTWC), official best track record for the storm. Latitude is 11°N ; longitude 146°E . $V_{max} \sim 10 \text{ m/s}$.

D2 - Pacific pretyphoon cloud cluster: Positions were obtained from ESSA satellite pictures and by extrapolation from JTWC best tracks. This data set is 'Stage 2' of Zehr (1976). It consists of that portion of each storm's track prior to one day before the first reconnaissance aircraft observation. Latitude is 10° N; longitude 153° E. $V_{max} \sim 10$ m/s or less.

D3 - Pacific intensifying cyclone: Tracks for these pretyphoon disturbances were obtained from satellite pictures and JTWC best tracks. This data set is Zehr's 'Stage 4'. It consists of the section of each storm's track beginning one day before the first reconnaissance aircraft observation and ending when the maximum sustained winds first attain 50 knots. Latitude is 13° N; longitude 144° E. $V_{max} < 50$ knots, average about 20 m/s.

D4 - Typhoon: Positions are from JTWC best tracks. All storm positions from the years 1961-1970 such that the central pressure of the storm was less than or equal to 980 mb and such that the latitude was less than 30° N are included. This data set has been analyzed in detail by W. Frank (1977a, 1977b). Latitude is 22° N; longitude 136° E. $V_{max} \sim 45$ m/s.

ATLANTIC DATA SETS

N1 - Atlantic cloud clusters: In collaboration with V. Dvorak of NOAA/NESS Applications Group, positions were obtained from satellite pictures of tropical weather systems which subjectively looked like they had potential for development into tropical storms. If a circulation center for the disturbance was visible, it was defined as the position of the system; otherwise the center of mass of the cloud area was used. Latitude is $\sim 20^{\circ}$ N; longitude $\sim 82^{\circ}$ W. $V_{max} \sim 10$ m/s or less.

N2 - Atlantic wave trough convection: N. Frank, director of the National Hurricane Center Miami (NHC), has tracked the movement of Atlantic easterly waves since 1968. Using N. Frank's tracks in the Caribbean for the years 1968-1974 a composite was made relative to the centers of these wave disturbances. Only wave systems which had a significant amount of cluster type convection associated with them were composited. The center of each system was defined such that the longitude was that of N. Frank's trough axis, and the latitude was the central latitude of convective activity as determined from geostationary satellite pictures. Latitude is $\sim 16^{\circ}$ N; longitude $\sim 72^{\circ}$ W. $V_{max} \sim 10$ m/s or less.

N3 - Atlantic non-developing depressions: Western Atlantic depressions which do not develop into tropical storms. Positions are from the annual reports 'Atlantic Tropical Systems of 1967-74' by Staff of National Hurricane Center published in Monthly Weather Review. Mean latitude is $\sim 21^{\circ}$ N; longitude 81° W. $V_{max} \sim 15$ m/s.

D1 - Prehurricane cloud cluster: Positions were obtained from satellite pictures, from past years' NHC Miami operational surface weather maps and from the summaries of individual storms published in the annual Monthly Weather Review articles, 'Atlantic Hurricane Season of 1961-74' by staff members of the National Hurricane Center. Positions for this data set precede positions for data set D2. Latitude is 18° N; longitude 72° W. $V_{max} \sim 10$ m/s or less.

D2 - Atlantic prehurricane depression: Positions for this data set and for data set D3 are from the official best tracks of the NHC. Data set D2 consists of all 12-hourly positions (up to a maximum of six positions per storm) immediately preceding data set D3. It represents

the depression before it begins any significant intensification.

Latitude is 21° N; longitude 75° W. $V_{max} \sim 15$ m/s.

D3 - Atlantic intensifying cyclone: This data set is made up of that portion of each storm's track such that:

- 1) 35 knots < estimated maximum sustained wind \leq 70 knots.
- 2) The last position such that $V_{max} \leq$ 35 knots is also included in the data set. (Thus, only systems that reach greater than 35 knots are considered.)
- 3) V_{max} increases with every time period (12 hours) within the data set.

This data set is thus the portion of the track when the system is actually intensifying through the tropical storm stage. Mean latitude is $\sim 22^{\circ}$ N; longitude $\sim 78^{\circ}$ W. $V_{max} \sim 20$ m/s.

D4 - Hurricane: Official best track positions of the National Hurricane Center for the years 1961-1974 were stratified according to the official estimated maximum sustained wind (V_{max}). Positions such that V_{max} was greater than or equal to 65 knots were included in this data set. Latitude is 23° N; longitude 79° W. $V_{max} \sim 45$ m/s.

1.4 Discussion

To retain the ability to make meaningful comparisons between systems which develop into storms and those which do not, no positions were included in non-developing data sets such that the system center was within 1° latitude of land within the following 24 hours.

The data were composited on the cylindrical coordinate grid described above. The number of soundings composited at various radii in each of the data sets is shown in Table 2.

The above 12 data sets are such that they can provide a complete description of tropical storm development. Data are included from two

TABLE 2

Number of rawinsonde observations included between $1\text{--}3^{\circ}$, $3\text{--}5^{\circ}$ and $5\text{--}7^{\circ}$ latitude distance from the center of each composite system.

	<u>2°</u>	<u>4°</u>	<u>6°</u>
<u>PACIFIC</u>			
N1 Cloud cluster	143	224	282
D1 Early pretyphoon cloud cluster	22	45	72
D2 Pretyphoon cloud cluster	151	281	352
D3 Intensifying cyclone	135	272	357
D4 Typhoon	203	521	787
<u>ATLANTIC</u>			
N1 Cloud cluster	170	393	548
N2 Wave trough cluster	197	364	477
N3 Non-developing depression	46	75	137
D1 Prehurricane cloud cluster	49	84	94
D2 Prehurricane depression	113	179	267
D3 Intensifying cyclone	111	227	299
D4 Hurricane	206	434	646

oceans so that regional peculiarities can be distinguished. Non-developing and developing systems at both the cluster stage and the depression stage are included. All stages of development are considered, including for comparison the fully developed typhoon or hurricane.

Table 3 summarizes the average geographical location of the disturbances in each data set. Table 4 shows the number of different individual disturbances in each data set. Table 5 lists the sea level pressures and low level winds associated with the various composite system.

TABLE 3

Mean position of the disturbances making up each composite data set.

	<u>Latitude</u>	<u>Longitude</u>
<u>PACIFIC NON-DEVELOPING</u>		
N1 Cloud cluster	11°N	149°E
<u>PACIFIC DEVELOPING</u>		
D1 Early pretyphoon cloud cluster	11°N	146°E
D2 Pretyphoon cloud cluster	10°N	153°E
D3 Intensifying cyclone	13°N	144°E
D4 Typhoon	22°N	136°E
<u>ATLANTIC NON-DEVELOPING</u>		
N1 Cloud cluster	20°N	82°W
N2 Wave trough cluster	16°N	72°W
N3 Non-developing depression	21°N	81°W
<u>ATLANTIC DEVELOPING</u>		
D1 Prehurricane cloud cluster	18°N	72°W
D2 Prehurricane depression	21°N	75°W
D3 Intensifying cyclone	22°N	78°W
D4 Hurricane	23°N	79°W

TABLE 4

Number of individual disturbances making up each composite data set.

	<u>Number</u>
<u>PACIFIC NON-DEVELOPING</u>	
N1 Cloud cluster	87
<u>PACIFIC DEVELOPING</u>	
D1 Early pretyphoon cloud cluster	46
D2 Pretyphoon cloud cluster	130
D3 Intensifying cyclone	130
D4 Typhoon	147
<u>ATLANTIC NON-DEVELOPING</u>	
N1 Cloud cluster	46
N2 Wave trough cluster	66
N3 Non-developing depression	22
<u>ATLANTIC DEVELOPING</u>	
D1 Prehurricane cloud cluster	23
D2 Prehurricane depression	63
D3 Intensifying cyclone	79
D4 Hurricane	73

TABLE 5

Mean sea level pressures and low level winds.

	<u>Composited mean wind speed at 950 mb averaged over the 0-4 area (m/s)</u>	<u>Composited tangential wind at 4° radius at 950 mb (m/s)</u>	<u>Estimate of maximum sus- tained sur- face wind (m/s)</u>	<u>Estimate of central sea level pres- sure (mb)</u>
<u>PACIFIC NON-DEVELOPING</u>				
N1 Cloud cluster	6.5	1.3	10	1008
<u>PACIFIC DEVELOPING</u>				
D1 Early pretyphoon cloud cluster	8.1	4.2	10	1007
D2 Pretyphoon cloud cluster	7.0	4.9	10	1005
D3 Intensifying cyclone	10.3	8.2	20	1000
D4 Typhoon	14.8	11.3	45	960
<u>ATLANTIC NON-DEVELOPING</u>				
N1 Cloud cluster	7.7	.2	10	1010
N2 Wave trough cluster	8.0	.6	10	1010
N3 Non-developing depression	7.0	3.5	15	1007
<u>ATLANTIC DEVELOPING</u>				
D1 Prehurricane cloud cluster	8.0	3.0	10	1007
D2 Prehurricane depression	7.7	5.0	15	1007
D3 Intensifying cyclone	9.9	5.8	20	1000
D4 Hurricane	13.9	8.9	45	980

2. BASIC DESCRIPTION OF DATA SETS

2.1 Large scale characteristics

The twelve composite data sets described in Chapter 1 represent average summertime tropical oceanic disturbances in the Northwest Pacific and Northwest Atlantic oceans. The mean low level (gradient level) and upper level (200 mb) wind circulations for these two regions at that time of the year are shown in Figs. 4 and 5. The mean positions of the composite data sets in each ocean are marked on the figures with a cross.

The Western Pacific systems exist in the low level easterlies just poleward of the monsoon equatorial trough. The easterly flow is deep extending upwards through the whole troposphere, so that the Pacific composite systems are still embedded in easterlies at the 200 mb level.

The Atlantic systems also exist in easterlies at low levels. They are further north, however. They are not associated with the Inter Tropical Convergence Zone (ITCZ), but are in the trade wind region. The trade wind easterlies are not quite as deep here, as they are closer to the ITCZ. Hence, at the 200 mb level the wind has changed direction; and at this level the West Atlantic data sets exist in mean northwest-easterly flow.

The Pacific systems exist in upper level easterlies, the Atlantic systems in upper level westerlies; but both sets of systems are in the region of the upper level subtropical ridge; so that they have westerlies poleward of them and easterlies equatorwards. They are also both just west of the Tropical Upper Tropospheric Trough, which is marked with a dashed line on Fig. 5. In the western part of the Northern Hemisphere oceans in summer, the upper level subtropical ridge branches in two,

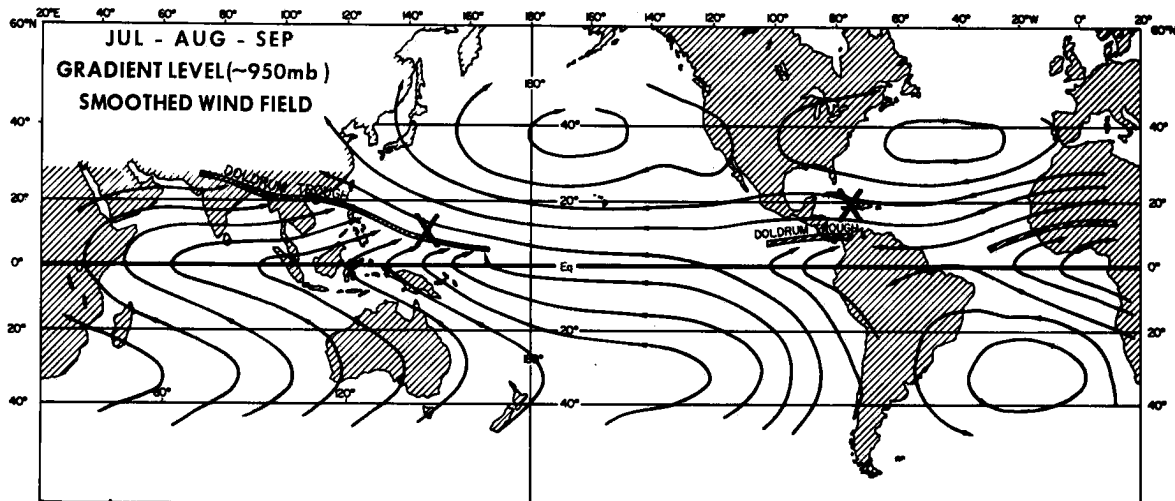


Fig. 4. Mean gradient level wind for the Northern Hemisphere summer months (from Gray, 1979). The crosses in the Northwest Pacific and the Northwest Atlantic represent the mean positions of the composite data sets in each region.

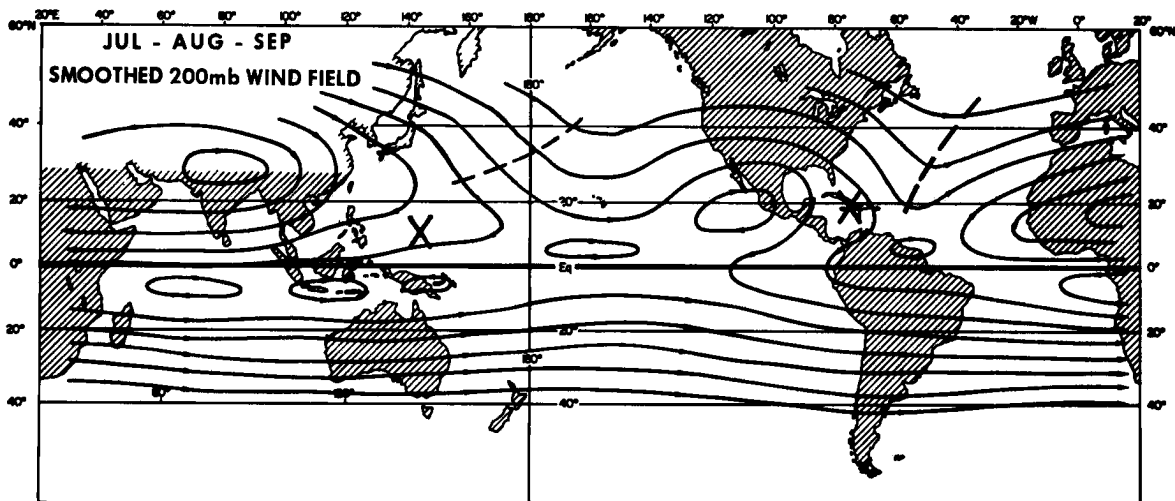


Fig. 5. Mean 200 mb level wind for the Northern Hemisphere summer months (Gray, 1979). The crosses in the Northwest Pacific and the Northwest Atlantic represent the mean positions of the composite data sets in each region. The dashed line shows the position of the tropical upper tropospheric trough.

one branch extending eastward and the other towards the northeast. The trough between these two ridges is what is referred to as the Tropical Upper Tropospheric Trough (TUTT). The TUTT varies greatly from day to day in intensity and position. Sadler in a series of papers (Sadler, 1967, 1975, 1976, 1978) has demonstrated that the initiation of tropical cyclones in the Western Pacific is often associated with the TUTT extending further westward than usual.

At the low levels both the Western Pacific systems and the Western Atlantic systems are embedded in easterly flow. The Pacific systems are associated with the monsoon equatorial trough. They thus exist in a region of strong mean background low level convergence and positive relative vorticity. The convergence is mainly $\frac{\partial U}{\partial x}$ convergence brought about by the deceleration of the easterlies as they approach the monsoon flow towards the west. The relative vorticity is mainly made up of the $-\frac{\partial U}{\partial y}$ component, with westerlies to the south and strong easterly winds to the north. McBride and Gray (1978) calculated mean summertime vorticity and vertical motion at the 850 mb level for the Northwest Pacific. They found the mean background vorticity to be $+3 \times 10^{-6} \text{ s}^{-1}$ and the vertical motion to be 30 mb/d upwards.

The Western Atlantic systems, on the other hand, are in the subsidence region of the trade winds. Here the long term mean summertime relative vorticity is negative ($-1.5 \times 10^{-6} \text{ s}^{-1}$ at 850 mb) and the background vertical motion is downwards (10 mb/d at 850 mb). Weather systems are often referred to as being in a 'coasting' or 'weakening' stage as they pass through this subsidence region.

2.2 The structure of cloud clusters and tropical storms

Pacific composite systems N1, D1, D2 and Atlantic composite systems

N1, N2 and D1 are cloud cluster data sets. The basic thermodynamic and dynamic structure of this type of weather system has been documented by Williams and Gray (1973) and Ruprecht and Gray (1976a, 1976b). The systems are embedded in deep tropospheric easterly flow, and they typically move with that flow towards the west at speeds of approximately 6 m/s. The directions and speeds of motion of all composite systems are presented in Table 6. The table shows that as the systems increase in intensity they slow down and move more towards the north. There is of course a great variability in movement, and the individual disturbances going into each composite can move in any compass direction and at speeds greatly varying from the composite average.

The mean thermodynamic and dynamic characteristics of Western Pacific and Western Atlantic summertime cloud clusters are shown in Fig. 6. The fields shown are the composite average fields from the Pacific D2 (Typhoon cloud cluster) and the Atlantic D1 (Prehurricane cloud cluster) data sets. Both these systems later develop into tropical storms. These particular systems have been chosen here to illustrate the mean features of a cloud cluster because they are well defined systems, so that the features of interest are easily observed. The variations on this basic structure which determine whether or not the systems will later develop into tropical storms are the subject of the following two chapters.

Figure 6a shows a vertical profile of $T_c - T_e$ where T_c is the mean temperature within the cluster region and T_e is the mean temperature of the "environment" or surrounding region. The temperature gradients

TABLE 6

Mean speed and direction of movement of composite data sets.

	Direction (from which disturbance is moving) (degrees)	Speed of Movement (m s^{-1})
<u>PACIFIC NON-DEVELOPING</u>		
N1 Cloud cluster	94	7.2
<u>PACIFIC DEVELOPING</u>		
D1 Early pretyphoon cloud cluster	90	7.2
D2 Pretyphoon cloud cluster	106	5.0
D3 Intensifying cyclone	118	4.4
D4 Typhoon	146	3.6
<u>ATLANTIC NON-DEVELOPING</u>		
N1 Cloud cluster	101	3.8
N2 Wave trough cluster	97	7.0
N3 Non-developing depression	135	3.1
<u>ATLANTIC DEVELOPING</u>		
D1 Prehurricane cloud cluster	109	4.9
D2 Prehurricane depression	135	3.2
D3 Intensifying cyclone	145	3.1
D4 Hurricane	130	2.9

between the cluster and its surroundings as revealed by the composited data are very small. Zehr (1976) pointed out that because of this smallness of the gradients, and because of the noise inherently present in meteorological data, the precise configuration of the temperature anomaly varies somewhat depending on the reference chosen to represent the cluster and its environment. In Fig. 6a the cluster area is defined as within 3° latitude radius of the center of the system; the environmental temperature is the average of the temperature values between 3 and 7 degrees to the east and west of the cluster position. The figure

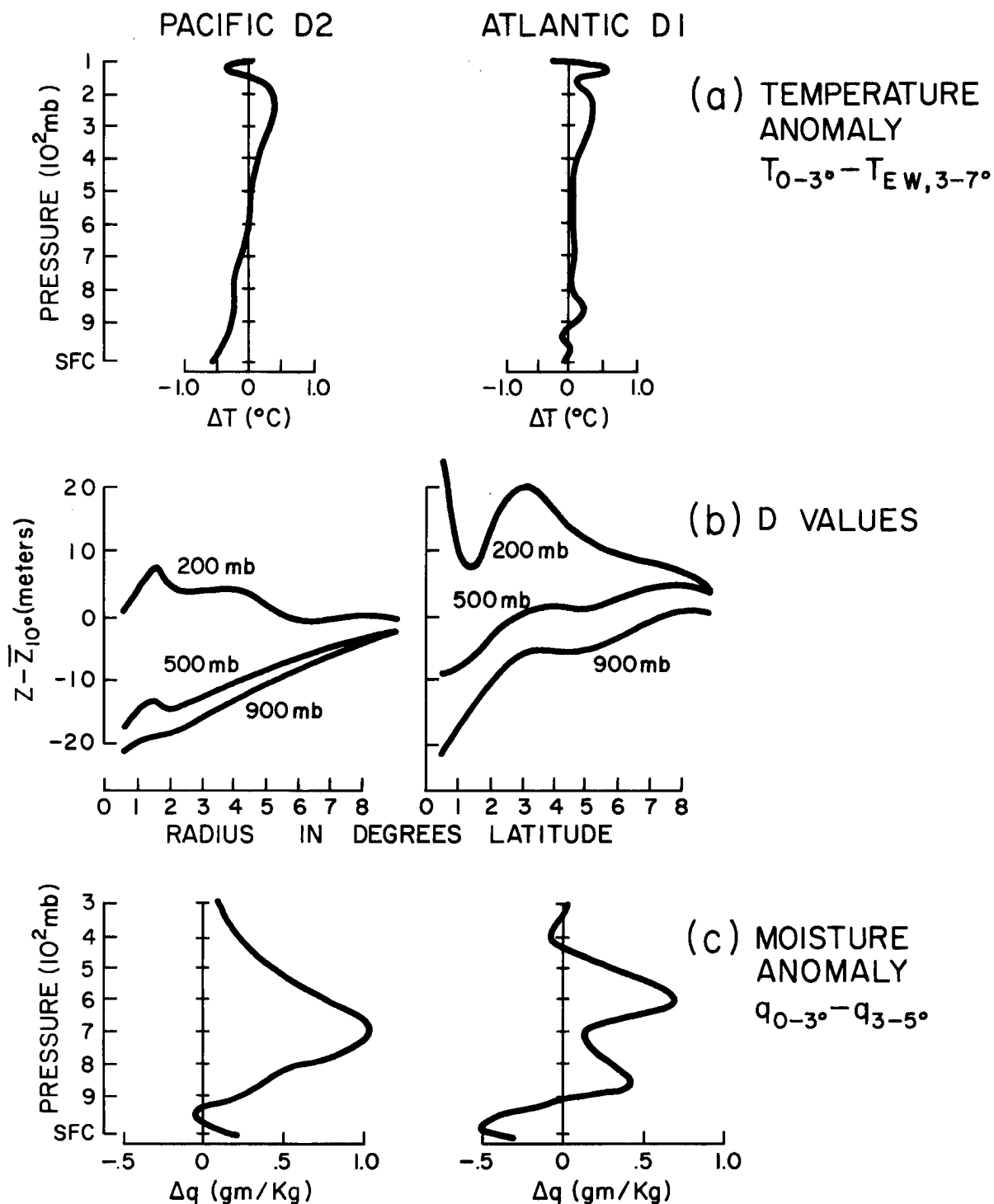


Fig. 6. Mean structure of West Pacific and West Atlantic cloud clusters.

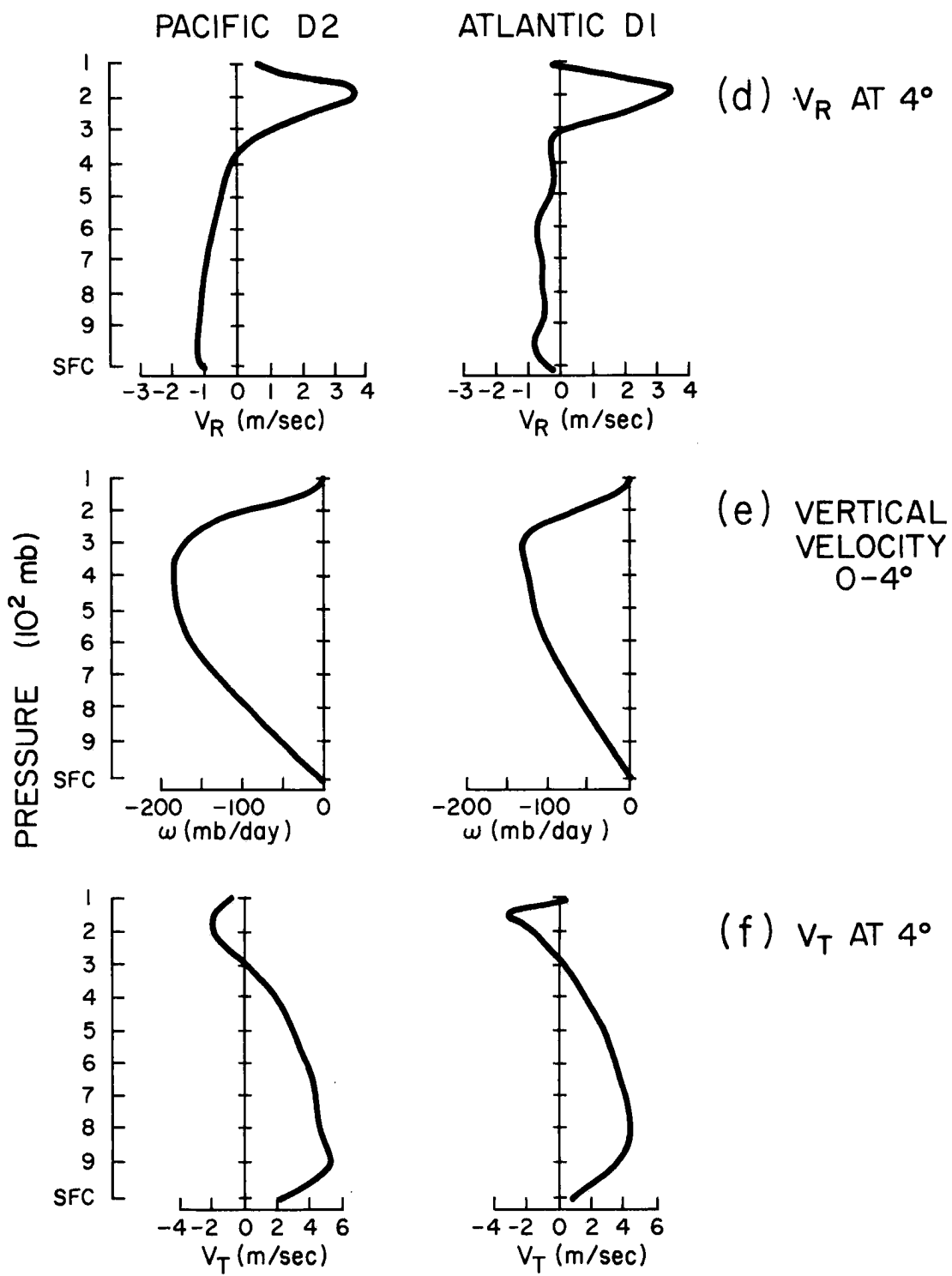


Fig. 6. Continued.

shows that cloud clusters in both oceans have a warm core in the upper levels centered at about the 250 mb level. Hydrostatically this observed upper level warm core implies a low pressure system with the strongest height gradients near the surface. This is observed, as shown in Fig. 6b which is a 2-dimensional cross-section of D values. The systems have very distinct inward height gradients at 500 and 900 mb. At 200 mb the height gradient is not as well defined, but is clearly outwards.

Part (c) of the figure shows a vertical profile of water vapor mixing ratio differences between the cluster ($r = 0-3^{\circ}$) and the environment ($r = 3-5^{\circ}$). The cluster is moister than its surroundings by about 0.6 g/kg in the middle troposphere.

Part (d) shows a vertical profile of radial wind V_R at 4° radius. There is inflow (or negative V_R) through most of the troposphere from the surface up to about 350 mb. A layer of strong outflow exists between 350 mb and 100 mb. The inflow extends through most of the troposphere and well above the layer of frictional influence. It is obviously therefore ageostrophic flow, flowing down the pressure gradients shown in Fig. 6b. Further discussion of this ageostrophic aspect of the inflow is reserved for section 2.4 below.

Part (e) of the figure shows vertical profiles of the kinematically derived vertical motion. The cluster is characterized by upward vertical motion through the whole troposphere, with the maximum value at about 350 mb.

The tangential component of the wind V_T is shown in Fig. 6f. The tangential wind is positive throughout the troposphere from the surface to 300 mb and negative or anticyclonic above that level. This is

consistent with the inflowing air bringing about vertical stretching or horizontal contraction of the vortex tubes and increased local vorticity. The outflowing air causes expansion of vortex tubes and generation of negative vorticity.

There are some major differences between Western Pacific and Western Atlantic cloud clusters which have not been shown in Fig. 6. Firstly, the typical Western Atlantic system has much weaker vertical motion than its counterpart in the Western Pacific. This is in agreement with the large difference the two regions have in background vertical motion. This large difference will be shown clearly when the vertical motion fields for all data sets are considered separately in Chapter 3.

Secondly, there is less moisture in the Western Atlantic. Averaging together the 3 cluster data sets in each ocean (Pacific N1, D1, D2; Atlantic N1, N2, D1) the mean precipitable water in the $0-4^{\circ}$ area for the Pacific systems is 5.8 gm/cm^2 , while for the Atlantic systems it is 5.0 gm/cm^2 . As shown in Fig. 6c, however, the horizontal gradient of moisture between cluster and environment is very similar in the two oceans. Taking the mean precipitable water over the $4-6^{\circ}$ area, the result in the Pacific is 5.6 gm/cm^2 , and in the Atlantic 4.8 gm/cm^2 . In both cases this is 0.2 gm/cm^2 less than in the $0-4^{\circ}$ area.

The structure of fully developed tropical storms as obtained from composite data has been described by W. Frank (1977a, 1977b) and by Núñez and Gray (1977). Figure 7 shows the composite thermodynamic and dynamic fields for the Pacific D4 typhoon and the Atlantic D4 hurricane data sets. The shape of each curve in this figure is very similar to the corresponding curve in Fig. 6. As far as broad scale characteristics

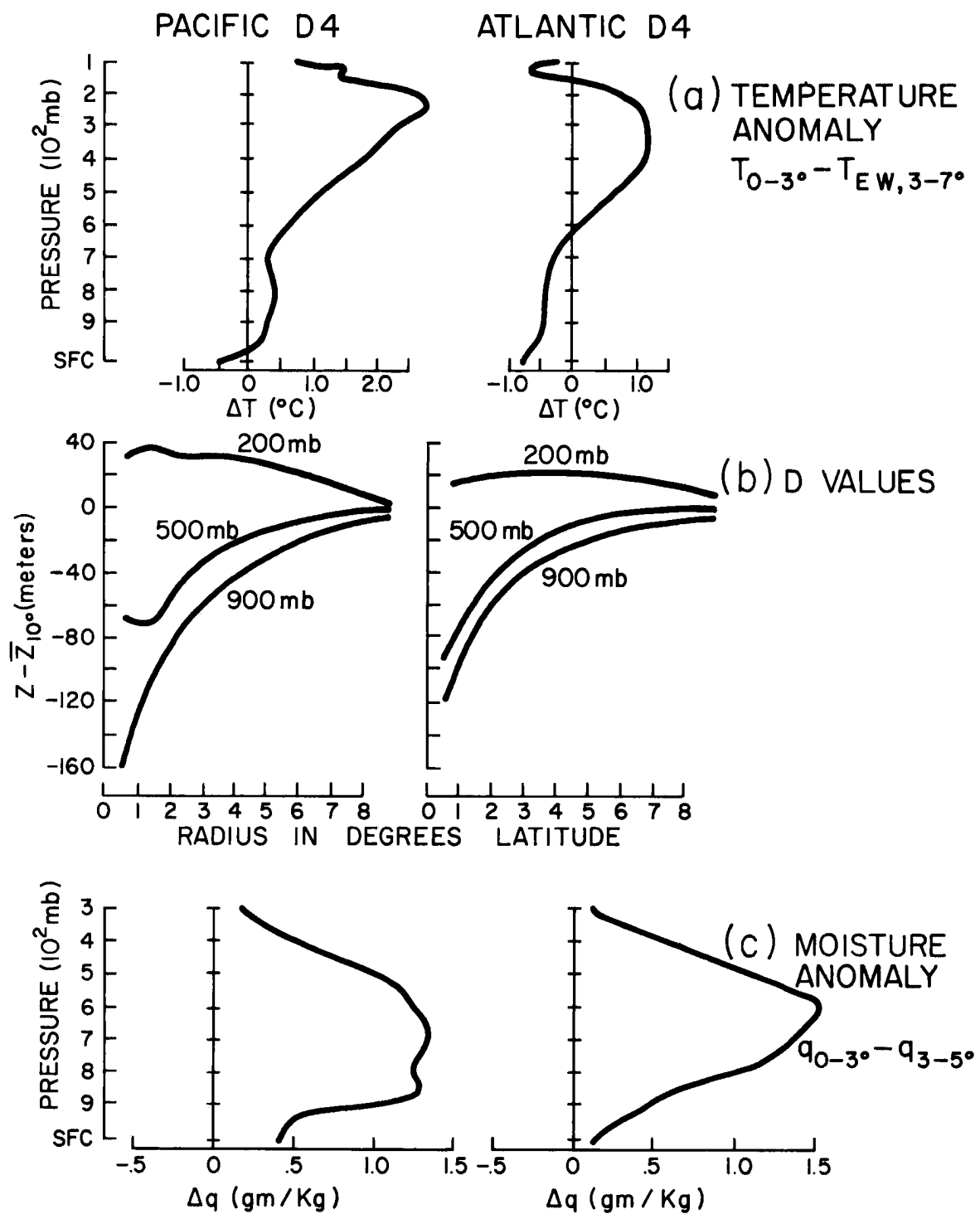


Fig. 7. Mean structure of composite Western Pacific typhoon and Western Atlantic hurricane.

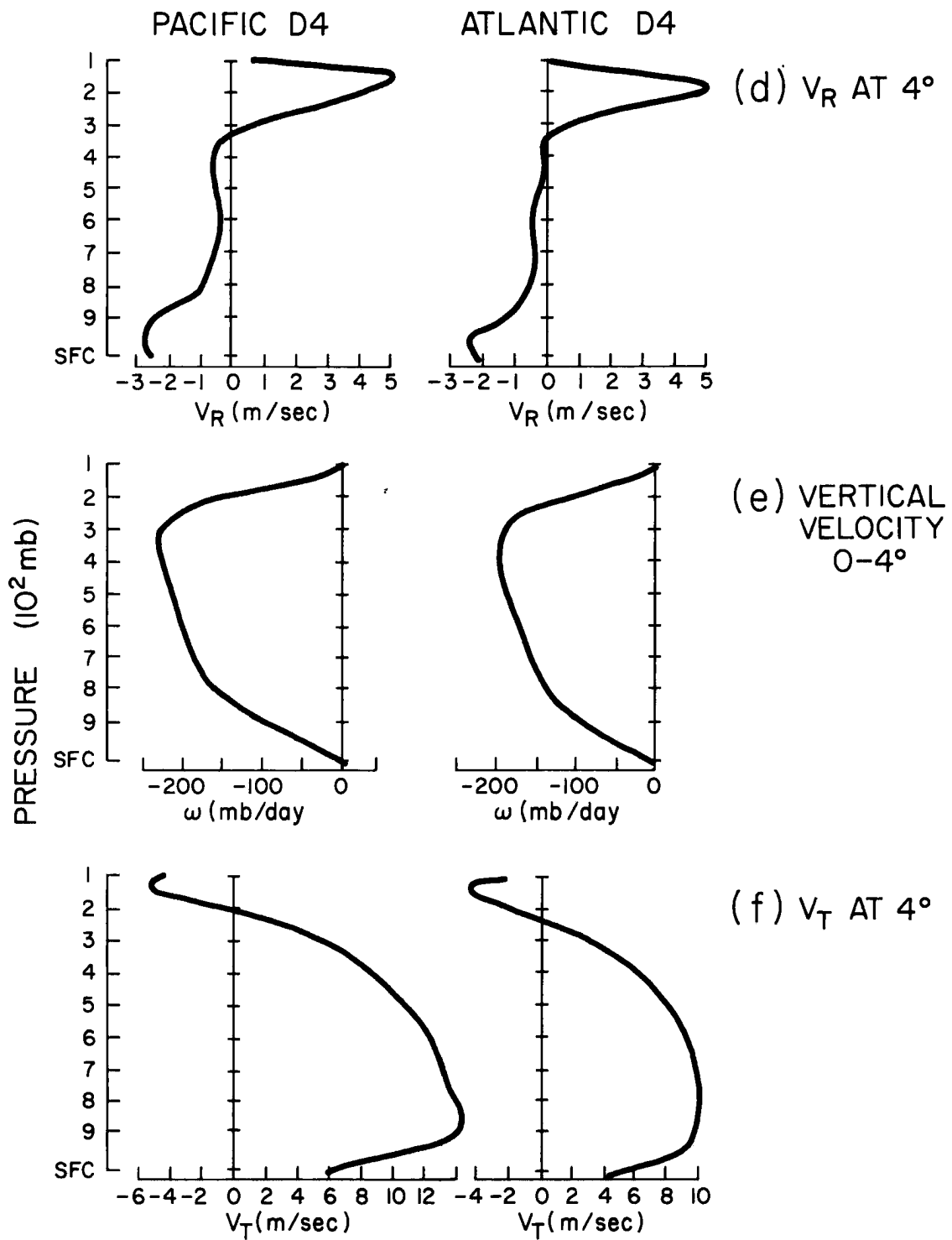


Fig. 7. Continued.

averaged over a $0\text{--}4^{\circ}$ latitude area are concerned, the difference between a cloud cluster and a tropical storm is one of magnitude. The upper level warm core (Fig. 7a), the lower and middle tropospheric inward height gradients (Fig. 7b) and the excess of moisture (Fig. 7c) are much more pronounced. The wind fields have correspondingly increased in magnitude (Fig. 7d, e and f), the largest increase being in the magnitude of the tangential wind V_T at each level (Fig. 7f).

2.3 Diurnal variation

It was demonstrated by Ruprecht and Gray (1976b) that tropical oceanic cloud clusters possess a very large diurnal variation in mass divergence and vertical velocity. No separate investigation has been performed on the diurnal variation of the data sets utilized in the current study; but McBride and Gray (1978) carried out an extensive analysis of twelve very similar data sets. In general, low level convergence and upward vertical velocity in tropical oceanic weather systems are greater in the morning than they are in the afternoon-evening. These features are particularly pronounced for cloud clusters, but become less prominent as the system intensifies towards the hurricane or typhoon stage. The physical cause of the diurnal variation has been extensively discussed by Gray and Jacobson (1977) and McBride and Gray (1978). The theory is that the deep convergence profile observed in tropical weather systems is maintained and diurnally modified by differences in the radiative-condensation heating profiles of the thick cirrus-shield covered weather systems and their surrounding clear areas.

Figure 8 shows the vertical profiles of divergence observed by McBride and Gray. The data sets in the current study are consistent

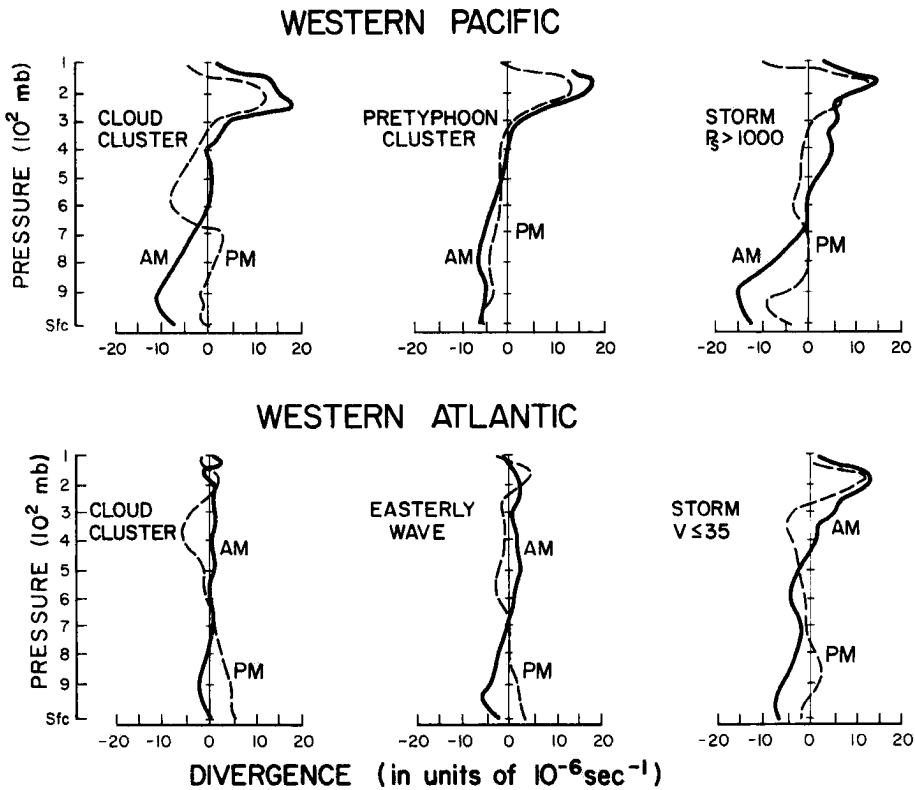


Fig. 8. Morning vs. nighttime divergence profiles for tropical Western Pacific and Western Atlantic weather systems (from McBride and Gray, 1978).

with McBride and Gray's observations. This can be seen in Fig. 9 which shows morning and evening vertical profiles of divergence and vertical velocity for the Atlantic D2 prehurricane depression data set.

In Chapter 10 some discussion will be made on the effect of this variation on the mechanism of tropical storm genesis and development. All other analyses of wind or divergence in this study are composites of all data, 00Z and 12Z combined; thus the diurnal variation has been filtered out of these fields.

The diurnal variation of the divergent component of the wind field which appears in the data is a real atmospheric effect. The composite data also show a diurnal variation in relative humidity and water vapor mixing ratio. This variation is spurious, and is due to design

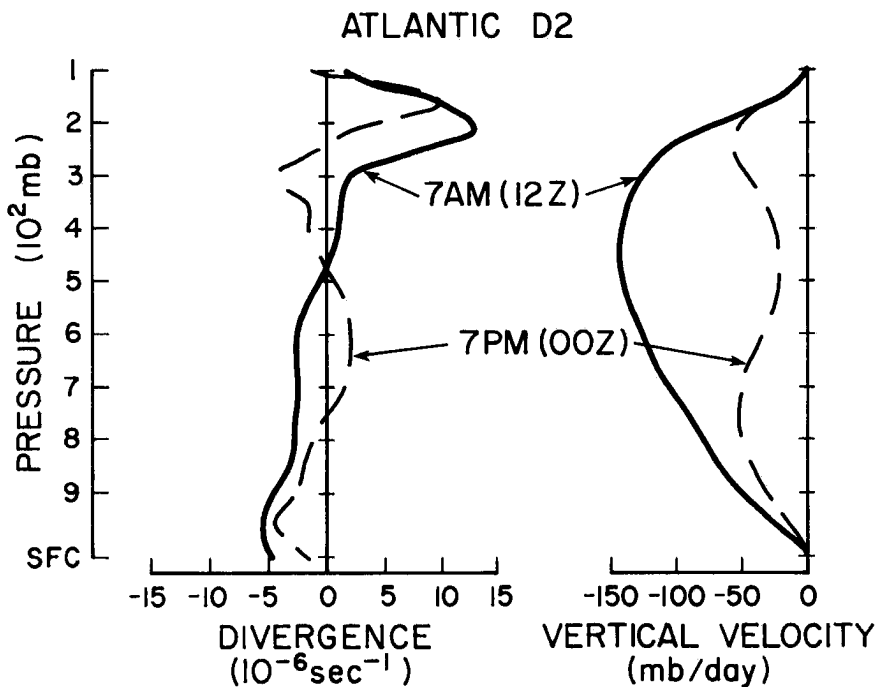


Fig. 9. Morning vs. nighttime profiles of divergence and vertical velocity averaged over the $0-4^{\circ}$ area for the Atlantic D2 pre-hurricane depression data set.

deficiencies in the humidity duct of the radiosondes used by the U.S. Weather Bureau prior to 1972. In those radiosondes airflow through the duct was severely restricted, and solar radiation penetrated the translucent plastic housing and warmed the hygristor to several degrees above the ambient temperature. The warmed hygristor measured the ambient moisture content but at an elevated temperature. It therefore registered a relative humidity lower than that actually present. All daytime measurements of humidity or moisture by radiosonde during that period can therefore not be considered reliable.

Data used in the current study are from radiosonde flights at 00 and 12 GMT. In the West Atlantic this corresponds approximately to 7 PM and 7 AM local time. The sun angle is low at both these times so the measured moisture values are considered reliable.

In the Western Pacific, on the other hand, 00Z is at 10 AM when the sun angle is high. It therefore is subject to moisture measurement errors, and in fact the Pacific data show consistently less moisture at 00Z than at 12Z. All Western Pacific 00Z moisture measurements have therefore been rejected, and all analyses of Pacific moisture shown or used in this study are actually analyses of 12Z or nighttime moisture.

2.4 Dynamic character of the weather systems

In the tropics, the low value of the Coriolis parameter allows the mass fields to adjust fairly rapidly to any perturbations. This effect allows only very weak gradients to exist in any thermodynamic or dynamic properties of the tropical troposphere.

In addition, the compositing procedure naturally acts as a smoothing operator, further diminishing the observed intensity of any existing gradients. Consequently, the analyses in this paper will emphasize differences between different data sets, rather than the absolute values of any parameter. This is satisfactory because the primary tropical cyclone forecast problem is one of distinguishing between systems that develop and those which do not. It is the system parameter differences which are of major interest and not the specific parameter magnitudes.

Some presentation of the dynamic features of the composite systems is nevertheless essential, both for completeness and for background necessary for the interpretation of the results that follow in later chapters.

Table 7 shows the ratio of divergence, to relative vorticity averaged over the $0\text{--}4^\circ$ area at various levels for each composite system. For all except the strongest systems this ratio is of the order of 20% in the low and middle troposphere. This 20% divergent component of the

TABLE 7

Ratio of divergence to relative vorticity averaged over the 0-4° area.

32

	<u>900 mb</u>	<u>700 mb</u>	<u>500 mb</u>	<u>300 mb</u>	<u>200 mb</u>	<u>150 mb</u>
<u>PACIFIC NON-DEVELOPING</u>						
N1 Cloud cluster	-0.4	-0.2	-0.3	-7.0	-1.7	-1.1
<u>PACIFIC DEVELOPING</u>						
D1 Early pretyphoon cloud cluster	-0.2	-0.1	-0.4	2.6	-1.2	-1.2
D2 Pretyphoon cloud cluster	-0.2	-0.2	-0.1	-8.1	-2.0	-1.5
D3 Intensifying cyclone	-0.2	-0.1	-0.1	0.2	-2.4	-1.7
D4 Typhoon	-0.2	-0.03	-0.04	0.1	-20.3	-1.2
<u>ATLANTIC NON-DEVELOPING</u>						
N1 Cloud cluster	0.4	0.1	-0.2	-0.7	-1.5	-1.3
N2 Wave trough cluster	-0.2	-0.1	0.5	-0.1	-0.8	-0.8
N3 Non-developing depression	-0.3	-0.2	0.2	1.7	-3.9	-1.4
<u>ATLANTIC DEVELOPING</u>						
D1 Prehurricane cloud cluster	-0.2	-0.1	-0.04	-0.7	-1.9	-0.7
D2 Prehurricane depression	-0.1	-0.02	0.01	-0.2	-4.6	-1.5
D3 Intensifying cyclone	-0.2	-0.1	-0.1	0.3	-1.5	-0.8
D4 Hurricane	-0.1	-0.05	-0.04	0.1	-2.2	-1.0

flow is very significant, and as shown in Fig. 6e leads to vertical velocities of approximately 150 mb/d. Actually, Table 7 strongly underestimates the divergent or ageostrophic character of the flow. McBride and Gray (1978) demonstrated that cloud clusters possess approximately a 2 to 1 diurnal variation of divergence, but no significant variation in relative vorticity. Such behavior can only be brought about by the divergent component of the wind's response to diurnally varying height gradients. This down-gradient character of the flow may not be accepted by some readers. The claim for it taking place is made here only for the tropics where the Coriolis parameter is small and only over the horizontal scale of a cloud cluster. Its existence under those conditions has been well substantiated by the numerical modelling study of Fingerhut (1978) and by the analytic studies of Paegle (1978) and P. Silva Dias (1979).

McBride and Gray (1978) demonstrated that for Western Pacific summertime cloud clusters a very large component of the lower and middle tropospheric mass convergence or inflow is forced by large scale background ITCZ convergence. In the West Atlantic on the other hand there is actually a small negative contribution from the large scale. It is also of interest to know the contribution to mass inflow from frictional convergence. Table 8 presents statistics on this aspect of the flow, averaged over the 0-4° area. The first column of the table gives the total mass inflow between the surface and the 350 mb level. The next two columns give the measured boundary layer inflow, between the surface and 900 mb, and between the surface and 850 mb respectively. Column (4) gives the contribution to the inflow due to friction, assuming a 100 mb thick boundary layer, and using the formula:

TABLE 8

Observed mass convergence and calculated frictional convergence (C_F) in $\text{gm/cm}^2 \text{d}^{-1}$. Convergence values are averaged over 0-4° radius area.

	(1)	(2)	(3)	(4)	(5)	(6)	(7)
	Observed Convergence sfc to 350 mb	Observed Convergence sfc to 900 mb	Observed Convergence sfc to 850 mb	Frictional Convergence C_F	Observed sfc-900 Observed sfc-350	Observed sfc-850 Observed sfc-350	C_F Observed sfc-350
<u>PACIFIC NON-DEVELOPING</u>							
N1 Cloud cluster	142	30	43	7	.2	.3	.05
<u>PACIFIC DEVELOPING</u>							
D1 Early pretyphoon cloud cluster	235	38	53	19	.2	.2	.1
D2 Pretyphoon cloud cluster	189	52	75	21	.3	.4	.1
D3 Intensifying cyclone	224	79	103	37	.4	.5	.2
D4 Typhoon	241	110	147	55	.5	.6	.2
<u>ATLANTIC NON-DEVELOPING</u>							
N1 Cloud cluster	10	-6	-10	2	--	--	.2
N2 Wave trough cluster	25	8	11	3	.3	.5	.1
N3 Non-developing depression	134	78	103	15	.6	.8	.1
<u>ATLANTIC DEVELOPING</u>							
D1 Prehurricane cloud cluster	133	31	43	15	.2	.3	.1
D2 Prehurricane depression	83	41	53	23	.5	.6	.3
D3 Intensifying cyclone	182	65	87	26	.4	.5	.1
D4 Hurricane	203	96	119	38	.5	.6	.2

The first column is the total observed convergence to 350 mb.

The second column is the observed convergence from the surface to 900 mb.

The third column is the observed convergence from the surface to 850 mb.

The fourth column is the calculated convergence due to frictional veering designated C_F .

The fifth column is the ratio of boundary layer convergence to total convergence: column (2) over column (1).

The sixth column is the ratio of boundary layer convergence to total convergence: column (3) over column (1).

The seventh column is the ratio of boundary layer convergence to total convergence: column (4) over column (1).

$$C_F \approx \frac{1}{10} \bar{\zeta}_T. \quad (2)$$

C_F is the convergence due to frictional turning of the winds, and $\bar{\zeta}_T$ is the vorticity at the top of the boundary layer. This equation is derived in McBride and Gray (1978) and Gray (1979).

Columns (5), (6) and (7) give the ratios of the boundary layer inflow (as gauged by the numbers in columns (2), (3) and (4) respectively) to the total inflow shown in column (1).

The last column of the table clearly shows that frictional convergence is not the dominant mechanism importing mass into the tropical weather system. For the cloud cluster data sets, most of the inward mass transport occurs above 900 mb. For all data sets C_F makes up only 5-20% of the observed total surface to 350 mb mass convergence.

Columns (5) and (6) show that for non-developing systems and in all stages of development for pretyphoon/prehurricane systems, there is a large amount of down pressure gradient flow above the boundary layer. Even in the D4 typhoon and hurricane data sets 50% of the mass inflow at 4° radius occurs above 900 mb.

Another dynamic parameter of interest is the non-linearity of the flow. It has in fact been hypothesized by Shapiro (1977a) that the transition from linear dynamics to non-linear dynamics is the essential factor leading to tropical cyclone genesis. One measure of the non-linear character of the flow is the ratio of the non-linear centrifugal term in the radial equation of motion to the linear Coriolis term. This can be equated to a Rossby number for the system:

Non-linear Character of $= \frac{V_T^2}{fR}$ = Centrifugal Acceleration/Coriolis Acceleration
the Flow

$$\begin{aligned}
 &= \frac{V_T^2}{fV_T} \\
 &= \frac{V_T}{fR} \\
 &= \text{Rossby Number, Ro.}
 \end{aligned} \tag{3}$$

f is the Coriolis parameter. R is the radius or distance from the system center. V_T is the tangential component of the wind.

The value of this parameter at 4° radius for each system is tabulated in Table 9. In the lower troposphere, values are consistently lower for non-developing systems than for the corresponding developing systems. At 900, 700, 500 mb all non-developing systems have $\text{Ro} \leq 0.2$, while developing systems have $\text{Ro} \geq 0.2$. As the system intensifies through the D1 to D4 stage, it moves north. f increases. This counteracts the increase in V_T , so that the Rossby number doesn't increase much.

2.5 Gray's climatological parameter

Gray (1975, 1979) in climatological studies of tropical cyclone genesis has demonstrated that the seasonal and geographical incidence of tropical cyclones is directly related to the seasonal and geographical distribution of the Seasonal Genesis Parameter (SGP).

TABLE 9

Rossby number, $V_T/f R$, for each composite system at 4° latitude radius.

	<u>900 mb</u>	<u>700 mb</u>	<u>500 mb</u>	<u>300 mb</u>	<u>200 mb</u>	<u>150 mb</u>
<u>PACIFIC NON-DEVELOPING</u>						
N1 Cloud cluster	0.14	0.16	0.16	-0.01	-0.16	-0.13
<u>PACIFIC DEVELOPING</u>						
D1 Early pretyphoon cloud cluster	0.40	0.38	0.37	0.02	-0.32	-0.28
D2 Pretyphoon cloud cluster	0.46	0.40	0.27	-0.01	-0.15	-0.18
D3 Intensifying cyclone	0.61	0.57	0.44	0.21	-0.10	-0.19
D4 Typhoon	0.58	0.56	0.46	0.23	-0.01	-0.18
<u>ATLANTIC NON-DEVELOPING</u>						
N1 Cloud cluster	0.02	0.06	0.06	0.01	-0.01	-0.01
N2 Wave trough cluster	0.05	0.04	-0.01	-0.02	-0.03	-0.04
N3 Non-developing depression	0.16	0.13	0.09	0.02	-0.03	-0.05
<u>ATLANTIC DEVELOPING</u>						
D1 Prehurricane cloud cluster	0.19	0.20	0.14	0.02	-0.08	-0.16
D2 Prehurricane depression	0.26	0.24	0.20	0.07	-0.02	-0.06
D3 Intensifying cyclone	0.27	0.26	0.21	0.07	-0.12	-0.16
D4 Hurricane	0.38	0.38	0.32	0.12	-0.07	-0.18

He defined this parameter to be:

$$SG = \begin{pmatrix} \text{Seasonal} \\ \text{Genesis} \\ \text{Parameter} \end{pmatrix} = \left[\begin{pmatrix} \text{Vorticity} \\ \text{Parameter} \end{pmatrix} \begin{pmatrix} \text{Coriolis} \\ \text{Parameter} \end{pmatrix} \begin{pmatrix} \text{Vertical} \\ \text{Shear} \\ \text{Parameter} \end{pmatrix} \times \right. \\ \left. \begin{pmatrix} \text{Ocean} \\ \text{Energy} \\ \text{Parameter} \end{pmatrix} \begin{pmatrix} \text{Moist} \\ \text{Stability} \\ \text{Parameter} \end{pmatrix} \begin{pmatrix} \text{Humidity} \\ \text{Parameter} \end{pmatrix} \right] \quad (4)$$

where

$(\text{Vorticity Parameter}) = \text{relative vorticity } + 5$, where 900 mb level relative vorticity is measured in units of 10^{-6} sec^{-1} .

$(\text{Coriolis Parameter}) = f \text{ or } 2\Omega \sin\phi$, where Ω is the rotation rate of the earth and ϕ denotes latitude. Units are sec^{-1} .

$(\text{Vertical Shear Parameter}) = 1/(S_z + 3)$ where $S_z = |\partial \nabla / \partial p|$ between 900 mb and 200 mb, determined in units of m/sec per 700 mb.

$(\text{Ocean Energy Parameter})$, E = the ocean thermal energy above 26°C down to a depth of 60 meters or

$$\text{E} = \int_{\text{Sfc}}^{60\text{m or where } T=26^{\circ}\text{C}} \rho_w C_w (T-26) dz \quad (5)$$

where ρ_w is ocean density (1 gm/cm^3)

C_w is the specific heat of water ($1 \text{ cal/gm - } ^{\circ}\text{C}$)

T is ocean temperature in $^{\circ}\text{C}$

E is measured in units of $10^3 \text{ cal/cm}^2 (.42 \text{ J/m}^2)$.

$(\text{Moist Stability Parameter}) = \partial h / \partial p + 5$ where h is moist static energy and $\partial h / \partial p$ between the surface and 500 mb is expressed in units of $^{\circ}\text{K}$ per 510 mb.

(Humidity
Parameter)

= $(\overline{RH} - 40) / 30$ where \overline{RH} is the mean relative humidity between 500 and 700 mb. Parameter is zero for $\overline{RH} < 40$, and 1 for $\overline{RH} \geq 70$.

Various tropical cyclone forecast offices in recent years have been using the SGP as a guide in forecasting storm development on a daily basis. The rationale for this is the assumption that statistical fluctuations of Genesis Potential above the seasonal value must put the potential above some threshold genesis potential necessary for storm development. To evaluate this hypothesis values of SGP averaged over the $0-3^{\circ}$ area have been calculated for each composite system (Table 10). All parameters have been calculated for each system from the composite output, except the ocean energy parameter, E. For this parameter climatological values have been used as a function of mean position of that data set, the actual values being taken from the mean graphs for July-September presented by Gray (1975, 1979).

The resultant value of SGP is given in the last column of the table. There is quite a large difference in both oceans between the values for developing versus non-developing data sets. The Pacific non-developing cloud cluster N1 has a value of 6, while the developing clusters D1, D2 have values around 30. The Atlantic non-developing clusters N1, N2 have the values 1 and 2, while the corresponding developing system D1 has the value 12. For the Atlantic depression data sets, the non-developing system N3 has the value 18, while the developing system D2 has a value more than twice as large, 38.

For the thermal parameters, E, $\partial h / \partial p$ and \overline{RH} , there is virtually no difference between developing and non-developing systems. There are some slight differences in the vertical shear parameter, but the big

TABLE 10

Seasonal Genesis Parameter (SGP) for the composite data sets. The first six columns give the component parameters. The product of these equals SGP, which is listed in the last column.

	Vorticity Parameter 10^{-6} s^{-1}	Coriolis Parameter 10^{-5} s^{-1}	Vertical Shear Parameter $\frac{700\text{mb}}{\text{s m}}$	Ocean Energy Para- meter $\frac{10^3\text{cal}}{\text{cm}^2}$	Moist Stability Parameter $^{\circ}\text{K}/510\text{mb}$	Humidity Parameter	SGP $\times 1.37 \times 10^{-8}$ $\text{cal}^{\circ}\text{K s}^{-1}$ cm^{-3}
<u>PACIFIC NON-DEVELOPING</u>							
N1 Cloud cluster	9.7	2.75	.107	18	12.0	1.0	6
<u>PACIFIC DEVELOPING</u>							
D1 Early pretyphoon cloud cluster	30.9	2.76	.189	18	11.8	1.0	34
D2 Pretyphoon cloud cluster	28.5	2.57	.182	18	11.3	1.0	27
D3 Intensifying cyclone	59.9	3.40	.138	16	11.7	1.0	53
D4 Typhoon	95.7	5.39	.197	12	8.9	1.0	108
<u>ATLANTIC NON-DEVELOPING</u>							
N1 Cloud cluster	2.0	4.99	.082	10	13.3	0.94	1
N2 Wave trough cluster	7.0	3.95	.063	12	15.3	0.68	2
N3 Non-developing depression	24.2	5.11	.121	10	13.5	0.89	18
<u>ATLANTIC DEVELOPING</u>							
D1 Prehurricane cloud cluster	23.5	4.44	.090	10	13.6	0.93	12
D2 Prehurricane depression	39.4	5.15	.162	10	12.5	0.92	38
D3 Intensifying cyclone	48.2	5.44	.108	10	12.4	0.99	35
D4 Hurricane	72.6	5.68	.117	10	10.8	1.00	52

differences are found in the low level relative vorticity, column (1).

Between the two oceans, the Coriolis parameter, f , is larger where genesis occurs in the Atlantic. This is mainly counteracted by a larger oceanic energy parameter, E , in the Pacific.

Overall, Table 10 shows that besides explaining the seasonal and geographical occurrence of tropical storms, SGP contains much of the information necessary for the day by day prediction of storm genesis. In particular all composite developing systems have values of SGP more than twice as large as their non-developing counterparts.

The Seasonal Genesis Parameter may also be thought of in the form of:

$$\begin{pmatrix} \text{Seasonal} \\ \text{Genesis} \\ \text{Parameter} \end{pmatrix} = (\text{Dynamic Potential}) \times (\text{Thermal Potential})$$

where

(6)

$$\text{Dynamic Potential} = (f) (\zeta_r + 5) [1 / (S_z + 3)]$$

$$\text{Thermal Potential} = (E) (\partial h / \partial p + 5) (\overline{RH} \text{ Parameter})$$

Table 11 shows the dynamic and thermal components of the Seasonal Genesis Parameter. There is no difference in Thermal Potential between developing and non-developing weather systems. The large differences that exist in SGP are all forced by differences in Dynamic Potential. This implies that the role of thermodynamic parameters in cyclone genesis is more a climatological one. The Thermal Potential is the potential for Cb convection. Tropical cyclones cannot form unless it has a large value, but its value is a function of geographical location and time of year and does not vary much on a day to day basis.

The dynamic parameters on the other hand have a large day to day

TABLE 11

Dynamic and thermodynamic components of SGP for the composite data sets.

	Dynamic Potential	Thermal Potential
	$\frac{700 \text{ mb} \cdot 10^{-11}}{\text{m-s}}$	$\frac{10^3 \text{ cal} \text{ } ^\circ\text{K}}{510 \text{ mb cm}^2}$
<u>PACIFIC NON-DEVELOPING</u>		
N1 Cloud cluster	2.9	216
<u>PACIFIC DEVELOPING</u>		
D1 Early pretyphoon cloud cluster	16.1	212
D2 Pretyphoon cloud cluster	13.3	203
D3 Intensifying cyclone	28.1	187
D4 Typhoon	101.6	107
<u>ATLANTIC NON-DEVELOPING</u>		
N1 Cloud cluster	0.8	125
N2 Wave trough cluster	1.7	125
N3 Non-developing depression	15.0	120
<u>ATLANTIC DEVELOPING</u>		
D1 Prehurricane cloud cluster	9.4	126
D2 Prehurricane depression	32.9	115
D3 Intensifying cyclone	28.3	123
D4 Hurricane	48.2	108

variation, and this shows up in the large differences in Dynamic Potential that exist between developing versus non-developing composite data sets.

2.6 Contribution from surface evaporation

Since the oceanic energy parameter, E, in the Western Pacific is much larger than in the Western Atlantic, one would expect the Pacific systems to enjoy a greater surface energy input through the surface sensible and latent heat fluxes. That this is so can be shown by the following simple calculation.

McBride and Gray (1978) performed background long-term-mean composites for the Northern Hemisphere summer in the Western Pacific and Western Atlantic. Their resultant background profiles of vertical motion are shown in Fig. 10. Background mean profiles of moist static energy, h , for each region were obtained by taking the mean value over the 3 to 9° area around data set N1 and N2 in the Atlantic and around data set N1 in the Pacific. These mean h profiles multiplied by the background vertical motion profiles of Fig. 10 yield a value for each region of the long-term mean export of h due to horizontal divergence, that is a value of $\int_{Sfc}^{100mb} \nabla \cdot \nabla h \frac{dp}{g}$. Converting to heating rate units, by dividing by the specific heat over the mass of the atmosphere, the results are a loss of $0.95^{\circ}\text{C}/\text{d}$ in the West Pacific and a loss of $0.05^{\circ}\text{C}/\text{d}$ in the West Atlantic.

The main sink of h in the troposphere is radiative cooling. Dopplick (1974) performed radiative transfer calculations for the earth's atmosphere using zonally averaged temperatures, water vapour and ozone concentrations and cloud amounts. Averaging his results for the period June — November, the following net radiative cooling rates are obtained for the 1000-100 mb tropospheric layer: $1.18^{\circ}\text{C}/\text{d}$ at the equator, $1.19^{\circ}\text{C}/\text{d}$ at 10°N , $1.19^{\circ}\text{C}/\text{d}$ at 20°N . The results of Bignell (1970) and Cox (1973) indicate that Dopplick's cooling rates (originally calculated in 1970) are probably an underestimate, due to the fact that he did not take into account the effect of the water vapor pressure dependent continuum absorption in the $8-12\mu\text{m}$ region. The mean background net radiative cooling for both regions, Western Pacific and Western Atlantic, will thus be taken to be $1.25^{\circ}\text{C}/\text{d}$.

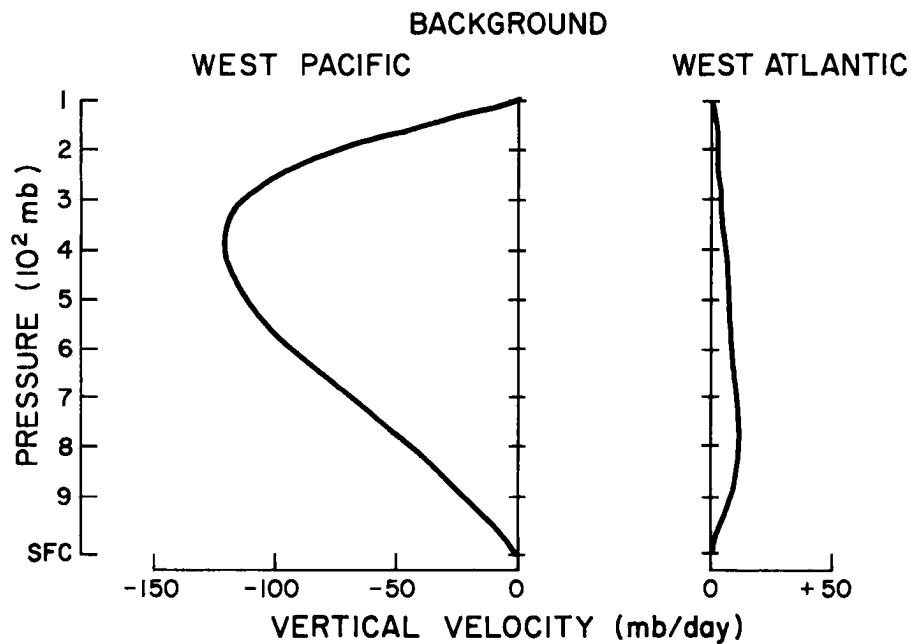


Fig. 10. Vertical velocity for the background or long-term mean composites (from McBride and Gray, 1978).

These two sinks of $\int \nabla \cdot \nabla h dp$ and radiative cooling, are balanced by the surface eddy flux. There must therefore be a surface flux large enough to heat the troposphere by $2.2^{\circ}\text{C}/\text{d}$ in the West Pacific and by $1.3^{\circ}\text{C}/\text{d}$ in the West Atlantic. Assuming a Bowen ratio of .1, this implies a surface evaporation rate of $0.75 \text{ gm/cm}^2 \text{ d}^{-1}$ in the Western Pacific and of $0.44 \text{ gm/cm}^2 \text{ d}^{-1}$ in the Western Atlantic.

3. COMPARISON: NON-DEVELOPING VS. DEVELOPING SYSTEMS

3.1 Pacific cluster: N1 vs. D1, D2

The Pacific N1 non-developing cloud cluster and the Pacific D2 pretyphoon cloud cluster were originally composited and analyzed by Zehr (1976). These two data sets include a similar number of observations and were used by Zehr to define the differences in structure between a system which would later develop into a typhoon and one which would not. Zehr found a number of differences between the two composite systems. A study of this type is subject, however, to the criticism that the findings may be symptomatic of the fact that development has already begun to take place in the pretyphoon systems. In other words the differences could be described as the differences between a non-developing cluster and a weak tropical cyclone, rather than between a non-developing and a developing cluster. To avoid this difficulty, the current study includes also an analysis of the pretyphoon data set composited by S. Erickson (1977). This data set (Pacific D1 early pretyphoon cloud cluster) is very much smaller than the others in terms of number of rawinsonde observations involved; but it consists of the very first one to two days existence of the pretyphoon system as observed by visual and infrared DMSP satellite imagery. Because of the greater amount of noise present in the smaller D1 data set, the main comparison made here will be between D2 and N1. The D1 data set will be referred to in order to show that the differences found are pertinent to the very beginning of the cluster's existence.

Figure 11 shows the vertical profiles of temperature anomaly (T_{0-3}° minus $T_{\text{east-west}, 3-7}^{\circ}$). The developing system has a better defined upper level warm core than does the non-developing; but the

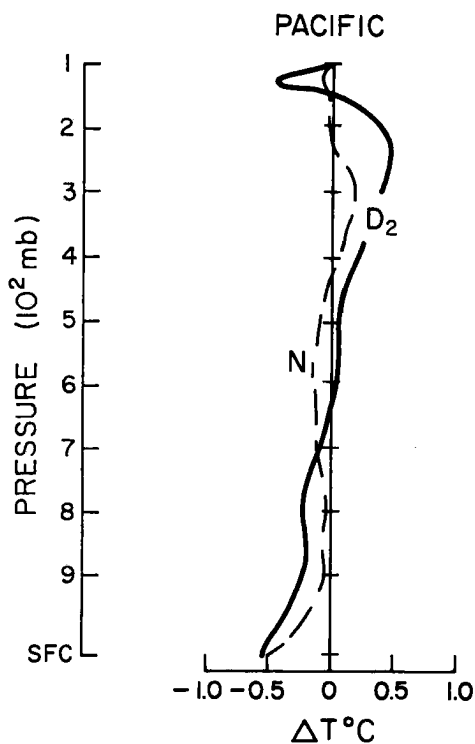


Fig. 11. Cluster minus environment vertical temperature profiles for the Pacific developing (D2) and non-developing (N1) cloud clusters. $T_{\text{cluster}} = T_{0-3^\circ}$; $T_{\text{environment}} = T_{\text{east-west}, 3-7^\circ}$.

gradients are small. Plan views of the temperature at 300 mb are shown in Fig. 12. A warm core can be seen for all three systems, but it is more distinct and of greater magnitude in the two developing systems. There are several features which should be noted in Fig. 12:

- (i) The warm "core" at 300 mb extends over a very large area. (The grid points along each radial arm are 2 degrees latitude or 222 km. apart).
- (ii) The warm core is distinct and obvious on the composite analyses for the developing systems; but in an individual atmospheric system it would be very hard to measure, being of the order of 1°C difference in temperature over several hundred kilometers.
- (iii) For all systems the temperature perturbation is quite symmetric. The only asymmetry seen is associated with the cold temperatures at the higher latitudes to the north.
- (iv) Besides having a greater temperature gradient the developing system also has a higher absolute value of temperature at

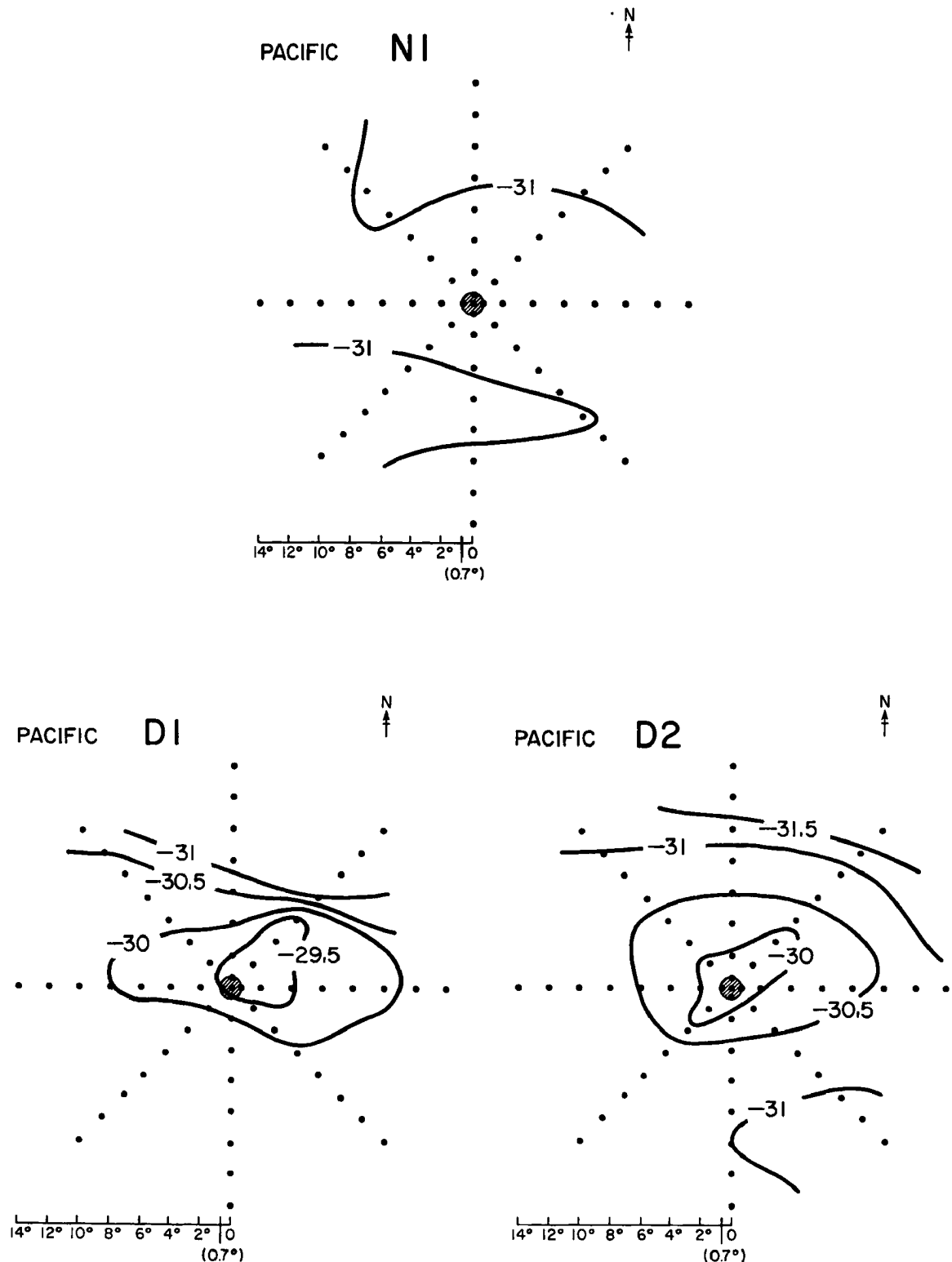


Fig. 12. Plan views of 300 mb temperature in $^{\circ}\text{C}$ for the Pacific N1 non-developing cloud cluster and for the developing (D1, D2) cloud clusters.

300 mb. The whole region out to 8° latitude in all directions around the developing cloud cluster is warmer than that around the non-developing cloud cluster.

Hydrostatically, the vertical integral of the differences in temperature between developing and non-developing systems is equivalent to a difference in low level pressure. Figure 13 shows plan views of the height of the 900 mb pressure level. There is a very obvious difference between developing and non-developing systems, the developing have a distinct area of low height or low pressure centered on the system. The 900 mb heights near the center of the developing cluster are approximately 1002 meters as compared with 1012 around the non-developing cluster. Converted to a difference in surface pressure this relates to only 1 mb. Thus, even though the differences in vertically integrated temperature show up clearly on composite analyses, they are of too small a magnitude to be useful in distinguishing between developing and non-developing disturbances in the individual cases.

The vertical lapse rate stabilities are very similar in the developing and non-developing systems; in fact, the greater middle level temperature in the developing case means that it actually has less potential buoyancy as measured by the vertical gradient of moist static energy h^* (Fig. 14).

Figure 15 shows vertical profiles of mixing ratio of water vapor for the cluster ($0-3^{\circ}$) minus its surroundings ($3-5^{\circ}$). The magnitude of the moisture anomaly is very similar in both systems, as is the absolute value of the moisture content. The precipitable water averaged over the $0-6^{\circ}$ area is 5.7 gm/cm^2 for the developing system (D2), and 5.6 gm/cm^2 for the non-developing system (N1).

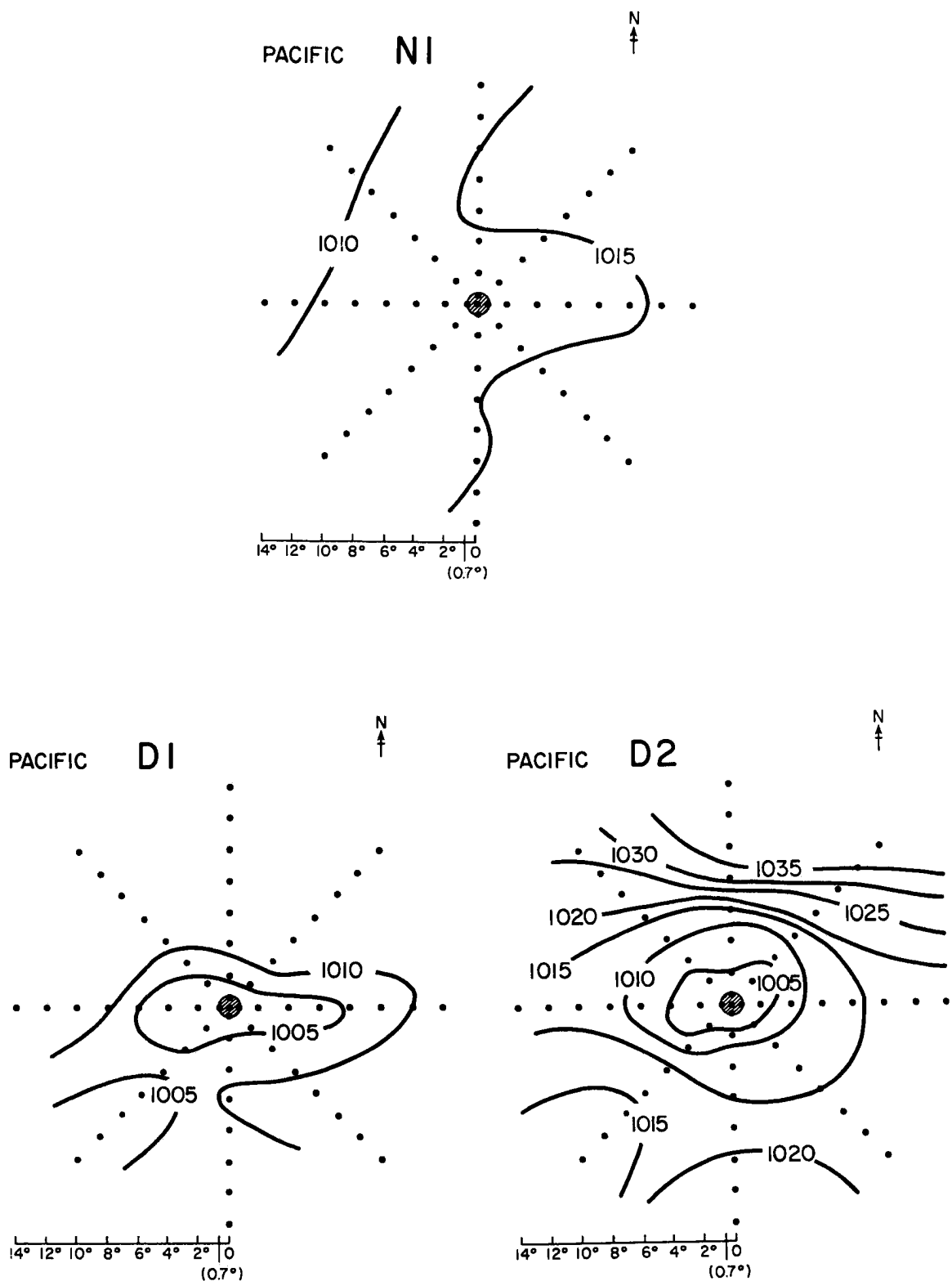


Fig. 13. Plan views of 900 mb heights in meters for Pacific N1 non-developing cloud cluster and for the developing (D1, D2) cloud clusters.

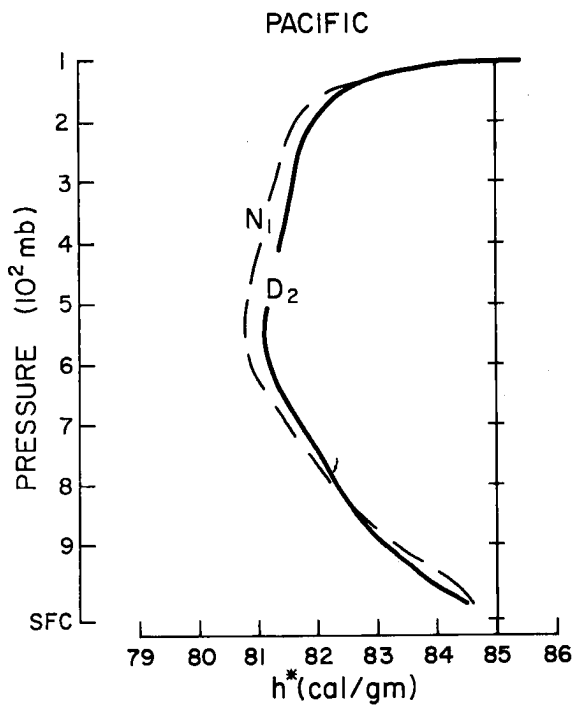


Fig. 14. Saturated moist static energy averaged over the 0-3° area for the Pacific N1 non-developing cloud cluster and D2 pretyphoon cloud cluster.

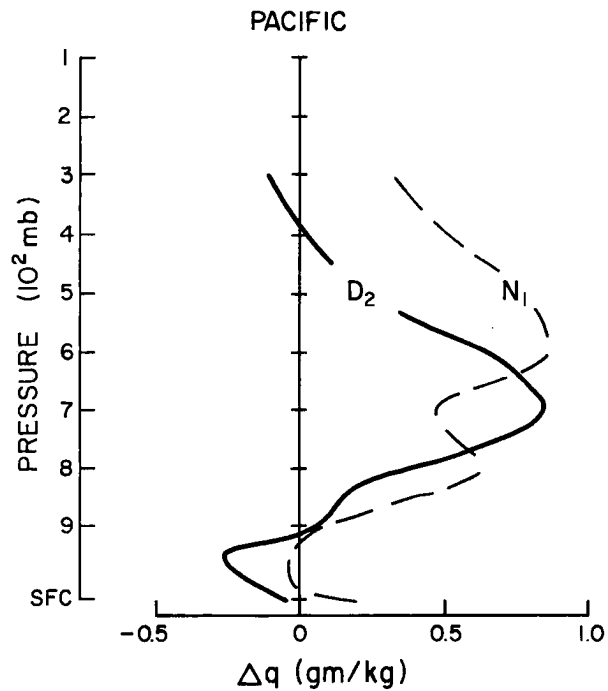


Fig. 15. Vertical profiles of mixing ratio of water vapor for the cluster (0-3°) minus its surroundings (3-5°) for the Pacific N1 and D2 systems.

Turning now to the wind or dynamic fields, the lower level (900 mb) and upper level (200 mb) flow patterns are shown in Figs. 16 and 17.

At 900 mb both developing and non-developing clusters have easterly trade wind flow to the north and westerly monsoon flow from the south. An area of convergence centered on the system can be seen in all cases. The main difference between the flow patterns is the magnitude of the wind, the composite developing systems having significantly stronger easterlies to their north.

One must be careful not to interpret Fig. 16 as implying that the developing systems have that much stronger low level winds. They do not. Table 5 (page 16) shows that averaged over the $0-4^{\circ}$ area the mean wind speed at 950 mb is 7 m/s in the D2 system and 6.5 m/s in the N1 system. The large difference in wind speed that shows up on the plan view in Fig. 16 is really a reflection of the difference in organization of the systems. Thus, the many rawinsonde observations going into each grid point in the non-developing case were highly variable in direction and yield a low magnitude mean vector wind. In the developing case, there was not much variability and the resultant vector mean had a high magnitude.

At 200 mb (Fig. 17) there is also a large difference between the developing and non-developing composite fields. The developing clusters have an anticyclone displaced about 3° latitude to the east of the system, whereas the non-developing cluster has no anticyclone.

Vertical profiles of the radial component of the wind at 4° radius and of the kinematically calculated vertical velocity averaged over the $0-4^{\circ}$ area are shown in Fig. 18. The developing systems have thirty

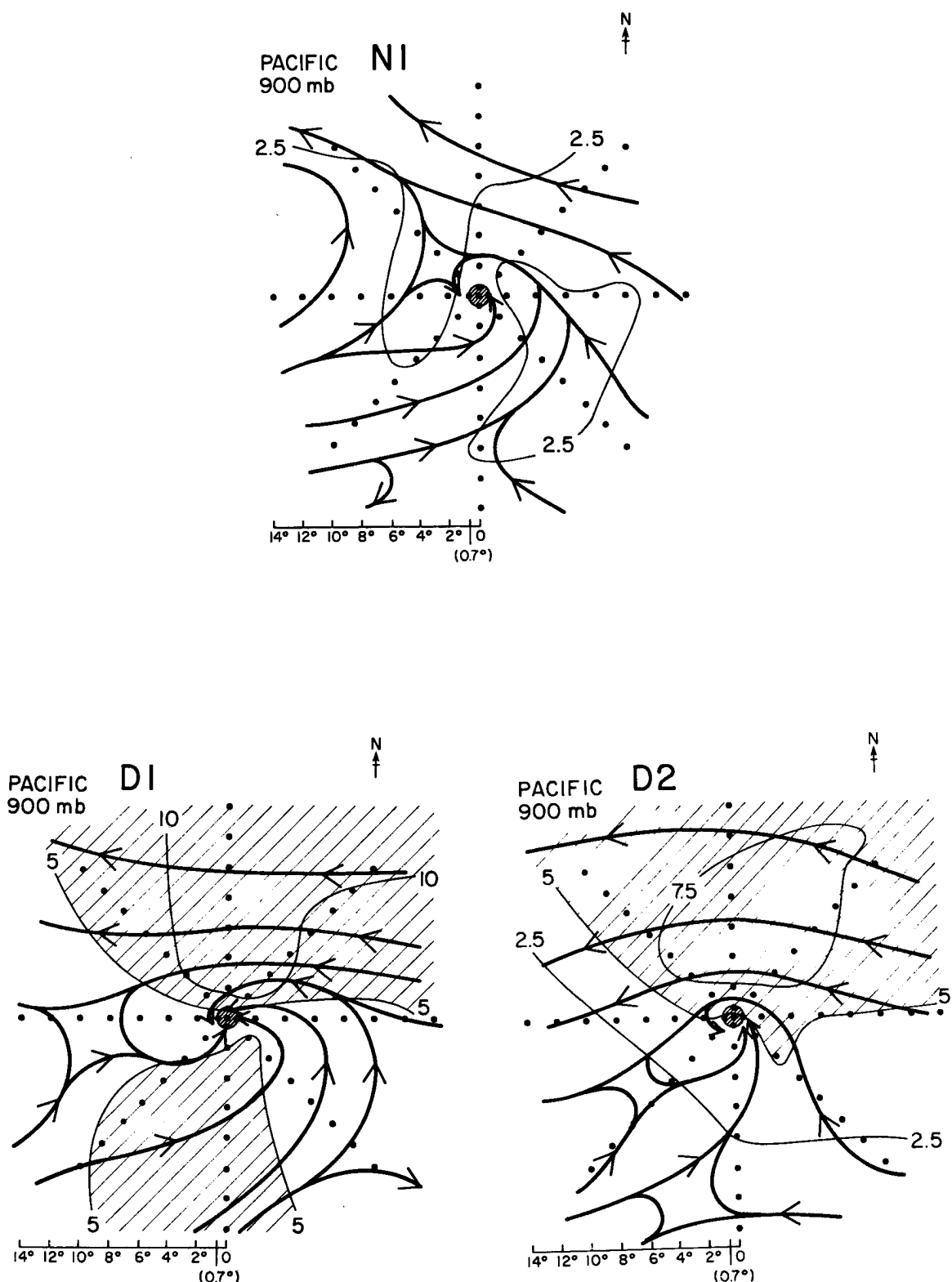


Fig. 16. 900 mb streamline and isotach analyses (m s^{-1}) for the Pacific non-developing (N1) and pre-typhoon (D1, D2) cloud clusters.

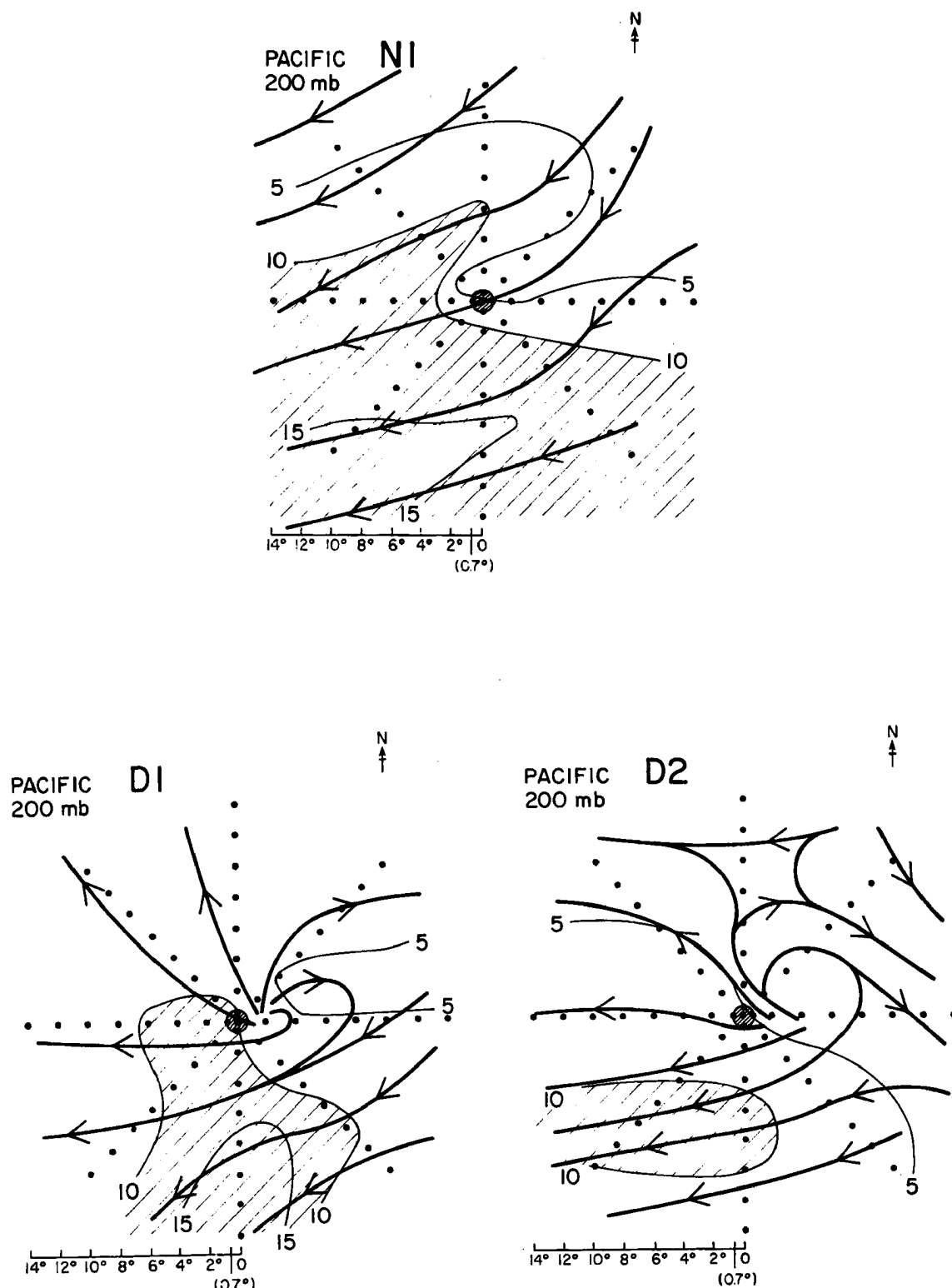


Fig. 17. 200 mb streamline and isotach analyses (m s^{-1}) for the Pacific non-developing (N1) and pre-typhoon (D1, D2) cloud clusters.

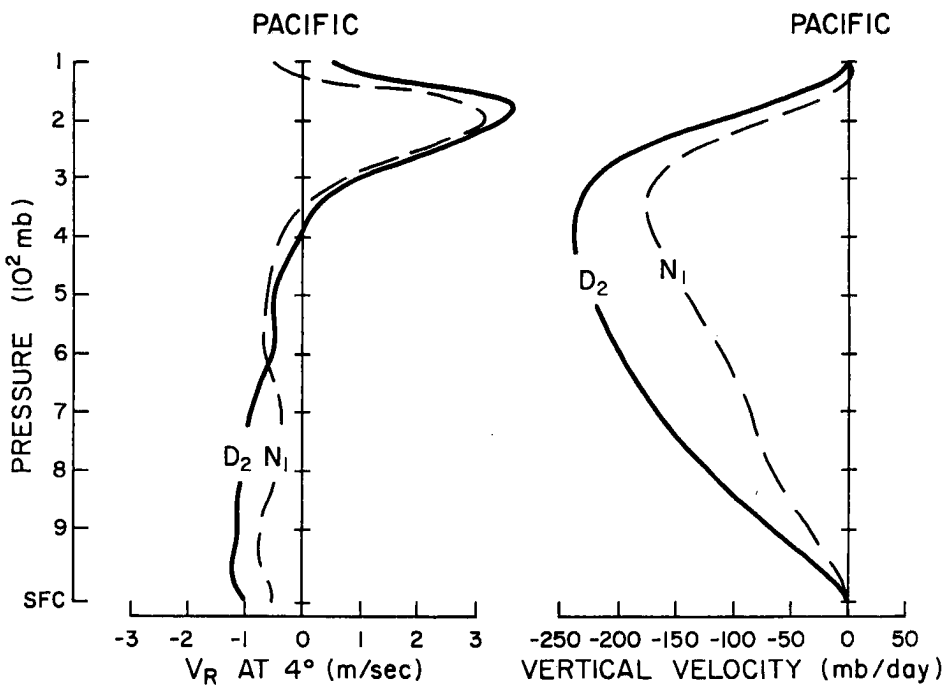


Fig. 18. Radial wind at 4° and vertical velocity averaged over the $0-4^{\circ}$ area for Pacific developing and non-developing cloud clusters.

percent more mass inflow and therefore greater upward vertical velocity than the non-developing systems.

Figure 19 shows symmetric vertical cross-sections of the tangential component of the wind. This field shows by far the most striking difference between the developing and non-developing systems, and as later discussion will show, also the most physically significant difference. The developing clusters are characterized by very large values of positive tangential wind, more than twice as large as the tangential wind in the non-developing clusters. There are several other aspects of the fields shown in Fig. 19 which are worthy of discussion:

- (i) The radius of maximum tangential wind is approximately 4° latitude or 444 km. This is a fundamental difference between the cloud cluster and the fully developed tropical storm which has its radius of maximum wind at approximately 35 km from the center.

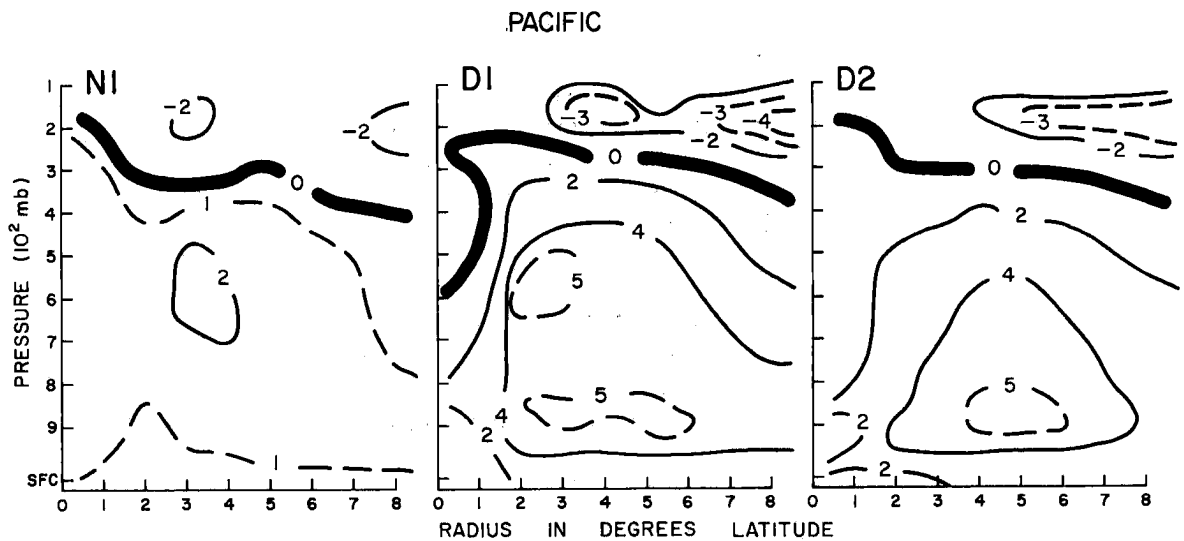


Fig. 19. 2-dimensional cross-section of V_T for the Pacific non-developing (N1) and pre-typhoon (D1, D2) cloud clusters.

- (ii) The very large difference that exists in tangential wind between developing and non-developing systems extends out to 8° radius. Since the relative vorticity averaged over a $0-R^\circ$ area is equal to $2V_T/R$, the developing system exists in a very large horizontal extent (at least an 8° latitude radius circle) of large positive relative vorticity. The vorticity averaged over this area is three times as large as that over the same area surrounding the non-growing system.
- (iii) The negative tangential wind observable at large radius in the upper troposphere for all systems is a reflection of the strong equatorial easterly winds to the south of all systems, which can be seen on the plan views in Fig. 17.
- (iv) The non-developing cloud cluster has its maximum value of V_T at approximately 600 mb. By thermal wind considerations this implies that the system is cold core below that level. As shown earlier, horizontal temperature gradients are very weak and hard to measure; so this consideration of the vertical variation of tangential wind is actually the most reliable indicator of the sign of the temperature anomaly. Of the developing systems, D2 has a clear low level wind maximum, and therefore a warm core all the way down to 900 mb. This may be symptomatic of the fact that development has already begun, since the D1 system has a very ambiguous temperature structure, with no clear temperature gradient being implied at all below the 500 mb level. Many authors in the past (e.g. Riehl, 1948; Yanai, 1961) have discussed the transition from a cold core to a warm core system as an important indicator of the potential of a system for development into a tropical storm. It has been shown here, and in earlier reports by Williams and Gray (1973), Ruprecht and Gray (1976a, b), Zehr (1976), S. Erickson (1977) that all

these systems are warm core in the upper levels, and therefore direct circulation. In the lower atmosphere the current observations reveal that if a transition does take place from cold core to warm core, it happens very early, at about the D1 stage. This is two to three days prior to the beginning of the JTWC Guam official best track for the system, which in turn is several days before the system develops into a tropical storm. This could have some operational potential as a predictor of tropical cyclone development: if the tangential component of the wind averaged around the circumference of a 3° latitude radius circle centered on the system is greater at 900 mb than it is at 500 mb, the system is much more likely to develop.

In summary, the comparison of Western Pacific non-developing versus developing cloud clusters yields the following results:

- 1) Both systems are warm cored in the upper levels. The warm area at 300 mb is much more pronounced in the developing system; following this the low level height anomaly is also much more pronounced. The actual magnitudes, however, of the temperature and height gradients are so small that they would be extremely difficult to measure for an individual system.
- 2) The developing or pretyphoon cloud cluster exists in a generally warmer atmosphere over a large horizontal scale, for example out to 8° latitude radius in all directions.
- 3) There is no obvious difference in vertical stability for moist convection between the systems.
- 4) The moisture anomaly and moisture content are similar for the developing and non-developing systems.
- 5) The composite fields yield a thirty percent greater upward vertical velocity for the developing system.
- 6) The developing system has an upper level anticyclone, while the non-developing does not.
- 7) The developing system exists in a very large area of low level positive tangential wind or positive relative vorticity. This is to some extent resultant from persistent low level easterlies to the north of the system.

Very similar results to the above were obtained by Zehr (1976).

One other difference that he pointed out was that the developing D2 cluster had a slower speed of movement than the non-developing N1.

Physically, this may be of some importance, but it is not a consistent

feature. Referring to Table 6, it is seen that the D1 system has the same speed of movement as the N1, and that in the Atlantic data sets there is no consistent difference in speed of movement between developing and non-developing systems.

3.2 Atlantic cloud clusters: N1, N2 vs. D1

In the West Atlantic Ocean, two non-developing cloud cluster data sets, N1 and N2, are available, and one developing, D1.

Vertical profiles of temperature anomaly, $T_{\text{cluster}} - T_{\text{environment}}$, for these systems are shown in Fig. 20. As has been discussed, data problems make these figures hard to interpret, but the most clearly defined upper level warm core is actually in the non-developing N1 data set. Looking at the larger scale, the plan views of 300 mb level temperature (Fig. 21) show only a slight hint of a warm core in the wave trough cluster N2 but a clearly defined warm core for both the non-developing N1 and the developing D1 systems. The effect of the temperature differences integrated through the troposphere shows up in the plan view of 900 mb level height (Fig. 22). The developing system is the only one with a clear low pressure center, but as in the Pacific the differences are very small and hard to measure. (A ten meter difference on Fig. 22 translates to only a one mb difference at the surface.)

An interesting feature of Fig. 22 is that all the Atlantic cluster systems exist in the middle of a region of strong north-south low level height gradient. Hydrostatically, this means that the region is one of a large north-south gradient of mean tropospheric temperature; by thermal wind considerations this is in agreement with the change in the mean wind across the grid from easterlies at 900 mb to westerlies at

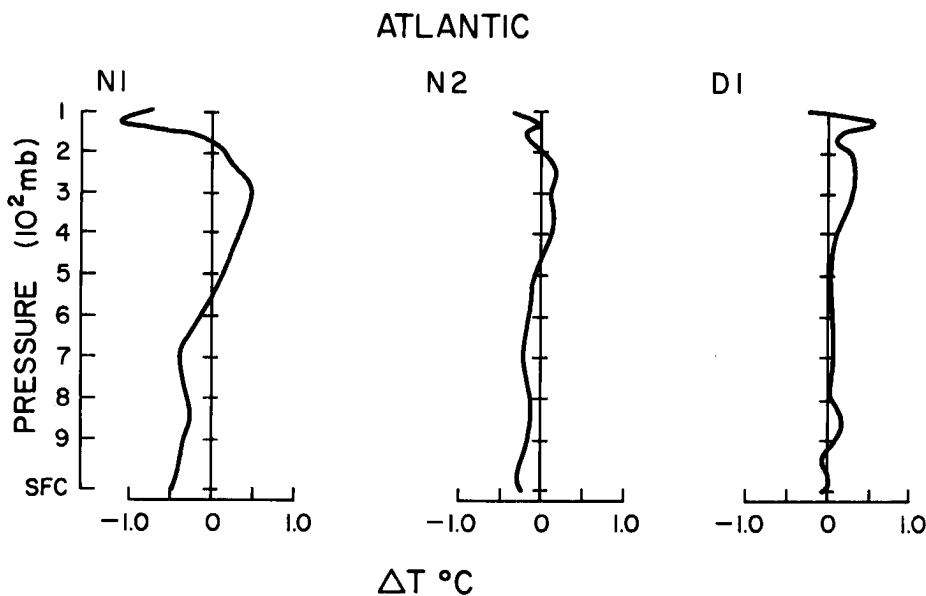


Fig. 20. Cluster minus environment vertical temperature profiles for the Atlantic non-developing (N1, N2) and pre-hurricane (D1) cloud clusters. $T_{\text{cluster}} = T_{0-3}^{\circ}$; $T_{\text{environment}} = T_{\text{east-west}, 3-7}^{\circ}$.

200 mb. Referring back to the 900 mb level heights for Pacific clusters in Fig. 13, there is no strong north-south height gradient. Correspondingly the cloud clusters in that region exist in easterlies at both lower and upper levels.

As in the Pacific the vertical velocity, horizontal gradient of moisture and total moisture content are very similar for developing and non-developing systems. The moisture anomalies are shown in Fig. 23. The total moisture contents over the $0-6^{\circ}$ area are 5.0 gm/cm^2 for the developing case D1 versus 4.9 and 4.8 gm/cm^2 for N1, N2.

The biggest difference that showed up in the Pacific between developing and non-developing clusters was in the tangential component of the wind, V_T . Vertical profiles of V_T at 2, 4 and 6° radius are shown in Fig. 24. The developing cluster has much greater positive

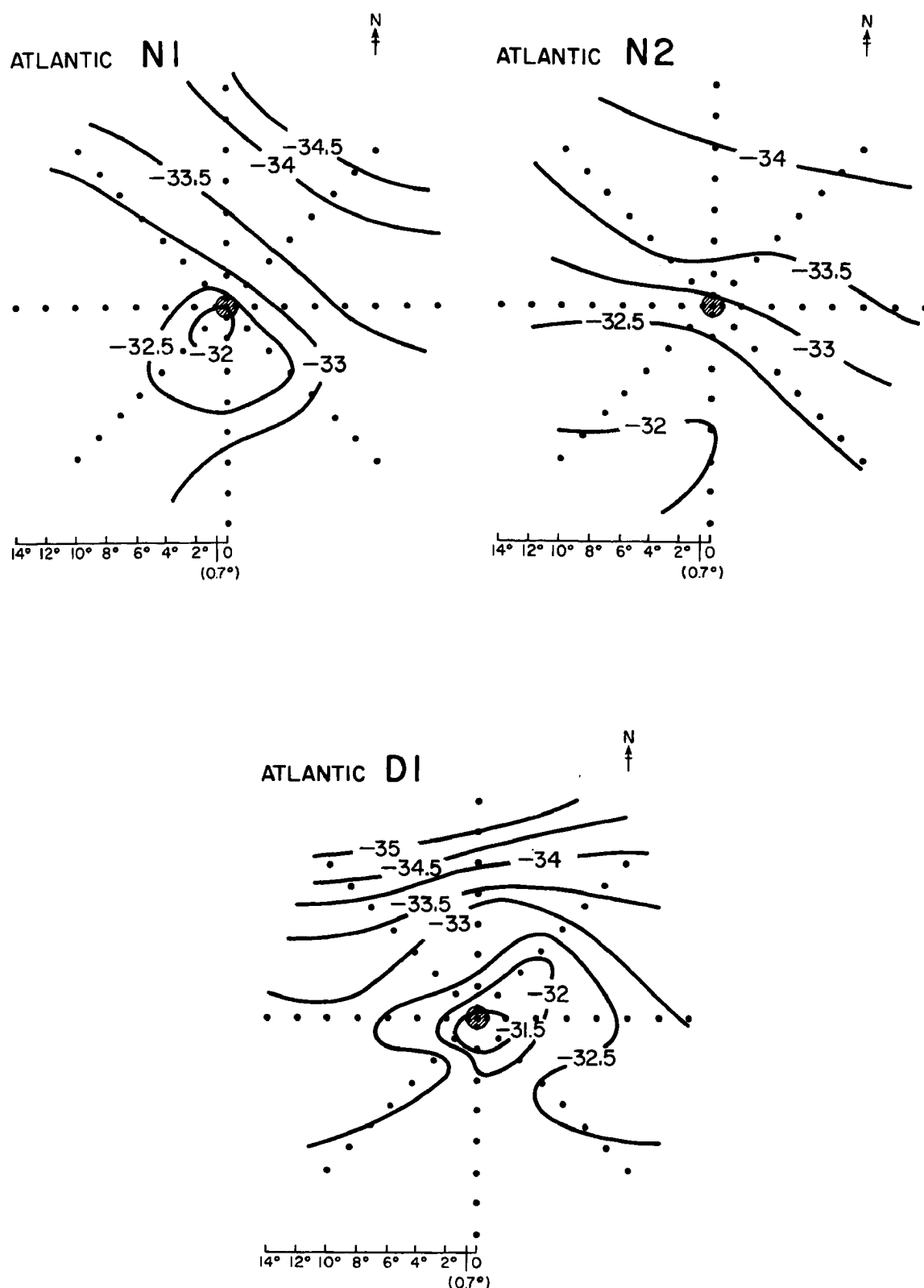


Fig. 21. Plan views of 300 mb temperature in $^{\circ}\text{C}$ for Atlantic non-developing (N1, N2) and developing (D1) cloud clusters.

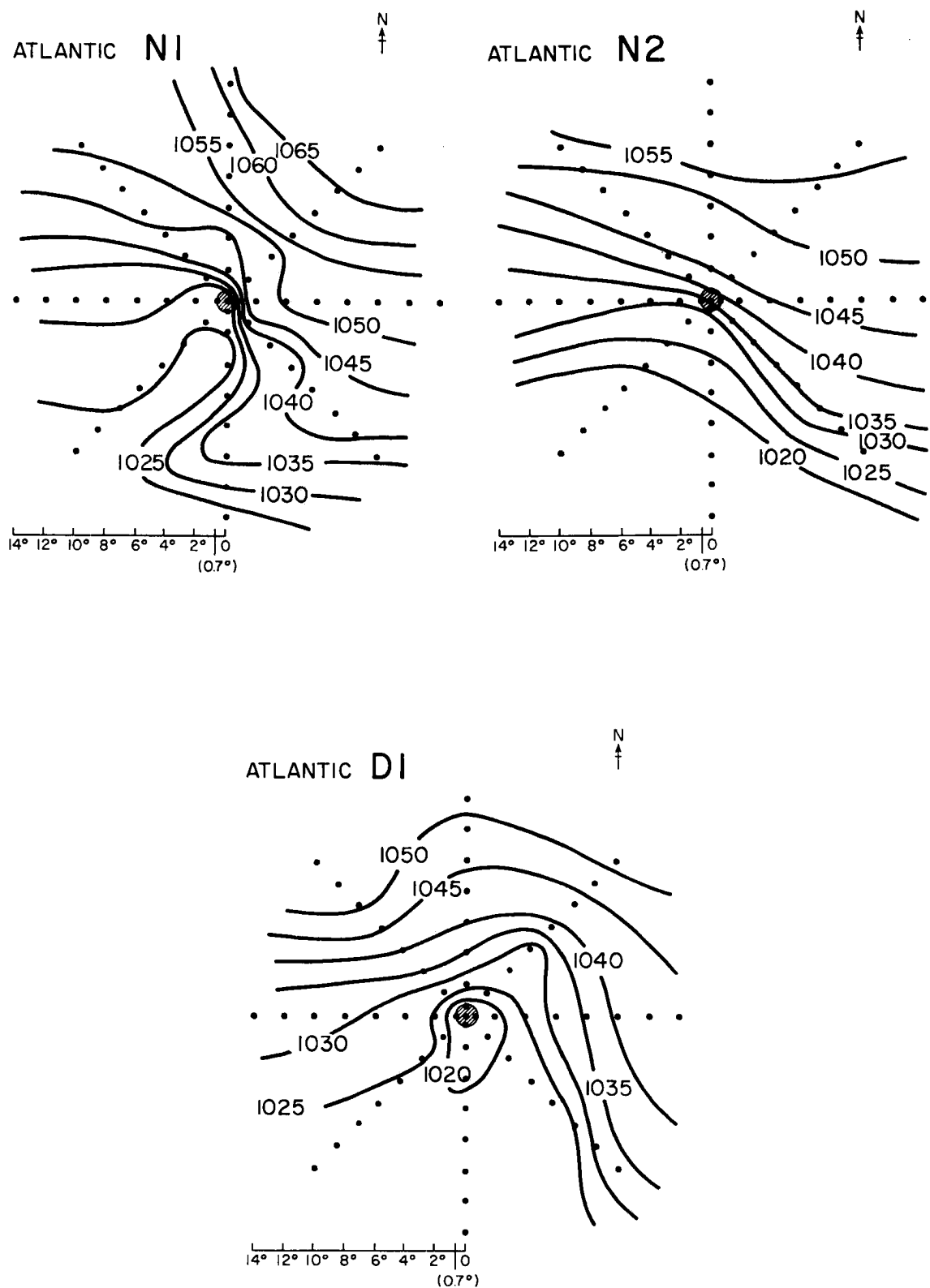


Fig. 22. Plan views of 900 mb heights in meters for Atlantic non-developing (N1, N2) and developing (D1) cloud clusters.

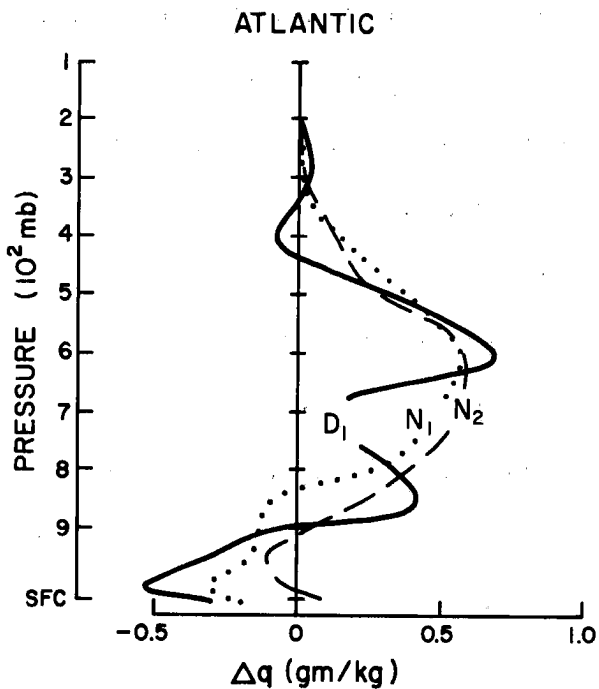


Fig. 23. Vertical profiles of mixing ratio of water vapor for the cluster (0-3°) minus its surroundings (3-5°) for the Atlantic developing (D₁) and non-developing (N₁, N₂) cloud clusters.

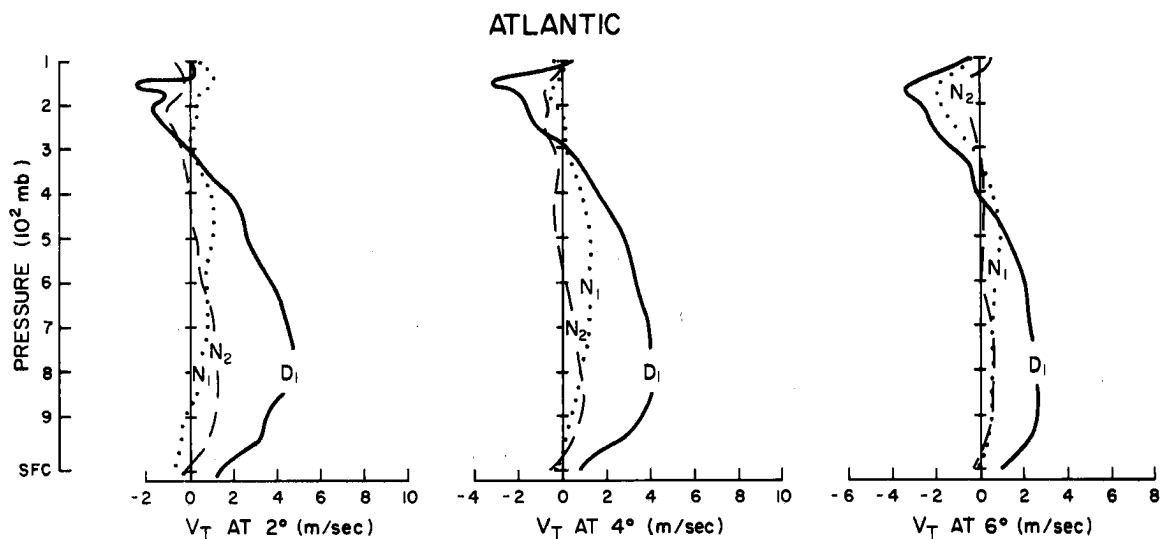


Fig. 24. Tangential wind (V_T) at 2°, 4° and 6° radius for the Atlantic developing and non-developing cloud clusters.

V_T at lower levels and much greater negative V_T at upper levels. These large differences extend out as far as 6° latitude radius and beyond. The N1 data set has maximum V_T around 500 or 600 mb implying that it is cold cored below that level; but the wave trough cluster N2 as well as the prehurricane cluster D1 has a low level maximum and therefore a warm core.

The 200 mb level flow patterns are shown in Fig. 25. The N2 wave trough cluster has no anticyclone. The N1 and the prehurricane D1 system both have an anticyclone displaced approximately 3° to the east of the system center. The large scale horizontal anticyclonic shear is very much greater for the developing system.

The vertical profiles of V_R at 4° and of $0-4^{\circ}$ vertical velocity are shown in Fig. 26. The typical Atlantic weather systems, as represented here by N1, N2 have very weak vertical motion associated with them. This is in agreement with the large scale long-term-mean vertical velocity in this region being downwards, as discussed in Chapter 2. The prehurricane system, however, does have substantial upward vertical motion, of the same order of magnitude as found in the Pacific systems in Fig. 18.

3.3 Atlantic depressions: N3 vs D2

The tropical depression represents a later stage of development than the cloud cluster. In the depression stage, by definition, there already exists a well defined closed vortex circulation at low levels. Approximately one third of depressions later develop into tropical storms. The structure of developing depressions will now be compared with the structure of those depressions which do not develop. The depressions making up the non-developing composite data set N3 are all from the

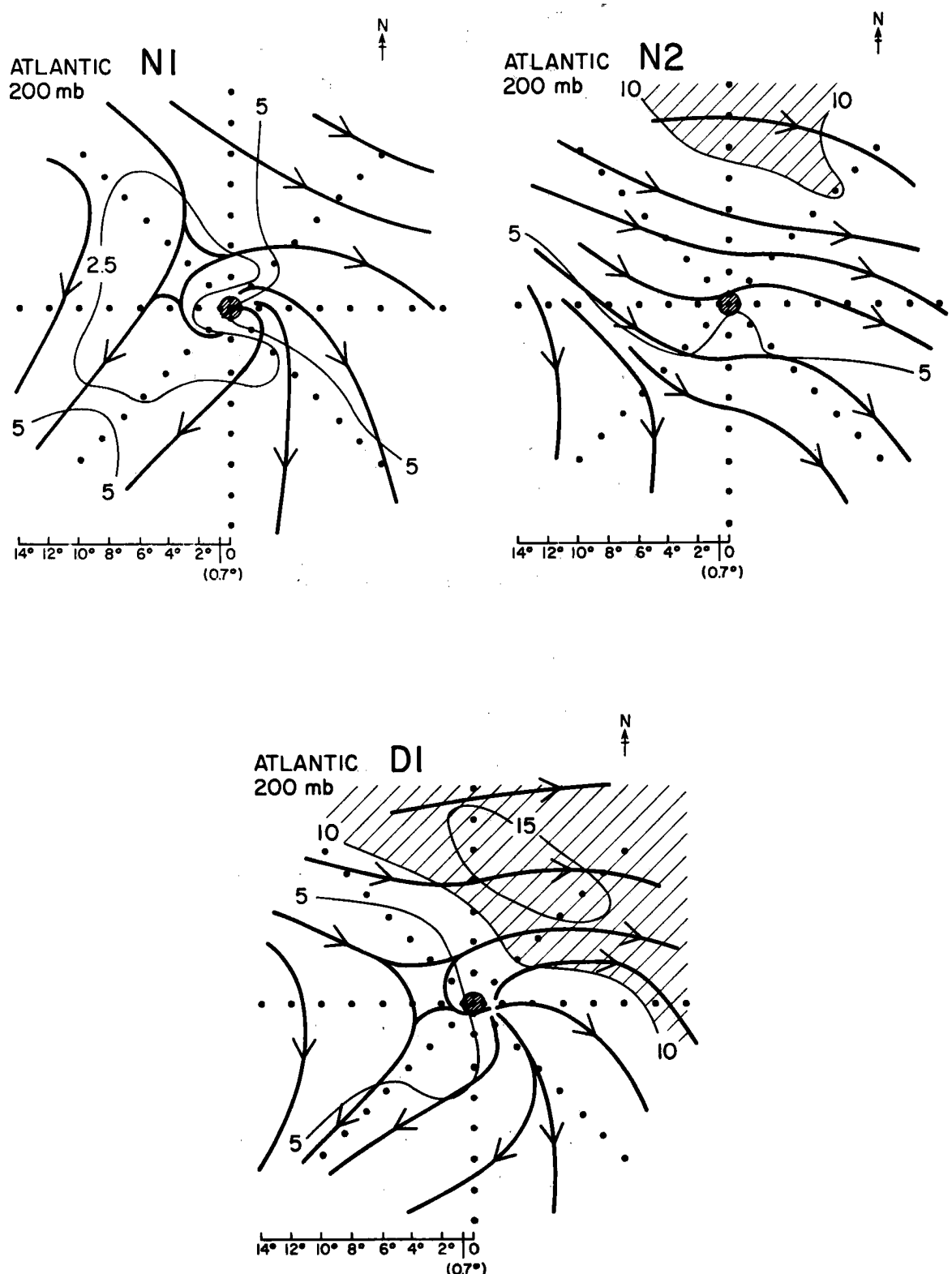


Fig. 25. 200 mb streamline and isotach analyses (m s^{-1}) for the Atlantic non-developing (N1, N2) and pre-hurricane (D1) cloud clusters.

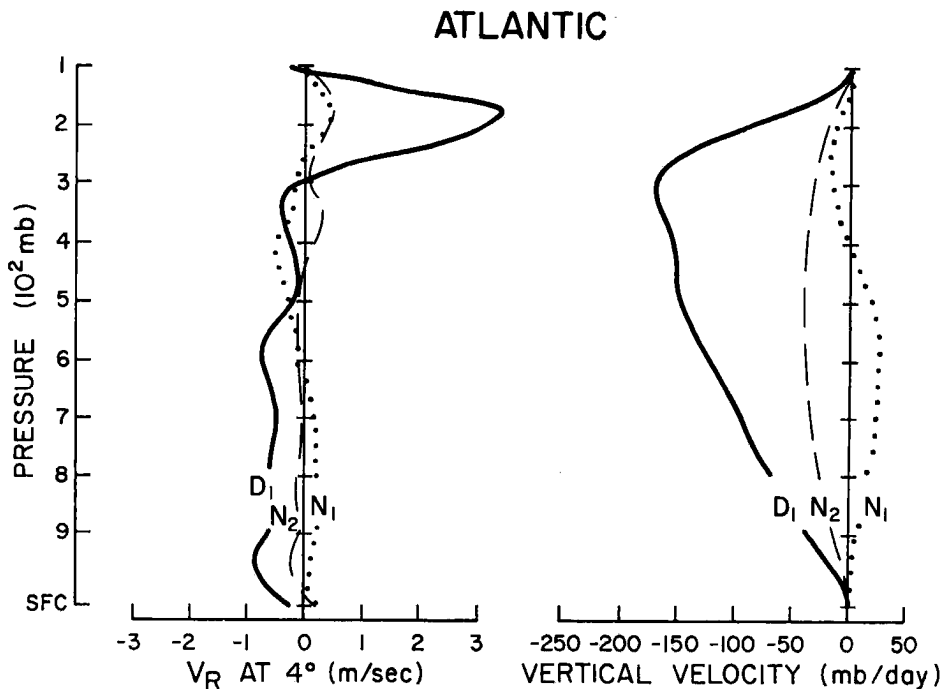


Fig. 26. Radial wind at 4° and vertical velocity averaged over the $0-4^\circ$ area for Atlantic developing and non-developing cloud clusters.

West Atlantic region, longitude greater than 55°W , latitude less than 30°N during the months of June to October. The sea surface temperature in that location and season is always well above $26\frac{1}{2}^\circ\text{C}$. In addition no positions were included in the N3 data set such that the system was within one degree latitude of land (including Cuba, Haiti, Jamaica and Puerto Rico) within the following 24 hours. Thus the lack of development must be attributed to dynamic and thermodynamic structure rather than to topographic or land versus sea influences.

The non-developing N3 and the prehurricane D2 depressions are both well defined tropical systems; so it would not be anticipated that all of the differences that were found between developing and non-developing clusters would carry over to them. For instance, they both have a well defined upper level anticyclone as shown in Fig. 27. The warm core is also of similar magnitude in the two systems as shown in

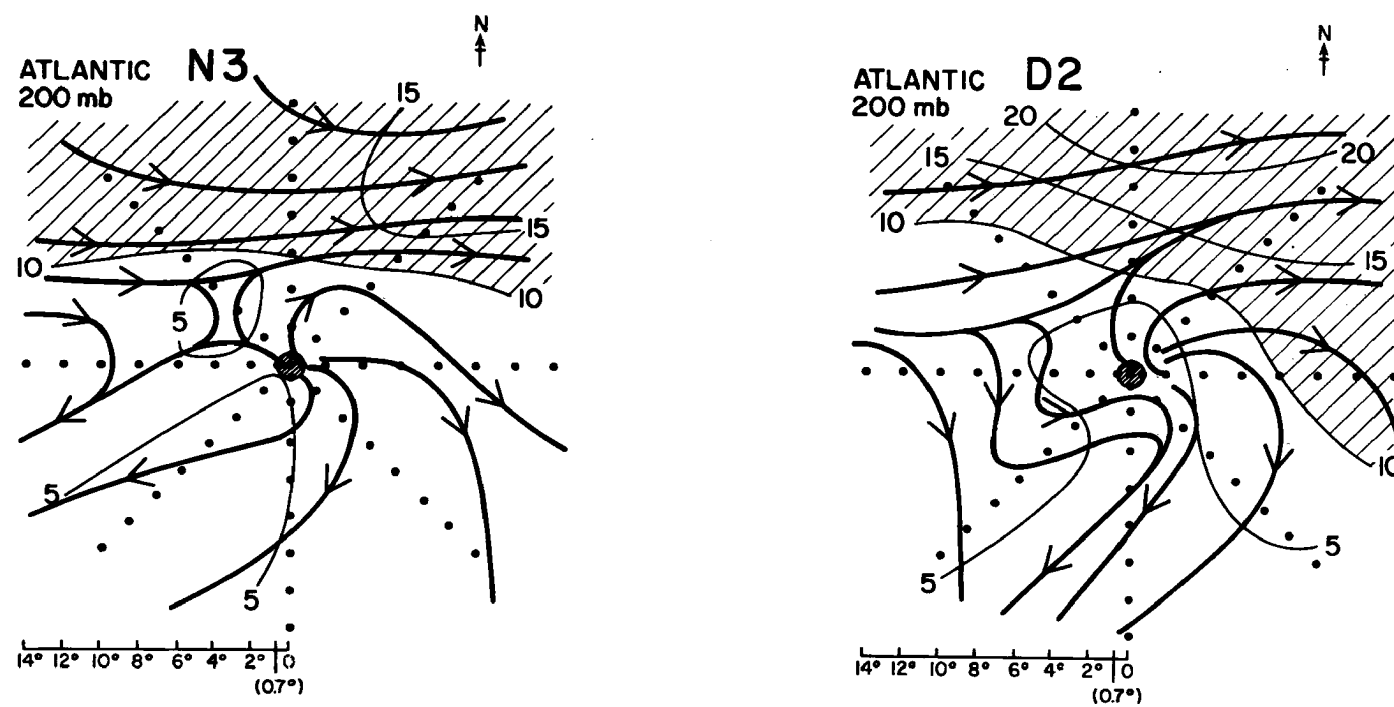


Fig. 27. 200 mb streamline and isotach analyses (m s^{-1}) for the Atlantic non-developing (N3) versus the pre-hurricane (D2) depression.

Fig. 28. Vertically integrated, however, the warm anomaly is better defined for the developing system. This can be seen in the better defined symmetric low level height gradient shown in Fig. 29.

The greater moisture anomaly actually is in the non-developing system (Fig. 30), but the large scale 0-6° moisture is much the same: 5.0 gm/cm² for the developing depression D2 as compared with 4.9 gm/cm² for N3.

The vertical velocity curves are shown in Fig. 31. The non-developing system has much more upward vertical velocity than the developing system.

The major difference between the two data sets is the tangential wind (Fig. 32). The low and middle level tangential winds for the developing depressions are twice as large as those for the non-developing, and the difference extends out to 6° radius and beyond. An inspection of the plan views in Fig. 27 also reveals a large difference in upper level anticyclonic tangential wind; but the difference does not show up until out to 8° and beyond.

In summary the major differences between developing and non-developing tropical depressions are: 1) the upward vertical motion is greater for the non-developing depression, and 2) the large scale low level vorticity is greater for the developing depression.

Some readers may question result number 1). It shows clearly in Fig. 31; but vertical velocity is a difficult parameter to measure. Further discussion and substantiating evidence will be presented in Chapters 7 and 9.

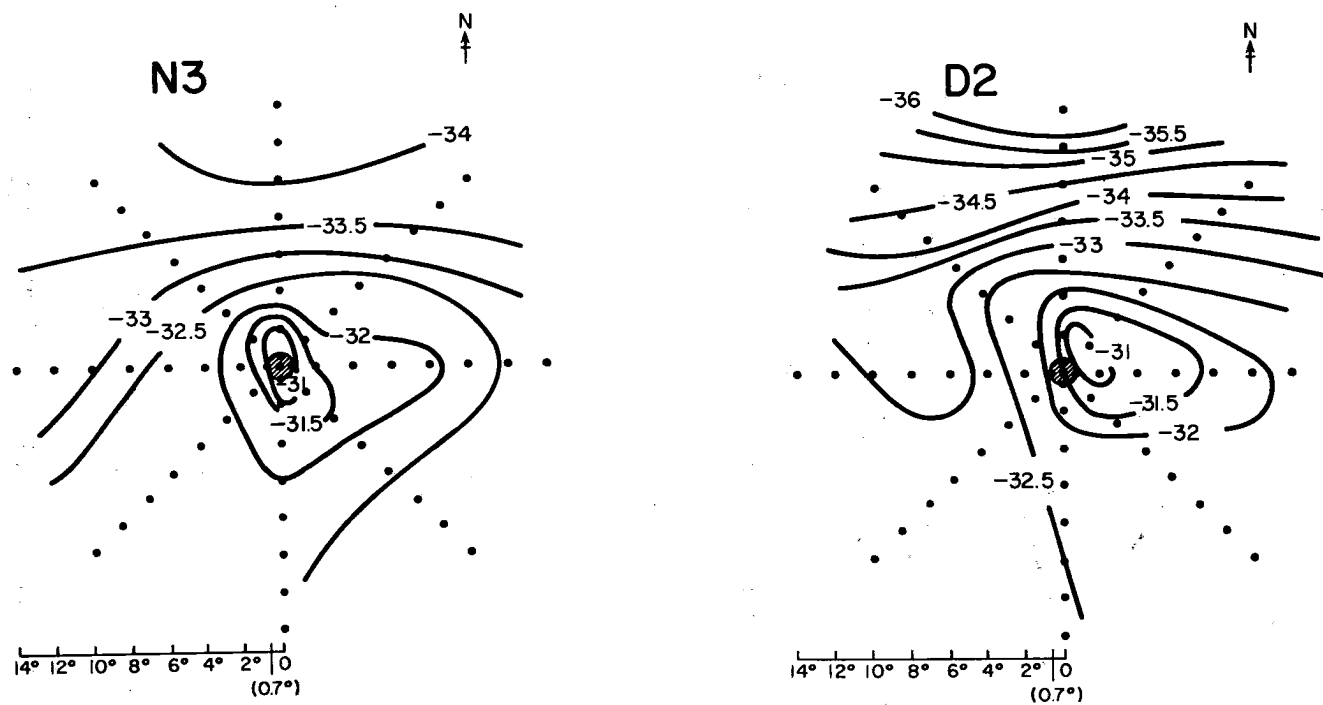


Fig. 28. Plan views of 300 mb temperature in $^{\circ}\text{C}$ for Atlantic non-developing (N3) versus pre-hurricane (D2) depressions.

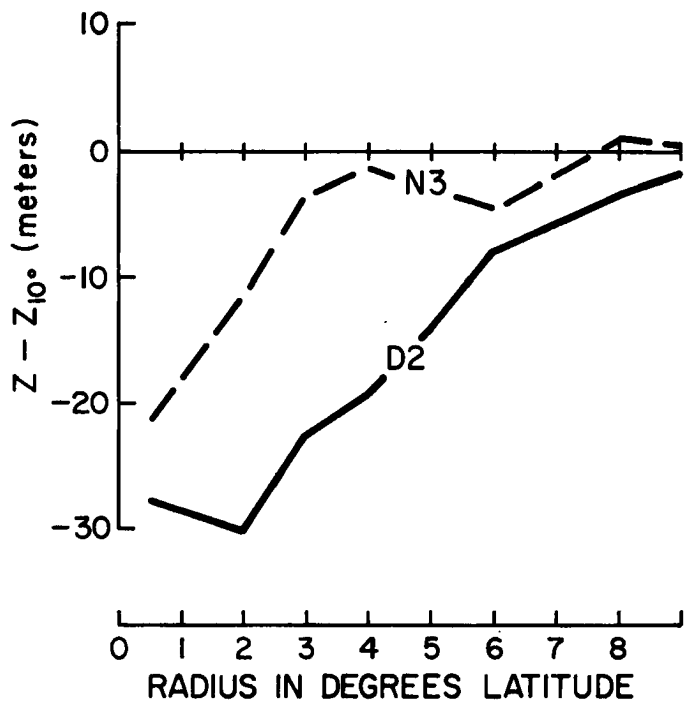


Fig. 29. D-values ($Z - Z_{10^\circ}$) in meters at 900 mb for the Atlantic non-developing (N3) versus developing (D2) depressions.

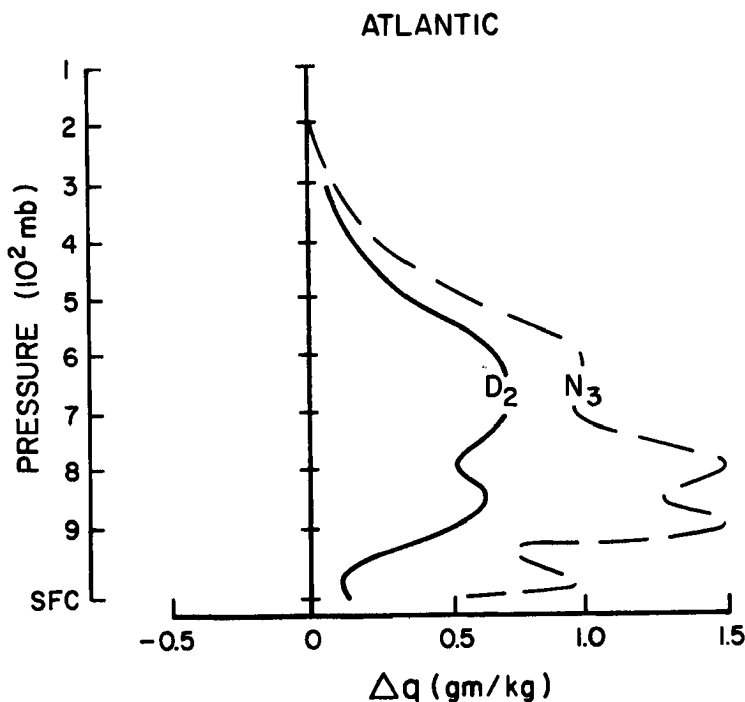


Fig. 30. q_{0-30} minus q_{3-50} for the Atlantic non-developing (N3) versus developing (D2) depression.

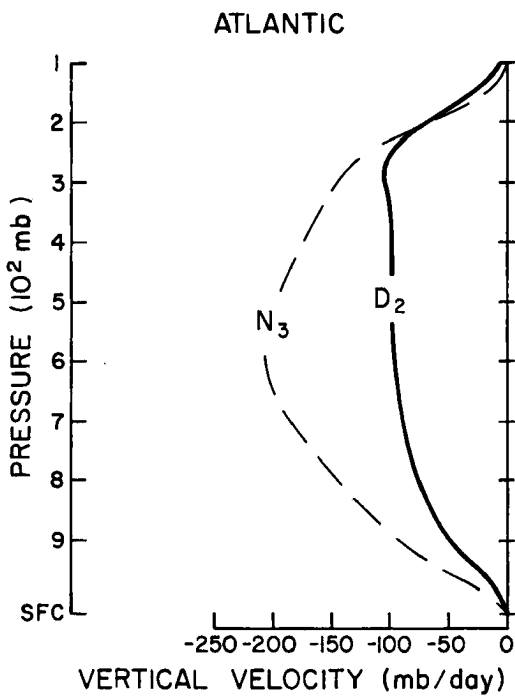


Fig. 31. Vertical velocity averaged over the $0-4^\circ$ area for the Atlantic non-developing (N₃) and pre-hurricane (D₂) depressions.

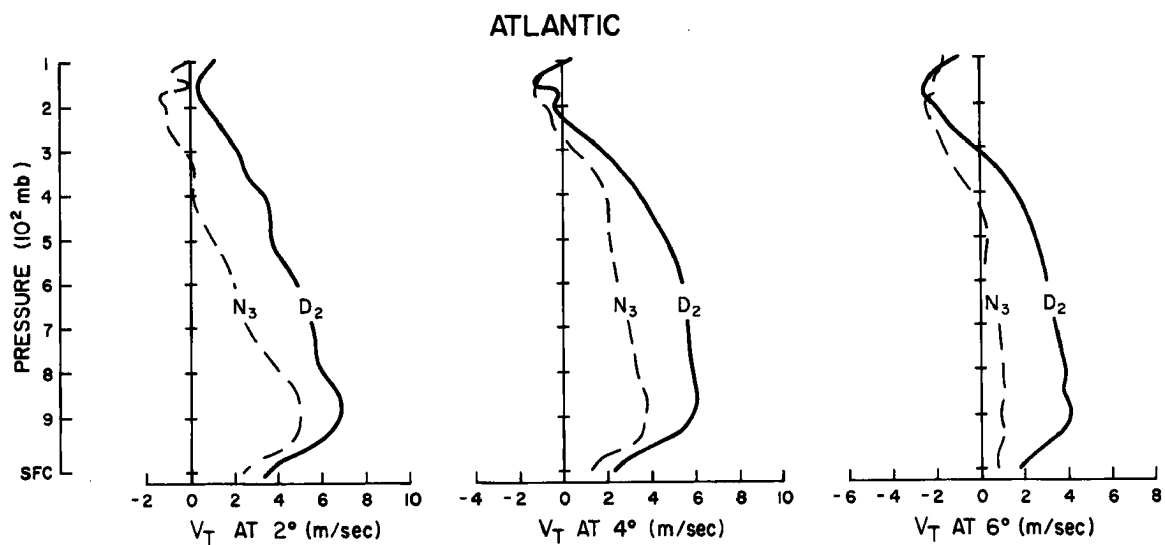


Fig. 32. V_T at 2° , 4° and 6° radius for the Atlantic depressions.

3.4 Discussion

One point which requires further emphasis is the very large horizontal scale of the differences between the developing and the non-developing data sets. The plan views of 300 mb level temperature in Figs. 12 and 21 show that the warm sector of the atmosphere extends over an 8° latitude radius circle, while the cloud cluster itself is only of radius approximately 3 degrees. The large differences that have been demonstrated to exist in the low level tangential wind also have a large horizontal extent. Fig. 33 shows plan views of V_T at 900 mb. In this figure the individual system motion vector has been subtracted from each rawinsonde wind field before the composite was made. It thus shows V_T in "motion" or "relative" coordinates. The positive tangential wind region extends over a 20° latitude diameter area. Conventional theories of cyclone development have depended on all positive relative vorticity being brought about by mass convergence and consequent contraction of vortex tubes. It is quite obvious from Fig. 33 that in the beginning or cluster stage of development there is already quite a large amount of positive relative vorticity present, and it extends over such a large scale that its origin must be external to the cluster or incipient cyclone system.

The comparison of clusters in sections 3.1 and 3.2 revealed that developing clusters had greater vertical motion than non-developing systems. In the Atlantic ocean, it seems a system must reach a stage of having of the order of 100 mb/d upward motion before it can begin the transition towards a tropical storm. In the Pacific, the average cloud cluster already has that much vertical motion.

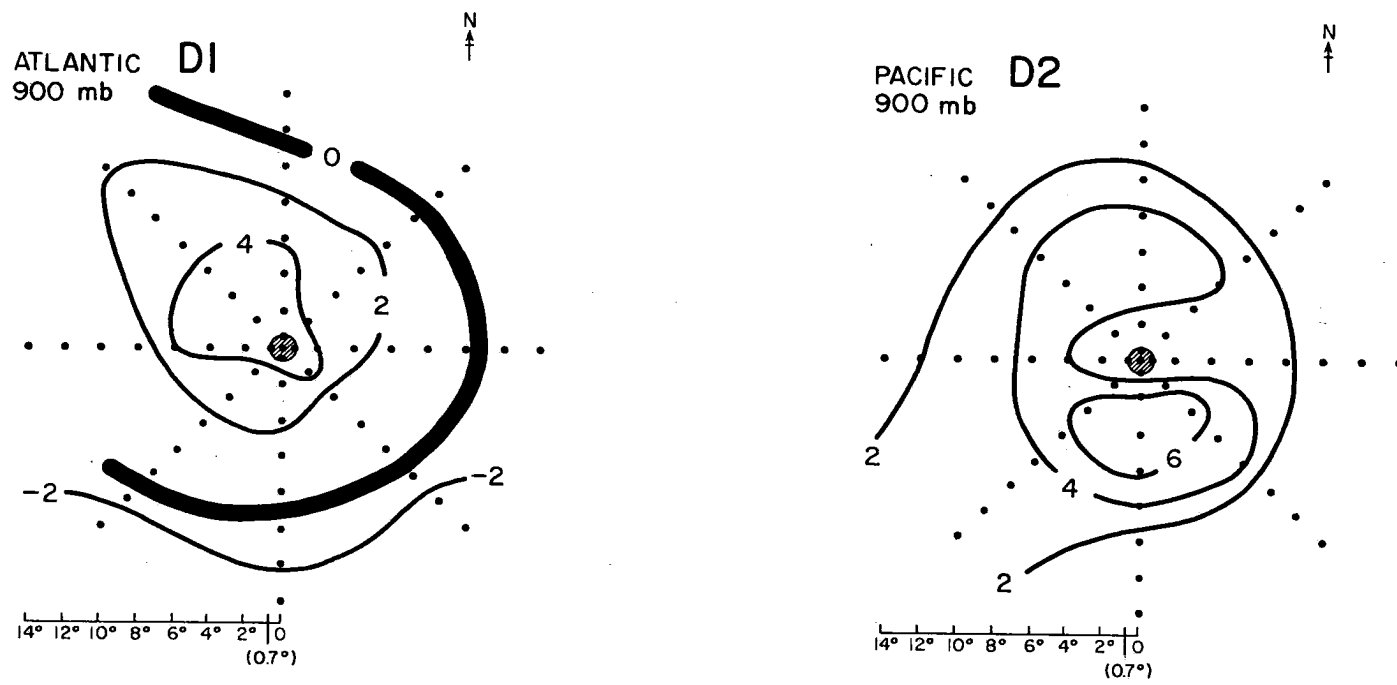


Fig. 33. Plan views of V_T in "motion" coordinates at 900 mb for the developing cloud cluster in each ocean (m s^{-1}).

In a satellite study of typhoon development Arnold (1977) showed that there exists a variability in deep penetrative convection and cirrus (and therefore in vertical motion) in pretyphoon cloud clusters of at least the same size as the mean cloudiness. The same variability exists in all later stages of development.

Given this variability, and the fact that for Atlantic depressions the composite non-developing system has greater vertical motion than the developing system (Fig. 31), it must be concluded that no importance can be placed on the differences in vertical motion found between Pacific developing and non-developing cloud clusters. The only restriction on development is that a cluster must reach a state of having approximately 100 mb/d upward motion averaged over the $0-4^{\circ}$ area.

Another result of this chapter which may require clarification concerns the existence or non-existence of the upper level anticyclone. The non-developing Pacific cluster and one of the Atlantic non-developing composite clusters have no anticyclone. All composite developing systems have an upper level anticyclone, and it is very clearly defined in the depression stage. If a cloud cluster is to develop into a tropical storm, it must develop an anticyclone at some stage; so this is a definite indicator of development. It is not infallible though, as in the Atlantic both the non-developing cloud cluster N1 and the non-developing tropical depression N3 have upper level anticyclones. S. Erickson (1977) visually inspected DMSP satellite images of 49 non-developing Pacific summertime cloud clusters and 53 pretyphoon clusters. By qualitatively following cirrus streaks on each image, he found that 10 out of the 49 (or 20%) of the non-developing had visible upper level

anticyclonic outflow, as compared with 34 out of 53 (or 64%) of the developing systems.

4. VERTICAL WIND SHEAR

One dynamic parameter which is important for tropical storm development is the presence of low vertical wind shear (Gray, 1968). Physically, low shear is required so that enthalpy and moisture can accumulate in a vertical column. A system with low wind shear will lose little moisture and heat energy through horizontal ventilation or blow-through and thus will be more likely to organize itself into a vertically stacked tropospheric system such as a tropical storm.

Plan views of the mean shear of the zonal wind $U_{200 \text{ mb}} - U_{900 \text{ mb}}$ for the Pacific data sets are shown in Fig. 34. The developing systems (D1, D2, D3) have a region of zero shear close to their center. The non-developing cluster (N1) has no such region.

Besides possessing small shear the developing data sets also show an additional characteristic of the tropospheric vertical shear field. Each system has a line of absolute zero shear close to its center. Taking into account the positioning problems inherent in the assembling of composite data sets, it is likely that the zero shear line lies directly above the developing system's center.

Further inspection of Fig. 34 shows that extremely strong horizontal gradients of vertical shear exist in the region extending about 5° latitude to the north and south of the developing systems. The vertical shears surrounding, but quite close to, the system are actually very strong. This effect stems partly from the superposition of an upper level anticyclone above a low level cyclone, but the strong shear pattern extends well out into the environment.

If the only role played by vertical wind shear in storm genesis is that it has to be low to prevent ventilation, why is absolute zero

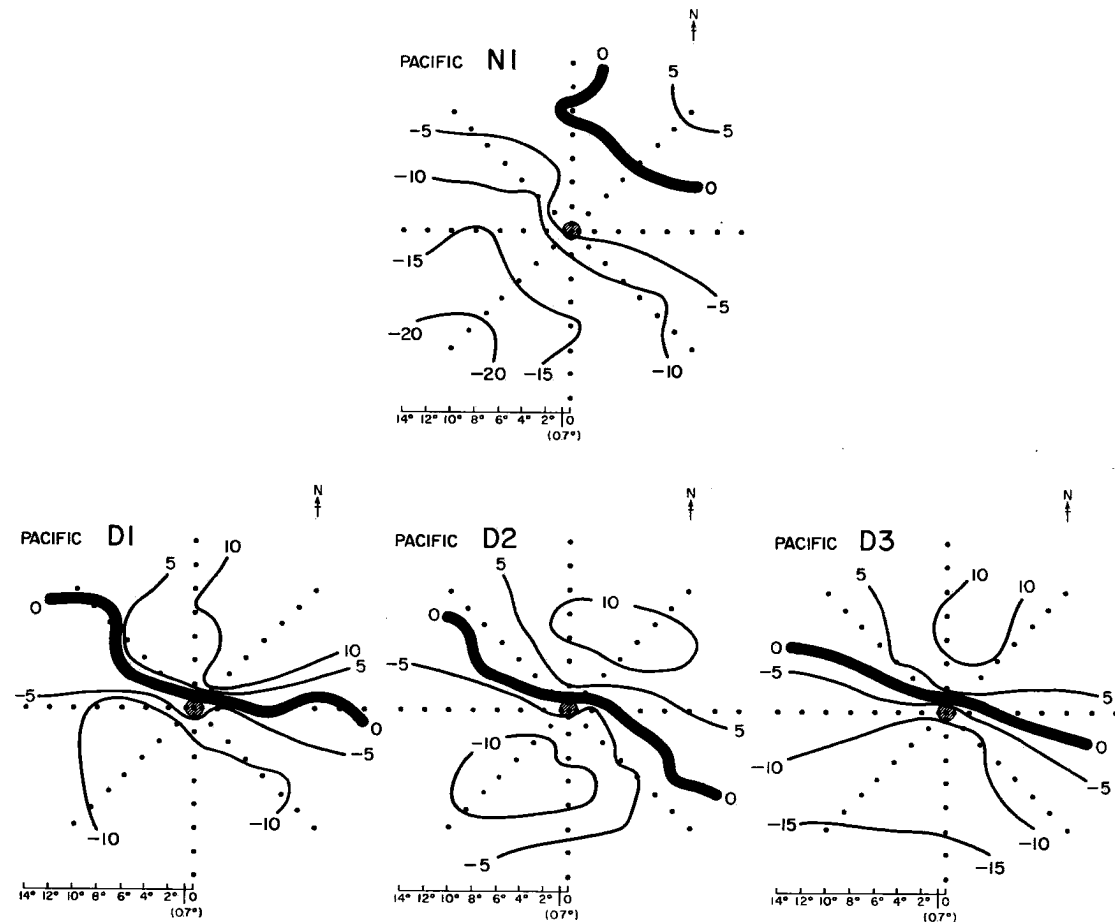


Fig. 34. Plan views of zonal shear, $U_{200 \text{ mb}} - U_{900 \text{ mb}}$ (m s^{-1}) for the Pacific data sets.

shear rather than just low shear observed on the composite plan views? Why also are such large zonal shears observed close to the system center to the north and the south?

Inspection of Fig. 34 leads to the conclusion that for tropical cyclone genesis in the West Pacific there is a requirement for the large scale environment to arrange itself to bring about the existence of an east-west extending line of zero tropospheric $\partial U / \partial p$ shear with a large gradient of this shear to the north and south.

Figure 35 shows the plan views of meridional vertical shear $V_{200 \text{ mb}} - V_{900 \text{ mb}}$ for the Pacific systems. Once again there is a striking difference between the non-developing cluster (N1) and the pretyphoon clusters (D1, D2). The non-developing system exists in a large area of low meridional vertical shear. The developing systems have zero shear over them with strong anticyclonic vertical shear to the east and west. Comparing Figs. 34 and 35, it is seen that the effect is much greater in the zonal than in the meridional shear pattern.

The plan views of zonal shear for the Atlantic systems are shown in Fig. 36. Comparing non-developing clusters N1, N2 with prehurricane systems D1, D2 and D3, the distinctive feature is that the prehurricane systems have very strong anticyclonic vertical shear north of them and zero or close to zero shear over them.

There is independent evidence for the strong shear to the north. Riehl (1975) documented several case studies of development of tropical storms in the Gulf of Mexico and Caribbean. In each of Riehl's cases, development was preceded by mid-tropospheric cold air advection 500 to 1500 km north of the system. By thermal wind considerations this

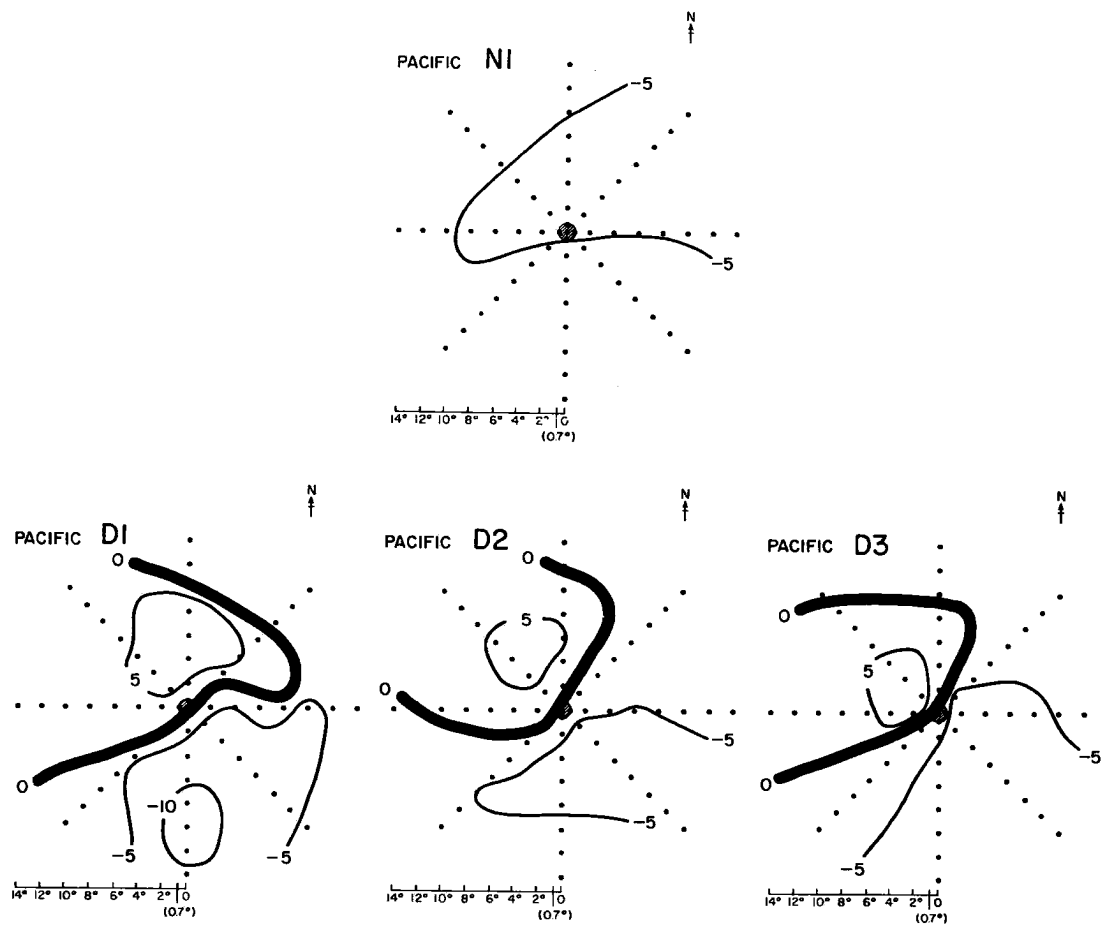


Fig. 35. Plan views of meridional shear, $V_{200 \text{ mb}} - V_{900 \text{ mb}}$ (m s^{-1}) for the Pacific data sets.

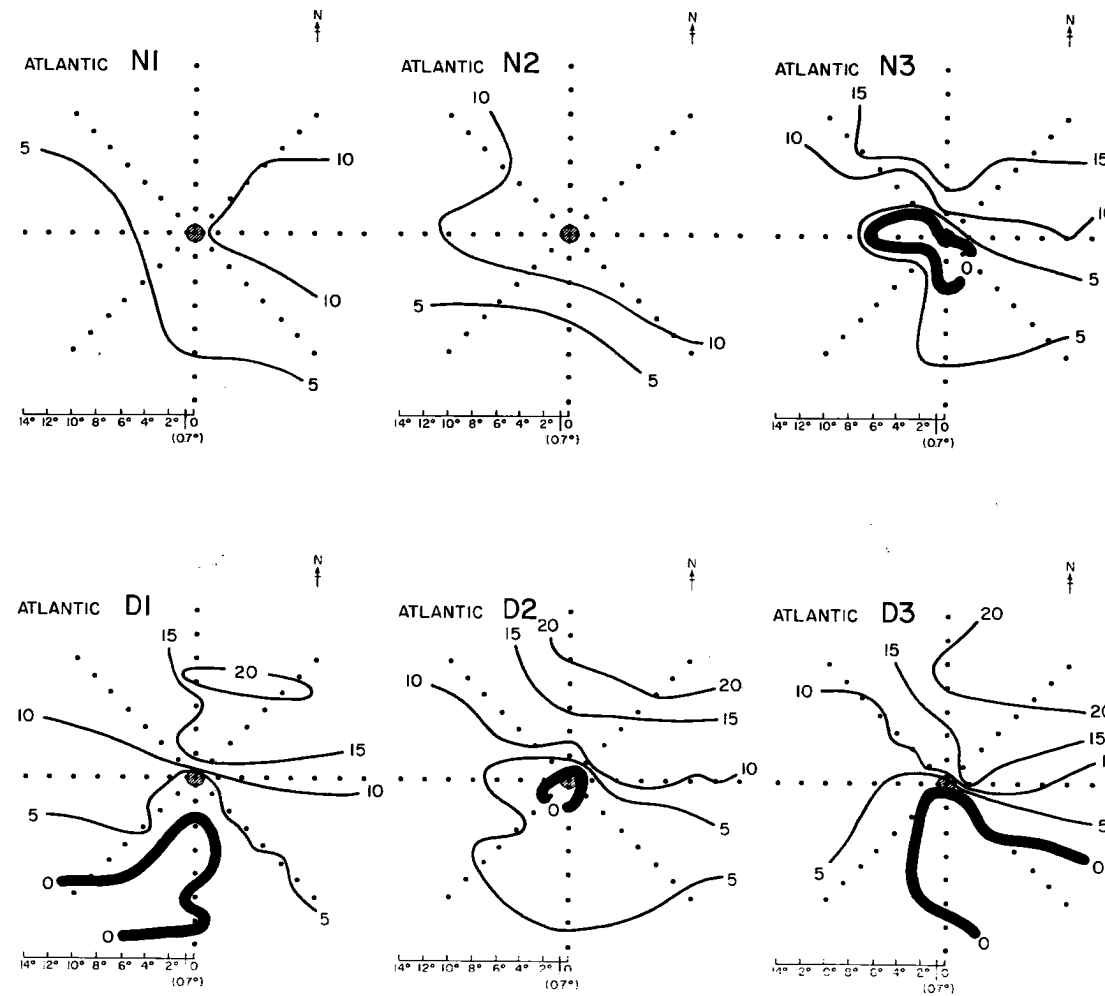


Fig. 36. Plan views of zonal shear, $U_{200 \text{ mb}} - U_{900 \text{ mb}}$ (m s^{-1}) for the Atlantic data sets.

implies an increase of positive zonal shear between the cold air and the system center.

The non-developing depression N3 also has the zero shear with strong positive shears to the north, indicating that these conditions are also highly favorable for the system to undergo the transition from cloud cluster to depression status. It should be noted, however, that for the N3 system the shear pattern does not extend over as large an area, particularly towards the north, as it does for the developing systems.

The Atlantic patterns of vertical shear of the meridional wind are shown in Fig. 37. The meridional shears in the Atlantic are stronger than in the Pacific. All developing Atlantic systems have a north-south extending line of zero vertical meridional shear going over the system center, positive shear to the west and very strong negative shear to the east. A difference also shows between developing D2 and non-developing N3 depressions, the positive - zero - negative pattern being better defined in the former case.

An inspection of the composites of Gray (1968) shows that the same situation exists in other tropical storm regions of the world. Figure 38 reproduced from Gray's paper is a plan view of the zonal shear for tropical disturbances in the South Pacific Ocean which later develop into tropical storms. Figure 39 is for prestorm disturbances in the North Indian Ocean. Both figures show the same features: an east-west line of zero zonal vertical shear accompanied by strong westerly shear to the poleward side and strong easterly shear to the equatorward side.

This result helps clear up some of the confusion that has existed in the past concerning vertical wind shear and tropical cyclone genesis.

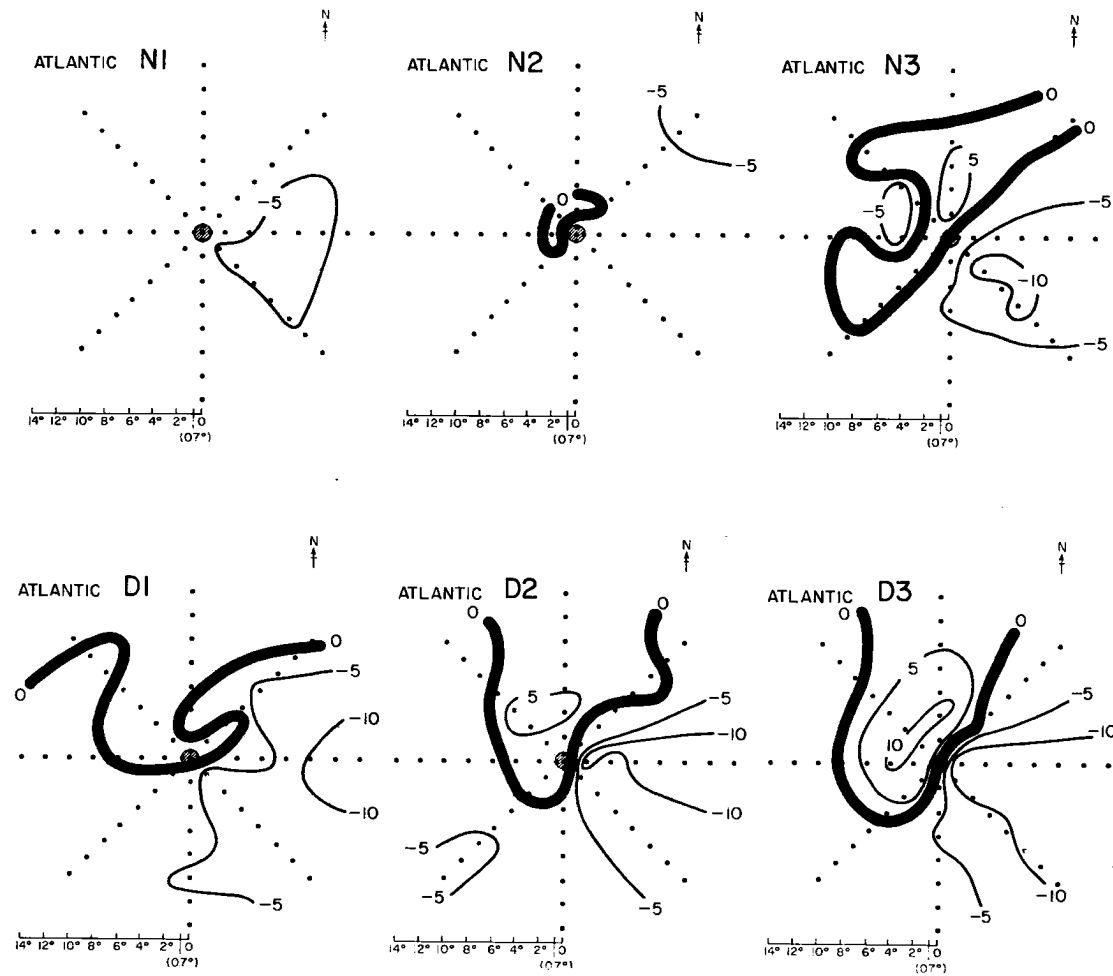


Fig. 37. Plan views of meridional shear, $v_{200 \text{ mb}} - v_{900 \text{ mb}}$ (m s^{-1}) for the Atlantic data sets.

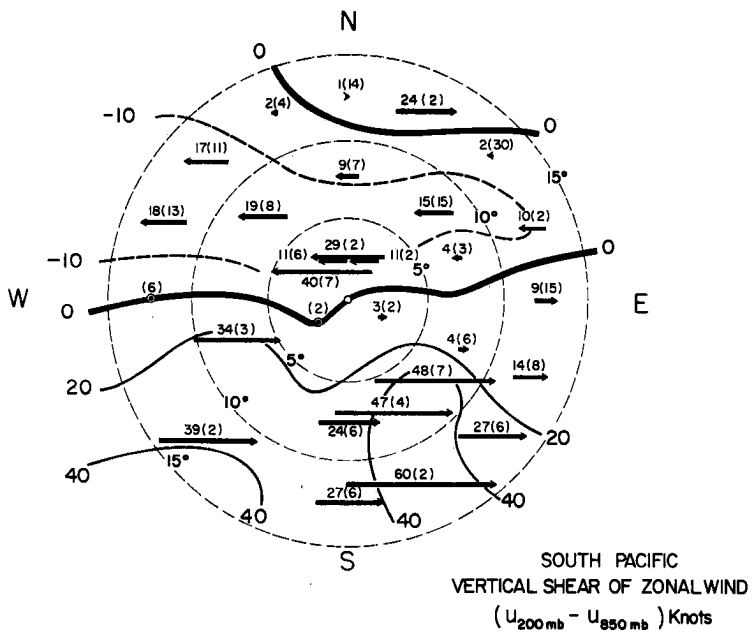


Fig. 38. Composite zonal vertical wind shear for average rawin information in each area relative to the center of 84 tropical disturbances in the South Pacific which later developed into tropical storms. Length of arrows proportional to wind shear in knots (at left). Values in parentheses are number of wind reports in each area average. Distance from the center is given by the lightly dashed circular lines at 5° latitude increments. (Reproduced from Gray, 1968).

There has been some resistance, for example, to acceptance of low tropospheric vertical shear as a cyclone genesis requirement. This hesitation has stemmed partly from synoptic observations of strong shears close to the developing systems. Forecast schemes based on low shear will give a high score to a tropical area of low shear. Such schemes work well on a climatological basis, but for individual situations the above data suggest that there is actually a requirement not only for very small vertical shear near the system center but also for two adjoining regions of strong 200-900 mb vertical shear of opposite sign on either side of the system.

The vertical shear pattern for the developing systems (D1, D2, D3 in either ocean) is a function of both the upper level and the lower

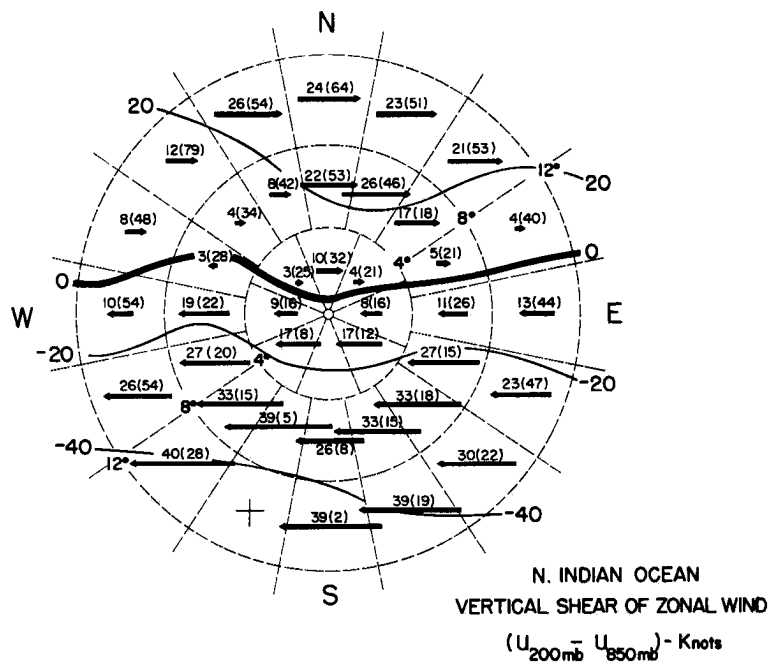


Fig. 39. Composite zonal vertical wind shear for average rawin information in each area relative to the center of 54 tropical disturbances in the North Indian Ocean which later developed into tropical storms. Length of arrows proportional to wind shear in knots (at left). Values in parentheses are number of wind reports in each area average. Distance from the center is given by the lightly dashed circular lines at 4° latitude increments. (Reproduced from Gray, 1968).

level flow and extends over a large region of the tropics, as far as 10° latitude distance from the center of the system. These ideas correspond well to the results of a number of previous researchers. Riehl (1948, 1950), Yanai (1961), Sadler (1967, 1975, 1976, 1978) and Dvorak (1975) have all placed emphasis on a requirement for a superposition of favorable upper level and lower level large scale flow features prior to disturbance intensification.

More specifically, Dvorak (1975) states that development will not take place underneath a unidirectional upper tropospheric flow pattern. Such a flow pattern is inconsistent with a large north-south gradient of $\partial U / \partial p$. Dvorak (personal communication) also states that development

in the Atlantic is inhibited by upper level northerly flow to the west of a disturbance. This is consistent with the requirement for a large value of $\partial/\partial x$ ($\partial V/\partial p$).

Sadler (1967, 1975, 1978) presents evidence that Northwestern Pacific cyclone genesis within the trade winds is associated with a westward extension of the tropical upper tropospheric trough (TUTT) existing to the northwest of the developing system. Sadler (1976) has also documented cases of low latitude (ITCZ) cyclone genesis taking place to the south of the TUTT. In the former situation the TUTT being to the west of the disturbance enhances the anticyclonic vertical shear close to the disturbance. In both situations the upper level westerlies to the south of the TUTT overlie trade winds, thus bringing about the required positive zonal shear to the north of the incipient disturbance.

Gray (1968) has shown that climatologically cyclone genesis usually takes place just to the poleward side of a monsoon or doldrum equatorial trough. A schematic north-south cross section of the usual zonal winds for such a trough are shown in Fig. 40. Note the positive zonal shear to the north and negative shear to the south.

Certain interpretations can be placed on this horizontal configuration of vertical shear. By thermal wind considerations it implies that the genesis takes place when the atmosphere is warm relative to its surroundings. The ITCZ is climatologically warm, and the required N-S and E-W gradients of shear can stem from the so called "sharpening up" of the ITCZ. As shown by Riehl (1975) they can also be brought about by cold air advection from the north in travelling middle latitude systems.

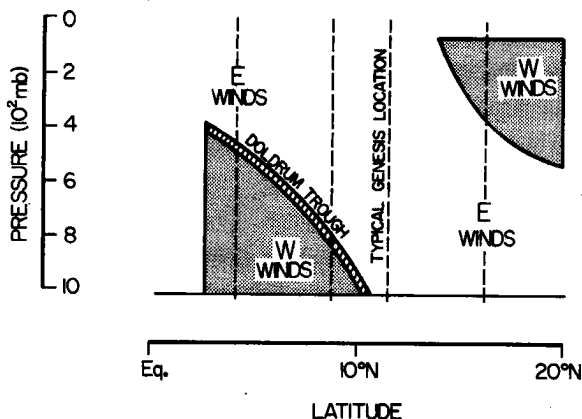


Fig. 40. Schematic north-south cross section of zonal winds relative to the position of a doldrum or monsoon equatorial trough.

Another interpretation is in terms of a vertical gradient of vorticity: a large north-south gradient of $-\frac{\partial U}{\partial p}$ in combination with a large east-west gradient of $\frac{\partial V}{\partial p}$

$$= \frac{\partial}{\partial y} \left(-\frac{\partial U}{\partial p} \right) + \frac{\partial}{\partial x} \left(\frac{\partial V}{\partial p} \right)$$

$$= \frac{\partial}{\partial p} \left(-\frac{\partial U}{\partial y} + \frac{\partial V}{\partial x} \right)$$

= a large vertical gradient of relative vorticity

Genesis potential for a developing disturbance may thus be quantified as:

$$GP = \zeta_{900 \text{ mb}} - \zeta_{200 \text{ mb}} \quad (7)$$

where ζ is relative vorticity. S. Erickson (1977) found large differences in GP between developing and non-developing Western Pacific cloud clusters.

Values of GP for the current study are shown in Table 12. Comparing the Pacific cluster (N1) with the Pacific pretyphoon clusters (D1, D2), it is seen that the latter developing systems have larger values of GP at all radii. Inspection of the data shows that at 2° and 4° the difference is due mainly to the developing systems having greater low level relative vorticity. The greatest difference in GP is at 6° , where the developing systems also have a contribution due to large scale 200 mb anticyclonic horizontal shear. Comparing Atlantic clusters (N1, N2 vs. D1) and depressions (N3 vs. D2), the same comments apply.

Table 13 shows genesis potential averaged for non-developing and developing data sets. At 6° radius this parameter is 3 times greater for the developing systems than for the non-developing systems. No other parameter differences are anywhere near as large. For comparison, Table 14 shows various other measured quantities averaged for non-developing versus developing data sets.

TABLE 12

Genesis Potential (GP). Mean relative vorticity differences between 900 mb and 200 mb for each composite data set.

$$GP = \bar{\zeta}_{900\text{mb}} \text{ Minus } \bar{\zeta}_{200\text{mb}} \text{ } (10^{-5} \text{ s}^{-1})$$

	<u>0-2°</u>	<u>0-4°</u>	<u>0-6°</u>
<u>PACIFIC NON-DEVELOPING</u>			
N1 Cloud Cluster	2.0	1.6	0.7
<u>PACIFIC DEVELOPING</u>			
D1 Early pretyphoon cloud cluster	6.0	4.0	2.3
D2 Pretyphoon cloud cluster	4.8	3.2	2.4
D3 Intensifying cyclone	8.5	4.8	3.0
D4 Typhoon	12.4	6.4	4.4
<u>ATLANTIC NON-DEVELOPING</u>			
N1 Cloud cluster	-0.5	0.4	0.7
N2 Wave trough cluster	2.1	0.6	0.4
N3 Non-developing depression	5.5	2.0	1.0
<u>ATLANTIC DEVELOPING</u>			
D1 Prehurricane cloud cluster	4.7	2.4	1.6
D2 Prehurricane depression	5.2	2.8	1.8
D3 Intensifying cyclone	9.8	4.2	2.8
D4 Hurricane	10.8	5.2	3.7

TABLE 13

Genesis Potential (GP) - Average of Developing and Non-developing data sets (10^{-5} s^{-1})

	<u>0-2°</u>	<u>0-4°</u>	<u>0-6°</u>
Average NON-DEVELOPING (Pacific N1; Atlantic N1,N2,N3)	2.3	1.1	0.7
Average DEVELOPING weak systems (D1,D2)	5.2	3.1	2.0
Average DEVELOPING all systems (D1,D2,D3)	6.5	6.0	2.3

TABLE 14

Comparison of developing versus non-developing data sets for various measured parameters. Values are averaged over the $0-4^{\circ}$ radius area.

	$\bar{U}_{sfc-100mb}$ (m/s)	$\bar{V}_{sfc-100mb}$ (m/s)	Composited wind speed at 950 mb (m/s)	Speed of movement of dis- turbance (m/s)	$\Delta h_{950-600mb}$ (cal/g)	$\Delta h^*_{950-600mb}$ (cal/g)	q_{700mb} (g/kg)	Precipitable water (g/cm ²)	ΔT_{300mb} (°C)	ΔT_{850mb} (°C)
Average NON-DEVELOPING (Pacific N1; Atlantic N1, N2, N3)	-3.0	0.6	7.3	5.3	2.7	3.0	6.9	5.2	0.3	-0.2
Average DEVELOPING (Pacific D1, D2; Atlantic D1, D2)	-3.2	1.0	7.7	5.1	2.6	3.1	7.8	5.6	0.3	-0.1

$\bar{U}_{sfc-100mb}$ is the pressure weighted average of the zonal component of the wind between the surface and 100 mb.

$\bar{V}_{sfc-100mb}$ is the pressure weighted average of the meridional component of the wind between the surface and 100 mb.

$\Delta h_{950-600mb}$ is the difference in moist static energy, h , between 950 mb and 600 mb.

$\Delta h^*_{950-600mb}$ is the difference in saturation moist static energy between 950 mb and 600 mb.

q_{700mb} is the mixing ratio at 700 mb.

ΔT is a measure of the temperature difference between the cluster ($0-3^{\circ}$) and its surroundings ($3-7^{\circ}$).

5. SUMMARY OF THE DIFFERENCES BETWEEN DEVELOPING AND NON-DEVELOPING TROPICAL DISTURBANCES

The main findings from the analysis of the composite fields in Chapters 3 and 4 are as follows:

- 1) Pre-typhoon and pre-hurricane systems are located in large areas of high values of low level relative vorticity. The low level vorticity in the vicinity of a developing cloud cluster is approximately twice as large as that observed with non-developing cloud clusters.
- 2) Mean divergence and vertical motion for the typical Western Atlantic weather system are well below the magnitudes found in pre-tropical storm systems.
- 3) Once a system has sufficient divergence to maintain 100 mb or more per day upward vertical motion over a 4° radius area, there appears to be little relationship between the amount of upward vertical velocity and the potential of the system for development.
- 4) Cyclone genesis takes place under conditions of zero vertical wind shear near the system center.
- 5) There is a requirement for large positive zonal shear to the north and negative zonal shear close to the south of a developing system. There is also a requirement for southerly shear to the west and northerly shear to the east. The scale of this shear pattern is over a 10° latitude radius circle with maximum amplitude at approximately 6° radius.
- 6) The large scale flow, therefore, rather than the properties of the system itself, appears to be the main differentiating factor for cyclone genesis.

These six findings can be synthesized into one parameter for the potential of a system for development into a hurricane or typhoon:

$$\text{Genesis Potential (GP)} = \zeta_{900 \text{ mb}} - \zeta_{200 \text{ mb}},$$

when applied over $0-6^{\circ}$ radius. As shown in Table 13, GP is three times greater for developing tropical weather systems than for non-developing systems.

All of the above factors relate to dynamic parameters or the wind fields around the disturbances. There are no consistent differences between developing and non-developing systems in thermodynamic parameters such as moisture content or vertical stability. This is in agreement with the analysis in section 2.5 of Gray's climatological genesis parameter. Of Gray's six climatological variables required for a region to spawn tropical cyclones, the three thermodynamic parameters were shown to be generally present throughout the whole season, whereas the three dynamic parameters had a large day to day variation.

The analysis of the composite fields in Chapter 3 does show some temperature differences between the developing and non-developing systems. The whole tropical region in which the developing disturbance is embedded is slightly warmer than the region surrounding the typical non-developing disturbance. This temperature difference is of a much smaller magnitude, however, than the difference in the wind fields.

Many past authors have emphasized warm-core versus cold-core differences between developing and non-developing disturbances. All composite tropical weather systems have an upper level warm core. In the lower atmosphere there are some differences. The Pacific non-developing cloud cluster has a low level cold core. In the Atlantic the N1 non-developing cloud cluster has a cold core, but the N2 non-developing cluster has a low level warm core. All developing data sets have low level warm cores. They also all exist in a very large horizontal extent of large low-level positive relative vorticity. The low-level warm core is on the cluster scale, but the vorticity is on a very much greater scale extending out to 10° latitude in all directions. The

vorticity difference therefore must be the dominant effect, since its large scale implies that its source is external to the system.

The appearance of a low level warm core is an indication that development has probably begun to take place; but the source or cause of this development must lie in the large scale vorticity fields.

6. INDIVIDUAL DAY CYCLONE GENESIS

In the previous chapters the composite data sets have been examined for consistent differences between systems that later develop into typhoons or hurricanes and systems which do not. Compositing is the first step in this study. By averaging together many different cases it smooths out interior class differences and enhances average system differences. Such mean differences have just been discussed.

The second step is to attempt an analysis of individual cases. This requires the separating of cases of cyclone development from prominent cases of non-development to see to what extent the composite characteristics fit the individual situations.

In this chapter the composite results are evaluated for 130 separate developing and non-developing tropical weather systems. In particular, the systems are examined for (i) high values of Genesis Potential (GP), (ii) the existence of an east-west extending line of zero tropospheric vertical shear, and (iii) the existence of a north-south extending line of zero meridional tropospheric vertical shear.

6.1 Atlantic tropical storms

During the hurricane season the National Hurricane Center in Miami routinely performs computer analyses over the North Atlantic Ocean of the wind fields at the 200 mb level and at the ATOLL level (Analysis of the Tropical Oceanic Lower Layer). Grid point values of these fields (at 1.5° grid resolution) were subtracted to provide fields of vertical shear by Mr. Mark Zimmer of the National Hurricane Center (NHC). This is representative of the vertical wind shear between 200 and 900 mb. Mr. Zimmer provided the author with maps of zonal and of meridional

shear for the Atlantic Ocean covering the region from the equator to 45° North, and from 35.5° West to 95° West. Data were provided twice daily for the hurricane seasons of 1975, 1976 and 1977. The data were taken from the operational data tapes of the NHC, so there were some retrieval problems and some periods of missing data. The Atlantic Ocean is a relatively data void area, so there are, of course, many deficiencies in the analyses. The data sources and the analysis techniques used by the NHC have been described by Wise and Simpson (1971). The 200 mb analysis includes both aircraft and satellite winds and is considered to be the most reliable upper air analysis. The ATOLL (~ 900 mb) is augmented by surface ship observations. These two levels are considered the best levels available in the tropics.

There were 22 named tropical cyclones in the Atlantic in the period 1975-1977. Hurricane Candice (1976) developed during a period for which no data were available. Hurricane Frances (1976) developed in a data void area in the Eastern Atlantic. The data available for that storm appeared to be grossly in error having the system directly under a vertical shear of greater than forty knots for the four twelve-hourly observation times prior to development. The existence of such large shear over a system at the point at which it becomes a named storm is in direct contradiction to all observational synoptic experience. It was considered sufficient reason to reject the data for that system.

Four storms, Doris (1975), Anna (1976), Holly (1976) and Babe (1977) had subtropical structure when they developed, including an upper level cold core and cyclonic circulation at 200 mb. Doris and Anna were officially numbered subtropical storms. The structure of Babe and Holly can be inferred from the archived upper level weather maps. Lawrence

(1977) states that for Holly:

"at 200 mb the flow was generally cyclonic over the developing storm as an upper low was located just to the north of the depression".

With regard to Babe, Lawrence (1978) states:

"gale-force winds within this band of convection led to the designation of Babe as a tropical storm..... This action was taken even though the system had not acquired tropical structure, in order not to confuse the public at a time of immediate threat"

At that time the storm was approaching the highly populated Gulf Coast.

For those reasons tropical cyclones Candice (1976), Frances (1976), Doris (1975), Anna (1976), Holly (1976) and Babe (1977) were removed from the data sample. For the remaining 16 tropical cyclones, the maps of the vertical shear of the zonal wind and of the meridional wind were examined for every 12 hours, beginning 60 hours before the point at which the system first reached a maximum sustained wind of 35 knots.

The former time is labelled -60, the latter 00.

Seven parameters were examined for each system. They are:

- (i) ΔU : the value of the vertical shear of the zonal wind at a point 6° latitude north of the position of the system minus the value of the shear at a point 6° south of the system; ΔU is proportional to $\partial/\partial y(-\partial U/\partial p)_{900-200mb}$;
- (ii) ΔV : the vertical shear of the meridional wind 6° west of the system minus the shear 6° east of the system; ΔV is proportional to $\partial/\partial x(\partial V/\partial p)_{900-200mb}$;
- (iii) $\Delta U + \Delta V$: this is proportional to $\zeta_{900mb} - \zeta_{200mb}$, averaged over the $0-6^{\circ}$ area;
- (iv) existence of a zonal zero line: the value of this parameter is YES if the vertical U shear is positive 6° to the north and negative 6° to the south; otherwise the value is NO;
- (v) existence of a meridional zero line: the value is YES if the vertical V shear is positive 6° to the west and negative 6° to the east;

- (vi) subjective existence of zonal zero line: the zero line often exists but does not meet the strict criteria of item (iv) above; for example the zonal zero line exists at position -60° for storm Amy shown in Fig. 4la, but the shear 6° to the south of the storm position is positive;
- (vii) subjective existence of meridional zero line.

The values of these parameters are listed for each 12-hour period for the 16 storms in Table 34 of the Appendix of this paper. Wind values are in knots.

Thirteen of the sixteen systems have high values of both ΔU and ΔV and also have both zonal and meridional zero lines existing prior to the cyclone development. The earliest consecutive three time periods having these characteristics for each system are underlined in the Appendix Table 34. Each of the 13 systems has ΔU and ΔV values both greater than 20 knots and both zonal and meridional zero lines during the underlined 3 time periods. The pattern typically sets up 48 hours prior to the time at which the system becomes a tropical storm. Three of the 16 systems, tropical storms Gloria (1976), Clara (1977) and Dorothy (1977), do not follow the pattern; given the paucity of synoptic observations over the Atlantic Ocean, this failing may be due to data problems.

The maps of zonal and meridional shear at representative times for the thirteen systems showing a positive response are displayed in Fig. 41. Point X on the figure is the position of the prestorm disturbance. Point T is the position at which it eventually becomes a named tropical storm. The important features of the figure are that every pre-storm disturbance has a large region of positive zonal shear to the north and negative zonal shear (shaded area) to the south. In the meridional shear it has a positive area immediately to the west and a negative area

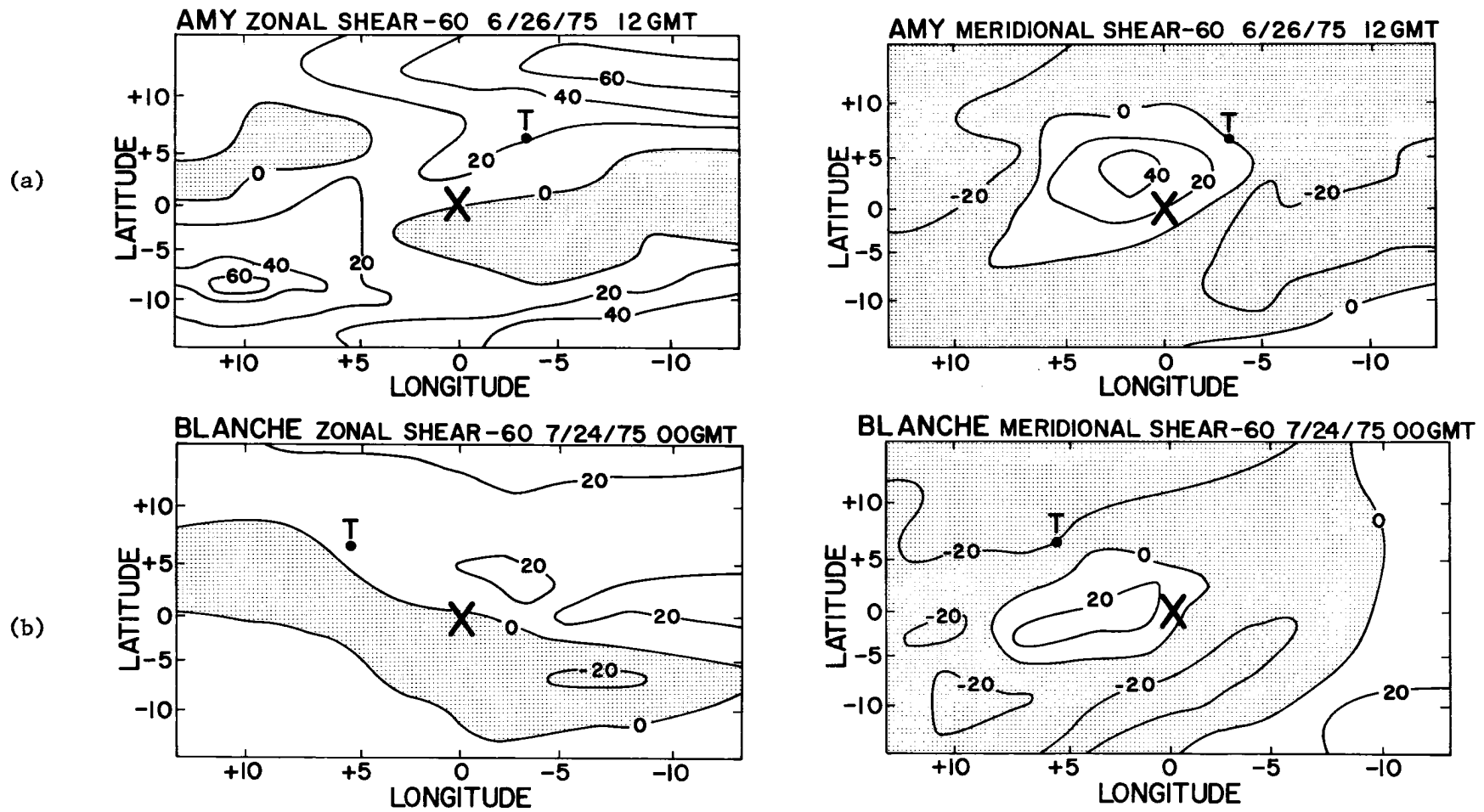


Fig. 4a-b. Maps of vertical shear (knots) of the zonal wind ($U_{200\text{mb}} - U_{\text{ATOLL}}$) and the meridional wind ($V_{200\text{mb}} - V_{\text{ATOLL}}$) surrounding pre-tropical storm disturbances. X marks the current position of the disturbances. T marks the position it will be in when it attains tropical storm status. The abscissa is degrees longitude; the ordinate is degrees latitude relative to the position of the disturbance. (a) is for 60 hours prior to the development of Tropical Storm Amy. (b) is for 60 hours prior to the development of Hurricane Blanche.

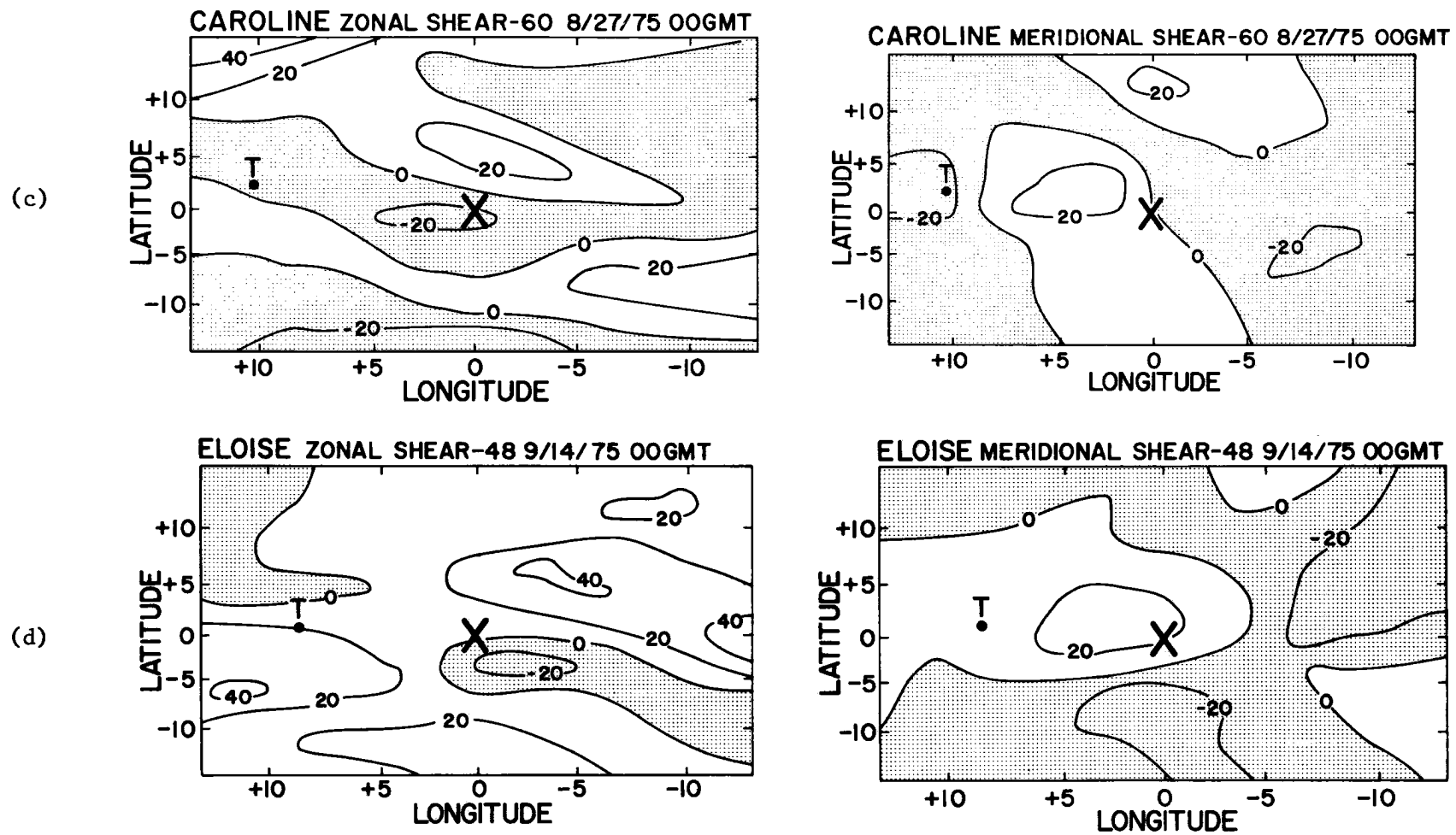


Fig. 41c-d. (c) 60 hours prior to the development of Hurricane Caroline. (d) 48 hours prior to the development of Hurricane Eloise.

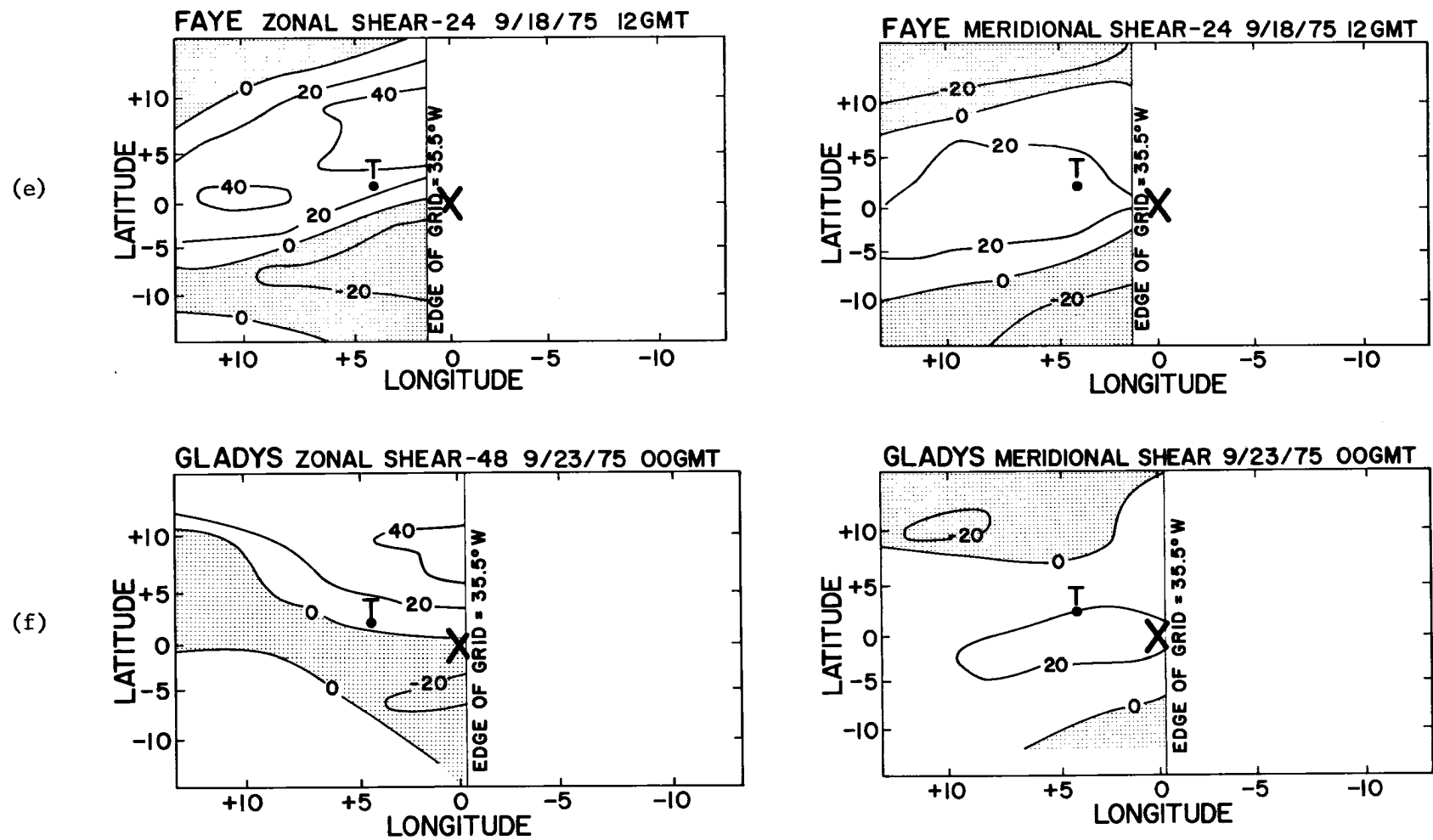


Fig. 4le-f. (e) 24 hours prior to the development of Hurricane Faye. (f) 48 hours prior to the development of Hurricane Gladys.

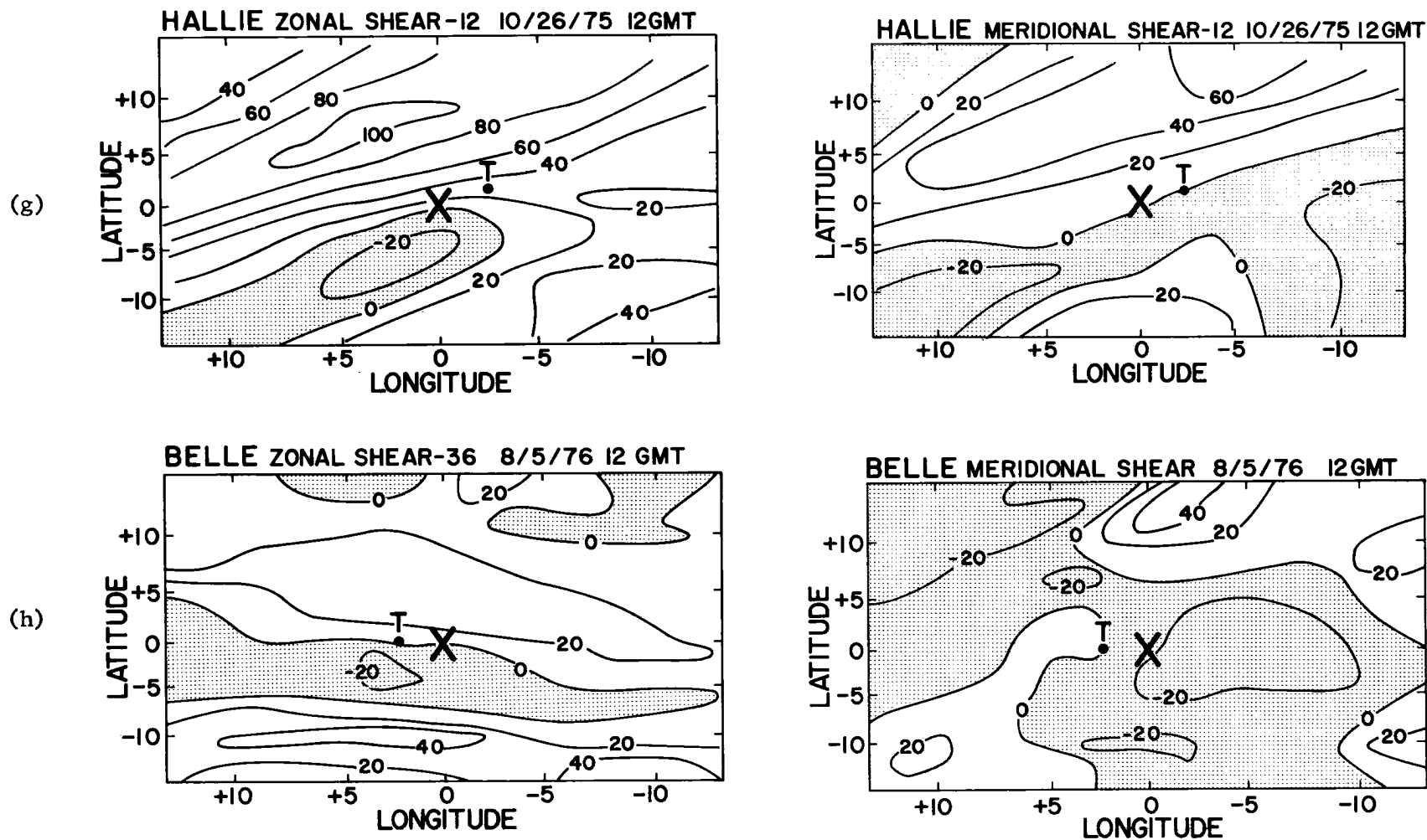


Fig. 41g-h. (g) 12 hours prior to the development of Tropical Storm Hallie. (h) 36 hours prior to the development of Hurricane Belle.

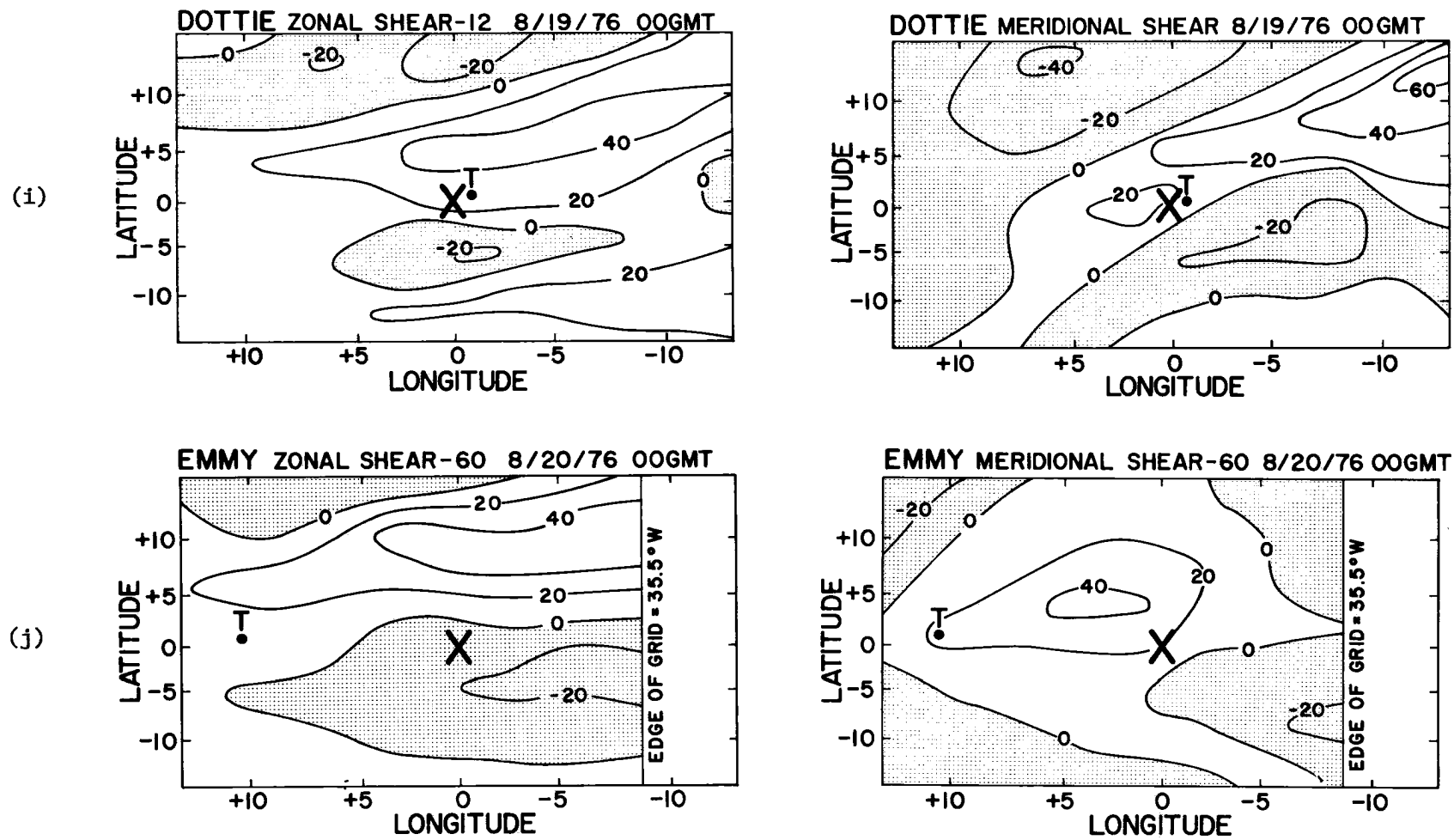


Fig. 41i-j. (i) 12 hours prior to the development of Tropical Storm Dottie. (j) 60 hours prior to the development of Hurricane Emmy.

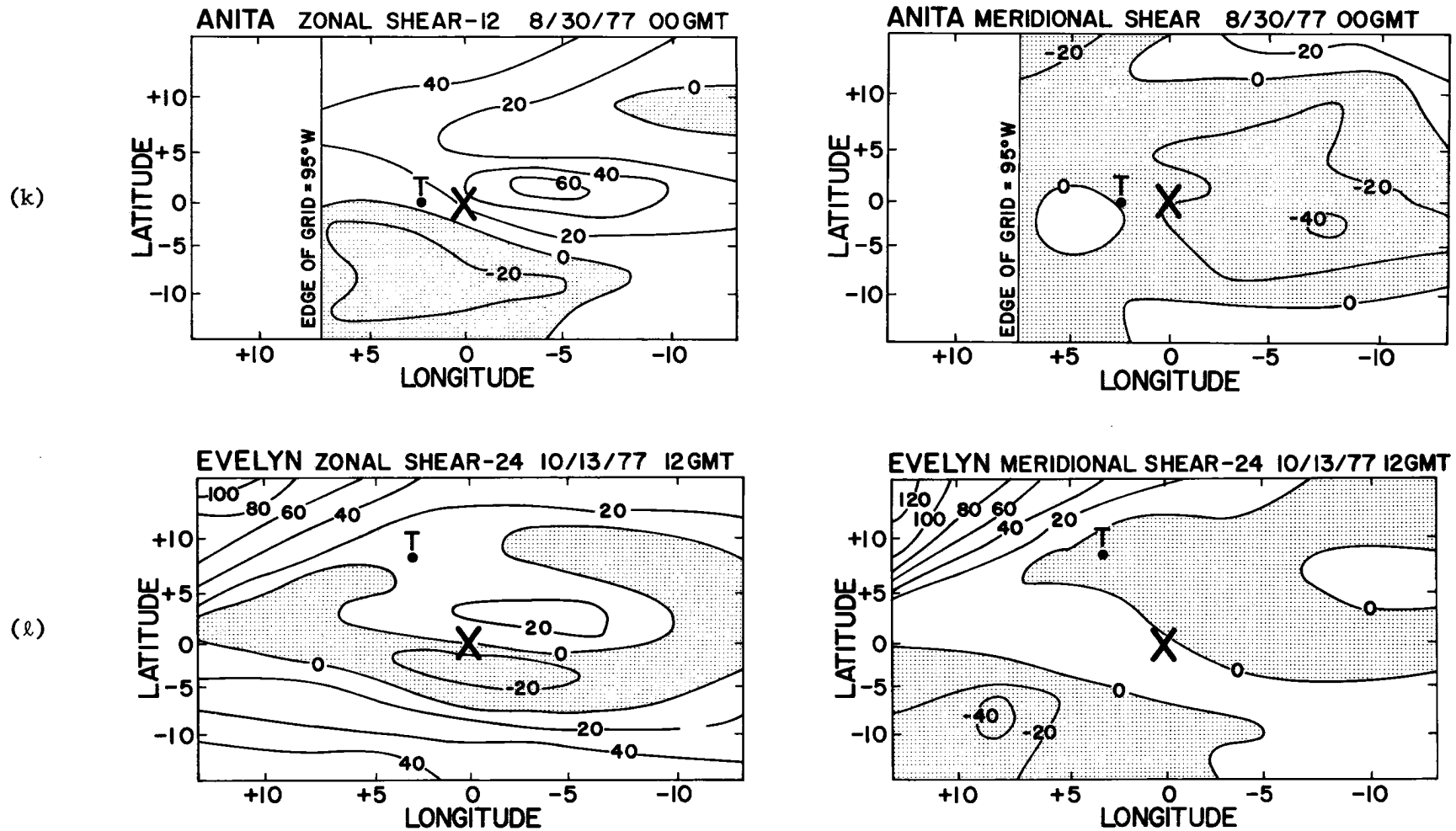


Fig. 41k-l. (k) 12 hours prior to the development of Hurricane Anita. (l) 24 hours prior to the development of Hurricane Evelyn.

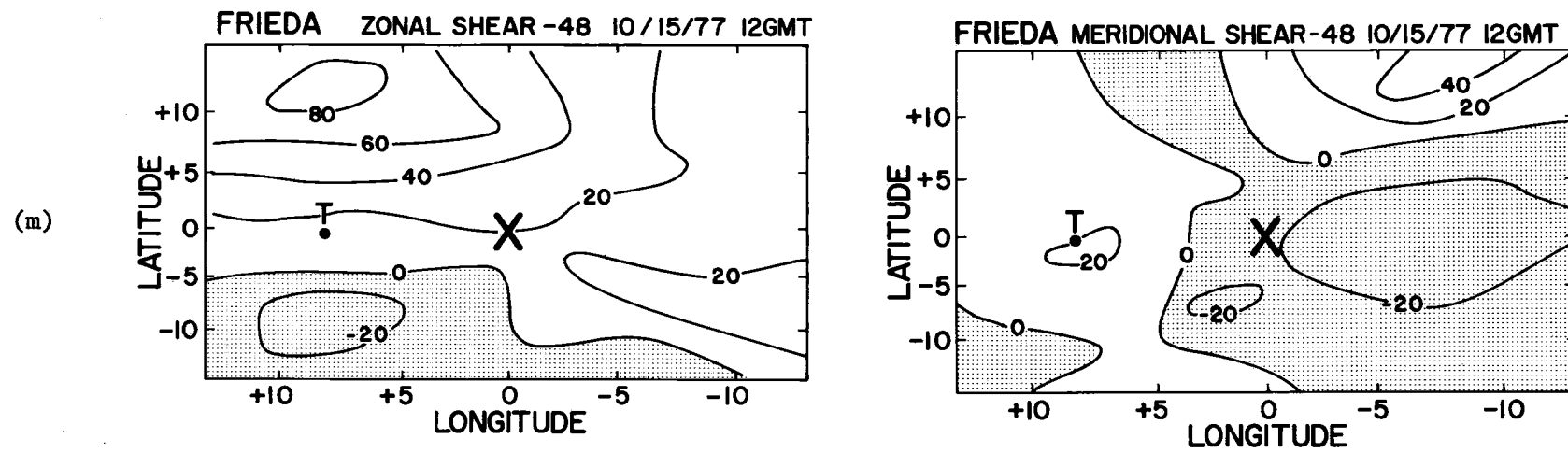


Fig. 41m. (m) 48 hours prior to the development of Tropical Storm Frieda.

to the east. The shears close to but not over the position of the disturbance are typically very large. It can be seen from the figure that this particular configuration of vertical shear extends over an area of 20 degrees latitude by 20 degrees longitude. It thus must be interpreted as being set up by the large scale surrounding flow rather than being caused by the disturbance itself.

The average values of ΔU , ΔV , $\Delta U + \Delta V$ and the number of YES and NO values for the zonal and meridional zero lines are shown in Table 15. The average values for the three earliest time periods having the required shear patterns are given in Table 16. For five systems the pattern is already established 60 hours before the storm develops. For four systems it sets up 48 hours before, for one system 36 hours before and for one system 24 hours. For tropical cyclone Dottie (1976) no data are available before point -24, but as shown in Fig. 4li the zero lines and high shear gradients are well established by that time.

Based on the above results it must be concluded that prior to the development of a tropical cyclone in the Western Atlantic it is necessary to have values of ΔU and ΔV both greater than 20 knots and also for there to simultaneously exist an east-west extending line of zero vertical shear of the zonal wind centered on the disturbance with positive shear to the north and negative shear to the south, and a north-south extending line of zero vertical shear of the meridional wind with positive shears to the west and negative shears to the east.

6.2 Atlantic depressions

An investigation was also performed on the transition from cloud cluster to tropical depression. Results for the storms of section 6.1

TABLE 15

Mean characteristics of the patterns of vertical shear for the sixteen pre-tropical storm disturbances. Values are in knots. ΔU is proportional to $\partial/\partial y(-\partial U/\partial p)_{900-200\text{mb}}$; ΔV is proportional to $\partial/\partial x(\partial V/\partial p)_{900-200\text{mb}}$; $\Delta U + \Delta V$ is proportional to $\zeta_{900\text{mb}} - \zeta_{200\text{mb}}$, averaged over the $0-6^\circ$ radius area centered on the system.

<u>Position</u>	<u>ΔU</u>	<u>ΔV</u>	<u>$\Delta U + \Delta V$</u>	<u>Zonal Zero Line</u>	<u>Meridional Zero Line</u>
-60	11	7	18	3 YES 10 NO	5 YES 8 NO
-48	17	10	24	6 YES 7 NO	7 YES 5 NO
-36	28	18	46	9 YES 5 NO	6 YES 7 NO
-24	35	27	64	8 YES 5 NO	9 YES 4 NO
-12	50	34	82	12 YES 4 NO	11 YES 4 NO
00	54	33	86	12 YES 4 NO	9 YES 6 NO
Mean	33	22	53	50 YES 35 NO (59%, 41%)	47 YES 34 NO (58%, 42%)

TABLE 16

Mean characteristics of the patterns of vertical shear for the three optimum time periods prior to the development of each tropical storm (values are in knots). These are not the three time periods with the highest values, but rather the earliest three time periods showing the required shear pattern. ΔU is proportional to $\partial/\partial y(-\partial U/\partial p)_{900-200\text{mb}}$; ΔV is proportional to $\partial/\partial x(\partial V/\partial p)_{900-200\text{mb}}$; $\Delta U + \Delta V$ is proportional to $\zeta_{900\text{mb}} - \zeta_{200\text{mb}}$, averaged over the $0-6^\circ$ radius area centered on the system.

<u>ΔU</u>	<u>ΔV</u>	<u>$\Delta U + \Delta V$</u>	<u>Zonal Zero Line</u>	<u>Meridional Zero Line</u>
—	—	—	28 YES 7 NO (80%, 20%)	25 YES 4 NO (86%, 14%)
37	28	65		

are presented in Table 17. Of the 16 storms pre-depression data were available for only 11. Here point -48 is 48 hours prior to the time at which the system was first designated a tropical depression (point 00).

Table 17 should be compared with the similar data relative to the point at which the system becomes a storm in Table 15. The total vorticity genesis parameter, $\Delta U + \Delta V$ is only 27 knots at the point at which the system becomes a depression as compared with 82 knots twelve hours before it becomes a storm. It has a 50% score for the presence of zonal zero lines and a 33% score for meridional zero lines at the depression stage, compared with 75% and 73% twelve hours prior to storm development. This implies that the establishment of the zero lines and the strong shear are more relevant to the transition to tropical storm than to the transition to depression.

TABLE 17

Mean characteristics of the vertical shear 48 hours, 24 hours and zero hours prior to the time at which the system is designated a tropical depression. Statistics are for the same systems that went into Table 15. ΔU is proportional to $\partial/\partial y(-\partial U/\partial p)_{900-200\text{mb}}$; ΔV is proportional to $\partial/\partial x(\partial V/\partial p)_{900-200\text{mb}}$; $\Delta U + \Delta V$ is proportional to $\zeta_{900\text{mb}} - \zeta_{200\text{mb}}$, averaged over the $0-6^\circ$ radius area centered on the system.

<u>Position</u>	<u>ΔU</u>	<u>ΔV</u>	<u>$\Delta U + \Delta V$</u>	<u>Zonal Zero Line</u>	<u>Meridional Zero Line</u>
-48	6	-11	-5	2 YES 9 NO	1 YES 10 NO
-24	22	5	27	5 YES 5 NO	3 YES 7 NO
00	19	8	27	5 YES 5 NO	3 YES 6 NO

6.3 Atlantic non-developing systems

From the period for which zonal and meridional shear data were available, tracks were made up for 63 tropical systems which did not

later develop into tropical storms. The positions for these systems were obtained as follows:

Non-developing tropical depressions (16 systems): The official tracks of Atlantic depressions were used as obtained from the National Hurricane Center. Only systems were used that died over the ocean. (Systems are from the 1975, 1976 and 1977 seasons.)

Dvorak systems (8 systems): These systems are from the same source as the systems making up the Atlantic cloud cluster N1 data set of Chapters 1 to 5. (Systems from 1975.)

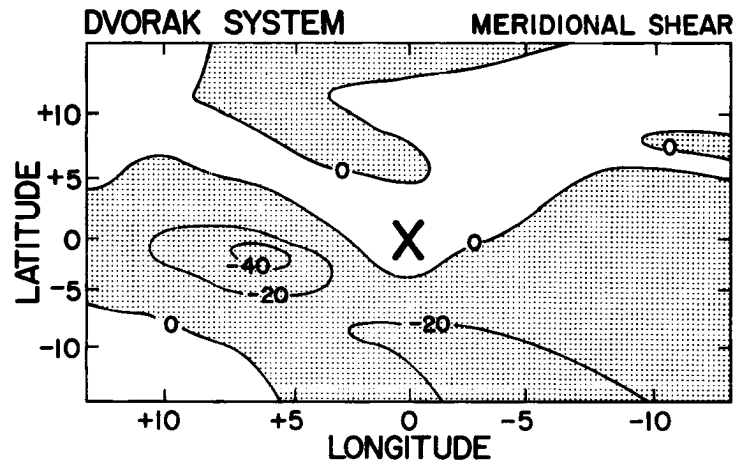
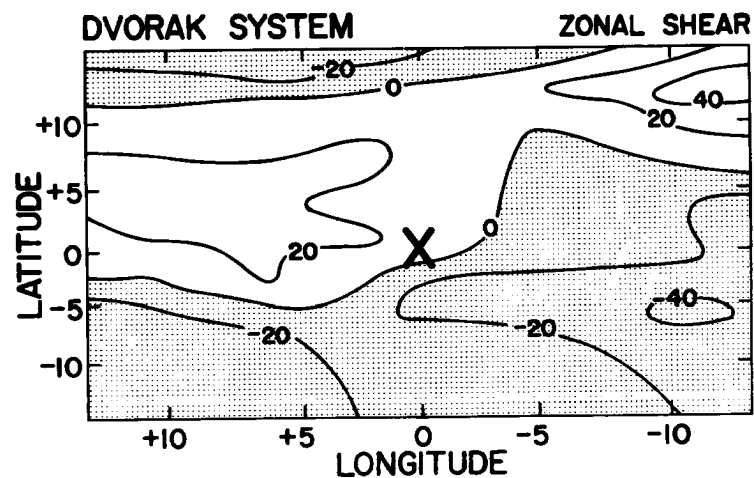
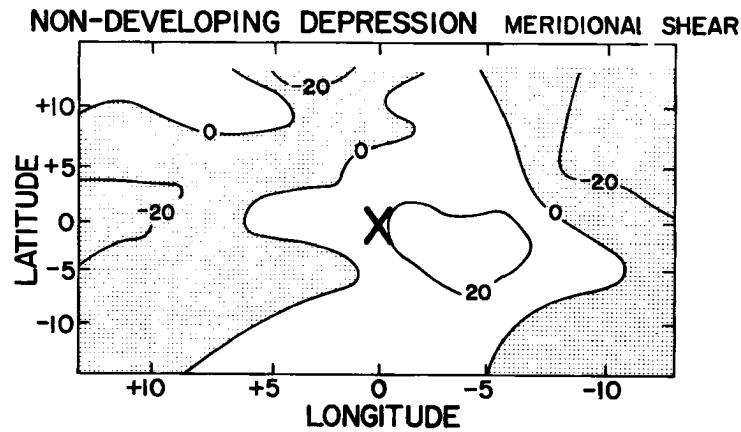
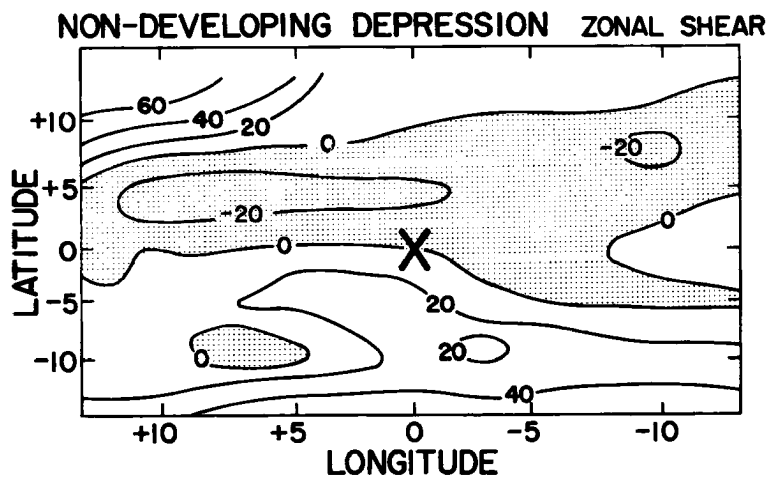
Frank systems (11 systems): These systems are from the same source as the systems making up the Atlantic wave trough cluster N2 data set of Chapters 1 to 5. (Systems from 1975.)

Shapiro systems (11 systems): Shapiro (1977a, b) of the National Hurricane and Experimental Meteorology Laboratory, NOAA, has also studied the differences between developing and non-developing tropical disturbances. The tracks of the systems which he used as non-developing cases were provided by him for this study. (Systems from 1976, 1977.)

McBride systems (17 systems): The author picked positions of prominent conservative (lifetime greater than 24 hours) cloud clusters in the Western Atlantic from geosynchronous satellite imagery. (Systems from 1976, 1977.).

Shear patterns for these systems were analyzed at only 12 GMT, though at least 2 satellite pictures per day were used in the actual positioning of the systems. For the 63 disturbances vertical shear data were available at 178 different 12 GMT time periods, an average of 2.8 per system. Four randomly chosen examples of the zonal and meridional vertical shear patterns surrounding the positions (marked X) of non-developing disturbances are shown in Fig. 42. The mean values of the shear parameters for the non-developing systems are shown in Table 18. The actual values at each of the 178 time periods are listed in the Appendix, Tables 36-43.

All the non-developing systems have very low values of ΔV . A zonal zero line exists for 25 percent of the positions and a meridional zero



101

Fig. 42. Maps of vertical shear of the zonal and meridional wind surrounding four non-developing tropical disturbances. The disturbances correspond to position numbers 2, 41, 81 and 94 listed in Appendix A.5.

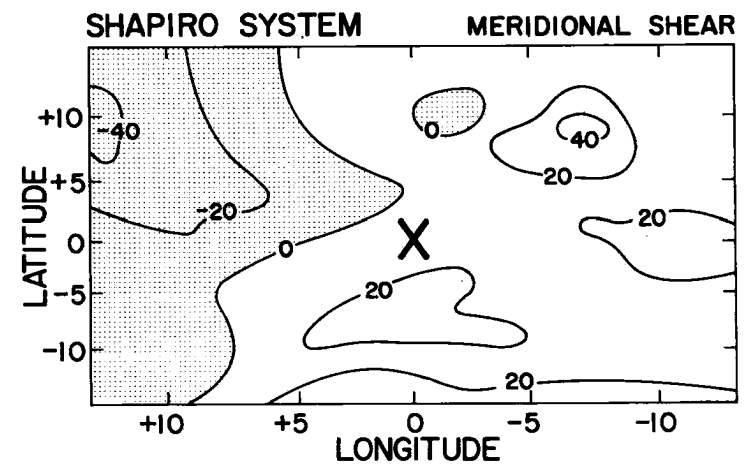
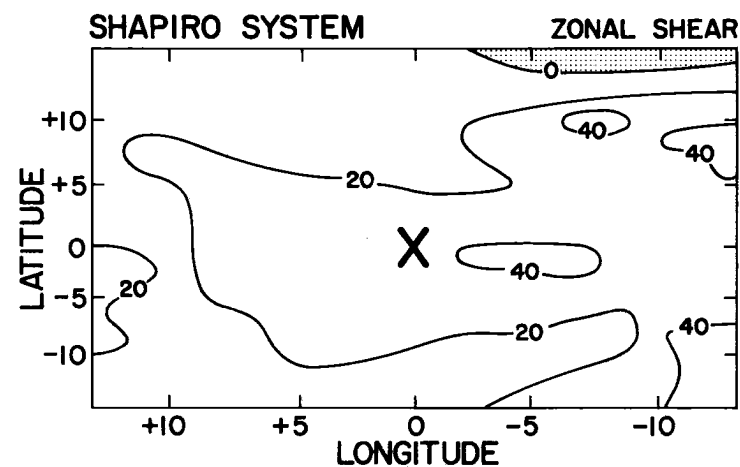
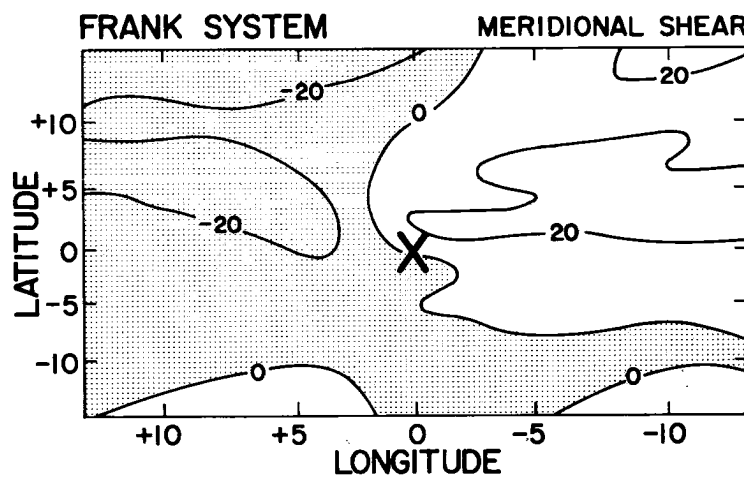
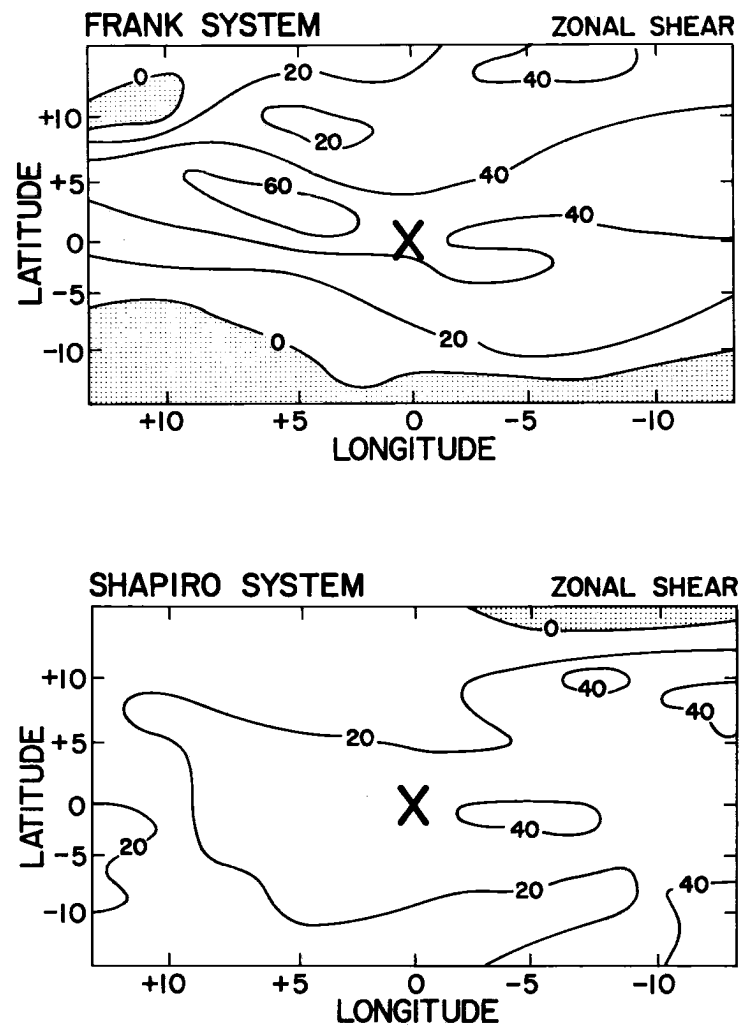


Fig. 42. Continued.

TABLE 18

Mean properties of the vertical shear for the 63 non-developing disturbances (values in knots). ΔU is proportional to $\partial/\partial y(-\partial U/\partial p)_{900-200\text{mb}}$; ΔV is proportional to $\partial/\partial x(\partial V/\partial p)_{900-200\text{mb}}$; $\Delta U + \Delta V$ is proportional to $\zeta_{900\text{mb}} - \zeta_{200\text{mb}}$, averaged over the 0-6° radius area centered on the system.

	<u>No. of Systems</u>	<u>No. of Positions</u>	ΔU	ΔV	$\Delta U + \Delta V$	Zonal Zero Line	Meridional Zero Line
Non-developing depressions	16	35	-1	-1	-2	3 YES 32 NO	11 YES 24 NO
Dvorak systems	8	25	23	-4	19	17 YES 8 NO	3 YES 22 NO
Frank systems	11	25	8	-13	-5	10 YES 15 NO	2 YES 23 NO
Shapiro systems	11	56	15	1	16	11 YES 45 NO	13 YES 43 NO
McBride systems	17	37	2	-7	-5	4 YES 33 NO	4 YES 33 NO
<hr/>							
	63	178	9	-4	5	45 YES 133 NO (25%, 75%)	33 YES 145 NO (19%, 81%)

line for 19 percent. This compares with 46 percent and 58 percent for prehurricane systems 48 hours before development.

It does seem, however, from Table 18 that large values of ΔU or ΔV shear or the existence of a zero line are fairly frequent events in the Western Atlantic. The important factor for tropical cyclone genesis is whether they exist concurrently and whether they persist for more than one day.

The 178 non-developing positions were examined for the concurrent appearance of (i) ΔU greater than 20 knots, (ii) ΔV greater than 20 knots, (iii) the existence of a zonal zero line, and (iv) the existence of a meridional zero line.

There were only 14 positions out of 178 (or 8%) such that three of the four criteria were met. By contrast, for the 16 developing systems considered in section 6.2, 13 (or 82%) of them had a period of at least 36 hours, such that 3 of the 4 criteria were met, sometime in the 60 hours prior to cyclone development.

Of the 63 non-developing systems only 2 (or 3%) had more than one time period satisfying 3 of the 4 criteria. If the vertical shear criteria were being used to predict cyclone genesis, these two systems (one Shapiro system and one Dvorak system) would have been predicted to develop. The shear criteria therefore appear to slightly overpredict genesis.

In summary, for the hurricane season of 1975-1977 in the Western Atlantic, the use of the vertical shear data would have correctly predicted the development of 13 out of 16 tropical storms. It would have correctly predicted non-development for 61 out of 63 non-developing

weather systems. The skill of operational forecasting of tropical cyclones is much below this success rate.

6.4 Pacific pretyphoon versus non-developing cloud clusters

In the Western Pacific no grid point data on vertical shear were available. Nevertheless, a limited test on the use of vertical shear as a predictor of tropical storms in this area was performed by subjectively picking wind values around clusters off weather maps. Typical examples of Joint Typhoon Warning Center (JTWC) Guam operational analyses at the surface and at 200 mb are shown in Fig. 43. Positions were tabulated for non-developing and pretyphoon cloud clusters from the years 1972 and 1974. Values of the U and V component of the wind at 200 mb and the surface were estimated from the weather maps at points 6° to the north, 6° to the south, 6° to the east and 6° to the west of each cluster. The positions of the clusters were those obtained in the DMSP satellite study of S. Erickson (1977). Weather maps were available at 182 time periods for 18 pretyphoon clusters and 31 non-developing cloud clusters. The wind values were picked off the weather maps without the knowledge of whether the position was for a developing or a non-developing system.

This method is crude, since there is no consistent and detailed wind information around most systems and guesses had to be made. The values are also biased greatly by whether or not the operational analyst drew either an upper level anticyclone or a low level cyclone over the system. Despite these drawbacks the method shows some predictive skill.

Wind values at all different time periods for a particular system were averaged together to yield one value per system. From the

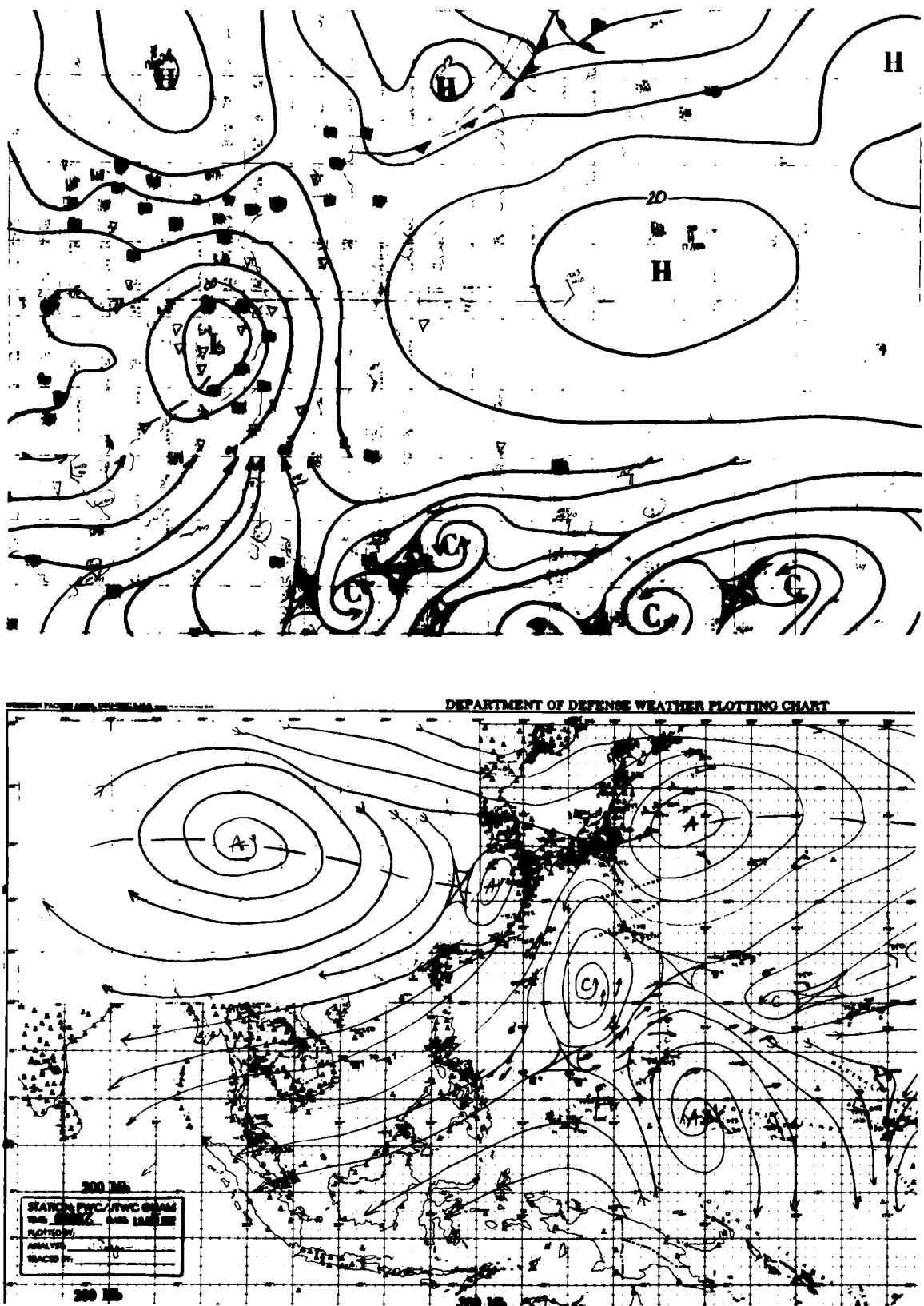


Fig. 43. Typical JTWC Guam operational analyses at the surface and 200 mb. Maps are for 00 GMT, 8/18/1972.

resultant numbers three parameters were extracted: (i) a value of $\Delta U + \Delta V$, following the same convention as used in the Atlantic, (ii) the existence of a zero line in the vertical shear of the zonal wind, and (iii) the existence of a zero line in the vertical shear of the meridional wind. The actual values of each parameter for each system are listed in the Appendix, Table 44.

The results are summarized in Table 19. Both the values of $\Delta U + \Delta V$ and the percentage of systems with zero lines are significantly greater for the developing systems.

The systems which had high values of $\Delta U + \Delta V$ were usually the same systems that had zero lines. Using the criteria that to develop into a typhoon a system must have zero lines in both zonal and meridional shear, the data give 10 out of 18 (56%) correct answers for the developing systems and 25 correct out of 31 (81%) for the non-developing.

Using the criteria that a system must have a mean value of $\Delta U + \Delta V$ greater than 40 knots gives 11 correct developing systems (61%) versus 22 correct (71%) non-developers.

Using the criteria that 2 out of the 3 conditions, zero line in zonal shear, zero line in meridional shear and $\Delta U + \Delta V$ greater than 40 knots, be met yields 11 correct developing systems (61%) and 21 correct non-developing predictions (68%).

These results are not as good as were obtained in the previous sections for the Atlantic, but they are very encouraging when the crudity of the approach and the poor quality of the Pacific wind data are taken into account.

In the Atlantic only vertical shear data were available, but in the Pacific separate wind values were used from each level. This allows

TABLE 19

Mean properties of the vertical shear (knots) for the Pacific pretyphoon and non-developing cloud clusters. $\Delta U + \Delta V$ is proportional to $\zeta_{900\text{mb}} - \zeta_{200\text{mb}}$, averaged over the $0-6^{\circ}$ radius area centered on the system.

	<u>$\Delta U + \Delta V$</u>	<u>Zonal Zero Line</u>	<u>Meridional Zero Line</u>
Non-developing systems (31 systems)	25	21 YES 10 NO (68%, 32%)	8 YES 23 NO (26%, 74%)
Developing systems (18 systems)	45	15 YES 3 NO (83%, 17%)	12 YES 6 NO (67%, 33%)

the opportunity to evaluate the magnitude of the separate contribution from each level, upper and lower, to $\Delta U + \Delta V$. U and V values of the wind added together with the appropriate signs give a contribution to $\Delta U + \Delta V$ at the surface of 16 knots (developing) versus 10 knots (non-developing). At 200 mb the contribution is 29 knots (developing) versus 15 knots (non-developing). This is tabulated in Table 20. The table shows that both the upper level and the lower level make important contributions to the observed differences in vertical shear between developing and non-developing weather system.

TABLE 20

$\Delta U + \Delta V$ (knots) for the Pacific cloud clusters. $\Delta U + \Delta V$ is proportional to $\zeta_{900\text{mb}} - \zeta_{200\text{mb}}$, averaged over the $0-6^{\circ}$ radius area centered on the system.

	<u>Contribution from the Surface</u>	<u>Contribution from 200 mb Level</u>	<u>Total</u>
Non-developing systems	10	15	25
Developing systems	16	29	45
Ratio of Developing/Non-developing	1.6/1	1.9/1	1.8/1

7. LARGE SCALE FLOW SURROUNDING THE PRE-STORM SYSTEM

7.1 The influence of external systems

The composite fields presented in Chapters 3 and 4 and the individual case studies presented in Chapter 6 have clearly demonstrated that an important prerequisite for tropical cyclone development is the simultaneous presence of upper level anticyclonic vorticity and low level cyclonic vorticity both over a large area, at least of the order of a 12° diameter circle. These features can be seen clearly on the NOAA operational National Hurricane Center 200 mb and surface analyses shown in Figs. 44 to 47.

Figure 44 shows the 200 mb level and surface maps 48 hours before the point at which Hurricane Eloise (1975) was named a tropical storm. The position of the prestorm depression is marked with a cross. A very large area of anticyclonic flow at 200 mb is already apparent. The source of this anticyclonic flow is three upper level cold lows to the west, the far north and the northeast of the system. The surface map for the same time shows a large area in which the flow has a cyclonic tangential component relative to the position of the disturbance. This flow is associated with a subtropical high to the northeast.

Figure 45 shows the maps 48 hours before the development of Gladys (1975). Once again a large area of upper level anticyclonic flow (outlined) and low level cyclonic flow (outlined) surround the system. The source of this flow is once again the surrounding weather systems.

Figure 46 for 60 hours before the development of Faye (1975) and Fig. 47 for 48 hours prior to Frieda (1977) show the same features.

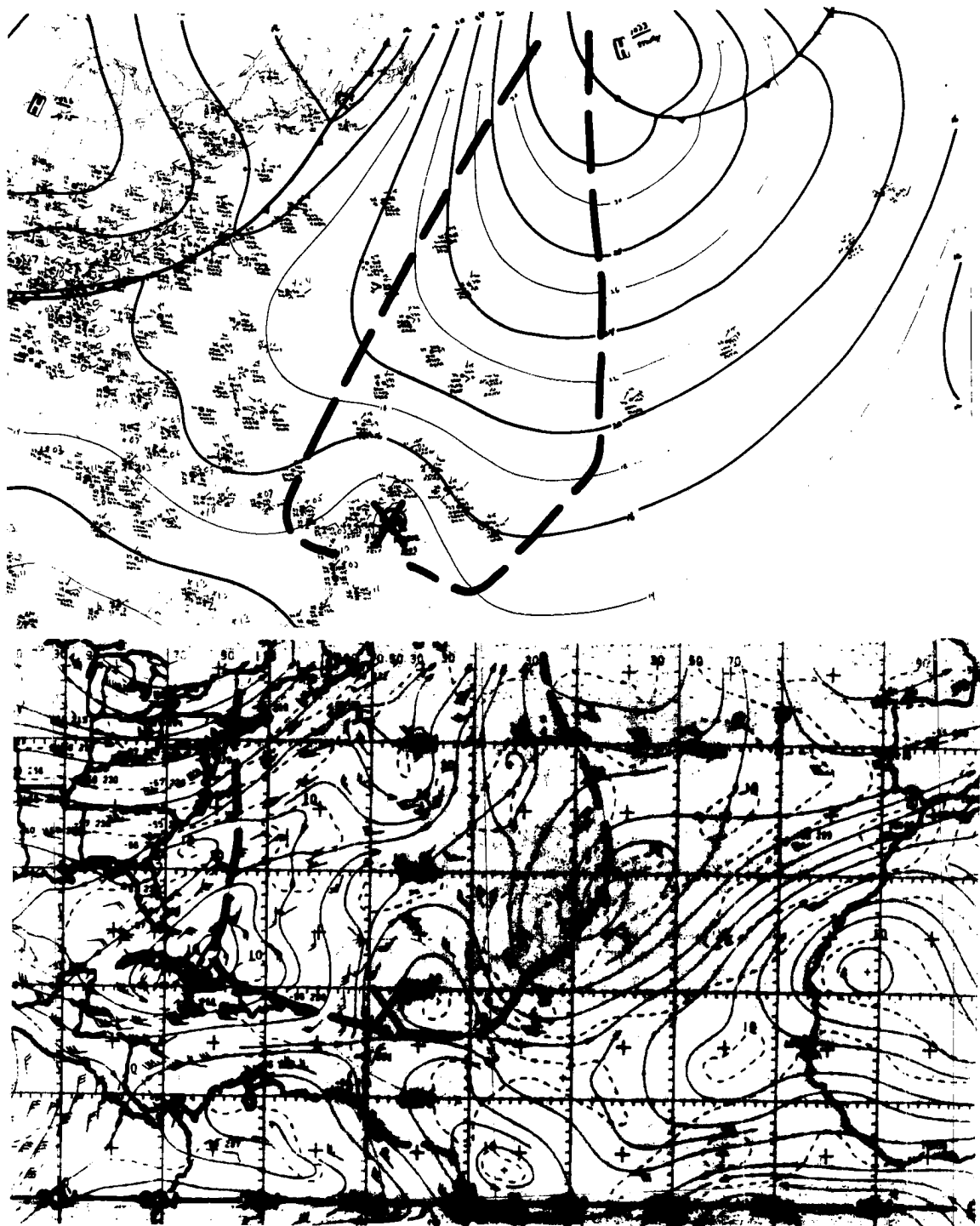


Fig. 44. Operational NHC surface and 200 mb analyses 48 hours before the time at which Hurricane Eloise (1975) first attained a maximum sustained wind speed of 35 knots. X marks the position of the pre-storm disturbance. The outlined region on the surface map marks the area where the wind has a cyclonic tangential component relative to the position of the disturbance. The outlined region on the 200 mb map marks the area where the wind has an anticyclonic tangential component relative to the position of the disturbance.

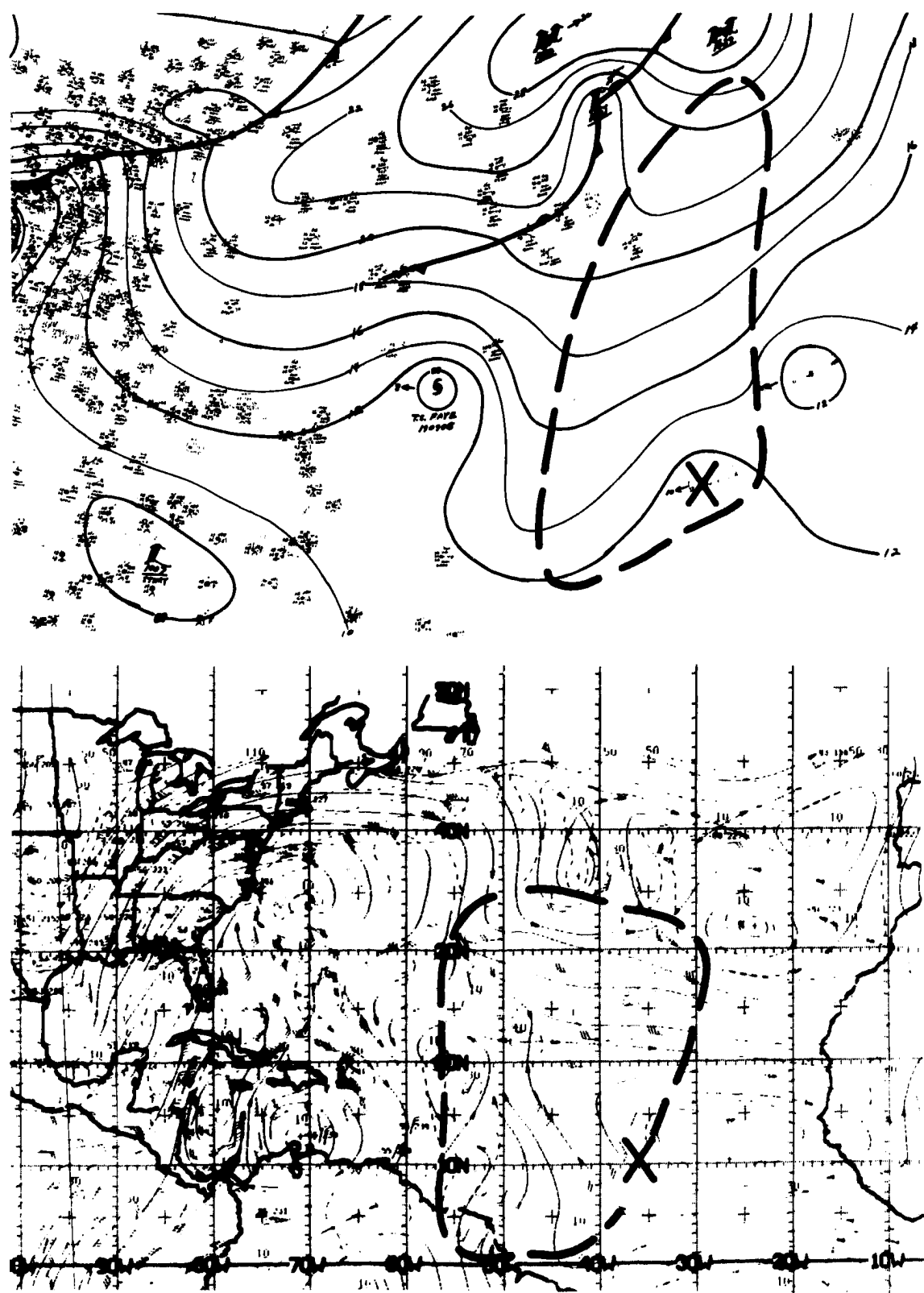


Fig. 45. Same as Fig. 44 but for 48 hours before the development of Gladys (1975).

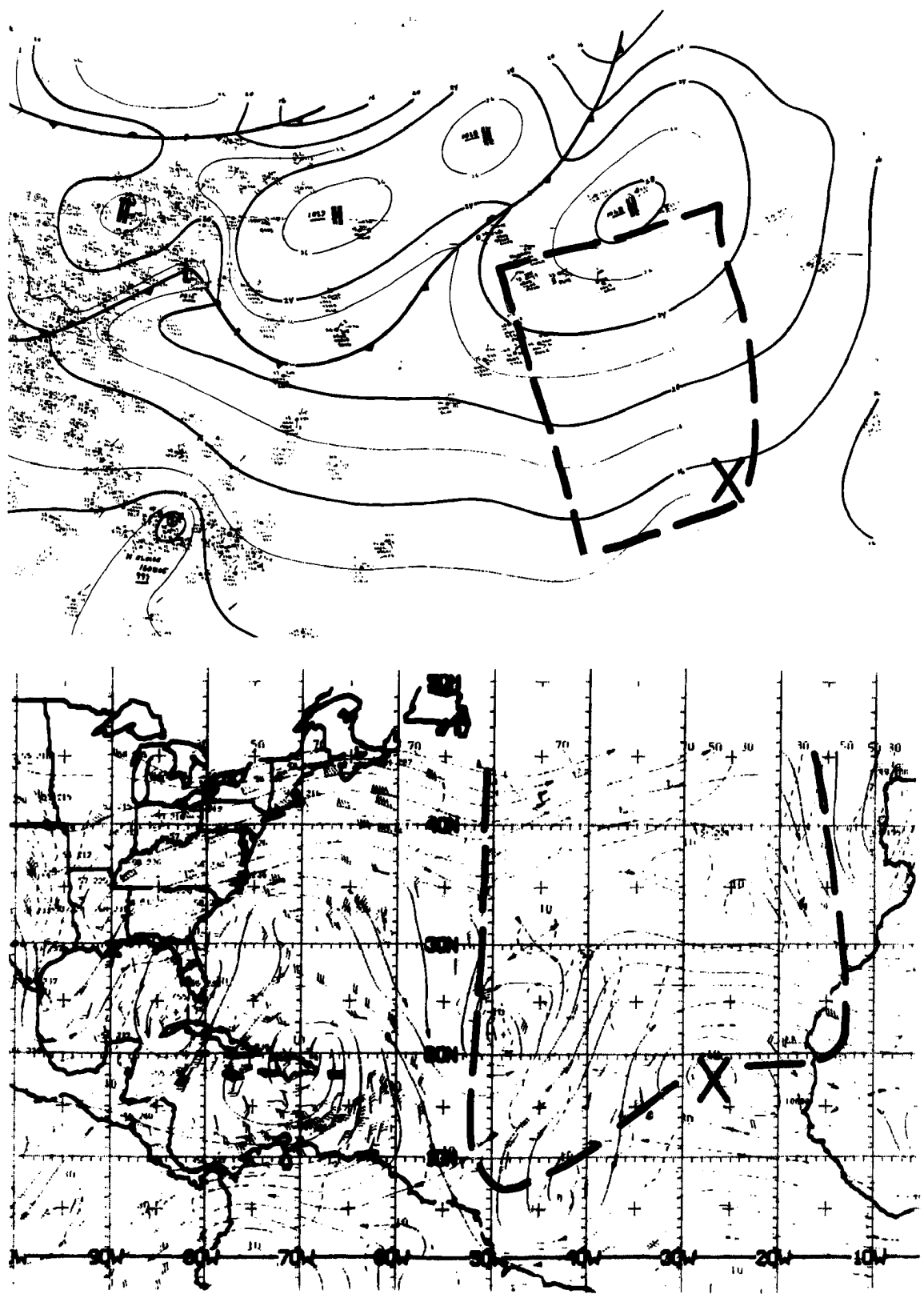


Fig. 46. Same as Fig. 44 but for 60 hours before the development of Faye (1975).

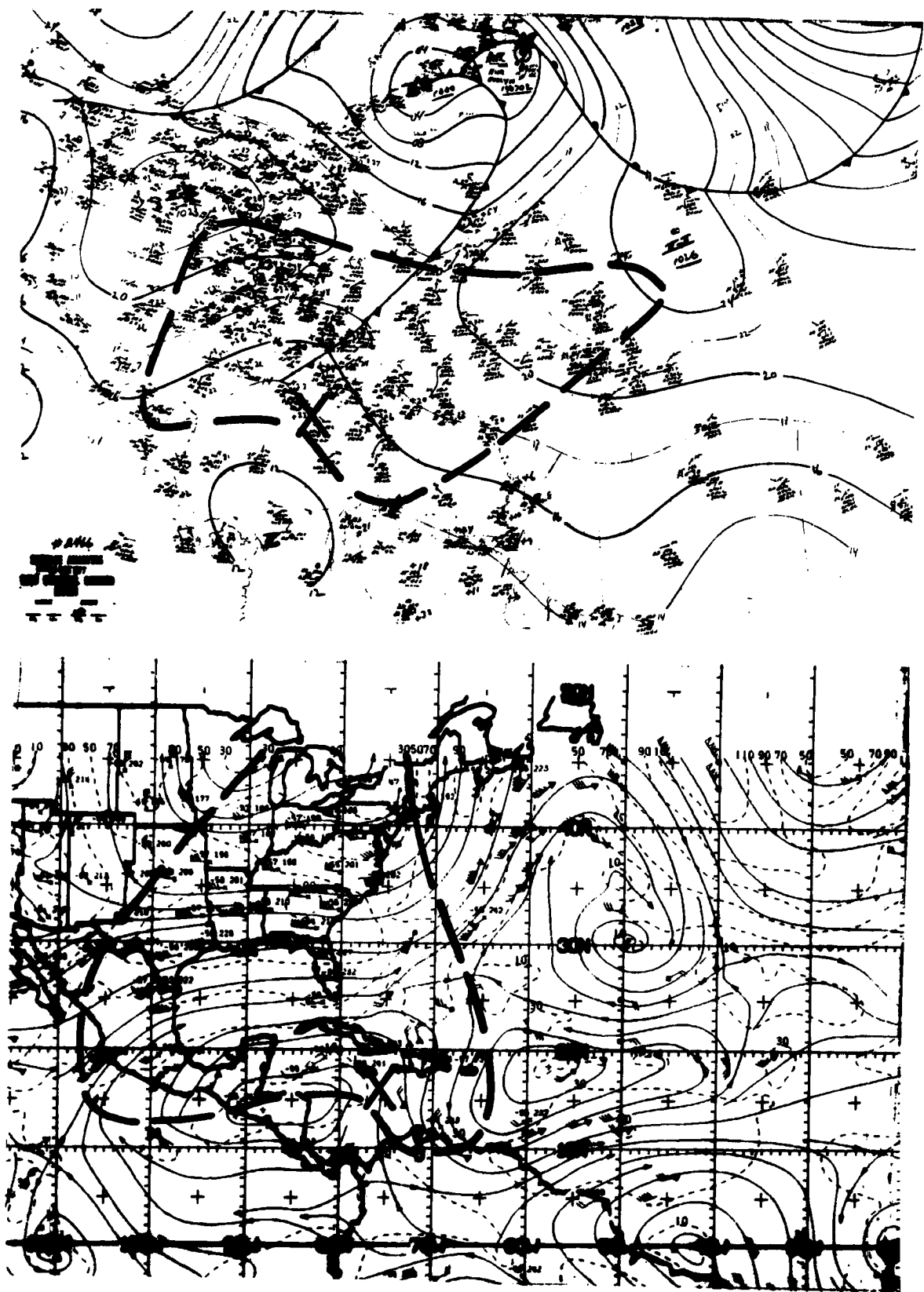


Fig. 47. Same as Fig. 44 but for 48 hours before the development of Frieda (1977).

For these cases there can be no doubt that large scale upper level anticyclonic flow and low level cyclonic flow exist over the area of the disturbance well before the time at which it becomes a tropical cyclone. This has particular significance in the upper levels because most previous works on tropical cyclone structure and development have included either the explicit or implicit assumption that the large upper level negative tangential winds around the system are the result of the Coriolis force acting on the outflowing air. Figures 44 to 47 reveal that at least in the early stages of development the surrounding region anticyclonic flow is the result of already existing mid-latitude westerlies to the north, equatorial easterlies to the south and large scale upper level troughs and ridges to the east and west. The source of the anticyclonic flow is thus external rather than internal to the developing system.

Is this also true once the system has become a fully developed hurricane or typhoon? The data indicate that it probably is. Figure 48 shows streamlines at the outflow level for the stage D4 typhoon and hurricane composite fields in each ocean. Both the Atlantic D4 composite hurricane and the Pacific D4 composite typhoon exist in the center of a large region of upper level negative tangential wind. A subjective appraisal of the figure indicates that much of this flow is the midlatitude westerlies flowing past to the north and the equatorial easterlies flowing past to the south.

Figure 49 shows plan views for the two systems of the radial component of the wind V_R at the outflow level. The Pacific system has two well defined outflow channels, one to the northeast and one to the southwest. The Atlantic system has only the one to the northeast.

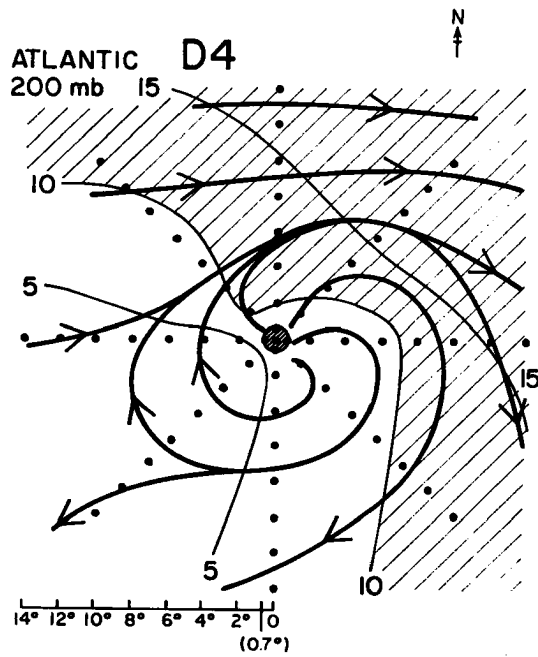
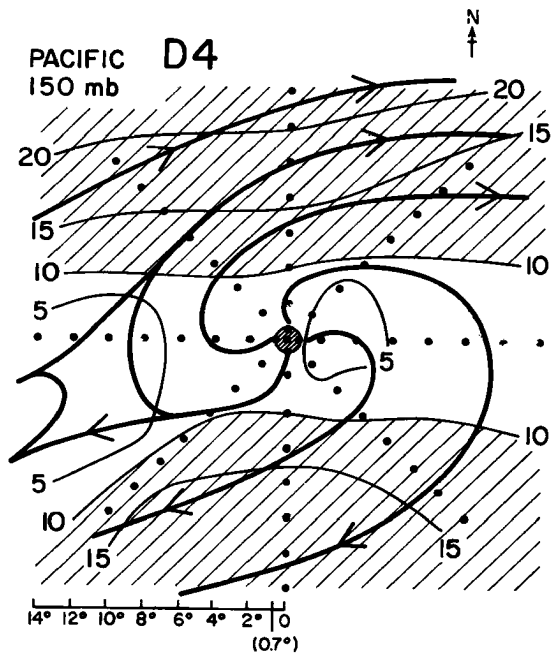


Fig. 48. Streamline and isotach analyses (m s^{-1}) at the outflow level for the stage D4 (typhoon and hurricane) composite system in each ocean.

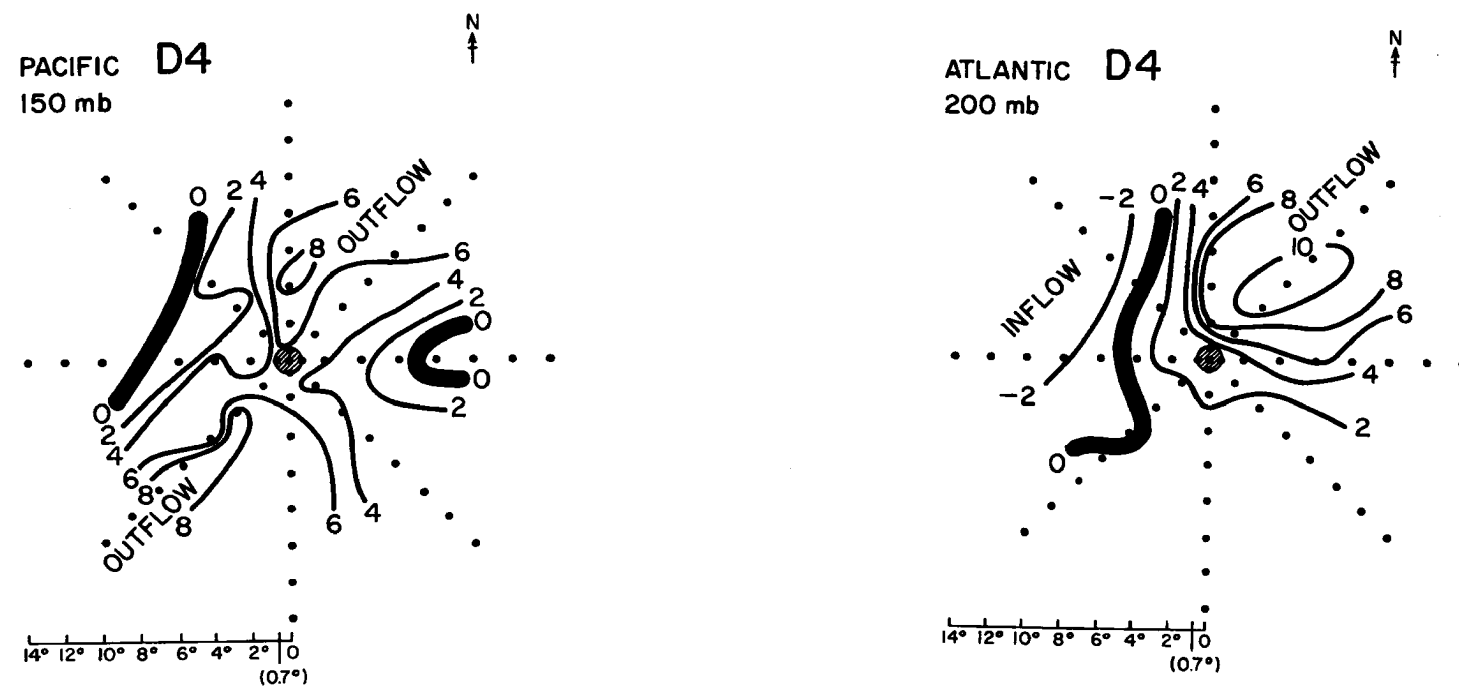


Fig. 49. Plan views of V_R (m s^{-1}) at the outflow level for the stage D4 (typhoon and hurricane) composite system in each ocean.

These features have been noted previously by W. Frank (1977a) and by Núñez and Gray (1977). A further look at the outflow plan views in Fig. 48, however, reveals that the outflow channels are not really representative of trajectories of air blowing directly out from the center of the cyclone, but rather are the radial component of the westerlies and easterlies blowing past the system. In other words, the outflow locations are primarily associated with the large scale surrounding circulations which happen to orient their flow pattern in a radial direction. The outflow is thus not an entity in itself but is strongly related to the surrounding region flow configuration.

In Chapter 2, Fig. 5, the mean upper level wind for the Northern Hemisphere summer months was shown. Referring back to that figure it can be seen that the mean position of the Pacific composite data sets has well defined westerlies to the north and also easterlies to the south. Thus, the composite D4 typhoon has two outflow channels or regions of anticyclonic flow, one being the system's link to the westerlies and the other its link to the easterlies.

In the mean position of the Atlantic composites, the easterlies to the south are very weak and poorly defined; thus the composite system does not typically link up with any anticyclonic large scale flow south of it, and there is no clearly defined negative tangential wind region or outflow region southwest of the system.

This interpretation of the regions to the northeast and southwest being predominantly regions of residual environmental negative tangential wind rather than regions of storm developed anticyclonic outflow depends on the concept of the storm circulation forming a link to the middle latitude westerlies and the equatorial easterlies. It belies

the principle of the source of the anticyclonic flow being spin-down of outflowing air.

This principle can be expressed mathematically by the conservation of absolute angular momentum, $M = RV_T + f R^2/2$. R is the radius; V_T is the tangential component of the wind and f is the Coriolis parameter.

Plan views of M at the outflow level are shown in Fig. 50. If the storm were a simple in, up and out circulation, then one would expect to see channels of constant M in the same region as the outflow channels on Fig. 49. No such regions exist on the plan views of absolute angular momentum, M . The dominant effects displayed on Fig. 50 are the increase of $(f R^2/2)$ with increasing R , and the increase of $(f R^2/2)$ with increasing latitude.

Of course air trajectories must obey the physical laws of motion; so M must be conserved in outflowing air. The figure shows that the storm circulation is not a simple one of air blowing in at low levels and out at upper levels. There is a large amount of cumulus mass recycling in the region of the storm (Gray, 1973; W. Frank, 1977b) constantly taking air from upper levels and replacing it with air from low levels.

7.2 Vorticity versus divergence

This paper has stressed the need for favorable upper and lower level relative vorticity or tangential wind fields. This goes against the historical treatments of the tropical cyclone development problem. Most authors in the past have emphasized the divergence or vertical motion field. Ramage (1974) and Sadler (1976, 1978) have stressed the importance of upper level outflow channels for cyclone development to occur. The current study interprets those anticyclonic outflow channels

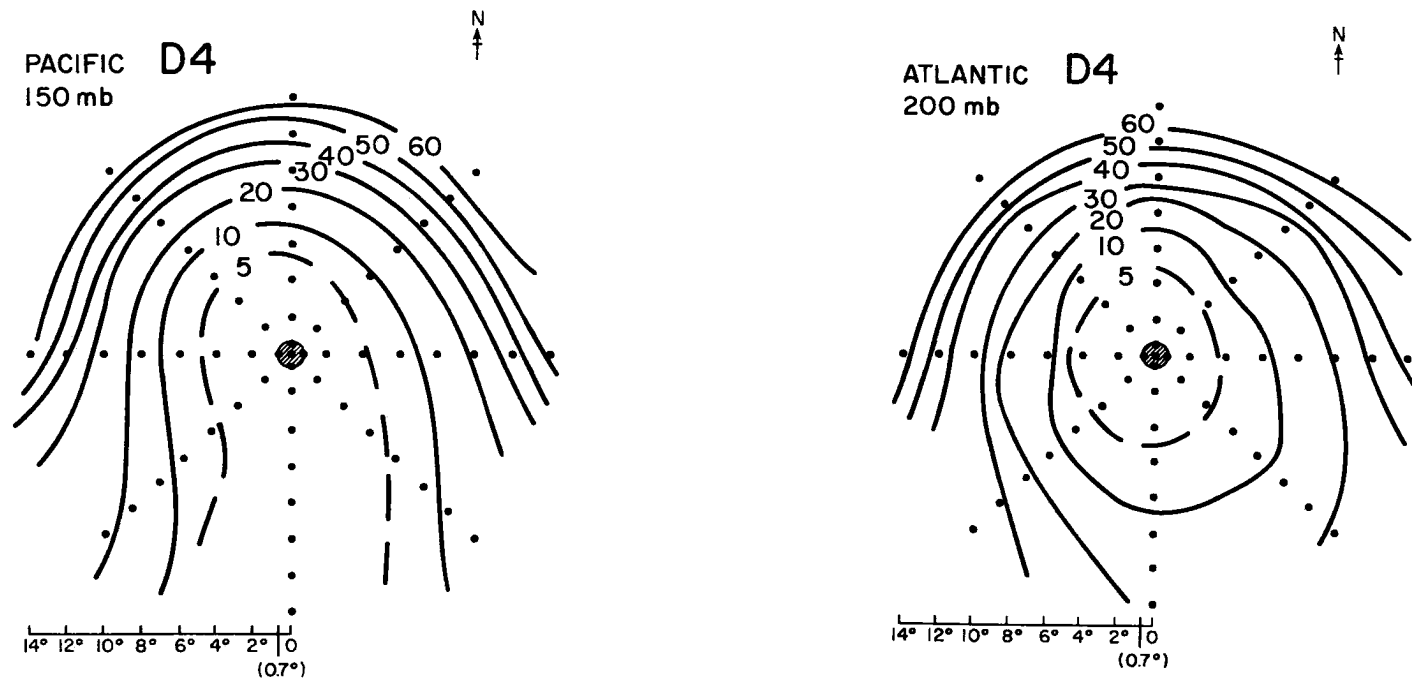


Fig. 50. Plan views of absolute angular momentum, $M = RV_T + f R^2/2$, at the outflow level for the stage D4 (typhoon and hurricane) composite system in each ocean. Units are $10^6 \text{ m}^2\text{s}^{-1}$.

as indicators of strong surrounding region anticyclonic flow and not necessarily of enhanced transverse circulation.

All current theoretical and numerical models of tropical cyclones (e.g. Anthes, 1977; Kurihara, 1975; Rosenthal, 1978; Yamasaki, 1977) have the rate of development mainly dependent on the strength of the vertical motion field and therefore on the strength of the low level mass inflow and upper level mass outflow.

There are now, however, several sets of observations available that indicate that the strength of the disturbance or cyclone's vertical motion fields is not related to its genesis or intensification potential.

Figure 51 shows vertical profiles of vertical velocity averaged over the $0\text{--}4^{\circ}$ area for Pacific composite data sets D1 to D4. Figure 52 shows the same data for the Atlantic systems. In both oceans, the upward vertical velocity actually decreases prior to the intensification to tropical cyclone stage. Thus, in both oceans, the vertical velocity in stage D2 is less than that in stage D1. This phenomenon was observed by Arnold (1977) in a study of the amount of convection around individual developing tropical weather systems using Defense Military Satellite Program (DMSP) data. Arnold had four stages of development for Pacific typhoons, stage I being the cloud cluster and stage IV the typhoon. He considered three quantitative measures of the amount of cloudiness or upward vertical motion: the percentage area of visible deep convective cells, the percentage area of cirrus at an infrared temperature of less than -50°C , and the percentage area of cirrus with temperature less than -63°C . For all three fields he found a decrease in the amount of cloudiness from stage I to stage II. His results are shown in Table 21.

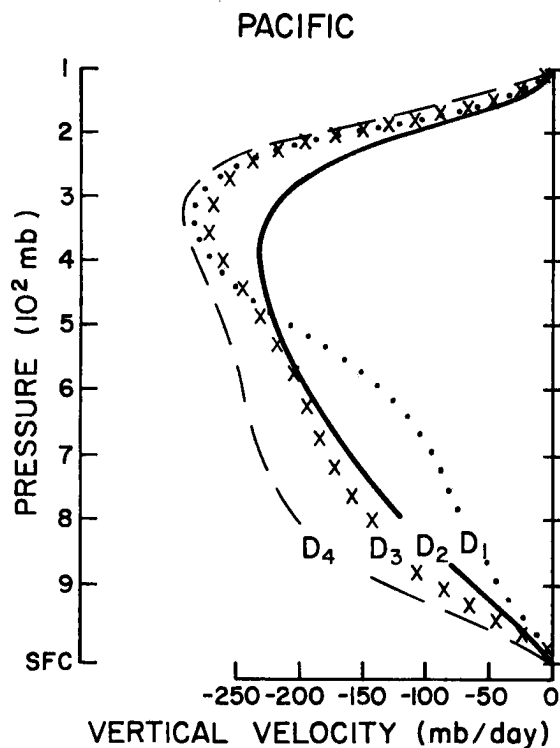


Fig. 51. Vertical velocity averaged over the $0-4^{\circ}$ area for Pacific composite data sets D1 to D4.

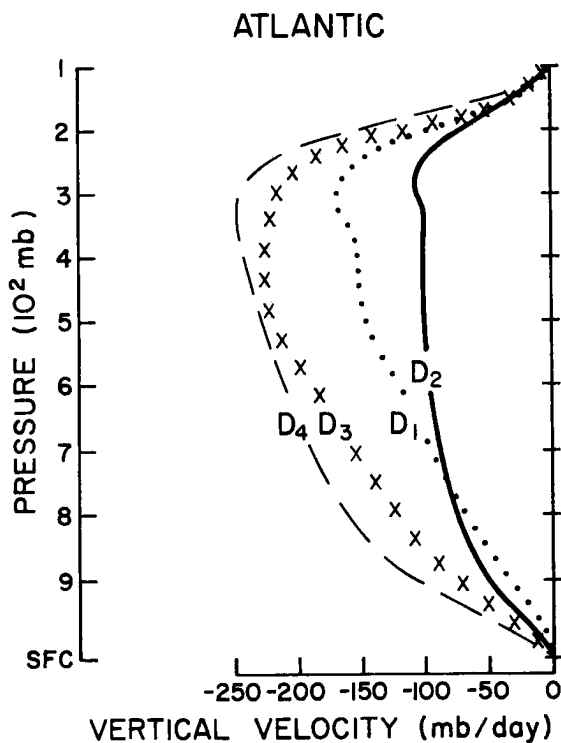


Fig. 52. Vertical velocity averaged over the $0-4^{\circ}$ area for Atlantic composite data sets D1 to D4.

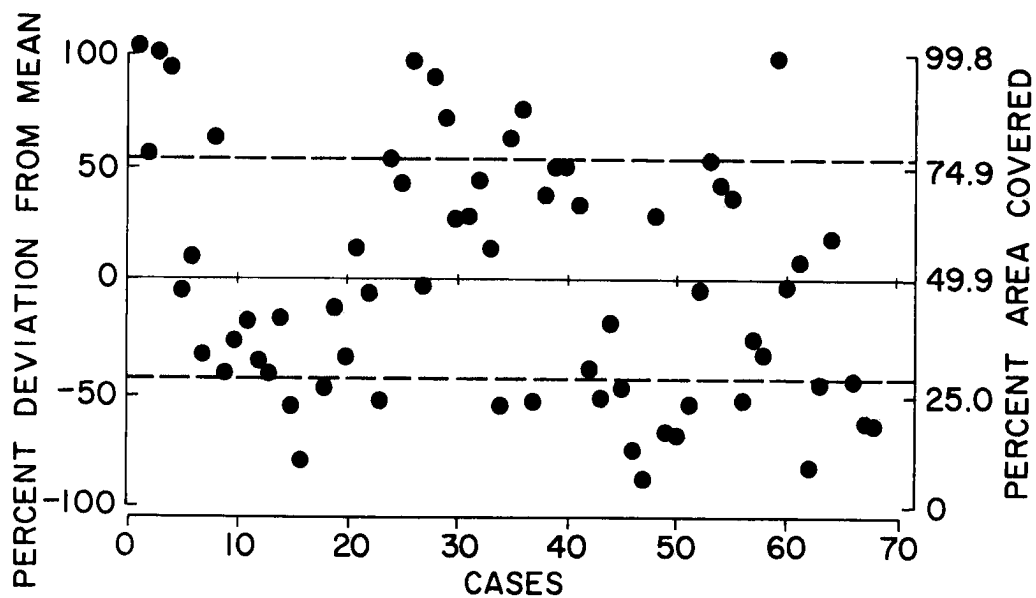
TABLE 21

Percentage of area covered by convective and cirrus clouds within the $R = 0-4.2^{\circ}$ region around tropical storms at different stages of development (adapted from Arnold, 1977).

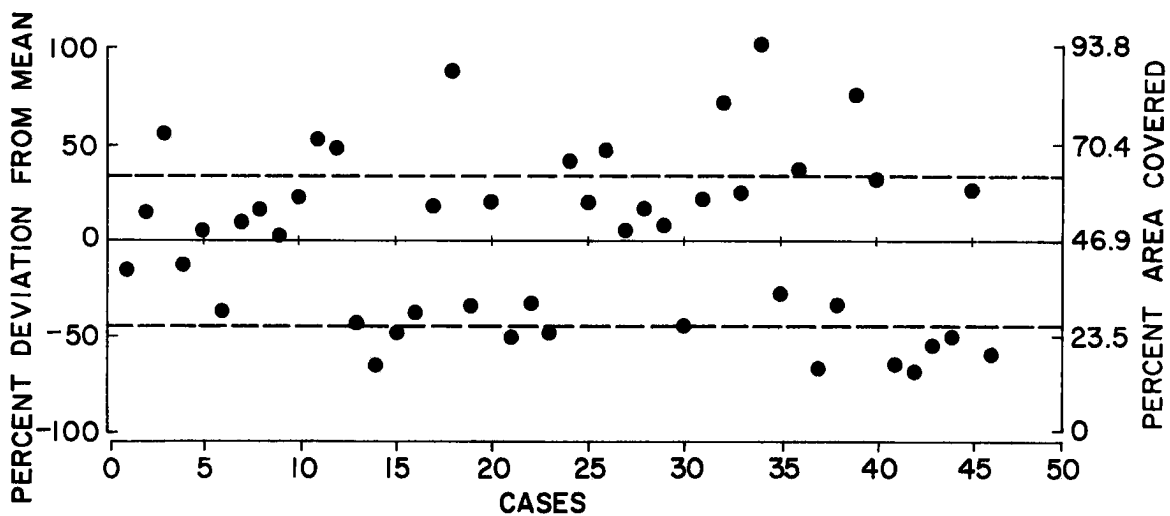
	I Cloud Cluster	II Depression	III Tropical Storm	IV Typhoon
Area of visible deep convective cells	3.2	2.1	2.2	4.5
Area of cirrus, $T < -50^{\circ}\text{C}$	49.9	46.9	47.5	62.8
Area of cirrus, $T < -63^{\circ}\text{C}$	16.1	10.7	13.2	32.8

Arnold (1977) also studied the variability of individual time period penetrative convection and cirrus cloudiness both of which are closely related to upper level vertical motion. He found that between different weather systems and at different times within the same system there is a variation in cloudiness of at least the same size as the mean cloudiness. This variability exists in all stages of development.

Figure 53 reproduced from Arnold's paper shows the individual values of percentage area of cirrus at a temperature less than -50°C for all the separate storms studied. The variability is so great that it renders meaningless any comparison of cloudiness or vertical motion between developing and non-developing systems. S. Erickson (1977) using the same techniques as Arnold compared developing versus non-developing Western Pacific cloud clusters. Figure 54 shows the individual values of percentage area of cirrus ($T < -50^{\circ}\text{C}$) for 50 developing cloud clusters (upper part of figure) and 50 non-developing clusters (lower part). The variations between different systems within each sample are

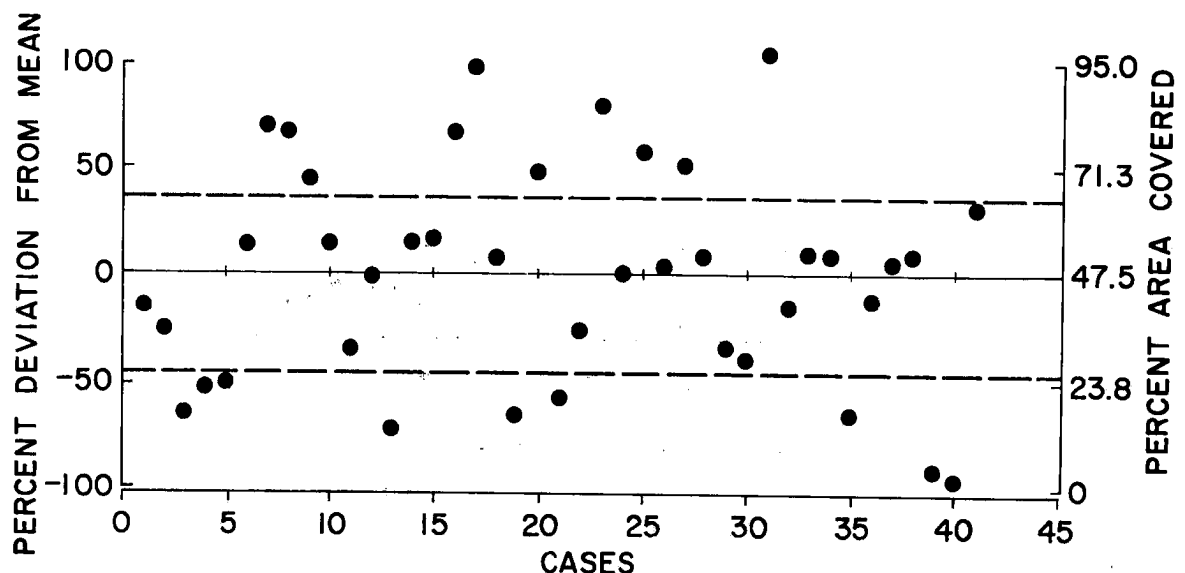


(a)

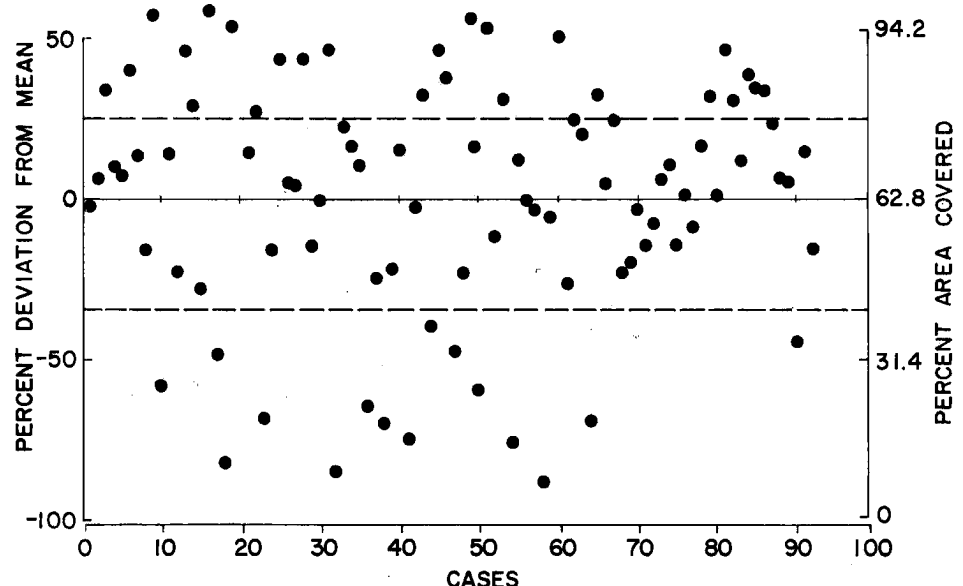


(b)

Fig. 53a-d. Percent area of cirrus ($T < -50^{\circ}\text{C}$) within the $R = 0-4.2^{\circ}$ region of different storms. The order of the cases is random (from Arnold, 1977). (a) Developing cluster (stage I); (b) Tropical depression (stage II); (c) Tropical storm (stage III); (d) Typhoon (stage IV). Dashed lines above and below the mean show the mean positive and negative deviations respectively.



(c)



(d)

Fig. 53. Continued.

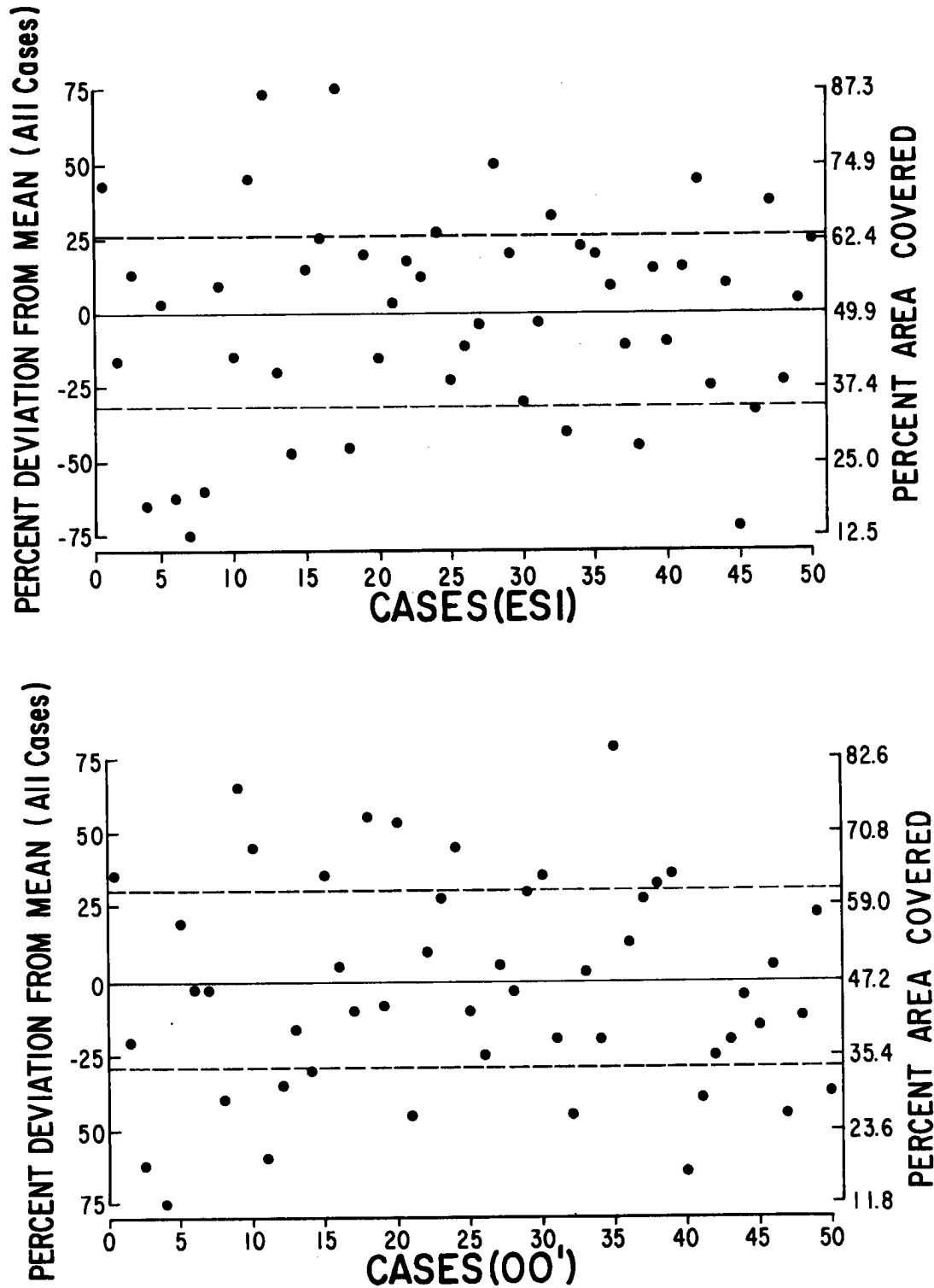


Fig. 54. Same as Fig. 53 but for 50 pretyphoon (ES1) and 50 non-developing (OO') Western Pacific cloud clusters (from S. Erickson, 1977).

orders of magnitude greater than the difference between the means of the two samples.

Besides Arnold's and Erickson's observations and the observations in Figs. 51 and 52, there are also the data presented in Chapter 3 (Fig. 31) which show that Atlantic prehurricane depressions have less vertical motion than non-developing depressions. Added together these observations make a forceful case for the argument that the potential of a disturbance for development is not directly related to the magnitude of the vertical motion field.

7.3 Discussion

A picture is emerging from both the composite data and the individual case data of tropical storm development being a result of large scale influences. It appears that the unique feature to specifying time and location of tropical cyclone genesis is not so much the characteristic of the individual meso-scale system itself. These systems are common and occur in all seasons and at most locations. Once the climatological conditions of genesis are met, it appears that favorable large scale changes in the tropical general circulation are the primary factors determining whether the often present individual organized meso-scale systems will intensify or not. It appears that genesis occurs when an organized tropical cloud cluster exists in a favorable large-scale environment. In particular, both low level positive relative vorticity and upper level negative relative vorticity over a very large surrounding area must be present. As shown in Chapter 4, these large scale vorticity requirements can also be interpreted in terms of vertical shear: large vertical shears of a particular configuration must be present close to the developing disturbance.

These results indicate that a realistic theory of tropical cyclone genesis and development must give primary consideration to the influence of the tropical system's surrounding flow patterns and much less consideration to the thermodynamic and convective aspects.

8. VERTICALLY INTEGRATED BUDGET ANALYSIS

In this chapter vertically integrated budgets of moisture, heat, angular momentum and kinetic energy will be analyzed for the composite data sets. The development of a tropical cyclone will be interpreted as an increase over the $0\text{--}6^\circ$ radius area of total heat content or of total angular momentum content.

8.1 The observed intensification from cloud cluster to typhoon/hurricane

The most distinctive feature of the mature tropical cyclone is its very strong tangential wind field. Figure 55 shows symmetric vertical cross-sections of the tangential component of the wind for the progression from stage D1 to stage D4. The hurricane force winds which cause most of the destruction to property and loss of human life occur within the $0\text{--}1^\circ$ radius area of stage D4 and are operating on a horizontal scale below the resolution of the data. The figure shows, however, that the storm spin-up and increase of tangential wind is actually taking place on the very much larger horizontal scale of the $0\text{--}8^\circ$ area.

The increase of tangential wind is the dynamic response of the atmosphere to a warming and subsequent increase in pressure gradients operating over the $0\text{--}8^\circ$ area. This large scale warming can be seen in the increase in low level height gradients shown in Fig. 56.

Besides temperature and tangential wind, the other parameters necessary to fully describe the state of the atmosphere are moisture content and the radial component of the wind. Neither of these increase substantially over the synoptic scale during tropical cyclone development and must be considered as being secondary in importance to the former two parameters.

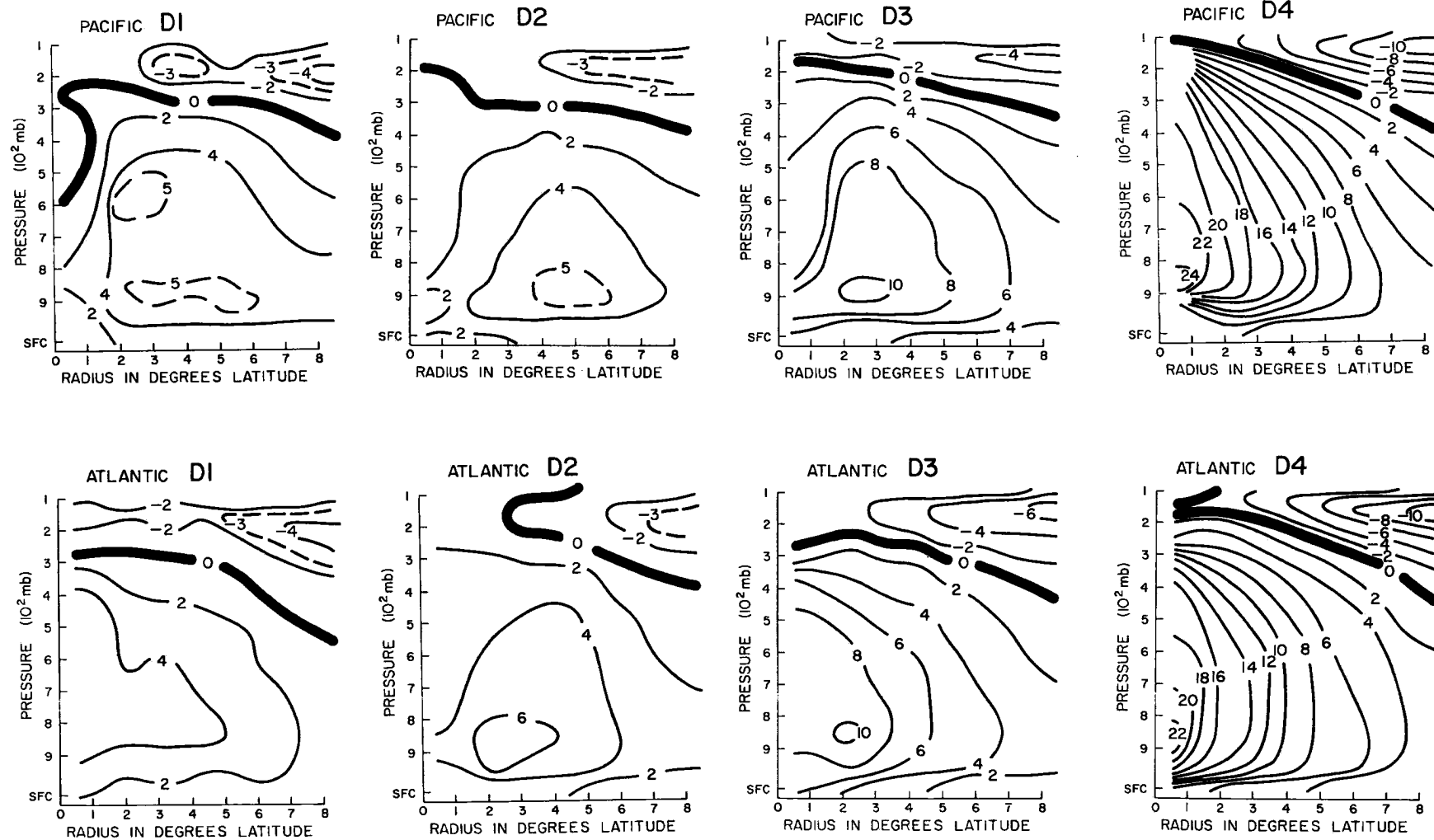


Fig. 55. Two dimensional cross sections of V_T for the progression from stage D1 to D4 in each ocean (m s^{-1}).

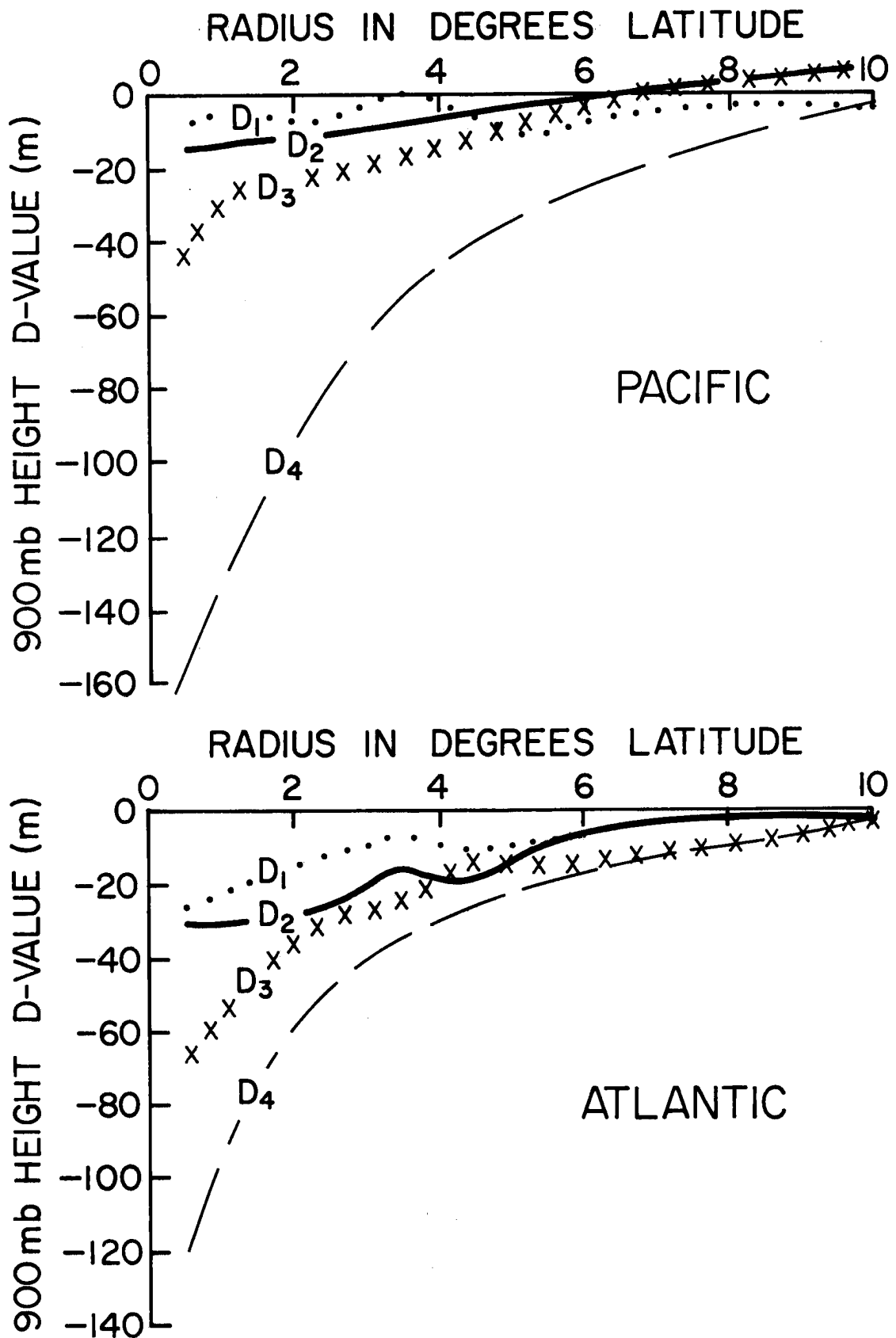


Fig. 56. D-values ($Z - Z_{\text{east-west}, 9-15^\circ}$) in meters for the progression from stage D₁ to stage D₄ in each ocean.

Figure 57 shows a comparison of the increase of total heat content ($s = c_p T + gz$) and of total moisture content (precipitable water) as the system intensifies from stage D1 to D4. Both parameters have been converted to units of $^{\circ}\text{K}$ by dividing by the specific heat multiplied by the mass of the atmosphere between the surface and the 100 mb level. The figure shows that the increase of sensible temperature as measured by change in s is very much greater than the increase in moisture, and that taken over a large area the total water vapor content actually decreases.

The comparison of the change with intensity of tangential wind versus that of radial wind is plotted in Fig. 58. The tangential component of the wind is represented in the figure by the vertical integral of relative angular momentum ($m = RV_T$) per unit area and of kinetic energy per unit area. The kinetic energy was obtained by compositing the square of the wind speed for each individual rawin sounding. The radial component of the wind is equal to the total mass flowing through the system and is represented in the figure by the vertical velocity at 300 mb. All parameters in Fig. 58 have been normalized so that they equal 1.0 at stage D4.

The figure clearly shows that the increase with time of angular momentum and of kinetic energy dominate any increase of vertical velocity.

The problem of tropical cyclone genesis is to explain the observed large scale increase of sensible temperature (s), kinetic energy (KE) and angular momentum (m) shown in Figs. 57 and 58. These changes apparently take place when a tropical oceanic cloud cluster with a sustained $0-4^{\circ}$ area upward vertical velocity exists in a region of large

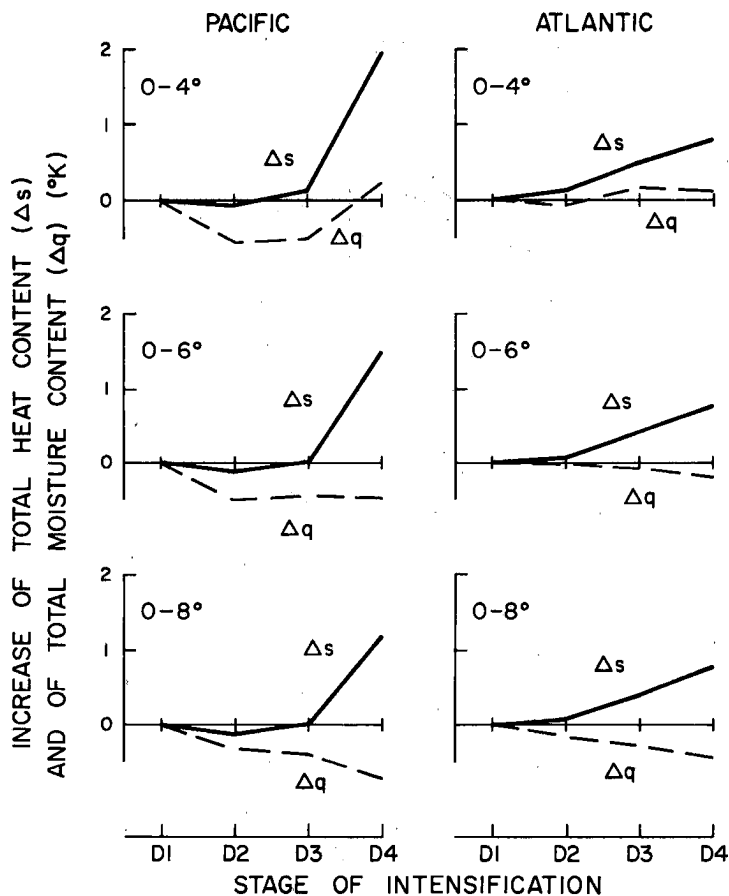


Fig. 57. The increase of total heat content ($s = c_p T + gz$) and of total moisture content (q) as the systems intensify from stage D1 to stage D4.

scale upper level negative relative vorticity and low level positive relative vorticity, or equivalently when it exists in a region of zero vertical wind shear surrounded by very strong anticyclonic vertical shear.

8.2 Heat budget

The main physical process which characterizes the development of a tropical storm is the increase of the sensible temperature of the atmosphere centered on and surrounding the pre-storm disturbance. The

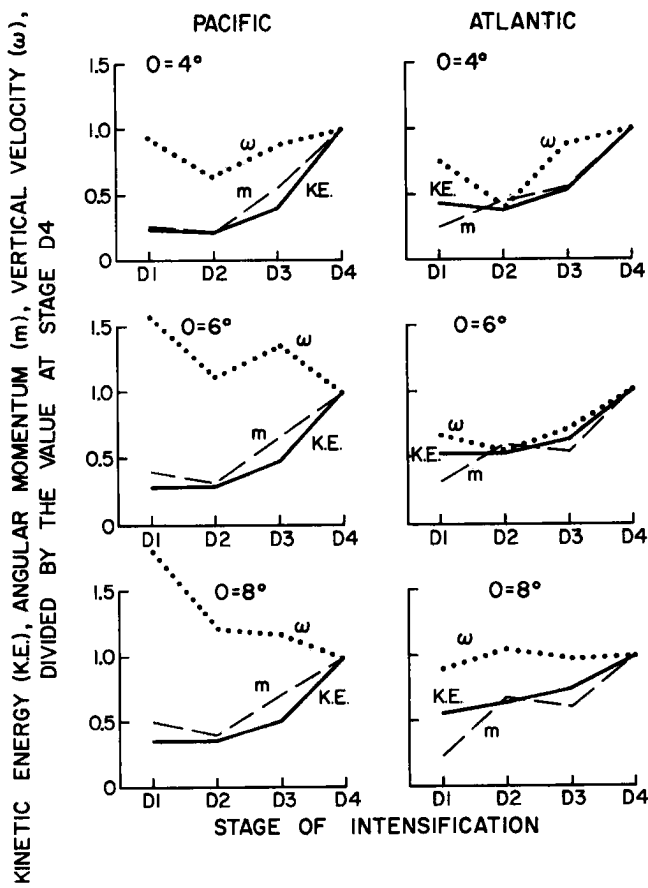


Fig. 58. The increase of relative angular momentum (m), kinetic energy (KE) and vertical velocity (ω) as the systems intensify from stage D1 to stage D4. Units are normalized so that they equal 1.0 at stage D4.

only energy source present is latent heat of condensation which is released in cumulus and cumulonimbus clouds.

Much research has been performed in recent years on how cumulus clouds warm the atmosphere. Gray (1973), Lopez (1973) and Yanai, Esbensen and Chu (1973) have shown that the latent heat released in cumulus clouds goes primarily into potential energy gain and increasing the temperature of the rising air parcel to that of the environmental temperature. The small extra (above environment) temperature increase of $1-2^\circ\text{C}$ of the rising cumulus or Cb parcel which is required for

buoyancy does not warm the environment unless it directly mixes out from the cloud at a higher temperature. It appears that the rising cumulus parcel typically continues rising until it loses its buoyancy and temperature excess. It then mixes with its environment at a temperature little different to (or even lower than) that of the environment. This does not directly warm the environment. Any heat transports out from the rising cloud are overcome by evaporation of the residual liquid-water particles as the clouds die. Although heavy rainfall may have occurred, there is typically no local region warming; instead there is often a local cooling of the immediate environment. This assessment has been substantiated by the observational studies of Kininmonth (1970) and Grube (1979).

In terms of a vertically integrated heat budget over a volume including the cloud cluster, the latent heat released in non-precipitating clouds does not increase the heat content of the volume, as it is counteracted by reevaporation within the same volume. The latent heat released as precipitation does, however, act as an energy source for the volume.

The increase of dry static energy $s = c_p T + gz$ integrated over the volume is governed by the equation:

$$\frac{\partial s}{\partial t} = - \nabla \cdot \nabla s + LP_o + Q_R + S_o \quad (8)$$

$- \nabla \cdot \nabla s$ is the convergence of s through the lateral boundaries of the volume. LP_o is the energy equivalent of the rain that falls in the volume. Q_R is the net radiative heating of the troposphere. S_o is the input of s from the eddy sensible heat flux at the sea surface.

From the composite data, typical magnitudes can be estimated for each term in this equation. Converted to units of $^{\circ}\text{C}/\text{d}$ averaged over the $0-6^{\circ}$ radius, surface to 100 mb, volume for the D2 data set in each ocean they are as follows:¹

$$\frac{\partial s}{\partial t} = - \nabla \cdot \nabla s + LP_o + Q_R + S_o$$

Pacific D2	.1	-4.7	5.7	-1.1	.2
Atlantic D2	.2	-2.5	3.6	-1.1	.2

($^{\circ}\text{C}/\text{d}$)

The increase of local sensible temperature $\frac{\partial s}{\partial t}$ is an order of magnitude smaller than the first three terms on the right hand side. Most of the latent heat energy LP_o is exported laterally through the boundaries of the region through conversion to the term $\nabla \cdot \nabla s$.

The portion of LP_o which is released within the volume acts to counteract the net radiative cooling Q_R . The physical processes by which this is accomplished were demonstrated by Gray (1972a, 1973). Gray performed simultaneous heat and moisture budgets on a tropical cloud cluster, and showed that the radiation is balanced by the residual between a large warming term due to adiabatic compression in the sinking air between clouds and a large cooling term due to reevaporation of cloud water. This is shown in Fig. 59.

The observations of Grube (1979) show that the scale on which this cloud induced warming and cooling takes place is of the order of 10-100 km. The down gradient response of the tropical atmosphere to mass

¹These magnitudes are estimated from the budget analyses presented later in this section. $\nabla \cdot \nabla s$ is from Table 23. LP_o is estimated from the moisture convergence in Table 24 and the surface evaporation in Table 25. S_o is approximately one tenth of the evaporation in Table 25.

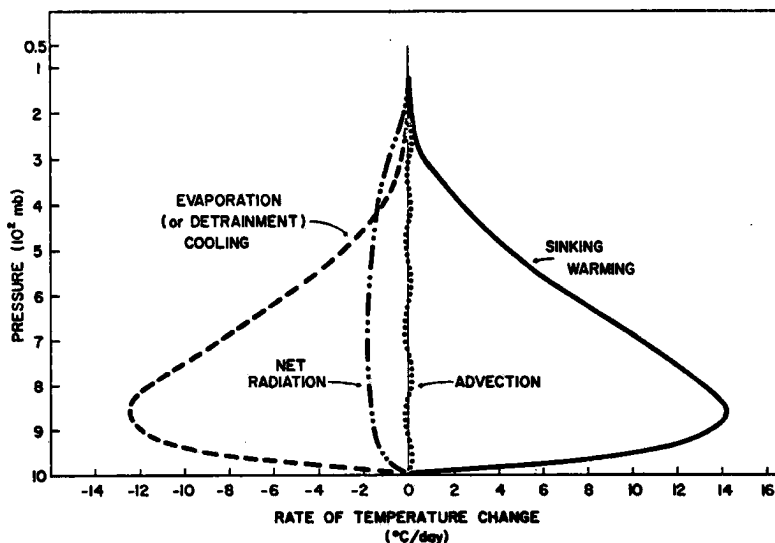


Fig. 59. Vertical distribution of components of heat balance in a steady state tropical cloud cluster (from Gray, 1973).

perturbations on this scale is very rapid and the atmosphere adjusts dynamically so that the heat is spread over a broader area within a few hours.

Because of the strong coupling of moisture and temperature it is more fruitful to consider the budget of moist static energy,

$$h = c_p T + gz + Lq.$$

The equation for the increase of h integrated over a volume is

$$\frac{\partial h}{\partial t} = H_o - \nabla \cdot \nabla h + Q_R \quad (9)$$

H_o is the input of h from the eddy sensible and latent heat fluxes at the sea surface. It approximately equals the surface evaporation.

$\nabla \cdot \nabla h$ is the export of h through the lateral boundaries. Q_R is the net radiative heating of the troposphere.

Looking at Fig. 57 it is seen that the moisture content q does not increase beyond that already present in the cloud cluster stage; thus any increase in h goes directly into increase of s or sensible temperature.

The term $\nabla \cdot \nabla h$ is the import and export of h by the mass circulation through the system. It was shown in Chapters 2 and 3 that in both cloud clusters and tropical storms there is mass convergence between the surface and the 300 mb level and an equal amount of mass divergence between 300 and 100 mb. The moist static energy h has a minimum near the 600 mb level. Therefore, the mean value of h in the 300-100 mb outflow layer is greater than the mean value in the surface-300 mb inflow layer. This means that the transverse or radial mass circulation exports h .

The divergence of moist static energy $\nabla \cdot \nabla h$ for the composite data sets was calculated by compositing the product $V_R h$ for individual soundings. To take into account the effect of the moving system, the motion vector of each individual cluster or storm was subtracted from V_R before the compositing was performed. As explained in Chapter 1, the compositing is carried out on a grid with eight azimuthal octants; so the export of h , $V_R h$, is obtained at eight points around the boundary. These exports are summed to yield the total export $\overline{V_R h}$. It was explained in Chapter 2 that for the Pacific data sets the 00 GMT values of moisture and therefore, of h could not be used. For these systems the composite average value of V_R at each octant was multiplied by the 12 GMT value of h for the same octant. This gave an estimation of $\overline{V_R h}$ at eight points around the perimeter of the cluster or storm volume.

The resultant values of $\nabla \cdot \nabla h$ for the composite systems are shown in Table 22. The values are in $^{\circ}\text{C}/\text{d}$ averaged over the respective $0\text{-}4^{\circ}$, $0\text{-}6^{\circ}$ and $0\text{-}8^{\circ}$ radius volumes. The Pacific D1 system has been omitted from this and all other budget analyses because of the very low data density of that data set.

The table shows that the mass circulation through every system exports energy. This export of h is the residual between an import of q and a larger export of s . The separate components $\nabla \cdot \nabla s$ and $\nabla \cdot \nabla q$ are shown in Tables 23 and 24 respectively.

The pretyphoon (Pacific D2) and prehurricane (Atlantic D1) cloud clusters consistently export more s and import more q than do the non-developing cloud clusters (Pacific N1, Atlantic N1, N2). To an extent the two effects cancel each other, but Table 22 shows that the developing cloud clusters generally export more h through their transverse circulations than do the non-developing cloud clusters.

Equation (9) describes the budget of h for the cloud cluster or storm volume. The term on the left hand side of the equation, $\frac{\partial h}{\partial t}$ is approximately zero for the non-developing cluster data sets and for the steady state typhoon and hurricane D4 data sets. It can be estimated for the D2 and D3 data sets by assuming that it takes 2 days to progress from one stage of intensity to the next. For the Atlantic N3 system it is assumed that it takes 2 days for this system to decay back to the h value observed in stage N1.

The radiation term Q_R is approximately $-1.1^{\circ}\text{C}/\text{d}$ for all systems. It is lower than the background value used in Chapter 2, to take into account the dampening of the infra red flux divergence by the thick cirrus clouds.

TABLE 22

The export of moist static energy due to horizontal divergence ($-\nabla \cdot \bar{V}h$). A negative sign denotes a loss of energy from the system. Values are expressed in equivalent mean surface to 100 mb temperature increase ($^{\circ}\text{C}/\text{d}$).

	<u>0-4°</u>	<u>0-6°</u>	<u>0-8°</u>
<u>PACIFIC NON-DEVELOPING</u>			
N1 Cloud cluster	-.5	-.5	-.5
<u>PACIFIC DEVELOPING</u>			
D2 Pretyphoon cloud cluster	-1.3	-.7	-.6
D3 Intensifying cyclone	-1.3	-1.0	-.6
D4 Typhoon	-2.6	-1.6	-1.0
<u>ATLANTIC NON-DEVELOPING</u>			
N1 Cloud cluster	-.3	-.5	-.3
N2 Wave trough cluster	-.1	-.2	0
N3 Non-developing depression	-1.7	-1.3	-.6
<u>ATLANTIC DEVELOPING</u>			
D1 Prehurricane cloud cluster	-1.0	-.5	-.5
D2 Prehurricane depression	-.8	-.5	-.3
D3 Intensifying cyclone	-1.2	-.7	-.9
D4 Hurricane	-1.4	-1.2	-.7

The remaining term H_o can now be estimated as a residual. This is done for the $0-6^{\circ}$ area in Table 25. The export term $\nabla \cdot \bar{V}h$ shown in the table is the average of the 3 values shown for each system in Table 22. The last column of Table 25 shows the implied surface evaporation E_o in cm/d , calculated by assuming a Bowen ratio of 0.1.

Budget calculations are extremely sensitive to the quality of the data; so none of the parameters in Table 25 can be considered as better than an approximation to the true value. In general, however, the

TABLE 23

The export of dry static energy due to horizontal divergence ($-\nabla \cdot \nabla s$). A negative sign denotes a loss of energy from the system. Values are expressed in equivalent mean surface to 100 mb temperature increase ($^{\circ}\text{C}/\text{d}$).

	<u>0-4°</u>	<u>0-6°</u>	<u>0-8°</u>
<u>PACIFIC NON-DEVELOPING</u>			
N1 Cloud cluster	-3.8	-3.1	-2.7
<u>PACIFIC DEVELOPING</u>			
D2 Pretyphoon cloud cluster	-6.9	-4.7	-3.2
D3 Intensifying cyclone	-7.6	-5.2	-2.9
D4 Typhoon	-10.6	-4.1	-2.9
<u>ATLANTIC NON-DEVELOPING</u>			
N1 Cloud cluster	.6	-.9	-.8
N2 Wave trough cluster	-.9	-1.0	-.1
N3 Non-developing depression	-6.3	-3.2	-2.4
<u>ATLANTIC DEVELOPING</u>			
D1 Prehurricane cloud cluster	-4.0	-2.4	-1.5
D2 Prehurricane depression	-3.5	-2.5	-1.5
D3 Intensifying cyclone	-6.3	-3.2	-2.1
D4 Hurricane	-7.5	-4.0	-1.8

evaporation values are close to the background values for each region calculated in Chapter 2.

The energy balance of Table 25 shows that tropical systems maintain themselves only through energy received from the ocean H_o . This agrees with synoptic observations that most tropical systems weaken or die when this ocean energy source is cut off. The vertical circulation through the organized weather system $\nabla \cdot \nabla h$ typically produces an energy depletion of the system.

The developing cluster data sets have slightly larger values of $\nabla \cdot \nabla h$ than do the non-developing clusters. The radiative cooling Q_R

TABLE 24

The import of water vapor due to horizontal convergence ($-\nabla \cdot \nabla q$). A positive sign denotes a gain of energy for the system. Values are expressed in equivalent mean surface to 100 mb temperature increase ($^{\circ}\text{C}/\text{d}$)

	<u>0-4°</u>	<u>0-6°</u>	<u>0-8°</u>
<u>PACIFIC NON-DEVELOPING</u>			
N1 Cloud cluster	3.3	2.6	2.2
<u>PACIFIC DEVELOPING</u>			
D2 Pretyphoon cloud cluster	5.6	4.0	2.6
D3 Intensifying cyclone	6.3	4.2	2.3
D4 Typhoon	8.0	2.5	1.9
<u>ATLANTIC NON-DEVELOPING</u>			
N1 Cloud cluster	-.9	.4	.5
N2 Wave trough cluster	.8	.8	.1
N3 Non-developing depression	4.6	1.9	1.8
<u>ATLANTIC DEVELOPING</u>			
D1 Prehurricane cloud cluster	3.0	1.9	1.0
D2 Prehurricane depression	2.7	2.0	1.2
D3 Intensifying cyclone	5.1	2.5	1.2
D4 Hurricane	6.1	2.8	1.1

is probably the same in each case, so for balance, the developing clusters must have slightly greater surface evaporation E_o or H_o . This inference is supported by the developing systems having slightly greater low level wind speeds, as shown in the first column of Table 5, page 16.

The h budget shows that for cyclone development to occur, either the h export by the transverse circulation $\nabla \cdot \nabla h$ must decrease, or the sea surface to atmosphere energy transfer H_o must increase. Both terms are of the order of magnitude of $1^{\circ}\text{C}/\text{d}$; the residual $\frac{\partial h}{\partial t}$ required for genesis is only $.1$ or $.2^{\circ}\text{C}/\text{d}$; so only a 10 percent change is required in $(H_o - \nabla \cdot \nabla h)$. Such a small change is below the level of accuracy of the current budget calculations.

TABLE 25

Budget of moist static energy, h , for the composite data sets averaged over the $0-6^{\circ}$ radius volume ($\delta^{\circ}C/d$).

	$\frac{\partial h}{\partial t}$	$\nabla \cdot \nabla h - Q_R$	$= H_o$	Implied Surface Evaporation E_o (cm/d)
<u>PACIFIC NON-DEVELOPING</u>				
N1 Cloud cluster	0	.5	1.1	1.6 .5
<u>PACIFIC DEVELOPING</u>				
D2 Pretyphoon cloud cluster	.1	.9	1.1	2.1 .7
D3 Intensifying cyclone	.7	1.0	1.1	2.8 .9
D4 Typhoon	0	1.7	1.1	2.8 .9
<u>ATLANTIC NON-DEVELOPING</u>				
N1 Cloud cluster	0	.4	1.1	1.5 .5
N2 Wave trough cluster	0	.1	1.1	1.2 .4
N3 Non-developing depression	-.1	1.2	1.1	2.2 .7
<u>ATLANTIC DEVELOPING</u>				
D1 Prehurricane cloud cluster	0	.7	1.1	1.8 .6
D2 Prehurricane depression	.1	.5	1.1	1.7 .6
D3 Intensifying cyclone	.2	.9	1.1	2.2 .7
D4 Hurricane	0	1.1	1.1	2.2 .7

The fact that the transverse circulation of the western ocean weather systems exports h from the systems is not a new observation. Many tropical researchers today use the Q_1 , Q_2 notation of Yanai, Esbensen and Chu (1973). In terms of that notation, it implies that the vertical integral of $Q_1 - Q_2$ is greater than zero. Physically, it means that for a steady state system the surface energy flux within the system is greater than the tropospheric radiative cooling, i.e. $H_o + Q_R$ is greater than zero.

The implications of these h budgets for tropical cyclone genesis are discussed more fully in the following chapter.

8.3 Kinetic energy budget

The export of kinetic energy through the lateral boundaries of the budget volume was obtained by compositing $\bar{V}_R \cdot \bar{V}^2$ for each individual sounding on the volume boundary. V is the magnitude of the actual horizontal wind. V_R is the radial component of the wind with the storm motion vector removed. Vertical profiles of $\bar{V}_R \cdot \bar{V}^2$ are shown in Fig. 60. All systems import kinetic energy in the surface to 300 mb inflow layer and export it in the upper tropospheric outflow layer. The export is greater than the import, so the cloud clusters and tropical storms act as sources of tropospheric kinetic energy. The effect of these horizontal transports on the kinetic energy content of the 0-4, 0-6 and 0-8° volumes is shown in Table 26. The table shows no obvious difference in the kinetic energy export from developing versus non-developing cloud clusters.

W. Frank (1977b, c) showed that for fully developed typhoons and hurricanes only 50 percent of the kinetic energy export is by the mean transverse circulation, the rest being carried out by horizontal eddies. The mean circulation transport by definition is equal to the composite mean \bar{V}_R at a given radius by the composite mean \bar{V}^2 at that radius, and is denoted $\bar{V}_R \bar{V}^2$. The composite of the product for individual soundings is denoted by $\bar{V}_R V^2$, and the eddy transport is defined as the difference $\bar{V}_R V^2 - \bar{V}_R \bar{V}^2$.

Figure 61 shows the total transports $\bar{V}_R V^2$ and the mean transports $\bar{V}_R \bar{V}^2$ at 6° radius for the Pacific data sets. The eddies are of the same magnitude as the mean flow and act in the same direction. The vertical integrals of the mean and eddy exports for the 0-6° volume are shown in Table 27.

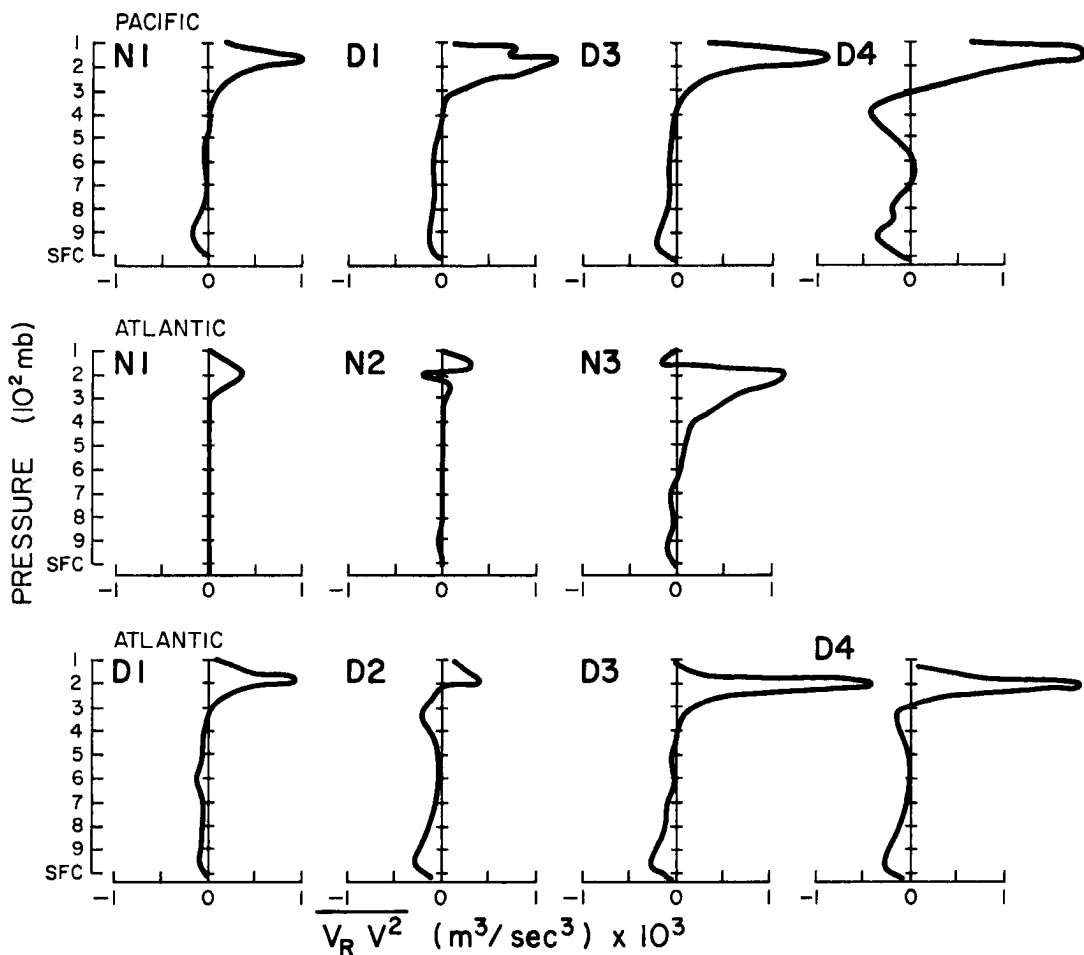


Fig. 60. Total horizontal transport of kinetic energy times two ($V_R V^2$) at $R = 6^\circ$ for all the composite data sets.

Kinetic energy is generated by down-gradient flow, $-\bar{\nabla} \cdot \bar{\nabla} \phi$. This was estimated for each composite system by taking the product $-\bar{V}_R \cdot \frac{\partial \bar{\phi}}{\partial R}$ at each radius and area averaging. This product is actually the generation by the mean radial circulation. Some visual smoothing was performed on the height fields before the calculation was made. Vertical profiles of the mean generation of kinetic energy $-\bar{\nabla} \cdot \bar{\nabla} \phi$ are shown in Fig. 62. The generation shows dual maxima with peaks at 950 and 150 mb. There is very little kinetic energy generation by the mean flow in the middle troposphere.

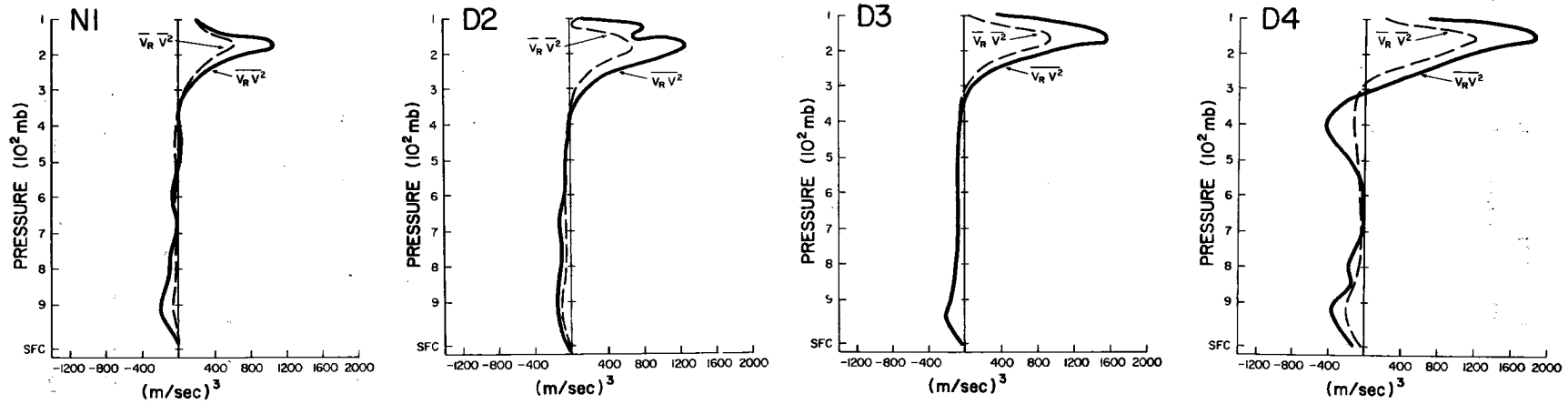
TABLE 26

The export of kinetic energy per unit area due to horizontal divergence. A negative sign denotes a loss of energy or export from the system.

	$-\nabla \cdot (\nabla \frac{1}{2} V^2) \text{ (W/m}^2\text{)}$		
	<u>0-4°</u>	<u>0-6°</u>	<u>0-8°</u>
<u>PACIFIC NON-DEVELOPING</u>			
N1 Cloud cluster	-2.5	-1.0	-2.1
<u>PACIFIC DEVELOPING</u>			
D2 Pretyphoon cloud cluster	-2.3	-1.4	-0.9
D3 Intensifying cyclone	-1.1	-1.7	-1.0
D4 Typhoon	-1.1	-1.2	-3.3
<u>ATLANTIC NON-DEVELOPING</u>			
N1 Cloud cluster	0.8	-0.5	-0.0
N2 Wave trough cluster	0.3	-0.0	-0.1
N3 Non-developing depression	-3.4	-2.0	-1.2
<u>ATLANTIC DEVELOPING</u>			
D1 Prehurricane cloud cluster	0.3	-0.4	-0.1
D2 Prehurricane depression	1.9	1.1	-0.0
D3 Intensifying cyclone	-2.0	-1.4	-1.5
D4 Hurricane	-1.2	-1.4	-1.1

The mean generation increases substantially as the system progresses from stage D1 to D4. This increase is mainly brought about by an increase in the height gradients, $\nabla\phi$, shown in Fig. 56.

It has been shown earlier (Figs. 51, 52 and 58) that there is very little increase in the total radial mass circulation ω . There is, however, an increase in the fraction of the mass inflow that takes place in the low levels where the height gradients are largest. Figure 63 depicts vertical profiles of the radial component of the wind, V_R , at 4° radius for the systems D1 to D4 in both oceans. The total inward



151

Fig. 61. Total horizontal transport of kinetic energy times two ($\bar{V}_R \bar{V}^2$) at $R = 6^\circ$ and transport by the mean circulation ($\overline{V_R V^2}$) at $R = 6^\circ$ for the Pacific systems. The difference between the curves is the horizontal eddy flux.

TABLE 27

The export of kinetic energy from the $0-6^{\circ}$ volume due to the mean and the horizontal eddy circulations. A negative sign denotes a loss of energy from the system.

$$-\nabla \cdot (\nabla \frac{1}{2} V^2), 0-6^{\circ} (W/m^2)$$

	Mean Circulation	Eddies	Total
<u>PACIFIC NON-DEVELOPING</u>			
N1 Cloud cluster	-0.7	-0.3	-1.0
<u>PACIFIC DEVELOPING</u>			
D2 Pretyphoon cloud cluster	-0.6	-0.8	-1.4
D3 Intensifying cyclone	-0.5	-1.2	-1.7
D4 Typhoon	-0.9	-0.3	-1.2
<u>ATLANTIC NON-DEVELOPING</u>			
N1 Cloud cluster	-0.2	-0.3	-0.5
N2 Wave trough cluster	-0.1	0.1	0.0
N3 Non-developing depression	-0.6	-1.4	-2.0
<u>ATLANTIC DEVELOPING</u>			
D1 Prehurricane cloud cluster	-0.3	-0.1	-0.4
D2 Prehurricane depression	-0.4	1.5	1.1
D3 Intensifying cyclone	-0.6	-0.8	-1.4
D4 Hurricane	-0.7	-0.7	-1.4

mass transport (or the integral of V_R from the surface to 300 mb) shows little increase from stage D1 to stage D4; but the values of V_R at 900 or 950 mb do increase. This is quantified in Table 8 of Chapter 2.

Column (1) of that table shows the total mass convergence; column (3) shows the mass convergence between the surface and 850 mb. The total convergence increases by only 20% from D1 to D4; but the proportion of this inflow taking place below 850 mb increases from .3 to .6. This concentration of the inflow into the low levels where $\nabla\phi$ is greatest

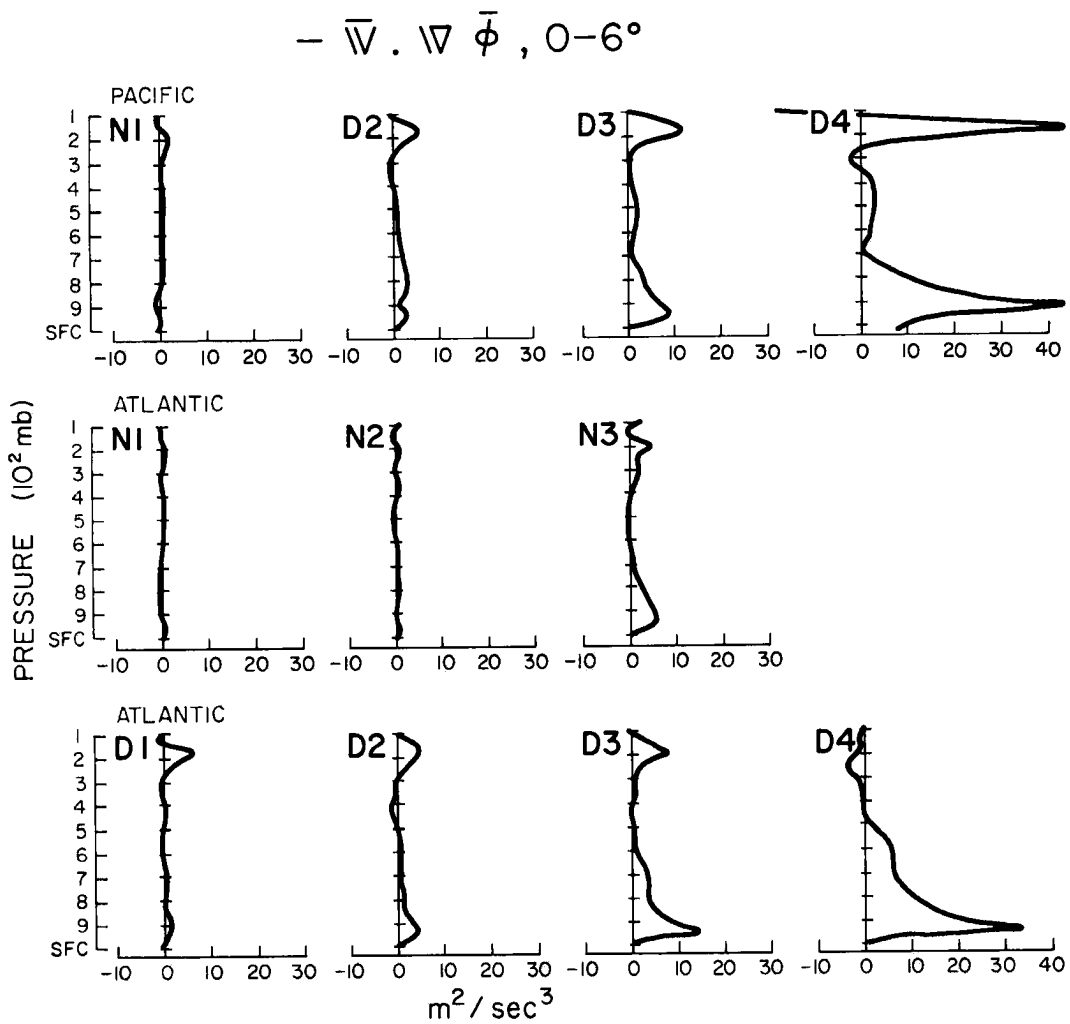


Fig. 62. Generation of kinetic energy by the mean circulation ($-\bar{\nabla} \cdot \nabla \bar{\phi}$) for the $0-6^\circ$ area.

enhances the product $-\bar{\nabla} \cdot \nabla \bar{\phi}$ i.e. the kinetic energy generation by the mean flow.

The dissipation of kinetic energy due to surface friction in the boundary layer is given by the equation:

$$\text{boundary layer dissipation} = \int v \frac{\partial \bar{v}' w'}{\partial z} dz$$

through the
depth of the
boundary layer

$$\begin{aligned} & \approx \overline{V} \frac{sfc}{\overline{V'w'}} \\ & = \overline{V} c_D |v|_{sfc}^2 \end{aligned} \quad (10)$$

\overline{V} is the mean wind speed in the boundary layer; $|v|_{surface}$ is the surface wind speed.

The winds at 900 mb are used in the calculation. $\overline{V} \approx .9 V_{900mb}$ and $V_{surface} \approx .8 V_{900mb}$, based on the oceanic boundary layer observations of Gray (1972b) and the tropical storm boundary layer observations of Bates (1977). The drag coefficient is calculated using the empirical formula of Garratt (1977):

$$c_D = (0.75 + 0.067 |v|_{surface}) \times 10^{-3} \quad (11)$$

There is also substantial dissipation of kinetic energy by turbulent processes above the boundary layer. Following Riehl and Malkus (1961), Miller (1962) and W. Frank (1977b) this internal dissipation is estimated as being equal to the surface dissipation.

The complete kinetic energy budget for the $0-6^{\circ}$ volume is shown in Table 28. The values of the time derivative in the first column were obtained by compositing the kinetic energy content and assuming that it takes 2 days for a system to progress from intensity stage D2 to stage D3, and 2 days for each of the progressions D3 to D4 and N3 to N1.

Some of the values of the horizontal export in column (2) of the table have been adjusted from the raw data values shown in earlier tables. The value for the Pacific D4 system has been adjusted following W. Frank (1977b). In performing a more complete energetic analysis of

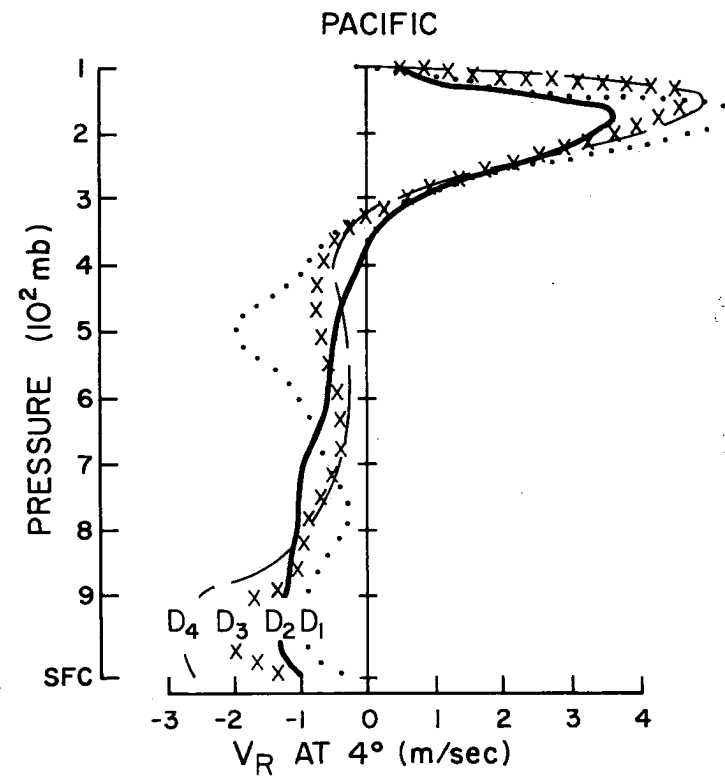
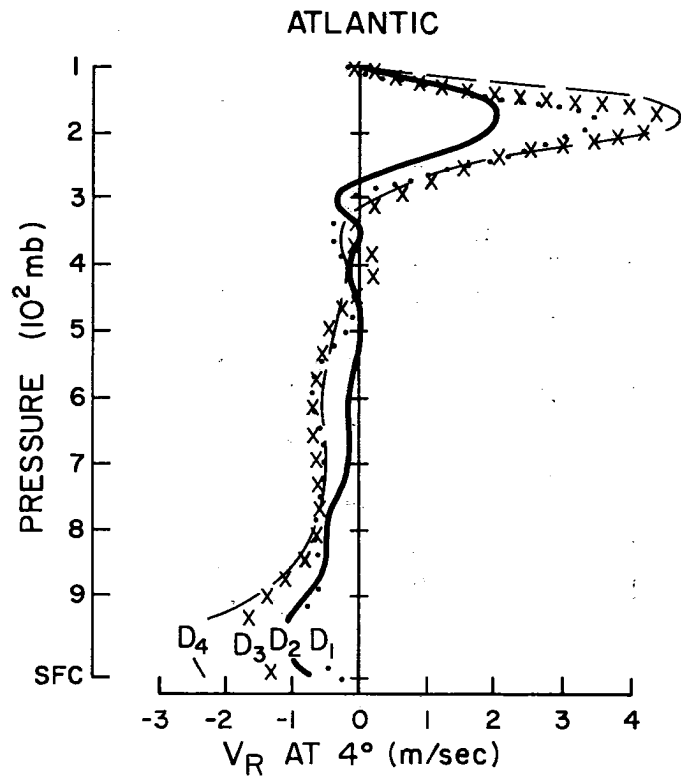


Fig. 63. The radial wind V_R at 4° for stages D₁ to D₄ in each ocean.

TABLE 28

Budget of kinetic energy over the $0-6^{\circ}$ radius area for the composite data sets (W/m^2).

	(1)	(2)	(3)	(4)	(5)	(6)
	$-\frac{\partial \text{KE}}{\partial t}$	$\nabla \cdot \nabla \text{KE}$	$\nabla \cdot \nabla \phi$	$\nabla \cdot \mathbf{F}$	Internal Dissipation	Residual
<u>PACIFIC NON-DEVELOPING</u>						
N1 Cloud cluster	0.0	-1.0	0.3	-0.3	-0.3	-1.3
<u>PACIFIC DEVELOPING</u>						
D2 Pretyphoon cloud cluster	-1.2	-1.4	1.3	-0.5	-0.5	2.3
D3 Intensifying cyclone	-3.6	-1.7	3.1	-1.4	-1.4	5.0
D4 Typhoon	0.0	-2.6	8.9	-5.4	-5.4	4.5
<u>ATLANTIC NON-DEVELOPING</u>						
N1 Cloud cluster	0.0	-0.5	0.0	-0.4	-0.4	1.3
N2 Wave trough cluster	0.0	0.0	0.1	-0.5	-0.5	0.9
N3 Non-developing depression	0.7	-2.0	1.3	-0.3	-0.3	0.6
<u>ATLANTIC DEVELOPING</u>						
D1 Prehurricane cloud cluster	0.0	-0.4	0.6	-0.6	-0.6	1.0
D2 Prehurricane depression	-0.4	-0.8	1.3	-0.5	-0.5	0.9
D3 Intensifying cyclone	-1.5	-1.4	2.9	-0.9	-0.9	1.8
D4 Hurricane	0.0	-1.4	4.9	-2.2	-2.2	0.9

Column (1) is minus the local time change

Column (2) is the horizontal convergence of kinetic energy

Column (3) is the generation of kinetic energy by the mean flow

Column (4) is the dissipation of kinetic energy in the frictional boundary layer

Column (5) is the dissipation by turbulent processes above the boundary layer

Column (6) is the residual of terms (1) to (5) and must be balanced by internal or eddy kinetic energy generation

this same data set, to obtain a physically realistic solution he had to radially smooth the horizontal transport of kinetic energy as shown in Fig. 64. The total horizontal export of kinetic energy for the Atlantic D2 system is inconsistent with the other systems, and has been replaced by twice the export by the mean circulation.

The last column of Table 28 shows the residual of all the other terms:

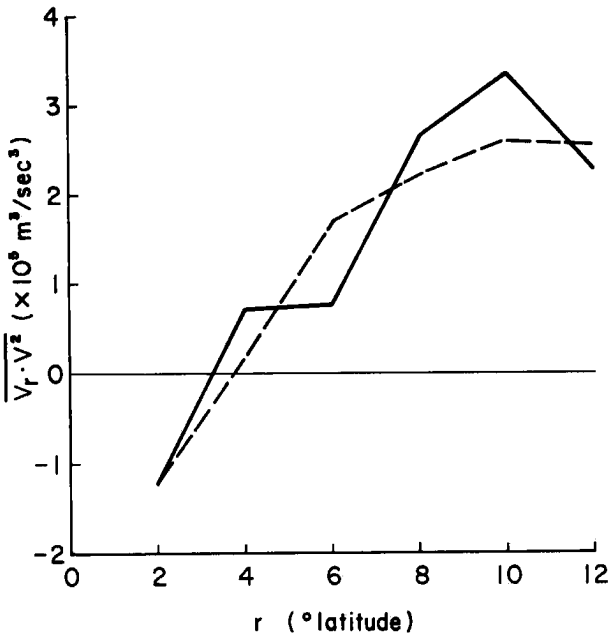


Fig. 64. Vertically integrated total horizontal flux of kinetic energy times 2 (solid line) for the Pacific D4 data set and smoothed curve used in budget calculations by W. Frank (1977b) (dashed curve).

$$\begin{aligned}
 & -\frac{\partial KE}{\partial t} + \text{horizontal convergence} + \text{mean generation} + \text{surface dissipation} \\
 & + \text{internal dissipation} = \text{Residual}.
 \end{aligned}$$

This residual must be balanced by the internal or eddy generation of kinetic energy. The values in the last column indicate that it is of the same order of magnitude as the generation by the mean flow. As will be discussed later it is probable that much of this internal kinetic energy generation is brought about by deep cumulus clouds existing in strong vertical wind shear.

8.4 Angular momentum budget

The conservation of relative angular momentum in cylindrical stationary coordinates may be expressed as

$$\frac{dm}{dt} = -Rf V_R - \frac{1}{\rho} \frac{\partial p}{\partial \theta} + R F_T \quad (12)$$

where $m = RV_T$ is the relative angular momentum; θ is the azimuthal angle; and F_T is friction in the tangential or θ direction.

Terms involving $\frac{\partial}{\partial \theta}$ drop out when integrated around a circle and vertical flux terms integrate to zero assuming no flux at 100 mb. The large scale vertically integrated angular momentum balance is thus:

$$(1) \quad (2) \quad (3) \quad (4)$$

$$\frac{\partial m}{\partial t} = -\nabla \cdot \nabla m - Rf V_R + RF_T \quad (13)$$

The first term is the local time change and is calculated in the same manner as for h and kinetic energy in the previous sections. The second term, the horizontal transport, is obtained by compositing $V_R m$ ($= V_R V_T R$) for individual soundings around the perimeter of the budget volume. Vertical profiles of this transport are plotted in Fig. 65. Negative values on the figure indicate an import of m ; so all systems import m , or act as sinks of relative angular momentum.

The vertical integrals of the horizontal divergence of m from the budget volumes are shown in Table 29.

The dashed curves on Fig. 65 represent the transports by the mean circulation $\bar{V}_R \bar{V}_T \bar{R}$. For the Atlantic systems and for the Pacific D4 typhoon, an appreciable part of the angular momentum import is carried by horizontal eddies. This can be seen in Table 30 which shows the mean and eddy components of the transport at $R = 6^\circ$.

The imports of relative angular momentum shown in Table 29 and 30 are consistently greater for developing systems than for non-developing weather systems. At 6° the Pacific pretyphoon cloud cluster D2 has 5 times as much import as the N1 non-developing cloud cluster. The

PACIFIC

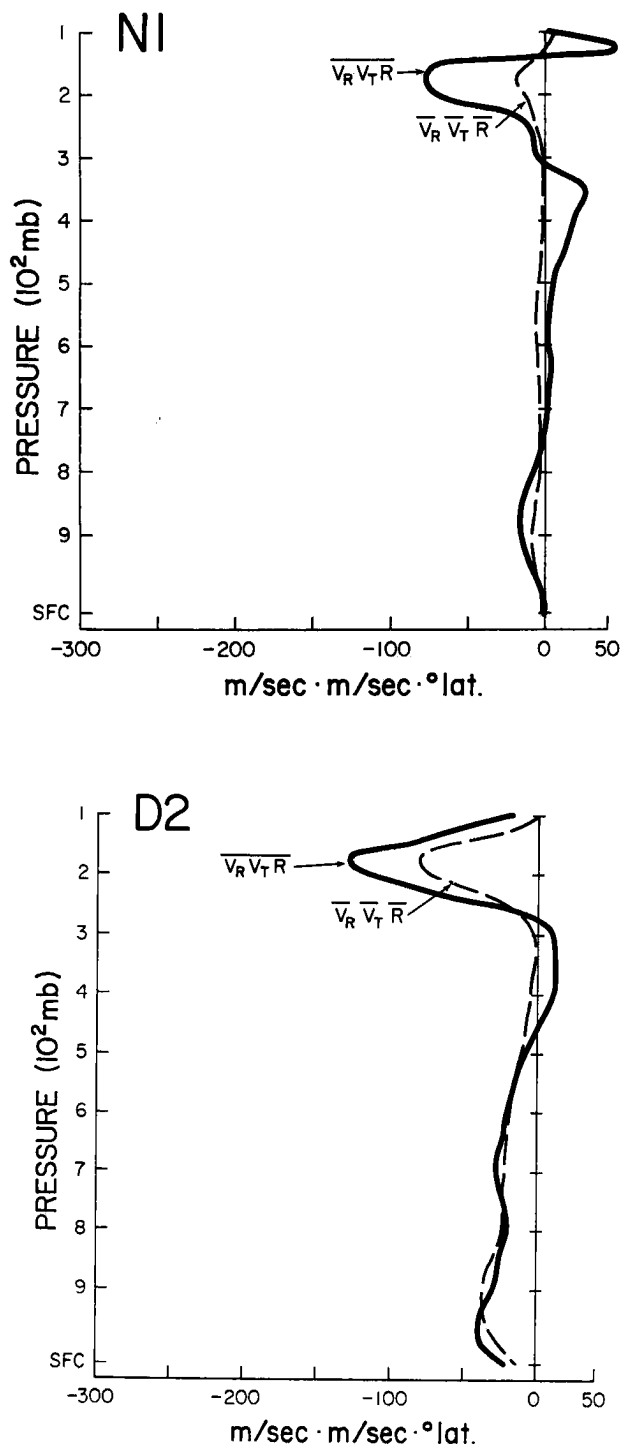


Fig. 65. Total horizontal flux of relative angular momentum ($\overline{V_R V_T R}$) and flux by mean circulation ($\overline{\overline{V_R} \overline{V_T} \overline{R}}$) at $R = 6^\circ$ for all composite data sets.

PACIFIC

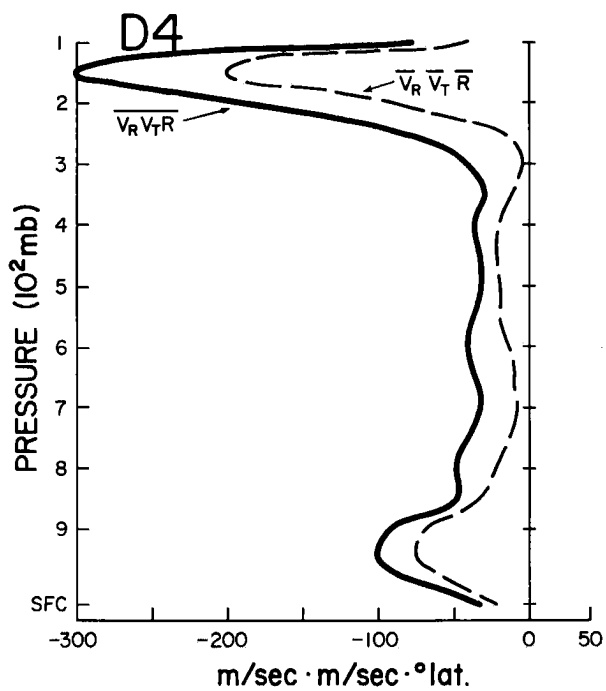
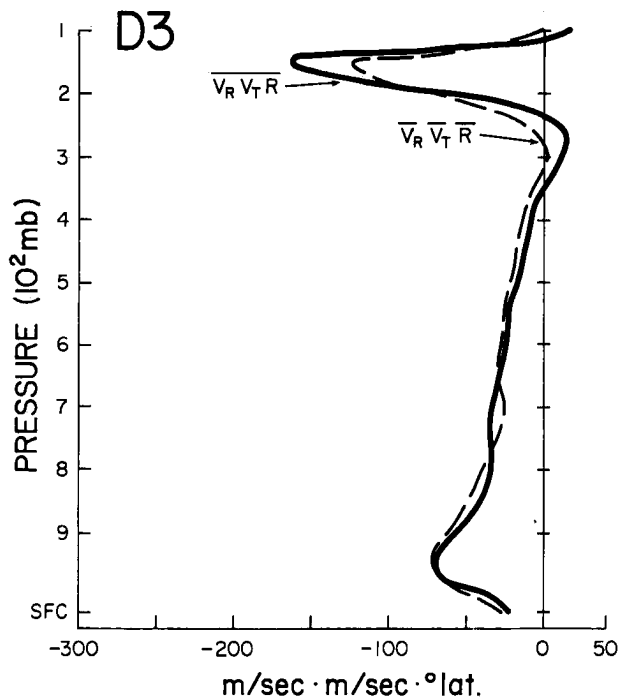


Fig. 65. Continued.

ATLANTIC

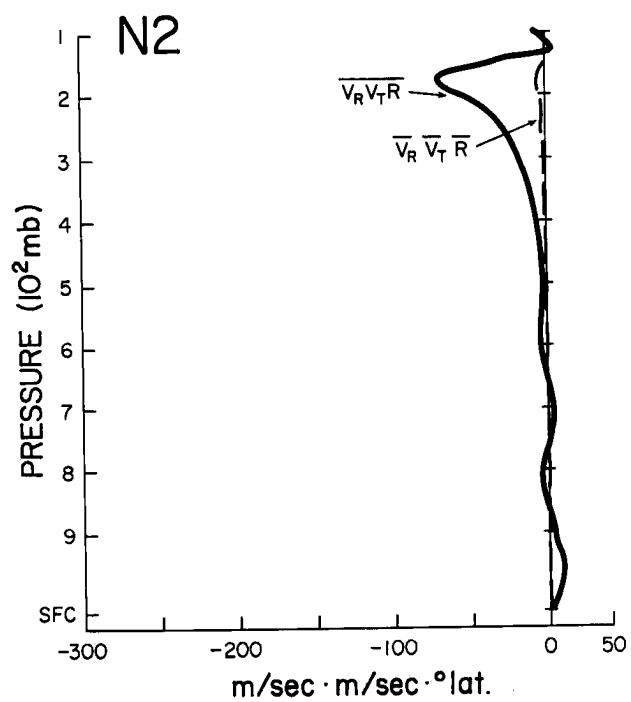
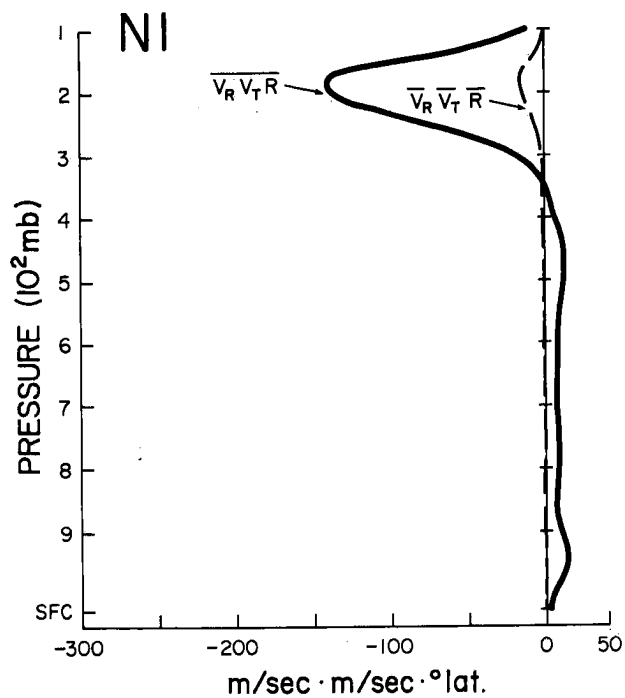


Fig. 65. Continued.

ATLANTIC

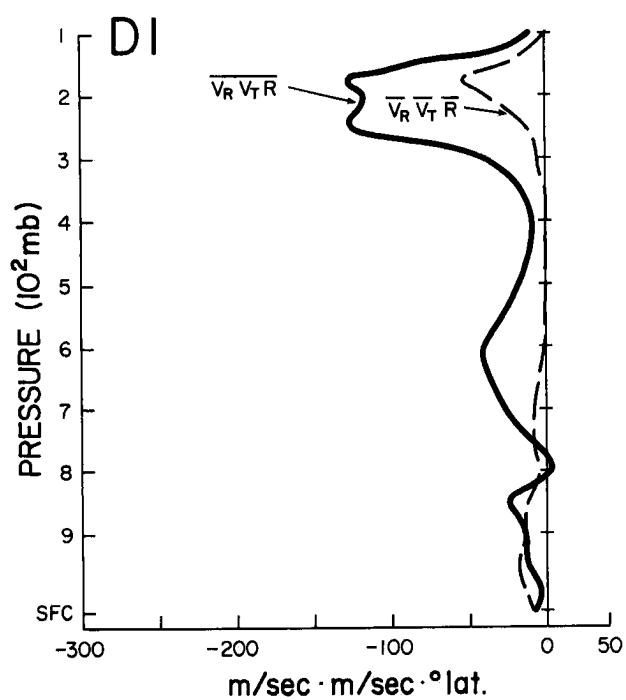
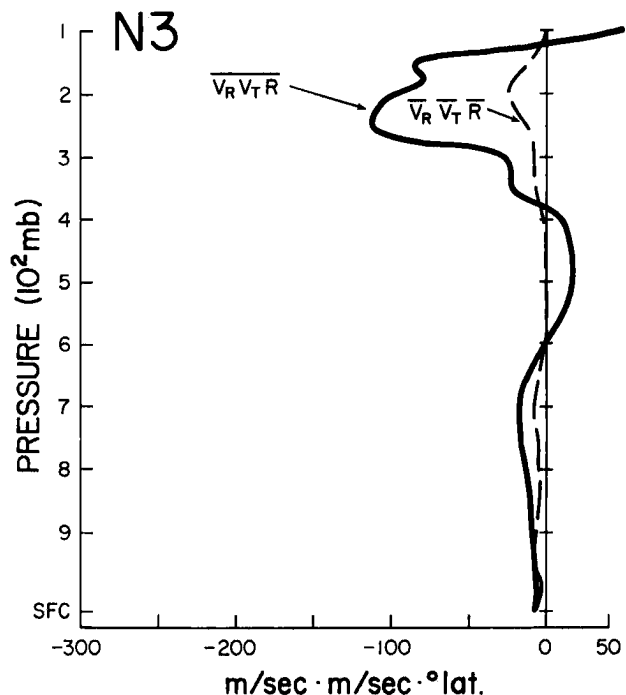


Fig. 65. Continued.

ATLANTIC

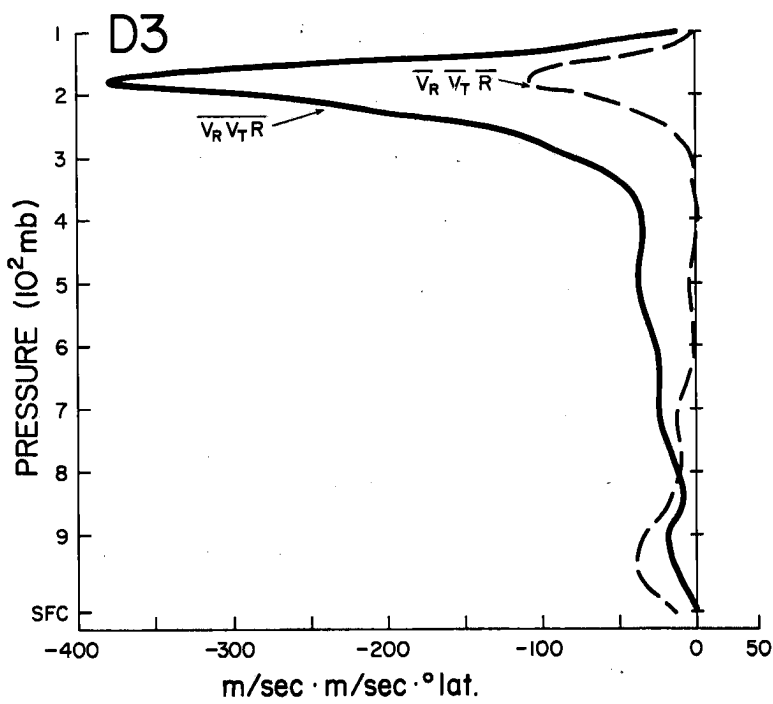
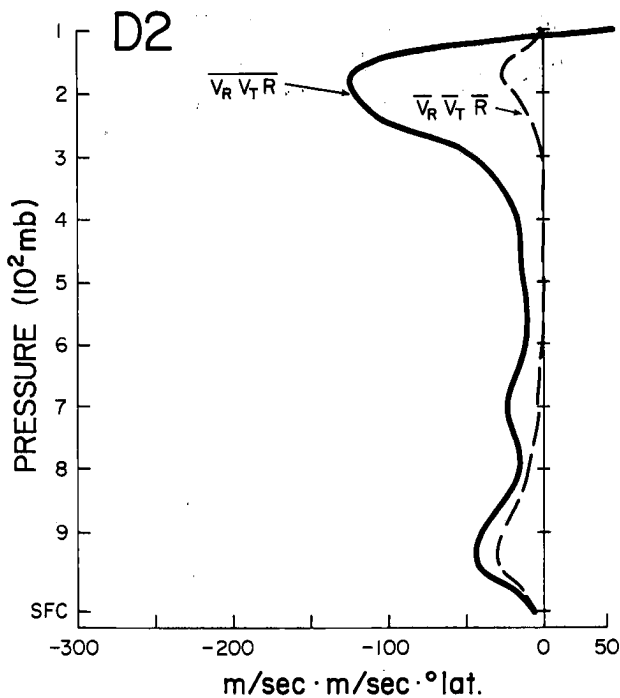


Fig. 65. Continued.

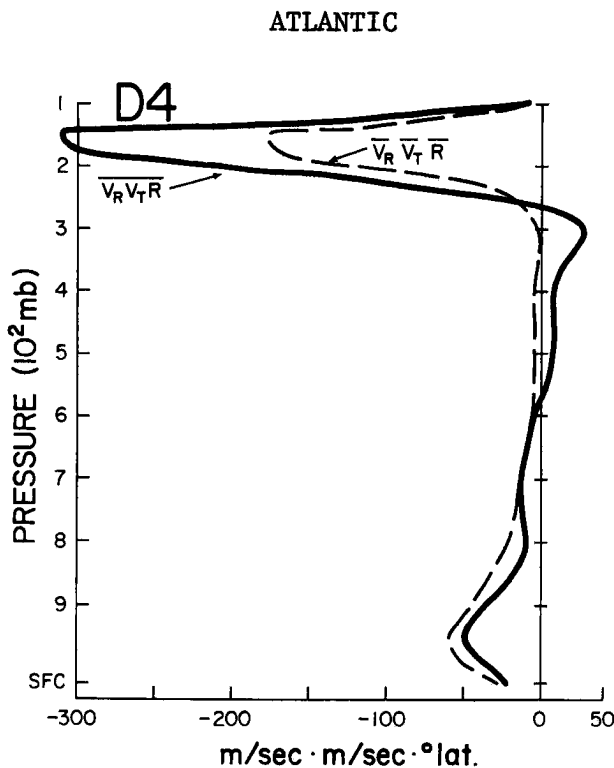


Fig. 65. Continued.

Atlantic D1 cloud cluster has better than 3 times greater import than either of the non-developing N1, N2 clusters. This is consistent with the greater outer radius vorticity fields for the developing systems which have been discussed at length in earlier chapters.

The effect of the large scale surrounding region vorticity or vertical shear on the angular momentum import is illustrated in Fig. 66. The schematic shows that if two cloud clusters have the same radial circulation, the system with the greater low level positive large scale relative vorticity imports more positive angular momentum through the product $(-V_R V_T)$. Also, if this system has greater upper level negative relative vorticity, it exports more negative angular momentum through the same product. Both effects cause an increase in positive angular momentum or a "spin-up" of the storm volume. The importance of the

TABLE 29

The horizontal convergence of relative angular momentum per unit area ($-\nabla \cdot \nabla m$). A positive entry denotes a gain of angular momentum. Units are in 10^4 kg/s^2 .

	<u>0-4°</u>	<u>0-6°</u>	<u>0-8°</u>
<u>PACIFIC NON-DEVELOPING</u>			
N1 Cloud cluster	-1.8	1.6	0.5
<u>PACIFIC DEVELOPING</u>			
D2 Pretyphoon cloud cluster	6.7	8.0	3.7
D3 Intensifying cyclone	11.9	10.3	5.5
D4 Typhoon	22.4	23.0	23.5
<u>ATLANTIC NON-DEVELOPING</u>			
N1 Cloud cluster	-3.6	3.8	0.5
N2 Wave trough cluster	2.4	2.7	2.9
N3 Non-developing depression	7.5	5.8	7.0
<u>ATLANTIC DEVELOPING</u>			
D1 Prehurricane cloud cluster	8.1	10.6	6.7
D2 Prehurricane depression	8.5	11.3	7.1
D3 Intensifying cyclone	8.7	19.0	18.3
D4 Hurricane	12.5	11.7	6.7

surrounding upper and lower tropospheric flow fields in the angular momentum budget of tropical storms has previously been stressed by Wachtmann (1968).

The separate contributions of the deep tropospheric inflow layer and of the upper tropospheric outflow layer to the relative angular momentum import are shown in Table 31. The large difference in angular momentum import between developing and non-developing weather systems is present in both layers. For the developing or pre-storm systems there is approximately an equal contribution from the inflow (surface to 300 mb) and from the outflow (300 to 100 mb) layers.

TABLE 30

The import of angular momentum ($-\nabla \cdot \mathbf{V}_m$) for the $0-6^{\circ}$ radius volume due to the mean circulation and due to horizontal eddies. A positive entry denotes a gain of momentum for the system. (Units 10^4 Kg/s^2).

	<u>Mean Circulation</u>	<u>Eddies</u>	<u>Total</u>
<u>PACIFIC NON-DEVELOPING</u>			
N1 Cloud cluster	1.3	0.3	1.6
<u>PACIFIC DEVELOPING</u>			
D2 Pretyphoon cloud cluster	7.3	0.7	8.0
D3 Intensifying cyclone	10.8	-0.5	10.3
D4 Typhoon	12.0	11.0	23.0
<u>ATLANTIC NON-DEVELOPING</u>			
N1 Cloud cluster	0.7	3.1	3.8
N2 Wave trough cluster	0.2	2.5	2.7
N3 Non-developing depression	1.9	3.9	5.8
<u>ATLANTIC DEVELOPING</u>			
D1 Prehurricane cloud cluster	2.7	7.9	10.6
D2 Prehurricane depression	2.4	8.9	11.3
D3 Intensifying cyclone	5.3	13.7	19.0
D4 Hurricane	9.5	2.2	11.7

The third term of Eq. (13), the Coriolis torque ($-f \mathbf{V}_R \cdot \mathbf{R}$), is usually assumed to integrate to zero over the total volume since the net radial mass flux is zero. This approximation is good at inner radii where f varies little. As pointed out by Anthes (1974) and W. Frank (1977b), however, the prevailing southerly wind component in the western oceans can cause an appreciable net spin-down of a storm at outer radii. The opposite (a net spin-up) would be true for a northerly flow.

To estimate the Coriolis torque, each composite system was assumed to exist at the mean latitude for that data set. A value of f was thus

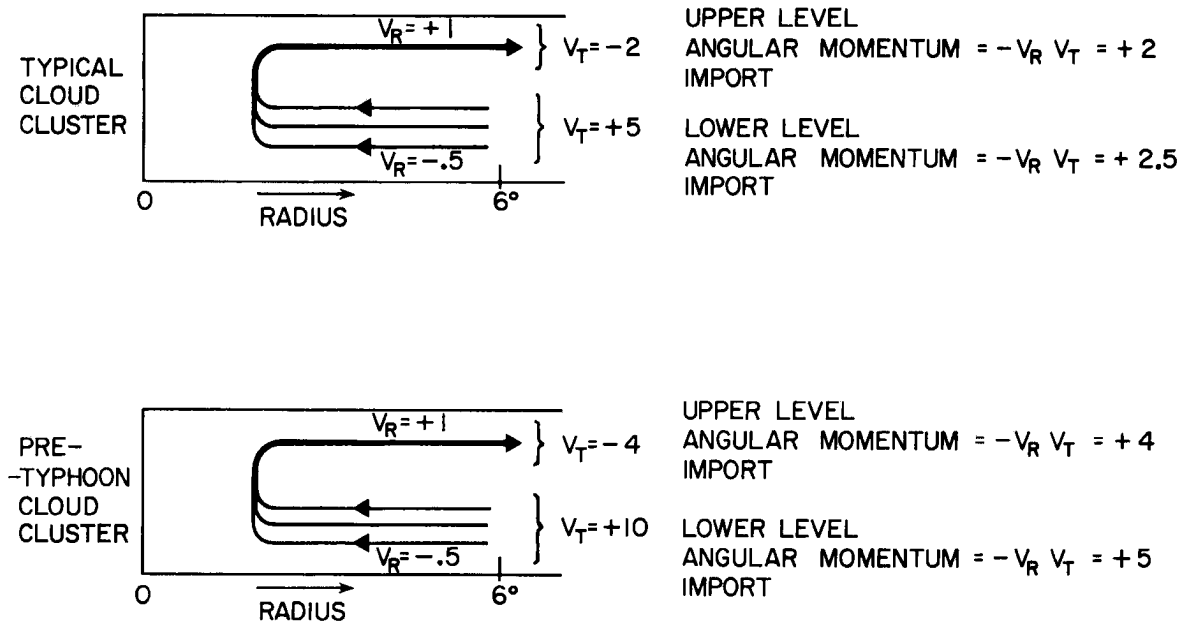


Fig. 66. Schematic representation of the effect of outer radius vorticity on the increase in angular momentum or the "spin-up" of a cloud cluster. Both clusters have the same radial circulation V_R . The lower cluster has greater outer radius tangential wind V_T and consequently imports more relative angular momentum. (Units are arbitrary.)

calculated for each octant on the composite grid, and area weighted values of $\overline{V_R} \overline{f} \overline{R}$ were calculated accordingly.

The dissipation of relative angular momentum (term (4) in Eq. 13) is equal to R times the surface tangential frictional stress, and is given by the equation:

$$\text{Dissipation} = R \rho c_D |v| V_T \quad (14)$$

The drag coefficient is the same as used in the previous section, and 900 mb winds are used scaled by .8 to approximate surface winds.

The resultant angular momentum budget for the $0-6^\circ$ volume is shown in Table 32. The second last column of the table is the residual of the three terms on the right hand side of Eq. 13. The last column is

TABLE 31

The separate contributions of the inflow and outflow layers to the import of angular momentum ($-\nabla \cdot \nabla m$) for the $0-6^{\circ}$ volume. A positive entry denotes a gain of momentum for the system. (Units are 10^4Kg/s^2).

	<u>Inflow Layer</u> (sfc-300 mb)	<u>Outflow Layer</u> (300-100 mb)
<u>PACIFIC NON-DEVELOPING</u>		
N1 Cloud cluster	-0.4	2.0
<u>PACIFIC DEVELOPING</u>		
D2 Pretyphoon cloud cluster	3.8	4.2
D3 Intensifying cyclone	6.5	3.8
D4 Typhoon	11.2	11.8
<u>ATLANTIC NON-DEVELOPING</u>		
N1 Cloud cluster	-1.8	5.6
N2 Wave trough cluster	2.1	0.6
N3 Non-developing depression	1.2	4.6
<u>ATLANTIC DEVELOPING</u>		
D1 Prehurricane cloud cluster	4.6	6.0
D2 Prehurricane depression	5.3	6.0
D3 Intensifying cyclone	6.1	12.9
D4 Hurricane	2.2	9.5

the measured value of $\frac{\partial m}{\partial t}$ or the left hand side of the equation. The equation as calculated from the data does not balance; so a constant percentage change was made to each term on the right hand side of the equation. The resulting "balanced" budget of relative angular momentum is shown in Table 33.

The relative angular momentum budget is dominated by the horizontal convergence ($-\nabla \cdot \nabla m$). This is proportional to $(-\nabla_R \cdot \nabla_T)$ on the perimeter of the volume. All the developing systems have very large values of angular momentum convergence. The Atlantic prehurricane cloud cluster has $2\frac{1}{2}$ to 3 times the convergence of the non-developing clusters.

TABLE 32

Vertically integrated budget of relative angular momentum for the $0-6^{\circ}$ volume (in units of 10^4 Kg/s^2).

	Import $-\nabla \cdot (\nabla m)$	Coriolis Torque RfV_R	+	Surface Frictional Dissipation $R F_T$	=	Residual	$\frac{\partial m}{\partial t}$ measured
<u>PACIFIC NON-DEVELOPING</u>							
N1 Cloud cluster	1.6	0.1		-0.5		1.2	0.0
<u>PACIFIC DEVELOPING</u>							
D2 Pretyphoon cloud cluster	8.0	-1.2		-1.7		5.1	6.3
D3 Intensifying cyclone	10.3	-3.2		-4.0		3.1	6.0
D4 Typhoon	23.0	-6.8		-8.3		7.9	0.0
<u>ATLANTIC NON-DEVELOPING</u>							
N1 Cloud cluster	3.8	-1.8		-0.2		1.8	0.0
N2 Wave trough cluster	2.7	-2.5		-0.2		0.0	0.0
N3 Non-developing depression	5.8	-2.8		-0.9		2.1	-1.5
<u>ATLANTIC DEVELOPING</u>							
D1 Prehurricane cloud cluster	10.6	-2.2		-1.0		7.4	0.0
D2 Prehurricane depression	11.3	-2.1		-1.7		7.5	-0.7
D3 Intensifying cyclone	19.0	-3.2		-2.4		13.4	5.5
D4 Hurricane	11.7	-3.5		-5.2		3.0	0.0

TABLE 33

Vertically integrated budget of relative angular momentum for the 0-6° area. Positive numbers indicate a gain of angular momentum. Values have been corrected slightly, as described in the text. (Units are 10^4 Kg/s^2).

	Import $(-\nabla \cdot \nabla m)$	Coriolis Torque	Surface Frictional Dissipation	$\frac{\partial m}{\partial t}$
<u>PACIFIC NON-DEVELOPING</u>				
N1 Cloud cluster	1.1	0.1	-0.7	0.5
<u>PACIFIC DEVELOPING</u>				
D2 Pretyphoon cloud cluster	8.4	-1.1	-1.6	5.7
D3 Intensifying cyclone	11.2	-2.9	-3.7	4.6
D4 Typhoon	20.6	-7.5	-9.2	3.9
<u>ATLANTIC NON-DEVELOPING</u>				
N1 Cloud cluster	3.2	-2.1	-0.2	0.9
N2 Wave trough cluster	2.7	-2.5	-0.2	0.0
N3 Non-developing depression	4.5	-3.4	-1.1	0.0
<u>ATLANTIC DEVELOPING</u>				
D1 Prehurricane cloud cluster	7.8	-2.8	-1.3	3.7
D2 Prehurricane depression	8.8	-2.6	-2.1	4.7
D3 Intensifying cyclone	11.7	-4.4	-3.3	4.0
D4 Hurricane	10.8	-3.8	-5.6	1.4

In the Pacific, the pretyphoon D2 cluster has 8 times as much angular momentum convergence as the N1 non-developing cloud cluster. These differences are directly caused by the differences in low level positive and upper level negative V_T between the systems, because as has been shown earlier the mass flow or V_R is much the same in each case.

8.5 Summary

The main findings from the budget analyses in this chapter are as follows:

- 1) All the composite weather systems export moist static energy h through their transverse circulation.
- 2) To bring about an increase in energy, h , the quantity $(H_o - \bar{V} \cdot \nabla h)$ must be increased.
- 3) All the composite weather systems export kinetic energy. The export takes place completely in the upper tropospheric outflow layer.
- 4) The kinetic energy budgets show a residual requirement for a generation of kinetic energy by sub-grid scale processes. This eddy generation appears to be of the same magnitude as the generation by the mean radial flow, $-\bar{V} \cdot \nabla \phi$.
- 5) Compared to non-developing systems, developing cloud clusters have twice to three times as much import of relative angular momentum through their lateral boundaries. This is directly related to the developing system having greater outer radius low-level positive and upper-level negative surrounding tangential wind fields.

9. THE PHYSICAL PROCESSES OF TROPICAL CYCLONE GENESIS

The only appreciable energy source present when a tropical cloud cluster undergoes the transformation into a tropical storm is the latent heat released in cumulus convection. In Chapters 3 and 8 it was shown that as the storm begins to develop and intensify, a warming of the troposphere takes place over a very large area. Figure 56 of Chapter 8 shows a decrease in the low level height fields as far out as 8° latitude radius from the system center.

The genesis and development of a tropical cyclone is the only situation in which a sustained and large scale warming takes place in the tropical troposphere. How is this warming brought about? The tropical atmosphere is normally very reluctant to warm, even under situations of very active and widespread deep cumulus convection. There have been many observational studies performed in recent years on tropical oceanic cloud clusters or weather disturbances (Reed and Recker, 1971; Williams and Gray, 1973; Gray, 1973; Yanai, Esbensen and Chu, 1973; Ruprecht and Gray, 1976a,b; W. Frank, 1978a). The main observational fact that has come out of these studies is that despite the very large amounts of precipitation falling in the cloud clusters, the warming (or $\frac{\partial s}{\partial t}$) realized on the scale of the cluster is approximately zero. As has been discussed in section 8.2, a portion of the energy released in the system as latent heat $L P_o$ acts to counter the radiative cooling Q_R ; the rest is exported from the system as potential energy through the term, $\nabla \cdot \nabla s$.

Grube (1979) examined every rawin sounding taken by the seven ships of the B-array during the sixty days of the GATE experiment which was

carried out in the Eastern Atlantic Inter Tropical Convergence Zone during the Northern Hemisphere Summer of 1974. The GATE B-array is approximately equivalent in area to a circle of $1\frac{1}{2}^{\circ}$ latitude radius. The average rainfall over the B-array for the 60 days of the experiment was 1.2 cm/d (W. Frank, 1978b) which is enough heat energy to warm the whole troposphere by $3.3^{\circ}\text{C}/\text{d}$. Despite this enormous amount of rain, Grube found no cases of simultaneous warming events at more than one ship in the array. She observed many cases of warming due to cumulus induced subsidence at single ships. These warming were characteristically changes of 1°C temperature averaged over the 200-500 mb layer. In every case the atmosphere reacted very quickly to counteract the warming so that the energy was spread over a very large area within a few hours. This has been verified in numerical modelling experiments by W. Fingerhut which are discussed in the Grube paper.

As has also been discussed in Chapter 8, the only means by which a Cb cloud can cause any appreciable temperature increase in its environment is by compensating subsidence. Somehow the favorable superposition of upper level anticyclonic flow and low level cyclonic flow described throughout this paper must decrease the export of potential energy $\nabla \cdot \nabla s$ and cause the compensating subsidence to be localized rather than spread over a broad region. In other words, it must somehow bring about a decrease in the energy exporting transverse circulation.

The vertically integrated h budget for a pretyphoon or prehurricane cloud cluster is described by the following equation, with typical values printed below it as estimated from the analysis in section 8.2:

$$\frac{\partial h}{\partial t} = H_o + Q_R - \nabla \cdot \nabla h$$

(15)

$$0 = 1.8 - 1.1 - 0.7$$

$$(^\circ\text{C/d})$$

The pre-cyclone cloud cluster is in a quasi-steady state with sea surface to atmosphere transfer H_o plus radiative heating Q_R equaling a net $H_o + Q_R$ greater than zero. For balance the transverse or radial circulation must export h from the system through the term $\nabla \cdot \nabla h$.

The local h content can be increased by increasing the surface evaporation H_o or by decreasing the radial circulation $\nabla \cdot \nabla h$. An increase of H_o acts to increase the water vapor content q which is converted to rainfall LP_o and exported as potential energy through the term $\nabla \cdot \nabla s$ or $\nabla \cdot \nabla h$. Apparently, to increase the warming within the cluster, the radial export through the term $\nabla \cdot \nabla h$ must be decreased.

It has been stressed throughout this paper that there is a large variability in radial circulation or vertical velocity between different systems of the same intensity or of the same type. Despite this variability a decrease in radial circulation, vertical velocity and mean cloudiness does show in the data between stage D1 and stage D2. This can be seen for cloudiness in Table 21 of Chapter 7, for vertical motion ω in Fig. 58 of Chapter 8 and for radial circulation V_R in Fig. 63 of Chapter 8.

As the incipient disturbance intensifies, the low level wind speeds increase and consequently the energy input H_o from the sea surface increases. The above quoted observational studies indicate that the

normal response of the tropical atmosphere to such an increase is to correspondingly increase the energy export $\nabla \cdot \nabla h$. A sustained warming and subsequent cyclone genesis and intensification can occur only if the flow fields are constrained to keep $\nabla \cdot \nabla h$ smaller than the sum of H_o and Q_R .

The observations of this paper indicate that such a relative decrease in $\nabla \cdot \nabla h$ takes place when the cloud cluster is embedded in a field of surrounding upper level anticyclonic flow and low level cyclonic flow. As has been discussed, the superposition of these fields leads to the presence of high anticyclonic vertical wind shear surrounding the cloud cluster at approximately 6° latitude radial distance from the center.

What effect does the vertical shear have on the properties of the westward moving ensemble of deep cumulus clouds, known as a 'cloud cluster'? In particular, how does it cause the latent heat released in these clouds to warm locally rather than be exported through the transverse circulation?

The effect of vertical wind shear on deep convection has been extensively studied by a group of scientists at Imperial College, London (Green and Pearce, 1962; Ludlam, 1963, 1966; Moncrieff and Green, 1972; Miller and Pearce, 1974; Moncrieff and Miller, 1976; Moncrieff, 1978). Their analytic and numerical results indicate that under certain conditions Cb convection acts to greatly increase the kinetic energy below cloud base and at the upper outflow level.

When the wind profile in which the deep convection is embedded is such that relative to the movement of the cloud the wind blows in opposite directions at upper and lower tropospheric levels, the effect

at the upper outflow level is to greatly increase the magnitude of the wind in the direction of the prevailing flow. This assessment has obtained recent support from the cloud modelling studies of Cotton and Tripoli at Colorado State University. Figure 67 from one of their recent model simulations clearly shows a large injection of kinetic energy into the mean flow at the outflow level. The clouds also apparently increase the kinetic energy below cloud base through the mechanism of the cloud downdraft spreading out horizontally as a density current (Benjamin, 1968; J. Simpson, 1969; Moncrieff and Miller, 1976).

The observations of Chapter 3 show that the prestorm cloud cluster characteristically has a large amount of deep cumulus convection, at least enough to equal 100 mb/d net upward motion averaged over the $0\text{--}4^{\circ}$ area. Away from the center of the system this convection exists in strong vertical shear such that the wind blows in opposite directions at upper and lower levels, for example low level trade winds and upper level westerlies to the poleward side of the cluster, low level westerlies and upper level easterlies on the equatorward side. Deep convection in such a vertical shear regime should increase the upper level negative and lower level positive tangential winds.

The cloud cluster's transverse circulation is predominantly an ageostrophic response to the cluster's pressure gradients, though there is a small contribution due to frictional convergence, as has been documented in Chapter 2. To decrease this circulation there must be a change induced in the wind-pressure balance of the surrounding tangential wind fields. It has been shown in Chapter 7 that the low level positive tangential winds and upper level negative tangential winds surrounding the prestorm disturbance are the result of already existing

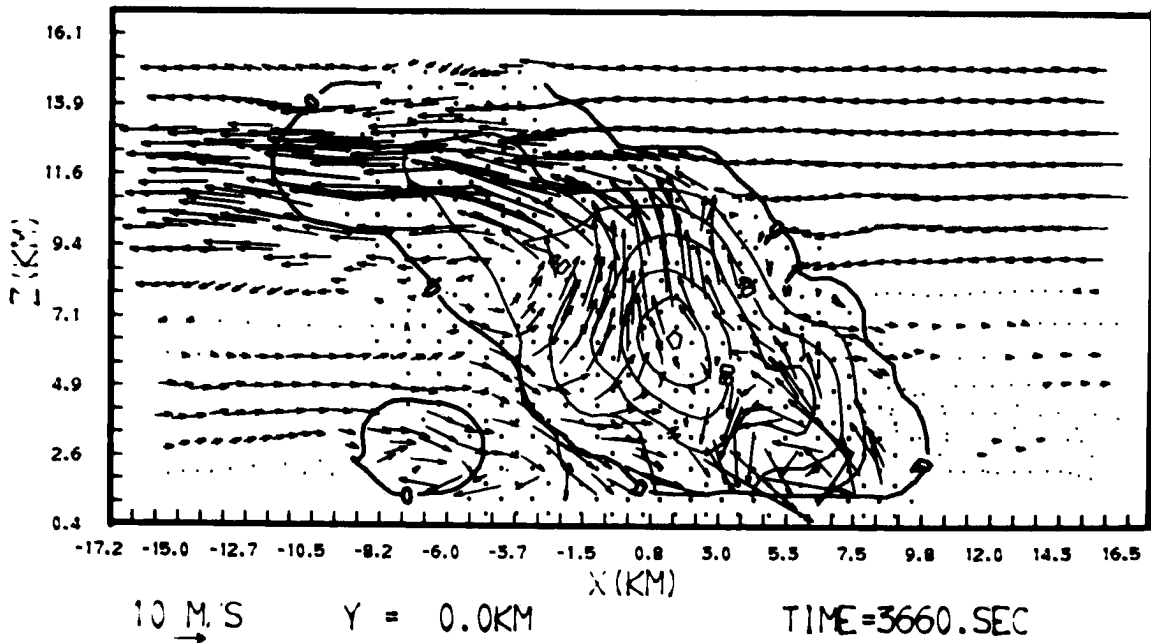


Fig. 67. Numerical output from recent cumulonimbus simulation by Cotton and Tripoli. Arrow lengths are proportional to wind speed.

surrounding lower and upper level weather systems. The wind fields for these systems are in dynamic balance with the height fields. Relative to the center of the prestorm cloud cluster, the tangential wind fields are in close to gradient balance.

The injection of kinetic energy from the clouds will change the wind-pressure acceleration balance and bring about supergradient (or less subgradient) winds at upper and lower levels. This should act to cause a reduction in the cyclone or disturbance's transverse circulation. The transverse circulation primarily acts to export moist static energy h from the system. This adjustment decreases the h export but leaves intact or slightly increases the low level h import, H_o , from the sea surface. There is a consequent energy accumulation and system intensification.

The adjustment is schematically represented in Fig. 68 where it is assumed that the initial balanced wind V_o is increased by C_b

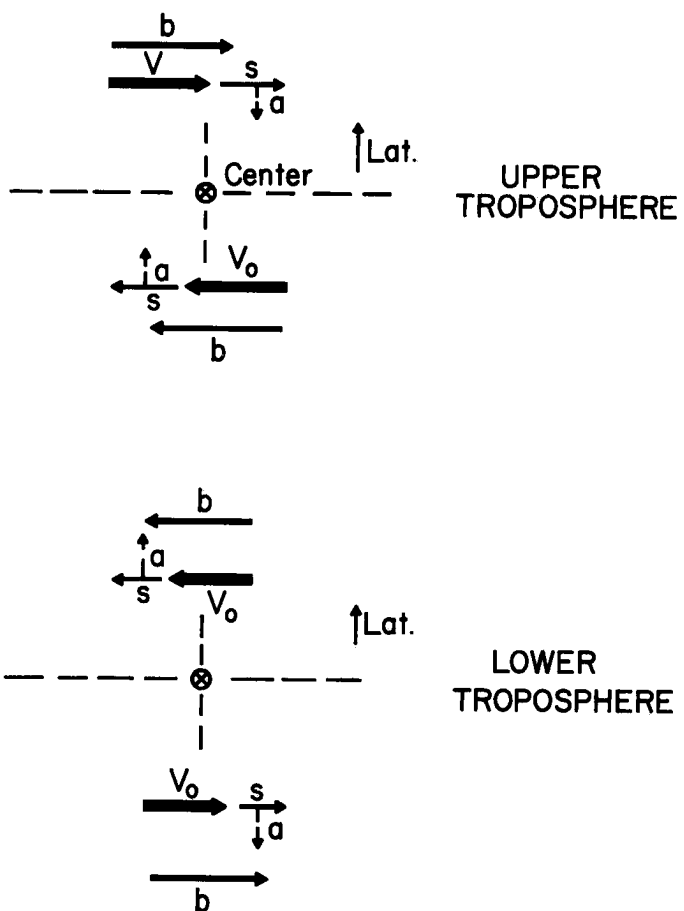


Fig. 68. Idealized view of how initial winds (V_o) poleward and equatorward of the developing disturbance are increased by amount s due to Cb convection, the direction of the resulting unbalanced acceleration a , and the magnitude of the resulting balanced wind b when wind and pressure come into adjustment (from Gray, 1979).

convection to a value of $V_o + s$ and a resulting outward acceleration (a) takes place to cause a reduction in the mean upper level divergence and lower level convergence. These radial wind alterations act to reduce the transverse circulation and bring about an adjustment of the wind-pressure fields. When the wind and pressure come into balance, the resulting wind is represented by b . Intensification may be thought of as a gradual step by step wind-pressure unbalancing and then wind-pressure adjustment to this unbalancing.

When vertical shear patterns do not permit the Cb convection to act in this manner, wind-pressure balances are not favorably altered and transverse circulation decreases and intensification does not occur. System weakening occurs when the wind-pressure ratio is one causing substantial subgradient winds.

Thus, the role which the strong surrounding vertical wind shear patterns of growing disturbances play may be that of allowing the outer radii Cb convection (often in the form of squall lines) to act to increase the lower and upper tropospheric wind-pressure ratios which, in turn, act to inhibit the system's transverse circulation. By previous reasoning this should lead to intensification. This tropical storm intensification hypothesis was first advanced by Gray (1979).

If the above proposed mechanism is correct, the role of cumulonimbus clouds in tropical cyclone genesis is not to act as sources of heat, but rather as sources of momentum. Schubert and Hack (1979) have recently provided some theoretical support for this idea. They have studied the linearized geostrophic adjustment in an axisymmetric vortex. In one model experiment they imposed an initial perturbation in the geo-potential field and solved analytically for the final adjusted state. In the tropics where the Coriolis parameter is small, and consequently the Rossby deformation radius is large, they find that the final state is one of approximately zero energy; that is the initial perturbation has been totally removed by gravity waves. This can physically be interpreted as corresponding to the above mentioned observational studies which show that no matter how much latent heat is released in a tropical cloud cluster, it is all exported out by the transverse circulation; and there is no local warming.

Schubert and Hack also performed the converse study of imposing an initial unbalanced vortex and solving for the final adjusted state. In the tropics the final state is such that 95% or more of the original kinetic energy is still present and the atmosphere has created a pressure gradient to balance it. These results generally support the idea that the cumulonimbus clouds in the pre-storm cluster can induce a tropospheric warming by acting as sources of kinetic energy.

Other researchers on Professor William M. Gray's project at Colorado State University are continuing this investigation to further explore this proposed mechanism for tropical cyclone development. Edwin Núñez has analyzed the wind-pressure relations at upper and lower levels around the data sets used in this study and around several additional composite systems. He is consistently finding more supergradient or less subgradient winds around developing systems than around non-developing systems. Wind-pressure imbalances such that the tangential wind is greater than required by the pressure gradients cannot result from any sensible heating mechanism, but must originate from some mechanism such as injection of kinetic energy from the sub-grid scale. Núñez's work is still in progress and will be reported on in a future Colorado State University Department of Atmospheric Science Project Report.

Fingerhut (1979) in a complementary study to the present one has developed an axially symmetric primitive equation model of a tropical cloud cluster which he allows to evolve into a tropical cyclone. His model is constructed to be consistent with the observations of the current paper. His cumulus parameterization is such that there is no net tropospheric warming at the grid point at which the cumulus exists.

He includes the observed surrounding region upper level negative and lower level positive tangential winds; and he invokes a large injection of Cb-induced upper and lower level kinetic energy. This model well simulates the transformation from cloud cluster to tropical cyclone.

More research is required on the effect of Cb convection on the dynamics of the cloud cluster or tropical storm environment. The mechanism proposed above involves a generation of horizontal kinetic energy by the clouds at cloud base and cloud top. Since the wind direction reverses with height, this means that the clouds are actually increasing the upper minus lower level vertical wind shear. It must be emphasized that this is a momentum or kinetic energy generation and not a momentum transfer. As previously discussed by Gray (1967), at all levels between cloud base and the upper outflow level the cloud mass fluxes are vertically transporting cyclonic momentum and thus are acting in the usually envisaged 'downgradient' sense. Figure 69 illustrates the type of process that may be operating. Part (a) shows the vertical shear as it exists around precyclone cloud clusters. Part (b) shows how the vertical transport of momentum by cumulus up and downdrafts reduces the wind shear. Part (c) shows the Cb induced upper and lower outflow level generation of kinetic energy in the direction of the mean flow; and part (d) shows the net effect of both processes. These detailed aspects of the clouds' role in the momentum and kinetic energy budgets are still somewhat speculative at this stage, however. Detailed vertically partitioned budget studies for the composite data sets are planned for Gray's research project in the near future to attempt to isolate these effects.

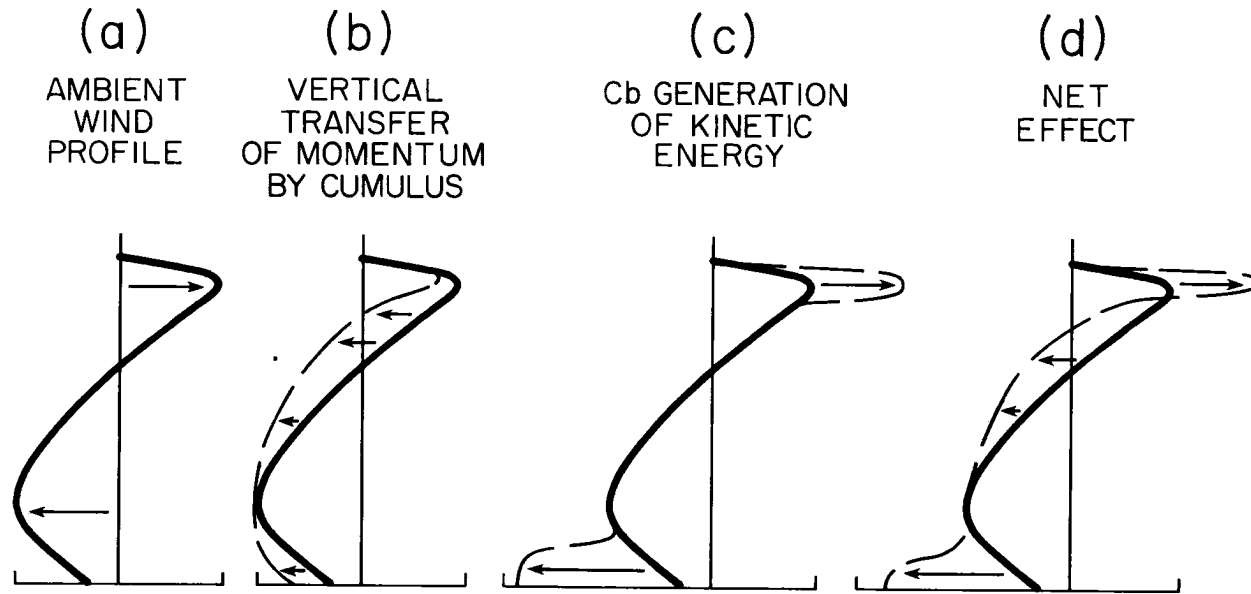


Fig. 69. Idealized picture of how Cb convection affects the tropospheric wind profile when the wind changes direction with height. Diagram a shows the ambient wind profile. Diagram b shows the vertical mixing of momentum by cumulus transports. This process acts to decrease the vertical shear. Diagram c shows the cumulonimbus generation of kinetic energy at cloud base and at cloud top. This acts to increase the vertical shear. Diagram d shows the net effect of processes b + c.

Some support for the hypothesis that the injection of mass from the cumulus up- and down-drafts increases the kinetic energy in the direction of the mean flow can be inferred from the work of McEwan (1976). He performed a rotating tank experiment whereby fluid was pumped from below through thin jets into the revolving tank. The effect of the extra injection of mass was to increase the total rotation rate of the fluid.

10. CONCLUDING REMARKS

The analysis of the composite data sets and of the 130 individual case studies has shown that prior to the development of a tropical cyclone the large scale atmosphere sets itself up so that there exists an east-west extending line of zero vertical shear of the zonal wind and simultaneously a north-south extending line of zero vertical shear of the meridional wind. There also exist very large horizontal gradients of this vertical shear with strong positive zonal shear to the north, strong negative zonal shear to the south, strong positive meridional shear to the west and strong negative meridional shear to the east of the developing system. These shear patterns are brought about by adjoining tropical and mid-latitude weather systems, so that it is the properties of the large scale surrounding flow rather than of the incipient disturbance that determine whether tropical cyclone genesis will occur.

The shear phenomenon can also be interpreted in terms of relative vorticity:

$$\text{Genesis Potential (GP)} = \zeta_{200 \text{ mb}} - \zeta_{900 \text{ mb}}$$

This parameter, when measured using tangential winds at 6° radius shows very large differences between developing and non-developing cloud clusters. It is three times greater for the developing systems than for the non-developing. The vorticity differences are concentrated in the lower and upper troposphere. As the lower and upper tropospheric maps are primary analysis levels in the tropics and since the

geostationary satellite will often be able to furnish winds at these levels, this finding has great potential as an operational forecast aid.

130 separate weather systems in the Atlantic and Pacific were examined to see to what extent the composite characteristics fit the individual situations. In the Atlantic grid-point vertical shear data were available. It was found that the use of the shear or vorticity criterion would have correctly predicted the development of 13 out of 16 tropical cyclones. It would have provided correct predictions for 61 out of 63 non-developing tropical weather systems.

Vertically integrated budgets of heat, momentum and kinetic energy were performed on the composite data sets. It was demonstrated that the transverse mass circulation through the cloud cluster exports moist static energy from the system. For development to occur this energy exporting transverse circulation must be inhibited. It was hypothesized that the inhibition was brought about by the deep cumulus clouds in strong vertical shear creating horizontal kinetic energy at their upper and lower tropospheric outflow levels. The extra kinetic energy causes a supergradient wind-pressure imbalance which decreases the radial flow.

The proposed theory of tropical cyclone genesis is dependent on the radial mass circulation exporting moist static energy h from the system. The western ocean cloud clusters export h because they have mass inflow through a deep tropospheric layer from the surface up to 300 mb and outflow in a thin layer between 300 and 100 mb. Moist static energy has a tropospheric minimum near 600 mb, so the inflowing air has a lower mean value of h than does the outflowing air.

The cyclone genesis mechanism is thus very dependent on the existence of the cloud cluster's very deep inflow layer. The observational

studies of Gray and Jacobson (1977) and McBride and Gray (1978) and the modelling work of Fingerhut (1978) indicate that the disturbance's deep inflow is maintained by the differences in the radiative-condensation heating profiles of the thick-cirrus shield covered weather systems and their surrounding clear areas. One important aspect of the forcing mechanism for the deep inflow is the fact that the cirrus covered cloud cluster has less net radiative cooling than the surrounding clear area; therefore in a relative sense it is a radiative heating maximum.

If this assessment is correct, it has important implications for numerical and analytic studies of tropical cyclone genesis. To realistically simulate cyclone genesis, the model weather system must have a deep layer of mass inflow, and to realistically include this it must incorporate the differential radiative properties of the weather system and its environment. The radiational differences are mainly caused by cloudiness differences. The cloudiness is believed to be much the same in non-developing and in pre-cyclone cloud clusters. Thus, radiation is not an important factor in distinguishing between a developing versus a non-developing system. It does, however, play an important role in the physical processes of storm genesis and must be included in any model of genesis.

The genesis theory has been proposed in terms of the h budget. Two major components of this budget, the radiation Q_R and the h export $\nabla \cdot \nabla h$, have a large diurnal variation. (The h export $\nabla \cdot \nabla h$ is carried out by the transverse circulation V_R . In Chapter 2 it was pointed out that this exhibits a 2 to 1 diurnal variation, mainly radiationally driven.) The effect of this variation on cyclone genesis has not yet been explored, but it must be taken into consideration in future work

on the subject. In particular the diurnal variation of radial wind implies that the system is exporting approximately twice as much h in the early morning (~ 7 AM local time) as it is in the evening (~ 7 PM local time).

For a steady state cloud cluster to be exporting h , this requires that the other terms in the budget $E_o + Q_R$ be greater than zero. In section 2.6 it was demonstrated that the Western Pacific has a greater value of surface evaporation E_o than does the Western Atlantic. It should therefore be much easier in the Western Pacific to form a cloud cluster such that $E_o + Q_R$ is greater than zero. This no doubt greatly influences the number of tropical storms in each region; and in fact the Western Pacific does have approximately three times more storms each year than the Western Atlantic (Gray, 1979).

Much research effort has been expended in recent years on the GATE area, or the ITCZ region of the Eastern Atlantic. That region has very small surface evaporation (approximately .3-.4 cm/d). Also, the convergence or mass inflow into a GATE weather system is mainly forced by large scale ITCZ convergence. In the Eastern Atlantic the ITCZ convergence is a low level phenomenon. Consequently, the mass inflow in a GATE cloud cluster is concentrated in the low levels. It is not a deep inflow; therefore the radial circulation does not export h . In terms of the model here proposed such a cluster cannot generate a tropical storm; and in fact there are no tropical cyclones in the Eastern Atlantic ITCZ region.

The theory of tropical cyclone genesis here proposed is that the required tropospheric warming is a result of an adjustment of the pre-storm disturbance's mass field to the wind field. The cloud influence

on cyclone genesis is not in proportion to the condensation energy released by the system but rather to the ability of the cloud to generate supergradient winds at lower and upper levels.

It is appropriate to comment on other existing theories of tropical cyclone development. The CISK theory first proposed by Ooyama (1964) and Charney and Eliassen (1964) depends on a positive feedback such that increased mass and moisture convergence bring about more local heating due to clouds which in turn increases the convergence. This theory has three basic deficiencies: (i) all the observational evidence of the current paper shows that genesis is not related to increased convergence or increased cloudiness; (ii) the theory is based on the cumulus convection acting as a direct heat source; as discussed earlier, it can act more effectively in the tropics as a source of momentum or kinetic energy; (iii) the positive feedback in the CISK models depends on the increased mass convergence being frictionally driven; it was shown in Chapter 2, Table 8, that boundary layer frictional convergence makes up only 5-20% of the total cloud cluster mass inflow. For these reasons the traditional CISK theory does not appear relevant to the transformation from cloud cluster to tropical cyclone.

Shapiro (1977a, b) has developed a criterion for cyclone genesis which basically looks for dynamic properties of the large scale flow which are inconsistent with an easterly wave or cloud cluster remaining in a linear state. Shapiro's work is in agreement with the current study in so far as it emphasizes the control by the large scale flow rather than the properties of the cluster itself. The major point of disagreement between Shapiro's work and the current study is that his criterion is a barotropic one and is based on the properties of the large scale

flow at just one level, such as 700 mb. The current study and many previous observational studies (Riehl, 1948, 1950; Yanai, 1961; Sadler, 1967, 1975, 1976, 1978; Gray, 1968; Zehr, 1976; S. Erickson, 1977; Dvorak, 1975) have shown that genesis depends on a superposition of favorable upper level and lower level large scale flow features.

The observations presented in this paper hopefully form a foundation for a theory or model of tropical cyclone genesis. The analysis of the composite data sets revealed differences in relative vorticity and vertical shear that exist between developing and non-developing oceanic tropical weather systems. The analysis of the individual case studies justified the compositing approach by verifying that these differences are actually present in the individual situations.

The composite analysis revealed the favorable large scale surrounding vorticity fields are present from the first day of existence of the pre-storm cloud cluster. The discussion in this paper has dealt with the physical processes that take place from the moment of existence of the cloud cluster in the favorable environment through to the existence of a fully developed typhoon or hurricane. The most obvious next step to further this research is to go back prior to the existence of the cloud cluster and to investigate the characteristics of the tropical general circulation which lead to the establishment of these favorable conditions. Some early research in this line was performed by Sartor (1968). More recent discussion has been presented by Gray (1975, 1979).

This paper has observationally investigated the genesis of tropical cyclones. Physical insight has been gained from the observations and discussion has been presented of the likely physical processes. To complete this theory, a mathematical treatment based on these physical

concepts is required. Fingerhut (1979) in a companion paper is performing such a treatment by simulating cyclone genesis with an axisymmetric primitive equation model.

ACKNOWLEDGEMENTS

The author gratefully acknowledges the support and guidance of his advisor, Professor William M. Gray.

This research was performed while the author was a member of W. M. Gray's tropical cyclone research project at Colorado State University. This study relied heavily on the previously assembled 10-year West Pacific and 14-year West Atlantic rawinsonde data sets of Professor Gray's project. Other members of the project whose work interrelated to the author's and discussions with whom greatly contributed to this research include: W. M. Frank, R. Zehr, S. L. Erickson, C. P. Arnold, W. A. Fingerhut and E. Núñez.

The research could not have been performed without the programming assistance of E. Buzzell, the technical assistance of Bonnie Weber and the fine technical and administrative assistance of Barbara Brumit.

The author is grateful to Mark Zimmer and Neil Frank of the National Hurricane Center, Vern Dvorak of NOAA/NESS Applications Group and Lloyd Shapiro of the National Hurricane and Experimental Meteorology Laboratory all of whom contributed their time and resources to the compilation of positions and tracks for the composite and individual case data sets.

Professors D. E. Stevens, W. H. Schubert and A. K. Betts reviewed the manuscript.

This research has been supported by the National Oceanic and Atmospheric Administration, National Hurricane and Experimental Meteorology Laboratory Grant No. NA 79 RAD 00002 and the National Science Foundation Grant No. ATM 78-18962, with supplementary support from the U.S. Navy Environmental Prediction Research Facility, Monterey, CA Grant No. N00228-76-C-2129.

BIBLIOGRAPHY

- Anthes, R., 1974: The dynamics and energetics of mature tropical cyclones. Rev. Geophys. Space Phys., 3, 495-522.
- Anthes, R., 1977: Hurricane model experiments with a new cumulus parameterization scheme. Mon. Wea. Rev., 105, 287-300.
- Arnold, C. P., 1977: Tropical cyclone cloud and intensity relationships. Dept. of Atmos. Sci. Paper No. 277, Colo. State Univ., Ft. Collins, CO, 154 pp.
- Bates, J., 1977: Vertical shear of the horizontal wind speed in tropical cyclones. NOAA Technical Memorandum ERL WMPO-39.
- Benjamin, T. B., 1968: Gravity currents and related phenomena. J. Fluid Mech., 31, 209-248.
- Bignell, K. J., 1970: The water vapor infra-red continuum. Quart. J. Roy. Meteor. Soc., 96, 390-403.
- Charney, J. C. and A. Eliassen, 1964: On the growth of the hurricane depression. J. Atmos. Sci., 21, 68-75.
- Cox, S. K., 1973: Infrared heating calculations with a water vapor pressure broadened continuum. Quart. J. Roy. Meteor. Soc., 99,
- Dopplick, T. G., 1974: Radiative heating in the atmosphere. In The General Circulation of the Tropical Atmosphere and Interactions with Extratropical Latitudes. Vol. 2, MIT Press, Cambridge, MA, 1-25.
- Dvorak, V. F., 1975: Tropical cyclone intensity analysis and forecasting from satellite imagery. Mon. Wea. Rev., 103, 420-430.
- Erickson, S. L., 1977: Comparison of developing vs. non-developing tropical disturbances. Dept. of Atmos. Sci. Paper No. 274, Colo. State Univ., Ft. Collins, CO, 81 pp.
- Fett, R. W., 1968: Typhoon formation within the zone of the inter-tropical convergence. Mon. Wea. Rev., 96, 106-117.
- Fingerhut, W. A., 1978: A numerical model of a diurnally varying tropical cloud cluster disturbance. Mon. Wea. Rev., 106, 255-264.
- Fingerhut, W. A., 1979: Numerical modelling of tropical cyclone genesis. Forthcoming Ph.D. Thesis, Dept. of Atmos. Sci., Colo. State Univ., Ft. Collins, CO.
- Frank, W. M., 1977a: The structure and energetics of the tropical cyclone, I: Storm structure. Mon. Wea. Rev., 105, 9, 1119-1135.

BIBLIOGRAPHY (cont'd)

- Frank, W. M., 1977b: The structure and energetics of the tropical cyclone, II: Dynamics and energetics. Mon. Wea. Rev., 105, 1136-1150.
- Frank, W. M., 1977c: Momentum and kinetic energy processes in the tropical cyclone. Volume of Conference Papers, 11th Technical Conference on Hurricanes and Tropical Meteorology, Dec. 13-16, Miami Beach, FL, Published by the Amer. Meteor. Soc., Boston, MA. 535-542.
- Frank, W. M., 1978a: The life cycles of GATE convective systems. J. Atmos. Sci., 35, 1256-1264.
- Frank, W. M., 1978b: Diagnostic analyses of the GATE A/B scale area at individual time periods. Dept. of Atmos. Sci. Paper No. 297, Colo. State Univ., Ft. Collins, CO, 102 pp.
- Garratt, J. R., 1977: Review of drag coefficients over oceans and continents. Mon. Wea. Rev., 105, 915-929.
- Gray, W. M., 1967: The mutual variation of wind, shear and baroclinicity in the cumulus convective atmosphere of the hurricane. Mon. Wea. Rev., 95, 55-74.
- Gray, W. M., 1968: Global view of the origin of tropical disturbances and storms. Mon. Wea. Rev., 96, 669-700.
- Gray, W. M., 1972a: Cumulus convection and larger scale circulations, Part III: Broadscale and meso-scale considerations. Dept. of Atmos. Sci. Paper No. 190, Colo. State Univ., Ft. Collins, CO, 80 pp.
- Gray, W. M., 1972b: A diagnostic study of the planetary boundary layer over the oceans. Dept. of Atmos. Sci. Paper No. 179, Colo. State Univ., Ft. Collins, CO, 95 pp.
- Gray, W. M., 1973: Cumulus convection and larger scale circulations, I: Broadscale and mesoscale considerations. Mon. Wea. Rev., 101, 839-855.
- Gray, W. M., 1975: Tropical cyclone genesis. Dept. of Atmos. Sci. Paper No. 234, Colo. State Univ., Ft. Collins, CO, 119 pp.
- Gray, W. M., 1979: Hurricanes/their formation, structure and likely role in the tropical circulation. Quart. J. Roy. Meteor. Soc., 105, 155-218. (Proceeding of Conf. of Meteor. over the Trop. Oceans).
- Gray, W. M. and R. Jacobson, Jr., 1977: Diurnal variation of deep cumulus convection. Mon. Wea. Rev., 105, 1171-1188.

BIBLIOGRAPHY (cont'd)

- Green, J. S. A. and R. P. Pearce, 1962: Cumulonimbus convection in shear. Tech. Note 12, Dept. of Meteor., Imperial College, London, 62 pp.
- Grube, P. G., 1979: Convection induced temperature change in GATE. Dept. of Atmos. Sci. Paper No. 305, Colo. State Univ., Ft. Collins, CO, 128 pp.
- Kininmonth, W. R., 1970: Thermal modification of the troposphere due to convective interaction. Dept. of Atmos. Sci. Paper No. 167, Colo. State Univ., Ft. Collins, CO, 36 pp.
- Kurihara, Y., 1975: Budget analysis of a tropical cyclone simulated in an axisymmetric numerical model. J. Atmos. Sci., 32, 25-59.
- Lawrence, M. B., 1977: Atlantic hurricane season of 1976. Mon. Wea. Rev., 105, 497-507.
- Lawrence, M. B., 1978: Atlantic hurricane season of 1977. Mon. Wea. Rev., 106, 534-545.
- Lopez, R. E., 1968: Investigation of the importance of cumulus convection and ventilation in early tropical storm development. Dept. of Atmos. Sci. Paper No. 124, Colo. State Univ., Ft. Collins, CO, 86 pp.
- Lopez, R. E., 1973: Cumulus convection and larger scale circulations, II: Cumulus and mesoscale interactions. Mon. Wea. Rev., 101, 856-870.
- Ludlam, F. H., 1963: Severe local storms: a review. Meteorological Monographs, 5, 1-30.
- Ludlam, F. H., 1966: Cumulus and cumulonimbus convection. Tellus, 18, 687-698.
- Martin, D. W. and V. E. Suomi, 1972: A satellite study of cloud clusters over the tropical North Atlantic Ocean. Bull. Amer. Meteor. Soc., 53, 135-156.
- McBride, J. L. and W. M. Gray, 1978: Mass divergence in tropical weather systems, Paper I: Diurnal variation, Paper II: Large scale controls on convection. Dept. of Atmos. Sci. Paper No. 299, Colo. State Univ., Ft. Collins, CO, 109 pp.
- McEwan, A. D., 1976: Angular momentum diffusion and the initiation of cyclones. Nature, 260, 126-128.
- Miller, B. I., 1962: On the momentum and energy balance of hurricane Helene (1958). NHRP Report No. 53, 19 pp. (Available from NOAA Weather Bureau, Miami office.)

BIBLIOGRAPHY (cont'd)

- Miller, M. J. and R. P. Pearce, 1974: A three-dimensional primitive equation model of cumulonimbus convection. Quart. J. Roy. Meteor. Soc., 100, 133-154.
- Moncrieff, M. W., 1978: The dynamical structure of two-dimensional steady convection in constant vertical shear. Quart. J. Roy. Meteor. Soc., 104, 543-567.
- Moncrieff, M. W. and J. S. A. Green, 1972: The propagation of steady convective overturning in shear. Quart. J. Roy. Meteor. Soc., 98, 336-352.
- Moncrieff, M. W. and M. J. Miller, 1976: The dynamics of simulation of tropical cumulonimbus and squall lines. Quart. J. Roy. Meteor. Soc., 102, 373-394.
- Núñez, E. and W. M. Gray, 1977: A comparison between West Indies hurricanes and Pacific typhoons. Volume of Conference Papers, 11th Technical Conference on Hurricanes and Tropical Meteorology, Dec. 13-16, Miami Beach, FL, Published by the AMS, Boston, MA, 528-534.
- Ogura, Y., 1964: Frictionally controlled, thermally driven circulation in a circular vortex with application to tropical cyclones. J. Atmos. Sci., 21, 610-621.
- Ooyama, K., 1964: A dynamical model for the study of tropical cyclone development. Geofisica Internacional, 4, 187-198.
- Ooyama, K., 1969: Numerical simulation of the life cycle of tropical cyclones. J. Atmos. Sci., 26, 3-40.
- Paegle, J., 1978: The transient mass-flow adjustment of heated atmospheric circulations. J. Atmos. Sci., 35, 1678-1688.
- Ramage, C. S., 1974: The typhoons of October 1970 in the South China Sea. Intensification, decay and ocean interaction. J. Appl. Meteor., 13, 739-751.
- Reed, R. J. and E. E. Recker, 1971: Structure and properties of synoptic-scale wave disturbances in the equatorial western Pacific. J. Atmos. Sci., 28, 1117-1133.
- Riehl, H., 1948: On the formation of typhoons. J. Meteor., 5, 247-264.
- Riehl, H., 1950: A model of hurricane formation. J. Appl. Meteor., 9, 917-925.
- Riehl, H., 1975: Further studies on the origin of hurricanes. Dept. of Atmos. Sci. Paper No. 235, Colo. State Univ., Ft. Collins, CO, 24 pp.

BIBLIOGRAPHY (cont'd)

- Riehl, H. and J. S. Malkus, 1961: Some aspects of Hurricane Daisy, 1958. Tellus, 13, 181-213.
- Rosenthal, S. L., 1978: Numerical simulation of tropical cyclone development with latent heat release by the resolvable scales, I: Model description and preliminary results. J. Atmos. Sci., 35, 258-271.
- Ruprecht, E. and W. M. Gray, 1976a: Analysis of satellite-observed tropical cloud clusters, Part I: Wind and dynamic fields. Tellus, 28, 391-413.
- Ruprecht, E. and W. M. Gray, 1976b: Analysis of satellite-observed tropical cloud clusters, Part II: Thermal, moisture and precipitation. Tellus, 28, 414-416.
- Sadler, J. C., 1967: The tropical upper tropospheric trough as a secondary source of typhoon and a primary source of trade wind disturbances. Hawaii Institute of Geophysics Report No. HIG 67-12, 44 pp. (Available from Dept. of Meteor., Univ. of Hawaii.)
- Sadler, J. C., 1975: Tropical cyclone initiation by the tropical upper tropospheric trough. UHMET 75-02. (Available from Dept. of Meteor., Univ. of Hawaii.)
- Sadler, J. C., 1976: A role of the tropical upper troposphere in early season typhoon development. Mon. Wea. Rev., 104, 1266-1278.
- Sadler, J. C., 1978: Mid-season typhoon development and intensity changes and the tropical upper tropospheric trough. Mon. Wea. Rev., 1137-1152.
- Sartor, J. W., 1968: Monthly climatological wind fields associated with tropical storm genesis in the West Indies. M.S. Thesis, Colo. State Univ., Ft. Collins, CO, 34 pp.
- Schubert, W. H. and J. J. Hack, 1979: Geostrophic and gradient adjustment in axisymmetric and asymmetric vortices. Paper presented at 12th Technical Conference on Hurricanes and Tropical Meteorology, AMS, April 24-27, New Orleans, LA.
- Shapiro, L. J., 1977a: Tropical storm formation from easterly waves: a criterion for development. J. Atmos. Sci., 34, 1007-1021.
- Shapiro, L. J., 1977b: A criterion for the development of tropical storms from easterly waves. Volume of Conference Papers, 11th Technical Conference on Hurricanes and Tropical Meteorology, Dec. 13-16, Miami Beach, FL, Published by the Amer. Meteor. Soc., Boston, MA, 9-14.

BIBLIOGRAPHY (cont'd)

- Silva Dias, P. L., 1979: Forthcoming Ph.D. Thesis, Dept. of Atmos. Sci., Colo. State Univ., Ft. Collins, CO.
- Simpson, J. E., 1969: A comparison between laboratory and atmospheric density currents. Quart. J. Roy. Meteor. Soc., 95, 758-765.
- Wachtmann, R. F., 1968: Role of angular momentum transports in tropical storm dissipation over tropical oceans. M.S. Thesis, Colo. State Univ., Ft. Collins, CO, 46 pp.
- Williams, K. T. and W. M. Gray, 1973: A statistical analysis of satellite-observed trade wind cloud clusters in the western north Pacific. Tellus, 21, 313-336.
- Wise, C. W. and R. H. Simpson, 1971: The tropical analysis program of the National Hurricane Center. Weatherwise, 24, 164-173.
- Yamasaki, M., 1977: The role of surface friction in tropical cyclones. J. Meteor. Soc. Japan, 55, 559-572.
- Yanai, M., 1961: A detailed analysis of typhoon formation. J. Meteor. Soc. Japan, 39, 187-214.
- Yanai, M., 1968: Evolution of a tropical disturbance in the Caribbean Sea region. J. Meteor. Soc. Japan, 46, 86-109.
- Yanai, M., S. Esbensen and J. Chu, 1973: Determination of bulk properties of tropical cloud clusters from large-scale heat and moisture budgets. J. Atmos. Sci., 30, 611-627.
- Zehr, R., 1976: Tropical disturbance intensification. Dept. of Atmos. Sci. Paper No. 259, Colo. State Univ., Ft. Collins, CO, 91 pp.

APPENDIX: LISTING OF INDIVIDUAL CASE VERTICAL SHEAR DATA

In Chapter 6 an analysis is presented of the fields of vertical wind shear around 130 separate tropical weather systems. This Appendix presents the actual values (in knots) of vertical shear for each system. In section A.5 the year, date and latitude and longitude of each position is listed.

A.1 Atlantic tropical storms

Seven parameters were examined for each system. They are:

- (i) ΔU : the value of the vertical shear of the zonal wind at a point 6° latitude north of the position of the system minus the value of the shear at a point 6° south of the system; ΔU is proportional to $\partial/\partial y(-\partial U/\partial p)_{900-200mb}$;
- (ii) ΔV : the vertical shear of the meridional wind 6° west of the system minus the shear 6° east of the system; ΔV is proportional to $\partial/\partial x(\partial V/\partial p)_{900-200mb}$;
- (iii) $\Delta U + \Delta V$: this is proportional to $\zeta_{900mb} - \zeta_{200mb}$, averaged over the $0-6^{\circ}$ area;
- (iv) existence of a zonal zero line: the value of this parameter is YES if the vertical U shear is positive 6° to the north and negative 6° to the south; otherwise the value is NO;
- (v) existence of a meridional zero line: the value is YES if the vertical V shear is positive 6° to the west and negative 6° to the east;
- (vi) subjective existence of zonal zero line: the zero line often exists but does not meet the strict criteria of item (iv) above; for example the zonal zero line exists at position -60 for storm Amy shown in Fig. 40a but the shear 6° to the south of the storm position is positive;
- (vii) subjective existence of meridional zero line.

The values of these parameters are listed in Table 34 for 16 Atlantic tropical storms from the years 1975, 1976, and 1977. Six positions are considered for each storm. Point -60 is 60 hours before the time at which the system first reaches a maximum sustained wind of 35 knots (point 00).

Thirteen of the sixteen systems have high values of both ΔU and ΔV and also have both zonal and meridional zero lines existing prior to the development of the storm. The earliest consecutive three time periods such that three of the four following criteria are met are underlined and marked with a parenthesis. Criteria: (a) ΔU greater than 20 knots, (b) ΔV greater than 20 knots, (c) the existence of a zonal zero line, and (d) the existence of a meridional zero line.

TABLE 34

Atlantic Tropical Storms

Storm	Position	(1)	(ii)	(iii)	(iv)	(v)	(vi)	(vii)
		ΔU	ΔV	$\Delta U + \Delta V$	Zonal Zero Line	Meridional Zero Line	Subjective Zonal Zero Line	Subjective Meridional Zero Line
1975 Amy	-60	$\frac{21}{43}$	$\frac{31}{47}$	$\frac{52}{90}$	N	$\frac{Y}{N}$	$\frac{Y}{Y}$	$\frac{Y}{Y}$
	-48	$\frac{-36}{45}$	$\frac{70}{65}$	$\frac{115}{141}$	$\frac{Y}{Y}$	$\frac{Y}{Y}$	$\frac{Y}{Y}$	$\frac{Y}{Y}$
	-36	$\frac{-24}{65}$	$\frac{76}{48}$	$\frac{141}{107}$	$\frac{Y}{Y}$	$\frac{Y}{Y}$	$\frac{Y}{Y}$	$\frac{Y}{Y}$
	-24	$\frac{-12}{48}$	$\frac{59}{53}$	$\frac{107}{97}$	$\frac{Y}{Y}$	$\frac{Y}{Y}$	$\frac{Y}{Y}$	$\frac{Y}{Y}$
	-12	$\frac{00}{44}$						
1975 Blanche	-60	$\frac{31}{18}$	$\frac{34}{7}$	$\frac{65}{25}$	$\frac{Y}{N}$	$\frac{Y}{Y}$	$\frac{Y}{Y}$	$\frac{Y}{Y}$
	-48	$\frac{-36}{26}$	$\frac{38}{4}$	$\frac{64}{30}$	$\frac{N}{N}$	$\frac{Y}{Y}$	$\frac{Y}{Y}$	$\frac{Y}{Y}$
	-36	$\frac{-24}{26}$	$\frac{44}{32}$	$\frac{30}{76}$	$\frac{Y}{N}$	$\frac{Y}{Y}$	$\frac{Y}{Y}$	$\frac{Y}{Y}$
	-24	$\frac{-12}{44}$	$\frac{54}{20}$	$\frac{76}{74}$	$\frac{N}{N}$	$\frac{Y}{Y}$	$\frac{Y}{Y}$	$\frac{Y}{Y}$
	-12	$\frac{00}{54}$						
1975 Caroline	-60	$\frac{28}{-48}$	$\frac{36}{-4}$	$\frac{64}{25}$	$\frac{Y}{N}$	$\frac{Y}{Y}$	$\frac{Y}{Y}$	$\frac{Y}{Y}$
	-48	$\frac{-36}{-11}$	$\frac{25}{-1}$	$\frac{21}{33}$	$\frac{N}{N}$	$\frac{Y}{Y}$	$\frac{Y}{Y}$	$\frac{Y}{Y}$
	-36	$\frac{-24}{-1}$	$\frac{Off\ grid}{9}$	$\frac{Off\ grid}{12}$	$\frac{N}{N}$	$\frac{N}{N}$	$\frac{N}{N}$	$\frac{N}{N}$
	-24	$\frac{-12}{9}$						
	00	$\frac{00}{12}$						

TABLE 34 (cont'd)

Storm	Position	(i)	(ii)	(iii)	(iv)	(v)	(vi)	(vii)
		ΔU	ΔV	$\Delta U + \Delta V$	Zonal Zero Line	Meridional Zero Line	Subjective Zonal Zero Line	Subjective Meridional Zero Line
1975 Eloise	-60	16	10	25	N	N	N	N
	-48	17	31	48	Y	Y	Y	Y
	-36	10	1	11	N	N	N	N
	-24	41	36	76	Y	Y	Y	Y
	-12	47	55	102	Y	Y	Y	Y
	00	48	48	95	Y	Y	Y	Y
1975 Faye	-60	Off grid	Off grid	Off grid	Y	Y	Y	Y
	-48	Off grid	Off grid	Off grid	Y	Y	Y	Y
	-36	Off grid	Off grid	Off grid	Y	Y	Y	Y
	-24	Off grid	Off grid	Off grid	Y	Y	Y	Y
	-12	116	Off grid	Off grid	Y	Y	Y	Y
	00	98	Off grid	Off grid	Y	Y	Y	Y
1975 Gladys	-60	Off grid	Off grid	Off grid	Y	Y	Y	Y
	-48	60	Off grid	Off grid	Y	Y	Y	Y
	-36	36	Off grid	Off grid	Y	Y	Y	Y
	-24	48	Off grid	Off grid	Y	Y	Y	Y
	-12	59	Off grid	Off grid	Y	Y	Y	Y
	00	64	Off grid	Off grid	Y	Y	Y	Y
1975 Hallie	-60	18	-45	-27	N	N	N	N
	-48	28	-80	-52	N	N	N	N
	-36	71	-32	38	Y	Y	Y	Y
	-24	68	19	87	Y	Y	Y	Y
	-12	103	14	117	N	N	N	N
	00	90	57	147	Y	Y	Y	Y

TABLE 34 (cont'd)

TABLE 34 (cont'd)

Storm	Position	ΔU	ΔV	$\Delta U + \Delta V$	Zonal Zero Line	Meridional Zero Line	Subjective Meridional Zero Line	
							N	Y
1977 Anita	-60	-5	-38	-43	N	N	N	N
	-48	33	2	35	Y	Y	Y	Y
	-36	39	13	52	Y	Y	Y	Y
	-24	29	-3	25	Y	Y	Y	Y
	-12	<u>31</u>	<u>31</u>	<u>61</u>	<u>Y</u>	<u>Y</u>	<u>Y</u>	<u>Y</u>
	00	<u>39</u>	<u>50</u>	<u>89</u>	<u>Y</u>	<u>Y</u>	<u>Y</u>	<u>Y</u>
1977 Clara	-60	17	44	62	N	N	N	N
	-48	21	20	41	N	N	N	N
	-36	48	21	68	N	N	N	N
	-24	46	12	58	N	N	N	N
	-12	112	38	150	Y	Y	Y	Y
	00	89	28	117	Y	Y	Y	Y
1977 Dorothy	-60	4	9	13	N	N	N	N
	-48	-1	7	6	Y	Y	Y	Y
	-36	-1	7	6	Y	Y	Y	Y
	-24	-9	13	4	Y	Y	Y	Y
	-12	2	15	16	N	N	N	N
	00	10	7	17	N	N	N	N
1977 Evelyn	-60	-43	-30	-73	N	N	N	N
	-48	-44	-22	-66	N	N	N	N
	-36	-7	-38	-44	Y	Y	Y	Y
	-24	<u>25</u>	<u>18</u>	<u>43</u>	<u>Y</u>	<u>Y</u>	<u>Y</u>	<u>Y</u>
	-12	<u>13</u>	<u>2</u>	<u>14</u>	<u>Y</u>	<u>Y</u>	<u>Y</u>	<u>Y</u>
	00	<u>60</u>	<u>57</u>	<u>117</u>	<u>N</u>	<u>N</u>	<u>N</u>	<u>N</u>

TABLE 34 (cont'd)

Storm	Position	ΔU	ΔV	$\Delta U + \Delta V$	Zonal Zero Line	Meridional Zero Line	Subjective Meridional Zero Line	
							N	Y
1977 Frieda	-60	19	37	56	N	N		
	-48	8	39	47	N	Y		
	-36	48	63	111	Y	Y		
	-24	56	54	110	Y	Y		
	-12	54	63	117	Y	Y		
	00	61	4	65	N	N		

A.2 Atlantic depressions

Pre-depression data were available for 11 of the 16 storms listed in A.1. Table 35 lists vertical shear data (parameters (i) to (v)) for 48 hours, 24 hours and zero hours prior to the time at which each system was officially designated a tropical depression.

TABLE 35

Pre-depression Stage

System	Position	(i)	(ii)	(iii)	(iv)	(v)
		ΔU	ΔV	$\Delta U + \Delta V$	Zonal Zero Line	Meridional Zero Line
1975 Amy	-48	2	8	10	N	N
	-24	25	36	61	Y	Y
	00	28	47	75	N	N
1975 Blanche	-48	-11	-30	-41	N	N
	-24	3	2	5	N	N
	00	31	18	49	Y	Y
1975 Caroline	-48	-8	-21	-29	N	N
	-24	5	-1	4	N	N
	00	-14	3	-11	N	N
1975 Eloise	-48	20	3	23	N	N
	-24	22	5	26	Y	N
	00	16	10	26	N	N
1975 Hallie	-48	1	-76	-75	N	N
	-24	-10	-49	-59	N	N
	00	-2	-80	-82	N	N
1976 Belle	-48	11	-19	-8	Y	N
	-24	52	29	81	Y	N
	00	35	31	66	Y	Y
1976 Gloria	-48	-46	-18	-64	N	N
	-24	Missing Data		Missing Data		Missing Data
	00	Missing Data		Missing Data		Missing Data
1977 Anita	-48	-7	-8	-15	N	N
	-24	11	-11	0	Y	N
	00	19	-3	15	Y	N

TABLE 35 (cont'd)

System	Position	(i) ΔU	(ii) ΔV	(iii) $\Delta U + \Delta V$	(iv) Zonal Zero Line	(v) Meridional Zero Line
1977 Evelyn	-48	7	11	18	N	N
	-24	24	-27	-4	N	N
	00	14	35	49	Y	N
1977 Frieda	-48	65	39	103	Y	Y
	-24	68	44	112	Y	Y
	00	60	--	--	Y	-

A.3 Atlantic non-developing systems

The values of parameters (i) to (v) are listed in Tables 36-43 for the 63 tropical systems which did not later develop into tropical storms.

Positions that meet three of the four criteria, (a) ΔU greater than 20 knots, (b) ΔV greater than 20 knots, (c) the existence of a zonal zero line, (d) the existence of a meridional zero line, are marked with a parenthesis.

TABLE 36
Non-developing Depressions (1975)

System Number	Position Number	(i)	(ii)	(iii)	(iv)	(v)
		ΔU	ΔV	$\Delta U + \Delta V$	Zonal Zero Line	Meridional Zero Line
1	1	-66	-56	-122	N	N
	2	-51	-37	-88	N	N
	3	-5	-45	-50	N	N
2	4	-8	-4	-12	N	N
	5	7	18	25	N	Y
3	6	-1	21	20	N	N
	7	-50	9	-41	N	Y
4	8	37	29	66	N	Y }
	9	-17	-7	-24	N	N
	10	-21	-31	-52	N	N
5	11	61	39	100	Y	Y }
	12	33	27	60	N	N
6	13	2	21	23	N	N
	14	11	19	30	N	Y

TABLE 37

Non-developing Depressions (1976)

System Number	Position Number	(i) ΔU	(ii) ΔV	(iii) $\Delta U + \Delta V$	(iv) Zonal Zero Line	(v) Meridional Zero Line
7	15	12	-35	-23	N	N
	16	-2	-42	-44	N	N
8	17	-8	-5	-13	N	N
	18	-18	-32	-50	N	N
9	19	19	-6	13	Y	N
10	20	-3	1	-2	N	N
	21	6	5	11	N	N
	22	14	18	32	N	Y
11	23	37	29	66	N	N
	24	15	18	33	N	N
	25	-21	-48	-69	N	N
12	26	26	-24	2	N	N

TABLE 38

Non-developing Depressions (1977)

System Number	Position Number	(i) ΔU	(ii) ΔV	(iii) $\Delta U + \Delta V$	(iv) Zonal Zero Line	(v) Meridional Zero Line
13	27	-50	-54	-104	N	N
	28	-49	-2	-51	N	N
14	29	35	22	57	N	N
15	30	6	9	15	N	Y
	31	8	23	31	N	Y
	32	46	21	67	Y	Y }
16	33	15	27	42	N	Y
	34	21	6	27	N	N
	35	-46	21	-25	N	Y

TABLE 39

Dvorak Systems (1975)

System Number	Position Number	(i)	(ii)	(iii)	(iv)	(v)
		ΔU	ΔV	$\Delta U + \Delta V$	Zonal Zero Line	Meridional Zero Line
17	36	35	-24	11	Y	N
	37	23	-3	20	N	N
	38	52	2	54	Y	N
18	39	1	-21	-20	N	N
	40	29	-16	13	Y	N
19	41	41	-24	17	Y	N
	42	45	-4	41	Y	N
	43	11	3	14	Y	N
20	44	-12	-22	-34	N	N
	45	15	-17	-2	Y	N
	46	-15	1	-14	N	N
	47	26	17	43	Y	N
	48	38	34	72	Y	Y }
	49	52	23	75	Y	Y }
	50	11	-33	-22	Y	N
21	51	71	-2	69	Y	N
	52	46	-1	45	Y	N
	53	38	8	46	Y	N
22	54	54	6	60	Y	Y }
	55	24	-20	4	Y	N
23	56	32	15	47	Y	N
	57	-26	-21	-47	N	N
	58	-35	-19	-54	N	N
24	59	25	10	35	N	N
	60	2	0	2	N	N

TABLE 40
Frank Systems (1975)

System Number	Position Number	(i) ΔU	(ii) ΔV	(iii) $\Delta U + \Delta V$	(iv) Zonal Zero Line	(v) Meridional Zero Line
25	61	12	-8	4	N	N
26	62	53	21	74	Y	Y }
	63	16	-28	-12	N	
	64	19	8	27	N	
27	65	-11	-3	-14	N	N
	66	-46	-17	-63	N	N
28	67	27	-3	24	N	N
29	68	41	-25	16	Y	N
	69	33	-19	14	Y	N
30	70	40	-7	33	Y	N
	71	29	23	52	Y	N
	72	63	-9	54	Y	N
	73	17	-4	13	Y	N
31	74	44	6	50	Y	N
32	75	-54	-7	-61	N	N
	76	-58	-23	-81	N	N
33	77	-39	-26	-65	N	N
	78	-34	-17	-51	N	N
	79	-34	-58	-92	N	N
34	80	19	-34	-15	N	N
	81	-9	-33	-42	N	N
	82	1	-12	-11	N	N
	83	-7	-35	-42	N	N
35	84	54	19	73	Y	Y
	85	33	-46	-13	Y	N

TABLE 41

Shapiro Systems (1976)

		(i)	(ii)	(iii)	(iv)	(v)
System Number	Position Number	ΔU	ΔV	$\Delta U + \Delta V$	Zonal Zero Line	Meridional Zero Line
36	86	39	-7	32	Y	N
	87	5	-19	-14	N	N
	88	-17	-33	-50	N	N
	89	3	1	4	N	N
	90	3	-3	0	N	N
37	91	-6	8	2	N	N
	92	3	13	16	N	N
	93	2	5	7	N	N
	94	-21	-16	-37	N	N
	95	25	-41	-16	N	N
	96	30	-1	29	N	N
38	97	17	6	23	N	N
	98	25	16	41	N	N
	99	2	4	6	N	N
	100	-5	-6	-11	N	N
	101	8	-5	3	N	N
39	102	4	1	5	N	N
	103	21	-15	6	N	N
	104	21	22	43	N	Y }
	105	-29	5	-24	N	N
	106	15	41	56	N	N
40	107	65	12	77	Y	Y
	108	-3	-4	-7	N	N
	109	28	3	31	N	N
	110	19	-2	17	N	N
	111	23	7	30	N	Y
	112	28	33	61	Y	Y }
	113	13	28	41	N	Y
	114	46	15	61	Y	N
	115	50	-9	41	Y	N
41	116	33	-18	15	Y	N
	117	37	-53	-16	Y	N
	118	14	-54	-40	N	N
	119	11	-16	-5	N	N

TABLE 41 (cont'd)

System Number	Position Number	(i) ΔU	(ii) ΔV	(iii) $\Delta U + \Delta V$	(iv) Zonal Zero Line	(v) Meridional Zero Line
42	120	24	-63	-39	N	N
	121	-32	-58	-90	N	N
	122	32	16	48	N	Y
	123	33	-6	27	N	N
	124	-2	-18	-20	N	N
	125	37	50	87	N	Y }
43	126	30	9	39	N	N
44	127	34	5	39	Y	N
	128	55	17	72	Y	N
	129	65	52	117	Y	Y }
	130	41	28	69	Y	Y }
	131	-14	-1	-15	N	N
	132	-1	19	18	N	Y
	133	-8	23	15	N	N
45	134	18	-17	1	N	N
	135	9	5	14	N	N
46	136	2	3	5	N	N
	137	-10	14	4	N	Y
	138	29	-7	22	N	N
	139	-37	-20	-57	N	N
	140	22	48	70	N	Y }
	141	19	48	67	N	Y

TABLE 42

McBride Systems (1976)

System Number	Position Number	(i) ΔU	(ii) ΔV	(iii) $\Delta U + \Delta V$	(iv) Zonal Zero Line	(v) Meridional Zero Line
47	142	41	15	56	N	Y
	143	4	1	5	N	N
	144	-58	-24	-82	N	N
	145	-39	7	-32	N	N
48	146	62	10	72	Y	N
	147	57	14	71	Y	N
49	148	-20	17	-3	N	N
50	149	14	3	17	N	N
51	150	13	9	22	N	N
	151	2	-6	-4	N	N
52	152	3	-15	-12	N	N
	153	23	3	26	N	N
53	154	16	-31	-15	Y	N
	155	32	-13	19	N	N
54	156	15	4	19	N	N
	157	33	-4	29	N	N
	158	7	-7	0	N	N
55	159	-6	-23	-29	N	N
56	160	36	13	49	N	N
	161	-10	-45	-55	N	N
57	162	-28	6	-22	N	N
	163	-4	12	8	N	N
	164	5	33	38	N	N
58	165	4	-1	3	N	N

TABLE 43

McBride Systems (1977)

System Number	Position Number	(i) ΔU	(ii) ΔV	(iii) $\Delta U + \Delta V$	(iv) Zonal Zero Line	(v) Meridional Zero Line
59	166	24	-52	-28	N	N
60	167	-65	-28	-93	N	N
	168	-1	-6	-7	N	N
61	169	14	-9	5	N	N
	170	12	-13	-1	N	N
	171	7	-20	-13	N	N
62	172	23	11	34	N	Y
	173	29	15	44	N	Y
	174	58	55	113	Y	Y }
63	175	-42	-23	-65	N	N
	176	-61	-55	-116	N	N
	177	-49	-48	-97	N	N
	178	-65	-45	-110	N	N

A.4 Pacific pretyphoon versus non-developing clusters

The values of parameters (iii), (iv) and (v) are listed in Table 44 for 18 Western Pacific pretyphoon cloud clusters and in Table 45 for 31 Western Pacific non-developing cloud clusters. The method of obtaining these values from Joint Typhoon Warning Center (JTWC) Guam operational weather maps is described in section 6.4. (Position numbers are the numbers used by S. Erickson (1977).) The latitude, longitude time and date corresponding to each position number are listed in Appendix A.5, Table 49.

TABLE 44
Pacific Pretyphoon Clusters

System Number	Position Number	$\Delta U + \Delta V$	Zonal Zero Line	Meridional Zero Line
		(iii)	(iv)	(v)
1	36-38	8.4	Y	Y
2	39-41, 43, 45	9.6	Y	N
3	73, 75, 77, 78	15.4	Y	Y
4	150, 151, 153	13.7	Y	Y
5	159-164	18.0	Y	Y
6	166, 168, 170, 172 175, 177	10.0	Y	N
7	174, 176, 178	13.0	Y	N
8	179-181	7.3	Y	N
9	248-251	10.9	Y	Y
10	284-288	-1.6	N	Y
11	289-293	9.3	Y	Y
12	294-297	14.3	Y	Y
13	298-300	13.3	Y	Y
14	301-303	11.0	Y	N
15	312	9.0	N	Y
16	313-315	-.4	N	N
17	319-321	22.9	Y	Y
18	322-325	20.1	Y	Y

TABLE 45
Pacific Non-developing Clusters

<u>System Number</u>	<u>Position Number</u>	<u>$\Delta U + \Delta V$</u>	<u>Zonal Zero Line</u>	<u>Meridional Zero Line</u>
1	20-23	14.1	Y	N
2	24-26	14.2	N	Y
3	27-29	7.3	N	N
4	30-32	19.9	Y	N
5	33-35	15.7	Y	Y
6	42,44,46	0.6	Y	N
7	47-51	-3.3	N	N
8	52-54,56	8.9	Y	Y
9	55,57-59	12.7	Y	Y
10	60,62,64	5.8	N	Y
11	61,63,65-69	2.5	N	N
12	70-72,74,76	0.1	Y	N
13	79-80	-4	N	N
14	121-124	6.9	Y	N
15	125-127	8.8	Y	N
16	128,130,132	14.4	Y	N
17	129,131,133	8.8	Y	N
18	134-136	1.8	Y	N
19	137-139	14.0	Y	Y
20	140-144	1.7	N	N
21	145-149	12.4	Y	Y
22	152,154,155	3.8	Y	N
23	156-158	5.1	Y	N
24	165,167,169, 171,173	9.1	Y	N
25	182-186	2.7	Y	N
26	187-191	9.1	Y	N
27	192-194	11.3	Y	N
28	195-197	7.4	Y	N
29	304-306	-9.3	N	N
30	307-311	0.2	N	N
31	316-318	-6.9	N	N

A.5 Listing of positions of individual systems

Tables 46, 47, 48, and 49 list the actual dates and positions of the 130 tropical systems studied in Chapter 6.

TABLE 46

Positions and time of the individual tropical weather systems studied in Chapter 6.

Atlantic Tropical Storms

System	Position Number	Month	Date	Time (GMT)	Latitude (Deg. North)	Longitude (Deg. West)
1975 Amy	-60	6	26	12	----	----
	-48	6	27	00	27.5	79.0
	-36	6	27	12	29.5	79.0
	-24	6	28	00	31.5	78.8
	-12	6	28	12	33.3	78.0
	00	6	29	00	34.4	75.8
1975 Blanche	-60	7	24	00	26.0	68.4
	-48	7	24	12	26.1	70.5
	-36	7	25	00	27.2	72.5
	-24	7	25	12	28.9	74.3
	-12	7	26	00	31.0	75.0
	00	7	26	12	33.4	73.5
1975 Caroline	-60	8	27	00	20.4	82.8
	-48	8	27	12	21.1	85.1
	-36	8	28	00	22.0	87.5
	-24	8	28	12	22.8	90.1
	-12	8	29	00	23.0	91.9
	00	8	29	12	23.2	93.2
1975 Eloise	-60	9	13	12	17.6	55.2
	-48	9	14	00	17.8	57.3
	-36	9	14	12	18.0	59.4
	-24	9	15	00	18.3	61.7
	-12	9	15	12	18.8	63.8
	00	9	16	00	19.0	65.6
1975 Faye	-60	9	17	00	17.5	28.0
	-48	9	17	12	17.0	30.0
	-36	9	18	00	17.4	32.0
	-24	9	18	12	17.8	34.4
	-12	9	19	00	19.0	36.4
	00	9	19	12	20.0	39.0

TABLE 46 (cont'd)

<u>System</u>	<u>Position Number</u>	<u>Month</u>	<u>Date</u>	<u>Time (GMT)</u>	<u>Latitude (Deg. North)</u>	<u>Longitude (Deg. West)</u>
1975 Gladys	-60	9	22	12	10.6	33.0
	-48	9	23	00	10.6	35.8
	-36	9	23	12	11.4	37.4
	-24	9	24	00	12.1	38.8
	-12	9	24	12	12.9	40.0
	00	9	25	00	14.2	41.0
1975 Hallie	-60	10	24	12	28.0	78.5
	-48	10	25	00	28.8	79.0
	-36	10	25	12	30.0	79.7
	-24	10	26	00	30.5	79.9
	-12	10	26	12	31.8	79.6
	00	10	27	00	33.5	77.5
1976 Belle	-60	8	4	12	23.5	67.0
	-48	8	5	00	24.0	69.0
	-36	8	5	12	25.0	71.0
	-24	8	6	00	25.0	72.0
	-12	8	6	12	25.5	73.0
	00	8	7	00	25.5	73.0
1976 Dottie	-12	8	19	00	24.5	82.5
	00	8	19	12	25.0	82.0
1976 Emmy	-60	8	20	00	14.0	45.0
	-48	8	20	12	14.0	48.0
	-36	8	21	00	14.0	50.5
	-24	8	21	12	14.5	53.0
	-12	8	22	00	15.5	54.0
	00	8	22	12	16.0	56.0
1976 Gloria	-60	9	25	00	21.0	51.0
	-48	9	25	12	21.5	53.5
	-36	9	26	00	22.0	56.0
	-24	9	26	12	23.0	58.0
	-12	9	27	00	24.0	58.0
	00	9	27	12	26.0	58.0
1977 Anita	-60	8	28	00	22.0	81.0
	-48	8	28	12	23.0	84.0
	-36	8	29	00	25.0	85.0
	-24	8	29	12	26.5	86.5
	-12	8	30	00	27.0	88.0
	00	8	30	12	27.0	90.0

TABLE 46 (cont'd)

System	Position Number	Month	Date	Time (GMT)	Latitude (Deg. North)	Longitude (Deg. West)
1977 Clara	-60	9	5	12	33.0	80.0
	-48	9	6	00	34.0	78.5
	-36	9	6	12	34.0	77.0
	-24	9	7	00	34.0	76.0
	-12	9	7	12	34.5	74.5
	00	9	8	00	35.0	72.0
1977 Dorothy	-60	9	25	00	23.5	74.0
	-48	9	25	12	25.5	74.0
	-36	9	26	00	27.0	73.0
	-24	9	26	12	28.0	72.0
	-12	9	27	00	29.5	70.0
	00	9	27	12	31.0	66.0
1977 Evelyn	-60	10	12	00	23.0	56.0
	-48	10	12	12	24.0	58.0
	-36	10	13	00	25.0	60.0
	-24	10	13	12	26.0	62.0
	-12	10	14	00	29.0	64.0
	00	10	14	12	35.0	65.0
1977 Frieda	-60	10	15	00	17.0	74.0
	-48	10	15	12	17.0	76.0
	-36	10	16	00	17.0	78.0
	-24	10	16	12	17.0	80.5
	-12	10	17	00	17.0	82.0
	00	10	17	12	17.0	84.0

TABLE 47

For this analysis, shear data were extracted always for the position at which the system was designated a tropical depression.

<u>Pre-depression Stage</u>					
System	Month	Date	Time (GMT)	Latitude (Deg. North)	Longitude (Deg. West)
1975 Amy	6	27	00	27.5	79.0
1975 Blanche	7	24	00	26.0	68.4
1975 Caroline	8	24	12	22.4	69.8
1975 Eloise	9	13	12	17.6	55.2
1975 Hallie	10	25	00	28.8	79.0
1976 Belle	8	6	12	25.5	73.0
1976 Gloria	9	26	00	23.0	58.0
1977 Anita	8	29	12	26.5	86.5
1977 Dorothy	9	27	00	29.5	70.0
1977 Evelyn	10	14	00	29.0	64.0
1977 Frieda	10	17	00	17.0	82.0

TABLE 48
Atlantic Non-developing Systems

<u>Non-developing Depressions (1975)</u>						
<u>System</u>	<u>Position Number</u>	<u>Month</u>	<u>Date</u>	<u>Time (GMT)</u>	<u>Latitude (Deg. North)</u>	<u>Longitude (Deg. West)</u>
1	1	6	24	12	32.0	52.0
	2	6	25	12	33.0	54.0
	3	6	26	12	33.0	58.0
2	4	7	4	12	30.0	73.0
	5	7	5	12	34.0	68.5
3	6	7	12	12	33.0	47.0
	7	7	13	12	31.0	49.0
4	8	9	11	12	32.0	62.0
	9	9	12	12	31.0	62.0
	10	9	13	12	36.0	59.0
5	11	9	7	12	17.0	46.0
	12	9	8	12	16.0	53.0
6	13	10	16	12	20.0	62.5
	14	10	17	12	21.0	66.0
<u>Non-developing Depressions (1976)</u>						
7	15	9	6	12	28.0	87.0
	16	9	7	12	28.0	89.0
8	17	9	23	12	21.0	45.0
	18	9	24	12	22.0	47.0
9	19	9	28	12	13.0	46.0
10	20	10	7	12	13.0	63.0
	21	10	8	12	13.0	66.0
	22	10	9	12	14.0	69.0
11	23	10	12	12	20.0	46.0
	24	10	13	12	22.0	47.0
	25	10	14	12	23.0	49.0
12	26	10	31	00	21.0	62.0

TABLE 48 (cont'd)

<u>System</u>	<u>Position Number</u>	<u>Month</u>	<u>Date</u>	<u>Time (GMT)</u>	<u>Latitude (Deg. North)</u>	<u>Longitude (Deg. West)</u>
<u>Non-developing Depressions (1977)</u>						
13	27	9	3	12	30.0	64.0
	28	9	4	12	28.5	63.0
14	29	9	19	12	10.0	45.0
15	30	10	1	12	10.0	46.0
	31	10	2	12	11.0	51.0
	32	10	3	12	12.0	56.0
16	33	10	2	12	28.0	45.0
	34	10	3	12	27.0	43.0
	35	10	4	12	29.0	43.0
<u>Dvorak Systems (1975)</u>						
17	36	7	3	12	12.0	66.0
	37	7	4	12	15.0	69.5
	38	7	5	12	14.0	77.0
18	39	7	15	12	13.0	82.0
	40	7	16	12	13.0	83.0
19	41	8	20	12	10.5	54.5
	42	8	21	12	12.0	64.0
	43	8	22	12	16.0	69.0
20	44	8	26	12	13.0	53.0
	45	8	27	12	13.0	58.0
	46	8	28	12	14.0	63.0
	47	8	29	12	14.0	68.0
	48	8	30	12	14.5	75.5
	49	8	31	12	16.5	78.5
	50	9	1	12	17.5	86.0
21	51	9	4	12	15.0	76.0
	52	9	5	12	15.0	79.0
	53	9	6	12	15.0	80.0
22	54	9	15	12	10.0	79.0
	55	9	16	12	14.5	80.0
23	56	9	26	12	12.0	71.5
	57	9	27	12	15.5	75.5
	58	9	28	12	17.5	79.0

TABLE 48 (cont'd)

<u>System</u>	<u>Position Number</u>	<u>Month</u>	<u>Date</u>	<u>Time (GMT)</u>	<u>Latitude (Deg. North)</u>	<u>Longitude (Deg. West)</u>
24	59	10	2	12	12.0	56.0
	60	10	3	12	12.0	62.5
<u>Frank Systems (1975)</u>						
25	61	7	4	12	15.0	70.5
26	62	8	4	12	13.0	51.0
	63	8	5	12	14.0	58.5
	64	8	6	12	14.0	67.5
27	65	8	16	12	17.5	62.5
	66	8	17	12	17.5	69.5
28	67	8	18	12	15.0	67.5
29	68	8	29	12	13.0	77.5
	69	8	30	12	15.0	84.5
30	70	8	31	12	15.0	55.5
	71	9	1	12	15.0	60.5
	72	9	4	12	15.0	77.0
	73	9	5	12	17.0	83.0
31	74	9	1	12	13.5	76.5
32	75	9	27	12	18.0	67.5
	76	9	28	12	18.0	73.0
33	77	10	5	12	15.0	60.0
	78	10	6	12	18.0	65.0
	79	10	7	12	19.0	69.5
34	80	10	14	12	17.5	60.0
	81	10	15	12	17.0	65.0
	82	10	16	12	17.0	69.0
	83	10	17	12	17.0	73.5
35	84	10	24	12	12.5	75.0
	85	10	25	12	12.5	80.5
<u>Shapiro Systems (1976)</u>						
36	86	9	6	12	14.0	55.0
	87	9	7	12	14.0	63.0
	88	9	8	12	14.0	69.0

TABLE 48 (cont'd)

<u>System</u>	<u>Position Number</u>	<u>Month</u>	<u>Date</u>	<u>Time (GMT)</u>	<u>Latitude (Deg. North)</u>	<u>Longitude (Deg. West)</u>
	89	9	9	12	14.0	76.5
	90	9	10	12	15.0	82.0
37	91	9	12	12	14.5	43.0
	92	9	13	12	15.0	46.5
	93	9	14	12	15.5	50.5
	94	9	15	12	16.0	55.0
	95	9	16	12	16.0	58.5
	96	9	17	12	16.0	63.0
38	97	9	14	12	11.5	42.0
	98	9	15	12	11.0	47.0
	99	9	16	12	11.0	53.0
	100	9	17	12	11.0	59.0
	101	9	18	12	11.0	65.0
39	102	9	24	12	21.0	42.0
	103	9	27	12	27.0	46.0
	104	9	28	12	27.5	48.0
	105	9	29	12	26.0	49.0
	106	9	30	12	26.0	52.0
40	107	9	28	12	11.0	45.0
	108	9	29	12	11.0	49.0
	109	9	30	12	11.0	52.5
	110	10	1	12	11.5	58.0
	111	10	2	12	12.0	62.0
	112	10	3	12	13.0	66.0
	113	10	4	12	13.0	70.0
	114	10	5	12	13.0	74.0
	115	10	6	12	13.0	79.0
41	116	10	2	12	10.0	47.0
	117	10	3	12	11.0	53.0
	118	10	4	12	12.0	59.0
	119	10	5	12	13.0	65.0
42	120	10	13	12	22.0	42.5
	121	10	14	12	23.0	46.0
	122	10	15	12	24.5	51.0
	123	10	16	12	27.0	54.5
	124	10	17	12	29.0	58.0
	125	10	18	12	31.0	61.0
43	126	10	31	12	14.0	42.0

TABLE 48 (cont'd)

<u>System</u>	<u>Position Number</u>	<u>Month</u>	<u>Date</u>	<u>Time (GMT)</u>	<u>Latitude (Deg. North)</u>	<u>Longitude (Deg. West)</u>
<u>Shapiro Systems (1977)</u>						
44	127	8	19	12	11.0	53.0
	128	8	20	12	13.5	60.0
	129	8	21	12	15.0	66.0
	130	8	22	12	16.0	72.0
	131	8	23	12	16.0	77.0
	132	8	24	12	17.0	82.0
	133	8	25	12	19.0	86.0
45	134	9	23	12	8.0	43.0
	135	9	24	12	8.0	50.0
46	136	10	1	12	11.0	44.0
	137	10	2	12	13.0	48.0
	138	10	4	12	20.0	55.0
	139	10	5	12	23.0	58.0
	140	10	6	12	27.5	60.0
	141	10	7	12	33.0	57.0
<u>McBride Systems (1976)</u>						
47	142	7	20	12	12.0	61.0
	143	7	21	12	15.0	66.0
	144	7	22	12	18.0	68.0
	145	7	23	12	23.0	75.0
48	146	7	28	12	13.0	62.0
	147	7	29	12	13.0	69.0
49	148	8	19	12	18.0	72.0
50	149	8	22	12	27.0	88.0
51	150	8	23	12	10.0	50.0
	151	8	24	12	12.0	60.0
52	152	9	6	12	12.0	53.0
	153	9	7	12	14.0	60.0
53	154	9	7	12	13.0	49.0
	155	9	8	12	13.0	56.0
54	156	9	16	12	13.0	53.0
	157	9	17	12	13.0	60.0
	158	9	18	12	13.0	66.0

TABLE 48 (cont'd)

<u>System</u>	<u>Position Number</u>	<u>Month</u>	<u>Date</u>	<u>Time (GMT)</u>	<u>Latitude (Deg. North)</u>	<u>Longitude (Deg. West)</u>
55	159	9	30	12	13.0	76.0
56	160	9	30	12	13.0	70.0
	161	10	1	12	14.0	75.0
57	162	10	23	12	11.0	45.0
	163	10	25	12	12.0	56.0
	164	10	26	12	14.0	61.0
58	165	10	29	12	15.0	48.0
<u>McBride Systems (1977)</u>						
59	166	8	19	12	14.0	68.0
60	167	8	24	12	22.0	67.0
	168	8	25	12	22.0	67.0
61	169	9	4	12	14.0	56.0
	170	9	5	12	14.0	62.0
	171	9	6	12	16.0	67.0
62	172	10	6	12	13.0	53.0
	173	10	7	12	14.0	60.0
	174	10	8	12	15.0	65.0
63	175	10	15	12	13.0	57.0
	176	10	16	12	14.0	59.0
	177	10	17	12	14.0	60.0
	178	10	18	12	14.0	60.0

TABLE 49

Pacific pretyphoon and non-developing cloud clusters (positions from S. Erickson (1977)).

<u>Position Number</u>	<u>Year</u>	<u>Month</u>	<u>Date</u>	<u>Time (GMT)</u>	<u>Latitude (Deg. North)</u>	<u>Longitude (Deg. East)</u>
20	1972	5	7	12	8.0	160.7
21	1972	5	8	00	8.6	159.7
22	1972	5	8	12	7.9	159.4
23	1972	5	9	00	7.8	159.3
24	1972	5	9	00	8.5	146.5
25	1972	5	9	12	7.5	142.5
26	1972	5	10	00	7.5	140.4
27	1972	5	12	00	13.1	158.0
28	1972	5	12	12	12.4	154.5
29	1972	5	13	00	11.7	151.0
30	1972	5	14	00	9.5	161.2
31	1972	5	14	12	9.0	160.0
32	1972	5	15	00	8.2	158.8
33	1972	5	19	00	7.4	156.0
34	1972	5	19	12	8.7	153.0
35	1972	5	20	00	10.0	150.0
36	1972	5	26	00	6.0	169.9
37	1972	5	26	12	6.1	166.6
38	1972	5	27	00	6.3	163.3
39	1972	5	27	00	11.0	140.2
40	1972	5	27	12	13.1	135.7
41	1972	5	28	00	15.2	131.1
42	1972	5	28	00	6.9	142.8
43	1972	5	28	12	15.4	127.6
44	1972	5	28	12	7.5	139.9
45	1972	5	29	00	15.6	124.1
46	1972	5	29	00	8.1	137.0
47	1972	6	06	00	7.8	136.1
48	1972	6	06	12	7.8	135.6
49	1972	6	07	00	7.8	135.0
50	1972	6	07	12	8.4	133.2
51	1972	6	08	00	9.0	131.5
52	1972	6	08	12	9.4	164.2
53	1972	6	09	00	9.0	162.8
54	1972	6	09	12	9.4	161.4
55	1972	6	09	12	13.0	169.5
56	1972	6	10	00	10.0	160.0
57	1972	6	10	00	13.2	169.0
58	1972	6	10	12	14.2	166.0
59	1972	6	11	00	15.2	163.0
60	1972	6	13	00	7.8	150.7
61	1972	6	13	00	14.3	156.9
62	1972	6	13	12	8.0	148.0
63	1972	6	13	12	13.4	153.1

TABLE 49 (cont'd)

<u>Position Number</u>	<u>Year</u>	<u>Month</u>	<u>Date</u>	<u>Time (GMT)</u>	<u>Latitude (Deg. North)</u>	<u>Longitude (Deg. East)</u>
64	1972	6	14	00	8.0	147.0
65	1972	6	14	00	12.5	149.3
66	1972	6	14	12	13.5	146.9
67	1972	6	15	00	14.4	144.5
68	1972	6	15	12	14.4	142.5
69	1972	6	16	00	14.5	140.5
70	1972	6	18	12	10.0	165.7
71	1972	6	18	12	9.9	164.0
72	1972	6	19	12	9.8	162.4
73	1972	6	19	00	9.3	147.3
74	1972	6	19	12	8.9	159.4
75	1972	6	19	12	10.0	146.1
76	1972	6	20	00	8.0	156.4
77	1972	6	20	00	10.7	144.9
78	1972	6	20	12	11.7	141.1
79	1972	6	30	00	5.0	139.6
80	1972	6	30	12	6.0	138.3
121	1972	8	02	12	11.5	141.0
122	1972	8	03	00	12.2	140.0
123	1972	8	03	12	11.7	138.8
124	1972	8	04	00	11.1	137.6
125	1972	8	10	00	15.7	130.9
126	1972	8	10	12	16.6	129.6
127	1972	8	11	00	17.5	128.3
128	1972	8	18	00	11.0	148.0
129	1972	8	18	00	10.3	134.0
130	1972	8	18	12	11.0	145.0
131	1972	8	18	12	10.7	132.2
132	1972	8	19	00	11.0	141.7
133	1972	8	19	00	11.0	130.4
134	1972	8	19	00	7.2	143.2
135	1972	8	19	12	8.1	140.3
136	1972	8	20	00	9.1	136.9
137	1972	8	21	00	7.8	156.0
138	1972	8	21	12	6.9	153.4
139	1972	8	22	00	6.0	150.8
140	1972	8	23	00	7.5	137.8
141	1972	8	23	12	7.2	136.9
142	1972	8	24	00	7.0	135.9
143	1972	8	24	12	7.9	135.0
144	1972	8	25	00	9.7	134.4
145	1972	8	27	00	13.0	145.8
146	1972	8	27	12	13.8	143.1
147	1972	8	28	00	14.5	140.4
148	1972	8	28	12	15.2	138.0
149	1972	8	29	00	15.8	135.5
150	1972	8	29	00	8.7	130.1
151	1972	8	29	12	10.0	127.8

TABLE 49 (cont'd)

<u>Position Number</u>	<u>Year</u>	<u>Month</u>	<u>Date</u>	<u>Time (GMT)</u>	<u>Latitude (Deg. North)</u>	<u>Longitude (Deg. East)</u>
152	1972	8	30	00	5.0	153.0
153	1972	8	30	00	11.3	125.4
154	1972	8	30	12	5.0	151.1
155	1972	8	31	00	5.0	149.1
156	1972	9	01	00	5.0	138.8
157	1972	9	01	12	5.0	137.4
158	1972	9	02	00	5.0	136.0
159	1972	9	05	00	13.9	145.2
160	1972	9	05	12	14.4	143.4
161	1972	9	06	00	14.9	141.6
162	1972	9	06	12	15.2	138.5
163	1972	9	07	00	15.5	135.4
164	1972	9	07	12	14.9	132.9
165	1972	9	08	00	9.0	153.6
166	1972	9	08	00	10.0	139.0
167	1972	9	08	12	9.0	150.6
168	1972	9	08	12	11.3	138.5
169	1972	9	09	00	8.9	147.6
170	1972	9	09	00	12.6	138.0
171	1972	9	09	12	8.7	145.8
172	1972	9	09	12	12.8	138.0
173	1972	9	10	00	8.5	143.9
174	1972	9	10	00	14.3	130.0
175	1972	9	10	00	13.1	138.0
176	1972	9	10	12	15.0	129.2
177	1972	9	10	12	13.2	137.5
178	1972	9	11	00	15.6	128.5
179	1972	9	15	00	13.4	154.5
180	1972	9	15	12	14.5	154.8
181	1972	9	16	00	15.5	155.0
182	1972	9	21	00	8.0	165.5
183	1972	9	21	12	7.6	163.8
184	1972	9	22	00	7.1	162.0
185	1972	9	22	12	7.3	160.3
186	1972	9	23	00	7.4	158.5
187	1972	9	24	00	10.0	168.0
188	1972	9	24	12	9.7	165.5
189	1972	9	25	00	9.5	163.0
190	1972	9	25	12	9.7	162.7
191	1972	9	26	00	10.0	162.5
192	1972	9	27	00	6.0	139.0
193	1972	9	27	12	6.5	136.9
194	1972	9	28	00	7.0	134.7
195	1972	9	29	00	7.0	134.0
196	1972	9	29	12	7.0	132.7
197	1972	9	30	00	7.0	131.3
248	1974	3	11	00	8.2	140.5
249	1974	3	11	12	8.2	141.2
250	1974	3	12	00	8.3	142.0

TABLE 49 (cont'd)

<u>Position Number</u>	<u>Year</u>	<u>Month</u>	<u>Date</u>	<u>Time (GMT)</u>	<u>Latitude (Deg. North)</u>	<u>Longitude (Deg. East)</u>
251	1974	3	12	12	8.4	143.7
284	1974	8	21	00	17.3	171.0
285	1974	8	21	12	17.3	168.8
286	1974	8	22	00	17.4	166.6
287	1974	8	22	12	18.1	164.0
288	1974	8	23	00	18.8	161.3
289	1974	9	07	00	14.0	166.9
290	1974	9	07	12	14.4	166.2
291	1974	9	08	00	14.8	165.5
292	1974	9	08	12	15.9	162.5
293	1974	9	09	00	17.0	159.5
294	1974	10	05	00	10.1	160.5
295	1974	10	05	12	10.1	155.8
296	1974	10	06	00	10.2	151.0
297	1974	10	06	12	10.4	147.0
298	1974	10	18	00	10.1	149.5
299	1974	10	18	12	10.7	146.4
300	1974	10	19	00	11.4	143.3
301	1974	10	21	00	9.2	151.4
302	1974	10	21	12	11.0	150.7
303	1974	10	22	00	12.7	150.0
304	1974	10	23	00	6.2	165.7
305	1974	10	23	12	7.1	163.8
306	1974	10	24	00	8.1	161.9
307	1974	10	28	00	5.1	156.4
308	1974	10	28	12	6.1	155.8
309	1974	10	29	00	7.1	155.2
310	1974	10	29	12	7.3	152.5
311	1974	10	30	00	7.5	150.0
312	1974	10	30	00	10.3	131.0
313	1974	10	31	00	2.3	146.0
314	1974	10	31	12	3.8	144.7
315	1974	11	01	00	5.2	143.3
316	1974	11	06	00	6.4	148.4
317	1974	11	06	12	5.7	145.2
318	1974	11	07	00	5.0	142.0
319	1974	11	12	00	13.0	124.5
320	1974	11	12	12	13.6	122.9
321	1974	11	13	00	14.3	121.2
322	1974	11	18	00	10.0	153.6
323	1974	11	18	12	10.1	150.8
324	1974	11	19	00	10.2	148.0
325	1974	11	19	12	9.8	146.8

W. M. GRAY'S FEDERALLY SUPPORTED RESEARCH PROJECT REPORTS SINCE 1967

CSU Dept. of
Atmos Sci.
Report No.

<u>Report Title, Author, Date, Agency Support</u>
104 The Mutual Variation of Wind, Shear, and Baroclinicity in the Cumulus Convective Atmosphere of the Hurricane (69 pp). W. M. Gray. February 1967. NSF Support.
114 Global View of the Origin of Tropical Disturbances and Storms (105 pp). W. M. Gray. October 1967. NSF Support.
116 A Statistical Study of the Frictional Wind Veering in the Planetary Boundary Layer (57 pp). B. Mendenhall. December 1967. NSF and ESSA Support.
124 Investigation of the Importance of Cumulus Convection and Ventilation in Early Tropical Storm Development (88 pp). R. Lopez. June 1968. ESSA Satellite Laboratory Support.
Unnumbered Role of Angular Momentum Transports in Tropical Storm Dissipation over Tropical Oceans (46 pp). R. F. Wachtmann. December 1968. NSF and ESSA Support.
Unnumbered Monthly Climatological Wind Fields Associated with Tropical Storm Genesis in the West Indies (34 pp). J. W. Sartor. December 1968. NSF Support.
140 Characteristics of the Tornado Environment as Deduced from Proximity Soundings (55 pp). T. G. Wills. June 1969. NOAA and NSF Support.
161 Statistical Analysis of Trade Wind Cloud Clusters of the Western North Pacific (80 pp). K. Williams. June 1970. ESSA Satellite Laboratory Support.
-- A Climatology of Tropical Cyclones and Disturbances of the Western Pacific with a Suggested Theory for Their Genesis/Maintenance (225 pp). W. M. Gray. NAVWEARSCHFAC Technical Paper No. 19-70. November 1970. (Available from US Navy, Monterey, CA). U.S. Navy Support.
179 A Diagnostic Study of the Planetary Boundary Layer over the Oceans (95 pp). W. M. Gray. February 1972. Navy and NSF Support.
182 The Structure and Dynamics of the Hurricane's Inner Core Area (105 pp). D. J. Shea. April 1972. NOAA and NSF Support.

W. M. GRAY'S FEDERALLY SUPPORTED RESEARCH PROJECT REPORTS SINCE 1967 (cont'd)

CSU Dept. of
Atmos. Sci.
Report No.

Report Title, Author, Date, Agency Support

- 188 Cumulus Convection and Larger-Scale Circulation, Part I: A Parametric Model of Cumulus Convection (100 pp). R. E. Lopez. June 1972. NSF Support.
- 189 Cumulus Convection and Larger-Scale Circulations, Part II: Cumulus and Meso-scale Interactions (63 pp). R. E. Lopez. June 1972. NSF Support.
- 190 Cumulus Convection and Larger-Scale Circulations, Part III: Broadscale and Meso-scale Considerations (80 pp). W. M. Gray. July 1972. NOAA-NESS Support.
- 195 Characteristics of Carbon Black Dust as a Tropospheric Heat Source for Weather Modification (55 pp). W. M. Frank. January 1973. NSF Support.
- 196 Feasibility of Beneficial Hurricane Modification by Carbon Black Seeding (130 pp). W. M. Gray. April 1973. NOAA Support.
- 199 Variability of Planetary Boundary Layer Winds (157 pp). L. R. Hoxit. May 1973. NSF Support.
- 200 Hurricane Spawned Tornadoes (57 pp). D. J. Novlan. May 1973. NOAA and NSF Support.
- 212 A Study of Tornado Proximity Data and an Observationally Derived Model of Tornado Genesis (101 pp). R. Maddox. November 1973. NOAA Support.
- 219 Analysis of Satellite Observed Tropical Cloud Clusters (91 pp). E. Ruprecht and W. M. Gray. May 1974. NOAA-NESS Support.
- 224 Precipitation Characteristics in the Northeast Brazil Dry Region (56 pp). R. P. L. Ramos. May 1974. NSF Support.
- 225 Weather Modification through Carbon Dust Absorption of Solar Energy (190 pp). W. M. Gray, W. M. Frank, M. L. Corrin and C. A. Stokes. July 1974.
- 234 Tropical Cyclone Genesis (121 pp). W. M. Gray. March 1975. NSF Support.

W. M. GRAY'S FEDERALLY SUPPORTED RESEARCH PROJECT REPORTS SINCE 1967 (cont'd)

CSU Dept. of
Atmos. Sci.
Report No.

<u>Report Title, Author, Date, Agency Support</u>	
--	Tropical Cyclone Genesis in the Western North Pacific (66 pp). W. M. Gray. March 1975. U.S. Navy Environmental Prediction Research Facility Report. Technical Paper No. 16-75. (Available from the US Navy, Monterey, CA). Navy Support.
241	Tropical Cyclone Motion and Surrounding Parameter Relationships (105 pp). J. E. George. December 1975. NOAA Support.
243	Diurnal Variation of Oceanic Deep Cumulus Convection, Paper I: Observational Evidence, Paper II: Physical Hypothesis (106 pp). R. W. Jacobson, Jr. and W. M. Gray. February 1976. NOAA-NESS Support.
257	Data Summary of NOAA's Hurricane Inner-Core Radial Leg Flight Penetrations 1957-1967, 1969 (245 pp). W. M. Gray and D. J. Shea. October 1976. NSF and NOAA Support.
258	The Structure and Energetics of the Tropical Cyclone (180 pp). W. M. Frank. October 1976. NOAA-NHEML and NOAA-NESS and NSF Support.
Unnumbered	Severe Thunderstorm Wind Gusts (81 pp). G. W. Walters. December 1976. NSF Support.
262	Diurnal Variation of the Tropospheric Energy Budget (141 pp). G. S. Foltz. November 1976. NSF Support.
--	Tropical Cyclone Research by Data Compositing (70 pp). W. M. Gray and W. M. Frank. July 1977. Naval Environmental Prediction Research Facility, Monterey, CA. NEPRF Technical Report TR-77-01. Navy Support.
274	Comparison of Developing vs. Non-developing Tropical Disturbances (81 pp). S. L. Erickson. July 1977. U. S. Army Support.
277	Tropical Cyclone Cloud and Intensity Relationships (154 pp). C. P. Arnold. November 1977. U.S. Army and NHEML Support.
--	New Results of Tropical Cyclone Research from Observational Analysis (106 pp). W. M. Gray and W. M. Frank. June 1978. Naval Environmental Prediction Research Facility, Monterey, CA. NEPRF Technical Report TR-78-01. Navy Support.

W. M. GRAY'S FEDERALLY SUPPORTED RESEARCH PROJECT REPORTS SINCE 1967 (cont'd)

CSU Dept. of
Atmos. Sci.

Report No.

Report Title, Author, Date, Agency Support

- | | |
|-----|--|
| 297 | Diagnostic Analyses of the GATE A/B-scale Area at Individual Time Periods (102 pp). W. M. Frank. November 1978. NSF Support. |
| 298 | Diurnal Variability in the GATE Region (80 pp). J. M. Dewart. November 1978. NSF Support. |
| 299 | Mass Divergence in Tropical Weather Systems, Paper I: Diurnal Variation, Paper II: Large-scale Controls on Convection (109 pp). J. L. McBride and W. M. Gray. November 1978. NOAA-NHEML Support. |
| 305 | Convection Induced Temperature Change in GATE (128 pp). P. G. Grube. February 1979. NSF Support. |

BIBLIOGRAPHIC DATA SHEET	1. Report No. CSU-ATS-308	2.	3. Recipient's Accession No.
4. Title and Subtitle OBSERVATIONAL ANALYSIS OF TROPICAL CYCLONE FORMATION		5. Report Date April, 1979	6.
7. Author(s) John L. McBride	8. Performing Organization Rept. No. CSU-ATS-308		
9. Performing Organization Name and Address Atmospheric Science Department Colorado State University	10. Project/Task/Work Unit No.		
12. Sponsoring Organization Name and Address NSF NOAA/NHEML NEPRF 18th & G. St. N.W. Coral Gables, FL Oakland, CA Washington, DC	11. Contract/Grant No. In #12		
Grant= ATM 78-18962 NA 79 RAD 00002 N00228-76-C-2129	13. Type of Report & Period Covered Project Report		
14.			
15. Supplementary Notes			
16. Abstracts This study investigates the genesis of tropical cyclones through a combination of the compositing approach and the case study approach. Twelve composite data sets are analyzed from the tropical Northwest Pacific and tropical Northwest Atlantic Oceans. Each data set is a composite average of approximately 80 individual disturbances. Four different types of non-developing oceanic tropical disturbances are composited. They are compared with pre-hurricane and pre-typhoon disturbances in each ocean composited at four different stages of intensification. In total 912 different tropical weather systems go into the composites and approximately 40,000 rawinsonde observations are used. Vertically integrated budgets of heat, momentum and kinetic energy are performed on the composite data sets and physical hypotheses are made on the mechanisms of tropical cyclone genesis and development.			
17. Key Words and Document Analysis. 17a. Descriptors Cyclone genesis Tropical cyclones			
17b. Identifiers/Open-Ended Terms			
17c. COSATI Field/Group			
18. Availability Statement	19. Security Class (This Report) UNCLASSIFIED	21. No. of Pages 230	
	20. Security Class (This Page) UNCLASSIFIED	22. Price	